University of Plymouth

PEARL **https://pearl.plymouth.ac.uk**

04 University of Plymouth Research Theses 01 Research Theses Main Collection

1994

THE DETERMINATION OF TRACE METALS IN SEA WATER USING ICP-MS

BLOXHAM, MARTIN JOHN

http://hdl.handle.net/10026.1/1073

http://dx.doi.org/10.24382/3271
University of Plymouth

All content in PEARL is protected by copyright law. Author manuscripts are made available in accordance with publisher policies. Please cite only the published version using the details provided on the item record or document. In the absence of an open licence (e.g. Creative Commons), permissions for further reuse of content should be sought from the publisher or author.

store

THE DETERMINATION OF TRACE METALS IN SEA WATER USING ICP-MS

M. J. BLOXHAM

Ph.D. 1994

This copy of the thesis has been supplied on the condition that anyone who consults it is understood to recognise that its copyright rests with its author and that no quotation from the thesis and no information derived from it may be published without the authors prior written consent.

Signed..
Date......6/1/95..............................

THE DETERMINATION OF TRACE METALS IN SEA WATER USING ICP-MS

By

MARTIN JOHN BLOXHAM, BSc

A thesis submitted to the University of Plymouth in partial
fulfilment for the degree of

DOCTOR OF PHILOSOPHY

Department of Environmental Sciences,
University of Plymouth,
Drake Circus,
Plymouth,
PL4 8AA.

In collaboration with:
Thornton Research Centre,
Shell Research Limited,
Chester,
CH1 3SH

November 1994

90 0220784 2

UNIVERSITY OF PLYMOUTH
LIBRARY SERVICES

Item No.	900 [illegible]07842
Class No.	T 551.4601 BLO
Contl. No.	X702992363

REFERENCE ONLY

LIBRARY STORE

ABSTRACT

THE DETERMINATION OF TRACE METALS IN SEA WATER USING ICP-MS

Martin John Bloxham

Inductively coupled plasma-mass spectrometry (ICP-MS) offers exceptional sensitivity and multi-element capability for trace metal analysis but the formation of polyatomic ions (particularly below m/z = 80) can cause serious interferences. Such species can be introduced *via* precursor atoms in atmospheric gases, the sample matrix or impurities in the argon support gas. This thesis describes the development of a portfolio of analytical methods coupled with ICP-MS detection for the determination of trace metals such as manganese, cobalt, copper, nickel, zinc, mercury and lead in complex matrices such as sea water. A literature review of coupled techniques is given in Chapter one.

Chapter two discusses the effect of sea water on the analytical performance of ICP-MS. Initial studies were carried out using a single channel flow injection (FI) manifold and included an investigation of the addition of nitrogen to the nebulizer gas flow of the ICP-MS for the reduction of the $ArNa^+$ polyatomic ion interference at m/z = 63 on the Cu signal. This was followed by a multivariate simplex optimisation for the suppression of the $ArNa^+$ polyatomic ion interference at m/z = 63 and non-spectroscopic interferences affecting other masses in sea water, for the determination of Cu, Cr, Mn, Ni, Co, Zn and Pb.

In Chapter three an on-line FI-ICP-MS matrix elimination method for the determination of trace metals such as Mn, Co, Cu, Zn and Pb in sea water is discussed. The method involved chelation of the analytes onto Chelex-100 or MetPac CC-1 iminodiacetate (IDA) resin, with the simultaneous removal of indirectly interfering matrix species, particularly Na and Cl ions. Results showing how the effects of the interferences were overcome, together with validation of the method by the analysis of open ocean, coastal and estuarine certified reference materials are reported.

Chapter four compares FI approaches coupled with AFS, ICP-AES and ICP-MS detectors for the determination of total mercury. Initial studies compared figures of merit for FI (conventional pneumatic nebulization) and FI-cold vapour generation (CVG) coupled with ICP-AES and ICP-MS. Detection limits for total Hg were improved by developing simple on- and off-line preconcentration procedures using a MetPac CC-1 micro-column incorporated in a FI manifold with conventional pneumatic nebulization. An AFS detector was then used in the development of a method for the determination of total mercury with an on-line bromide/bromate oxidation step.

In chapter five an LC-ICP-MS method for the speciation of Hg in sea water samples is described. The method involved the separation of mercury(II) chloride, methylmercury chloride and ethylmercury chloride on a C_{18} ODS stationary phase with an ammonium acetate/acetonitrile/2-mercaptoethanol mobile phase. In order to achieve the necessary detection limits required for the determination of mercury in real sea water samples (< 50 ng l^{-1}), an off-line preconcentration method using a dithiocarbamate resin was used.

CONTENTS

CHAPTER 1 INTRODUCTION 1

1.1 Inductively coupled plasma mass spectrometry 1

1.1.1 Historical development 1

1.1.2 Instrumentation and operation 2

1.1.3 Analytical applications 6

1.1.4 Interferences 10

1.1.4.1 Spectroscopic interferences 11

1.1.4.2 Non-spectroscopic interferences 15

1.1.5 The use of nitrogen-argon plasmas for the removal of spectroscopic and non-spectroscopic interferences 16

1.2 FI and LC coupled with atomic spectrometry 18

1.2.1 Flow injection analysis 18

1.2.1.1 Basic principles 19

1.2.1.2 On-line sample treatment 19

1.2.2 FI coupled with atomic spectrometry 22

1.2.2.1 Preconcentration using chelation exchange resins 23

1.2.2.2 Simultaneous preconcentration and matrix removal using chelation exchange resins 23

1.2.3 Liquid chromatography 29

1.2.3.1 Basic principles 29

1.2.3.2 Chromatographic parameters 31

1.2.4 LC coupled with atomic spectrometry 34

1.2.4.1 Environmental applications of LC-ICP-MS 37

1.2.4.2 Clinical and industrial applications of LC-ICP-MS 39

1.3 Trace metals in sea water 50

1.3.1 Sea water composition 50

1.3.2 Metal speciation and complexation 51

1.3.3 Mercury speciation 54

1.4 Research objectives 56

CHAPTER 2 DETERMINATION OF TRACE METALS IN SEA WATER USING MIXED GAS PLASMAS **58**

2.1 Experimental 59

2.1.1 Instrumentation 59

2.1.2 Gas addition 60

2.1.3 Reagents 60

2.1.4 Simplex optimisation 63

2.1.5 Flow injection manifold 66

2.2 Results and discussion 66

2.2.1 Determination of trace metals in saline and non-saline matrices by ICP-MS 66

2.2.2 Preliminary univariate search 70

2.2.3 Simplex optimisation of operating conditions for the removal of $ArNa^+$ with nitrogen addition to the nebulizer gas flow using an FI sample introduction procedure 73

2.2.4 Simplex optimisation of operating conditions for the removal of ArNa$^+$ with nitrogen addition to the nebulizer gas flow using a continuous nebulization sample introduction procedure 77

2.3 Conclusions 84

CHAPTER 3 ON-LINE REMOVAL OF MATRIX INTERFERENCES IN SEA WATER BY FLOW INJECTION WITH INDUCTIVELY COUPLED PLASMA-MASS SPECTROMETRIC DETECTION 85

3.1 Experimental 87

3.1.1 Instrumentation 87

3.1.2 Flow injection manifold 87

3.1.3 Reagents 89

3.1.4 Certified reference materials 90

3.2 Results and discussion 93

3.2.1 Preconcentration of trace metals using Chelex-100 93

3.2.1.1 Properties of Chelex-100 93

3.2.1.2 Optimisation of the FI procedure 95

3.2.2 Preconcentration of trace metals using Metpac CC-1 98

3.2.2.1 Properties of Metpac CC-1 98

3.2.2.2 Optimisation of the FI procedure 99

3.2.2.3 Preconcentration of copper from sea water 104

3.2.3 Coupling of FI Metpac CC-1 preconcentration with ICP-MS detection 107

3.2.3.1 Reagent purity 107

3.2.3.2 Analysis of synthetic sea water 107

3.2.3.3 Standard additions 108

3.2.3.4 Validation of the procedure 109

3.3 Conclusions 115

CHAPTER 4 DETERMINATION OF TOTAL MERCURY IN SEA WATER BY FLOW INJECTION WITH ATOMIC SPECTROMETRIC DETECTION **116**

4.1 Atomic fluorescence spectrometry 117

4.2 Experimental 120

4.2.1 Instrumentation 120

4.2.2 Reagents 123

4.2.3 Analysis of TORT-1 lobster hepatopancreas 125

4.2.4 FI procedures 125

4.2.4.1 Single channel FI manifold for ICP-AES and ICP-MS detection 125

4.2.4.2 Cold vapour generation FI manifold for ICP-AES and ICP-MS detection 126

4.2.4.3 FI preconcentration manifold for ICP-MS detection 126

4.2.4.4 Cold vapour generation FI manifold for AFS detection 129

4.3 Results and discussion 132

4.3.1 Determination of inorganic mercury in saline and non-saline matrices by FI with ICP-AES and ICP-MS 132

4.3.1.1 FI-ICP-AES 132

4.3.1.2 FI-ICP-MS 134

4.3.2 On-line preconcentration of total mercury with ICP-MS detection 138
4.3.2.1 Optimisation of the procedure 138
4.3.2.2 Figures of merit 142
4.3.2.3 Validation using TORT-1 CRM 146
4.3.2.4 Analysis of a Sutton Harbour sample 146
4.3.3 FI-cold vapour generation-AFS 148
4.3.3.1 Optimisation of the procedure 149
4.3.3.2 Figures of merit 156
4.3.3.3 Validation using TORT-1 CRM 158
4.3.3.4 Analysis of Sutton Harbour samples 158
4.4 Conclusions 161

CHAPTER 5 SPECIATION OF MERCURY IN SEA WATER BY LIQUID CHROMATOGRAPHY WITH ATOMIC SPECTROMETRIC DETECTION **164**
5.1 Experimental 165
5.1.1 Instrumentation 165
5.1.2 Reagents 166
5.1.3 Analysis of TORT-1 lobster hepatopancreas 167
5.1.4 Off-line preconcentration procedure 167
5.2 Results and discussion 168
5.2.1 Optimisation of acetonitrile concentration 168
5.2.2 Effect of synthetic sea water on the chromatographic separation 172
5.2.3 Figures of merit 172

5.2.4 Validation using TORT-1 lobster hepatopancreas CRM 175

5.2.5 Determination of mercury in discharge water samples 178

5.2.6 Analysis of Plymouth Sound sea water samples 180

5.3 Conclusions 182

CHAPTER 6 GENERAL CONCLUSIONS AND FUTURE WORK **184**

6.1 General conclusions 184

5.3 Future work 186

CHAPTER 7 REFERENCES **189**

LIST OF TABLES

1.1 ICP-MS, ICP-AES and GFAAS detection limits (3 σ) for a range of elements found in environmental samples such as sea water. 9

1.2 Common polyatomic ion interferences. 12

1.3 Examples of trace metal determinations using chelating resins. 27

1.4 Classification of modes of LC. 30

1.5 LC-ICP-MS applications (environmental). 40

1.6 LC-ICP-MS applications (clinical and industrial). 47

1.7 The major ions of sea water. 51

1.8 Speciation and concentration data for selected trace elements in sea water. 53

2.1 ICP-MS scan parameters. 61

2.2 Standard operating conditions for the ICP-MS. 62

2.3 Simplex optimisation start conditions for 1 % v/v synthetic sea water. 65

2.4 Limits of detection (3 σ) for the metals of interest in 2 % v/v nitric acid and a 10 % v/v synthetic sea water matrix using continuous nebulization. 68

2.5 Limits of detection (3σ) for the metals of interest in 2 % v/v nitric acid and a 10 % v/v synthetic sea water matrix using flow injection (200 μl sample loop). 68

2.6 The effect of nitrogen addition on the signal-to-blank ratio (S/B) for 100 $\mu g\ l^{-1}$ copper. 71

2.7 Simplex optimum conditions for the removal of $ArNa^+$ interference with nitrogen addition (10 % v/v synthetic sea water) using FI. 74

2.8 Simplex optimum conditions for the removal of $ArNa^+$ interference with nitrogen addition (1 % v/v synthetic sea water) under continuous nebulization. 78

2.9 Comparison of limits (3σ) of detection for the analytes of interest under simplex optimised conditions and standard operating conditions. 83

3.1 FAAS operating conditions for the determination of copper. 88

3.2 ICP-MS time resolved analysis parameters and isotopes used for each element. 88

3.3 Thirteen metals for which certified values have been established in the NASS-3 CRM. 92

3.4 Selectivity for divalent cations. 94

3.5 Effect of synthetic sea water concentration on the retention and elution of sodium. 100

3.6 Effect of synthetic sea water pH on the breakthrough and retention of 5.0 mg l^{-1} copper. 101

3.7 Effect of buffer concentration on the retention and breakthrough of copper (5.0 mg l^{-1}) and sodium (100 % v/v synthetic sea water). 102

3.8 Optimum FI Conditions. 104

3.9 Figures of merit for 200 and 2000 µl sample injections for Cu over the range 10-100 µg l^{-1}. 105

3.10 Figures of merit for the Merck corrosion test mixture. 108

3.11 NASS-3 open ocean sea water certified reference material results. The uncertainties represent 95 % confidence limits for an individual subsample (n=3). 111

3.12 CASS-2 near shore sea water certified reference material results. The uncertainties represent 95 % confidence limits for an individual subsample (n=3). 112

3.13 SLEW-1 estuarine water certified reference material results. The uncertainties represent 95 % confidence limits for an individual subsample (n=3). 113

4.1 Varian Liberty 200 operating conditions. 120

4.2 Merlin AFS detector operating conditions. 123

4.3 Figures of merit using either conventional (Meinhard) nebulization or cold vapour generation. 133

4.4 Figures of merit using either conventional (Meinhard) nebulization or cold vapour generation. 137

4.5 Figures of merit for the on-line preconcentration of mercury. 144

4.6 TORT-1 certified reference material results. 146

4.7 Figures of merit for the off-line total mercury preconcentration procedure. 147

4.8 Total mercury concentrations in two environmental samples. 148

4.9 Bromide/bromate and hydroxylammonium chloride concentrations. 151

4.10 FI-CVG-AFS conditions for the on-line oxidation of organic mercury species. 154

4.11 Figures of merit for the on-line determination of mercury(II) chloride and methylmercury chloride in 100 % v/v synthetic sea water. 156

4.12 TORT-1 certified reference material results. 158

4.13 Sutton Harbour total mercury concentrations. 159

4.14 Comparison of detection limits. 163

5.1 Physical properties of Metalfix Dithiochel resin. 167

5.2 Retention data for mercury(II), methylmercury and ethylmercury chloride (10 μg l^{-1}) using a 0.06 M ammonium acetate, 0.005 % v/v 2-mercaptoethanol mobile phase with varying concentrations of ACN. 169

5.3 Figures of merit for mercury(II), methylmercury and ethylmercury chloride spiked in Milli-Q de-ionised water and synthetic sea water. 175

5.4 TORT-1 certified reference material results. 178

5.5 Comparison of mercury concentrations in North Sea discharge waters using LC-ICP-MS and vacuum distillation/cold cell AAS. 178

5.6 Methylmercury and mercury(II) chloride concentrations in two Plymouth Sound samples. 181

LIST OF FIGURES

1.1 Schematic representation of a standard ICP Torch. 2

1.2 Sample introduction system. 4

1.3 Typical extraction interface. 6

1.4 Schematic of ICP-MS instrument. 7

1.5 Schematic diagram of a simple single line FI manifold. 19

1.6 Structures of two typical chelating compounds. 24

1.7 Schematic diagram of the basic LC system. 29

1.8 Illustration of parameters for retention time and resolution. 32

1.9 Cycling of mercury in the environment. 55

2.1 Calibration of the percentage mix gas added through the Signal gas blender. 61

2.2 Fixed step size simplex optimisation with two variables, X and Y. 64

2.3 Schematic diagram of the FI manifold. 66

2.4 Effect of increasing sea water concentration on the ^{63}Cu signal. 69

2.5 Effect of sea water concentration on the signal at m/z=63 with and without nitrogen addition to the nebulizer gas flow. 71

2.6 Univariate searches of the effect of (a) nebulizer gas and (b) auxiliary gas on the $Co^+/ArNa^+$ ratio. 75

2.6 Univariate searches of the effect of (c) forward power and (d) nitrogen addition on the $Co^+/ArNa^+$ ratio. 76

2.7 Simplex history. 78

2.8 Univariate searches of the effect of (a) nebulizer gas and (b) auxiliary gas on the $Co^+/ArNa^+$ ratio. 80

2.8. Univariate searches of the effect of (c) forward power and (d) nitrogen addition on the $Co^+/ArNa^+$ ratio. 81

3.1 A schematic diagram of the FI manifold. 89

3.2 Effect of synthetic sea water concentration on the breakthrough of copper (carrier stream, 1.5 M ammonium acetate buffer; acid eluent, 3.0 M nitric acid). 95

3.3 Effect of ammonium acetate buffer concentration on the breakthrough of Cu in 10 % v/v synthetic sea water. 96

3.4 Investigation of the retention of sodium on Chelex-100. 97

3.5 The structure of MetPac CC-1 chelating resin. 99

3.6 Effect of buffer pH on the retention of 5 mg l^{-1} copper. 102

3.7 Effect of nitric acid concentration on the elution characteristics for 5 mg l^{-1} copper. 103

3.8 Effect of sample loop size on the quantitative retention of 1.0 mg l^{-1} copper. 105

3.9 Replicate injections (n = 10) of 1.0 μg l^{-1} copper in 100 % v/v synthetic sea water. 106

3.10 Standard additions calibration graph. 109

3.11 Typical peak profiles for replicate injections of spiked NASS-3 samples. 114

4.1 Gas-liquid separator for the tin(II) chloride scheme. 119

4.2 Schematic diagram of the PS Analytical Merlin atomic fluorescence detector. 122

4.3 Schematic diagram of the cold vapour generation FI manifold for ICP-AES and ICP-MS detection. 127

4.4 Schematic diagram of the FI preconcentration manifold with ICP-AES or ICP-MS detection. (a) Mercury preconcentration step, (b) Mercury elution step. 128

4.5 Schematic diagram of the cold vapour generation FI manifold for AFS detection. 130

4.6 Calibration graphs for de-ionised water or synthetic sea water using either conventional (Meinhard) nebulization or cold vapour generation. 133

4.7 Modified gas-liquid separator for the tin(II) chloride reduction system. 135

4.8 Effect of modified gas-liquid separator and nebuliser flow rates on the signal to background ratio for mercury(II) chloride. 135

4.9 Calibration graphs for de-ionised water or synthetic sea water using either conventional (Meinhard) nebulization or cold vapour generation. 137

4.10 Optimisation of hydrochloric acid eluent concentration (thiourea concentration maintained at 1.0 % m/v). 141

4.11 Optimisation of thiourea concentration (hydrochloric acid concentration maintained at 2.0 M). 141

4.12 Optimisation of thiourea concentration in carrier stream. 143

4.13 Effect of sample volume on the response for mercury(II) chloride (5.0 $\mu g\ l^{-1}$). 143

4.14 Calibration graph for mercury(II) chloride and methylmercury chloride in 100 % v/v synthetic sea water. 144

4.15 Replicate 100 ng l^{-1} mercury peaks. 145

4.16 Effect of bromide/bromate reaction coil length on the detection of mercury(II) chloride and methylmercury chloride. 150

4.17 Effect of bromide/bromate and hydroxylammonium chloride concentration on the determination of mercury(II) chloride and methylmercury chloride. 150

4.18 Effect of Bromide/bromate reaction coil temperature on the determination of mercury(II) chloride and methylmercury chloride. 153

4.19 Effect of hydroxylammonium chloride reaction coil length on the determination of mercury(II) chloride and methylmercury chloride. 153

4.20 Effect of sample volume on the determination of mercury(II) chloride and methylmercury chloride. 155

4.21 The effect of incomplete oxidation of methylmercury when injecting 2000 ul sample volumes. 155

4.22 Calibration graph for mercury(II)chloride and methylmercury chloride in 100 % v/v synthetic sea water. 156

4.23 Replicate injections of 50 ng l^{-1} mercury(II) chloride (a) and methylmercury chloride (b) in 100 % v/v synthetic sea water. 157

4.24 Location of sampling positions in Sutton Harbour. 160

5.1 The chromatographic separation of the mercury(II), methylmercury and ethylmercury chloride (10 µg l^{-1}) using a 0.06 M ammonium acetate, 0.005 % 2-mercaptoethanol mobile phase with 3 % ACN. 170

5.2 The chromatographic separation of the mercury(II), methylmercury and ethylmercury chloride (10 µg l^{-1}) using a 0.06 M ammonium acetate, 0.00 5% 2-mercaptoethanol mobile phase with 1 % ACN. 171

5.3 Effect of synthetic sea water on the separation of methylmercury chloride, mercury(II) chloride and ethyl mercury chloride using a mobile phase containing 1.0 % v/v ACN. 173

5.4 Calibration graph for mercury(II), methylmercury and ethylmercury chloride spiked in Milli-Q de-ionised water and synthetic sea water. 174

5.5 Chromatogram of Methyl- Ethyl- and mercury(II) chloride (0.25 µg l^{-1}) in synthetic sea water. 176

5.6 Replicate injections of TORT-1 lobster hepatopancreas extract. 177

5.7 Chromatogram of (a) a North Sea discharge water and (b) Milli-Q spiked with mercury(II), methylmercury and ethylmercury chloride (5 µg l^{-1}). 179

5.8 Calibration graph for methylmercury and mercury(II) chloride in Milli-Q after preconcentration on dithiocarbamate resin. 181

ACKNOWLEDGEMENTS

I would like to offer my sincere thanks to Professor Paul Worsfold and Dr Steve Hill for their guidance and support over the last three years.

I am grateful to the Thornton Research Centre, Shell Research Limited, for an Extramural Research Grant for this work. I would like to thank everyone in Pervasive Technology, and particularly Margaret Allen, John Lambert, Brian McCourt, Denise and Val.

Thanks (from the Nomadic atomic boy) to the 106 boys, past and present; and in particular, Dave, Nick, Slim, Kev, Trev, Anthony, Ian and Tony (have trolley will travel!!).

Super love is extended to Niki and Jackie but not to Paul (just a manly hand shake) and hearty yomps to the other ex Bladderacks, Steve and Ash. (I soon will be able to put it in the box!).

A special thankyou is also extended to the Nicholson family, and in particular Hazel and Victor, who's advice in 1988 enabled me to change my life.

AUTHORS DECLARATION

At no time during the registration for the degree of Doctor of Philosophy has the author been registered for any other university award.

The work was financed with the aid of an extramural research grant from Thornton Research Centre, Shell Research Limited.

The work described in this thesis has entirely been carried out by the author. Relevant scientific seminars and conferences were regularly attended at which work was often presented; external institutions were visited for consultation purposes, and several papers were prepared for publication.

Signed......................................
Date..........16\1\95.......................

CHAPTER 1

Introduction

CHAPTER 1: INTRODUCTION

1.1 INDUCTIVELY COUPLED PLASMA MASS SPECROMETRY

1.1.1 HISTORICAL DEVELOPMENT

Inductively coupled plasma-mass spectrometry (ICP-MS) was first expressed as a concept in 1970. It was apparent before the commercial release of inductively coupled plasma atomic emission spectrometry (ICP-AES) that matrix elements such as Ca, Al and Fe made the choice of interference free spectral lines for trace element analysis very difficult. It was concluded by Gray[1] that atomic mass spectrometry was potentially the only viable successor to ICP-AES. However, the potential problems associated with ion extraction from the atmospheric environment of the ICP were considerable since ions could not be analysed until they were in high vacuum. Collaboration between Houk *et al.*in the USA, and Gray *et al* in the UK, and the work of Douglas and French. during the late 1970s resulted in solutions being found to the problems associated with the ion extraction interface, the extraction of ions from the gas at high temperatures (c. 8000 K) and the effects of RF electric fields on mass analysis and ion detection of the ICP[1-7].

The first success in ICP-MS was reported by Houk *et al*[3] in 1980 when analyte ions were extracted from an ICP. In 1982 Date and Gray [4,8] obtained the first mass spectra from an ICP source. By 1983 two commercial instruments were launched, the PlasmaQuad, based on the UK system manufactured by VG Isotopes Ltd (now Fisons Ltd), and the Canadian Elan system manufactured by Sciex (now Perkin Elmer Ltd). Since this time ICP-MS has experienced rapid growth, and there are now at least six manufacturers with over 1500 instruments worldwide.

1.1.2 INSTRUMENTATION AND OPERATION

The ion source in ICP-MS is generated by coupling the energy from a radio frequency generator to an appropriate gas flowing through a quartz glass torch. The standard Fassel torch is shown in Figure 1.1.

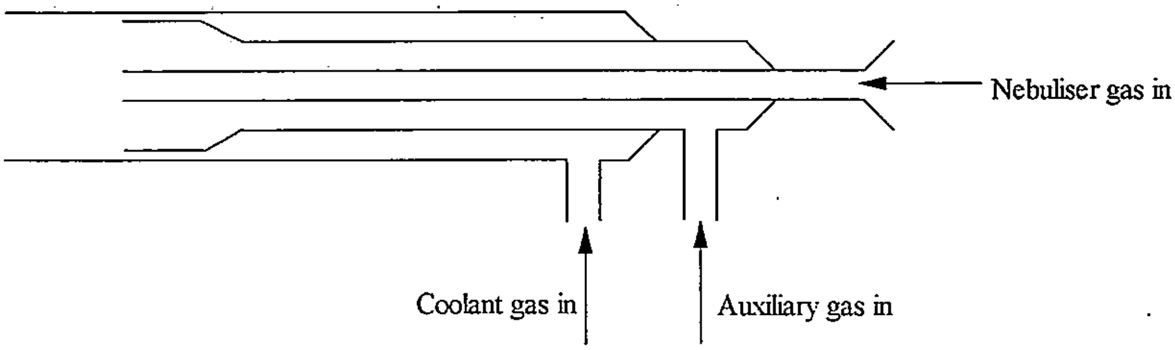

Figure 1.1 Schematic representation of a standard ICP Torch.

This consists of an outer tube within which are two concentric tubes terminating short of the torch mouth. Each annular region formed by the tubes is supplied with gas by a side tube entering tangentially so that it creates a vorticular flow. The innermost of the three gas flows (the nebulizer or injector gas) carries the aerosol from the sample introduction system at about 1.0 l min^{-1}. This produces a high velocity jet of gas which punches a hole in the base of the plasma. This central, or axial tunnel is cooler than the rest of the plasma but at 5000-6000 K is hot enough to atomise most samples and cause varying degrees of ionisation of the constituent elements. The outer or coolant gas flow (usually 10-15 l min^{-1}) protects the torch walls and acts as the main plasma support gas. The second or auxiliary gas flow (0-1.5 l min^{-1}) ensures that the hot plasma is kept clear of the tip of the nebuliser flow. The gas most commonly used is argon although other gases are occasionally used, sometimes as additions to the main supply, *e.g.* nitrogen.

The RF energy is transferred to the plasma via a load coil of 2-4 turns of fine copper tube cooled by water. This is located with its outer turn about 5 mm below the mouth of the torch. The energy is delivered at incident power levels of between 1 and 2 kW, usually at a frequency of 27.12 MHz. The plasma is formed when the gas is seeded with electrons from a Tesla coil. These electrons accelerate in the magnetic field and ionisation of some of the gas atoms occurs. Collisions cause further ionisation, and the plasma becomes rapidly self sustaining at a temperature of between 6000 and 10000 K, although the degree of ionisation of argon is only about 0.1 % at these ionisation temperatures. At the forward RF powers usually used (1-2 kW) the plasma is not in local thermal equilibrium.

The ICP requires any sample to be introduced into the nebuliser gas flow as a gas, vapour or aerosol of fine droplets or as solid particles[2]. Most systems are equipped with a pneumatic system as standard in which a high velocity gas stream produces a fine droplet dispersion of the analyte solution. A number of nebuliser designs exist including the concentric glass or Meinhard type, the cross flow and the De Galan nebulizer and the Babbington type of which the Ebdon nebulizer is a variety. The larger droplets produced by the nebuliser are removed by a spray chamber which allows only those below about 8 μm diameter to pass on to the plasma. The spray chamber is required because these larger droplets can cause signal fluctuations, plasma instability and can eventually extinguish the plasma. The small droplets below 8 μm carry only 1-2 % of the solution metered to the nebuliser by the peristaltic pump. The standard sample introduction system is shown in Figure 1.2.

Although inefficient, the pneumatic nebuliser is still the most common form of sample introduction for liquids because of its convenience, reasonable stability and ease of use. Other techniques are becoming more widely used, however. Liquid sample introduction can

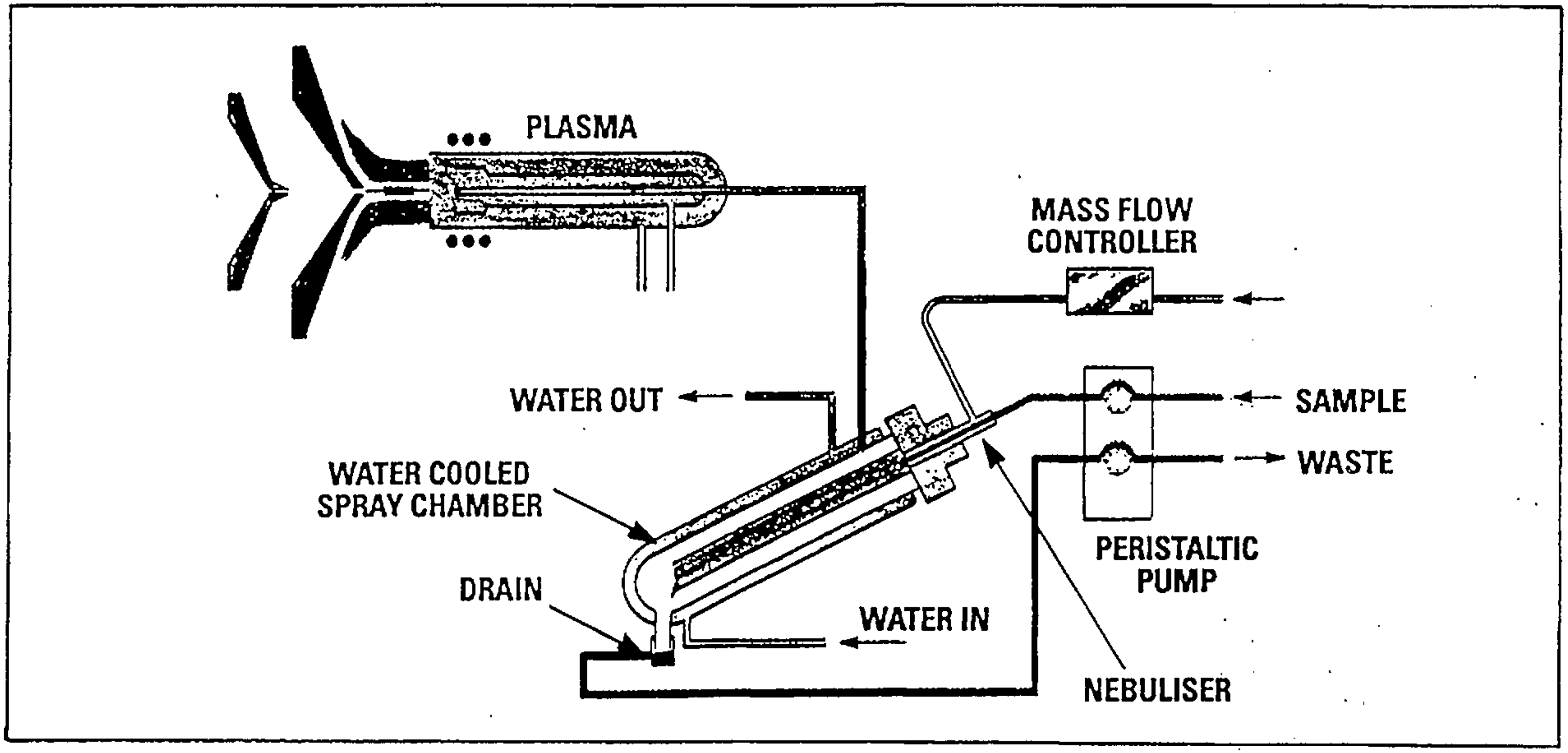
PLASMA
MASS FLOW CONTROLLER
WATER OUT
SAMPLE
WASTE
WATER COOLED SPRAY CHAMBER
PERISTALTIC PUMP
DRAIN
WATER IN
NEBULISER

Figure 1.2 Sample introduction system[23].

be achieved using ultrasonic nebulizers[9], thermospray vaporisers[10-12] and direct injection nebulizers (DIN)[13] which can improve nebulization and transport efficiencies. In addition thermospray vaporisers and DIN allow the direct injection of a variety of common LC solvents (*e.g.* up to 100% methanol, acetonitrile and methyl isobutyl ketone). Organic solvents can also be introduced following some form of desolvation[14-20] to remove a large proportion of the organic solvent (up to 80%) prior to its reaching the plasma. The introduction of gaseous samples to the ICP has also been performed using hydride generation[21] and direct injection[22].

Once the sample has entered the plasma it is desolvated and vaporised. The constituent analytes are then disassociated, excited and ionized. Extracting ions from the plasma into the vacuum system of the mass spectrometer is achieved using a two stage rotary pumped interface. A schematic diagram of a typical extraction interface is shown in Figure 1.3. The interface consists of two nickel cones enclosing an intermediate pressure region between the plasma and the mass spectrometer. The ions are extracted through a 1 mm orifice in the sampler cone from a region several aperture diameters across. A supersonic jet forms behind the aperture and the temperature drops. This results in relatively few collisions in the jet and the ion population is essentially 'frozen' at bulk plasma levels. The jet consists of a freely expanding region called the zone of silence. To avoid losses of ions due to scattering and collisions from shock waves (called barrel shock and Mach disc) surrounding the zone of silence, the skimmer tip is positioned inside the Mach disc. Thus the central core of the zone of silence (about 1 %) passes through the skimmer cone orifice (0.75 mm diameter) into the second vacuum stage. A rapid pressure drop occurs behind the skimmer and the ion optics take over as the transport process[2].

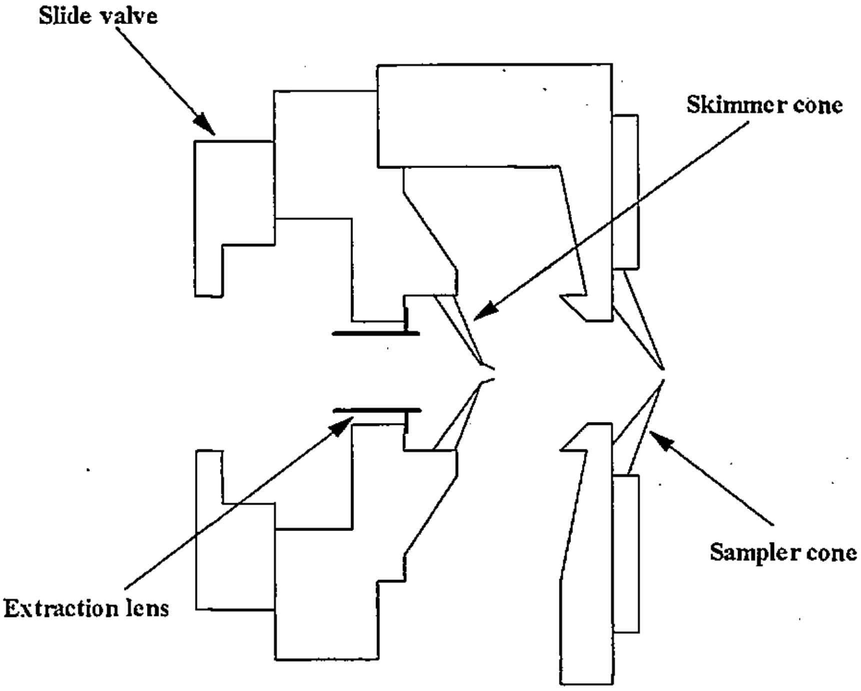

Figure 1.3 Typical extraction interface.

The ion optics consist of a series of electrostatic lenses, which serve to extract positive ions and focus the ion beam before passing into the quadrupole mass filter. The quadrupole then separates the ions with respect to their mass to charge ratio (m/z), the denominator of which is normally one. The ions are detected using an electron multiplier, the data from which is transferred to a computer via a multi-channel analyser. The complete instrumental system is drawn schematically in Figure 1.4.

1.1.3 ANALYTICAL APPLICATIONS

ICP-MS is a highly sensitive technique with detection limits for many elements in the range 0.01 - 0.1 $\mu g\ l^{-1}$. Limits of detection (based on the blank signal plus three standard deviations of the blank signal) for a range of elements found in environmental samples such as sea water are summarised in Table 1.1. These detection limits can be up to three orders of magnitude better than those reported for ICP-AES, and better than or equivalent to those reported for graphite furnace atomic absorption spectrometry (GFAAS).

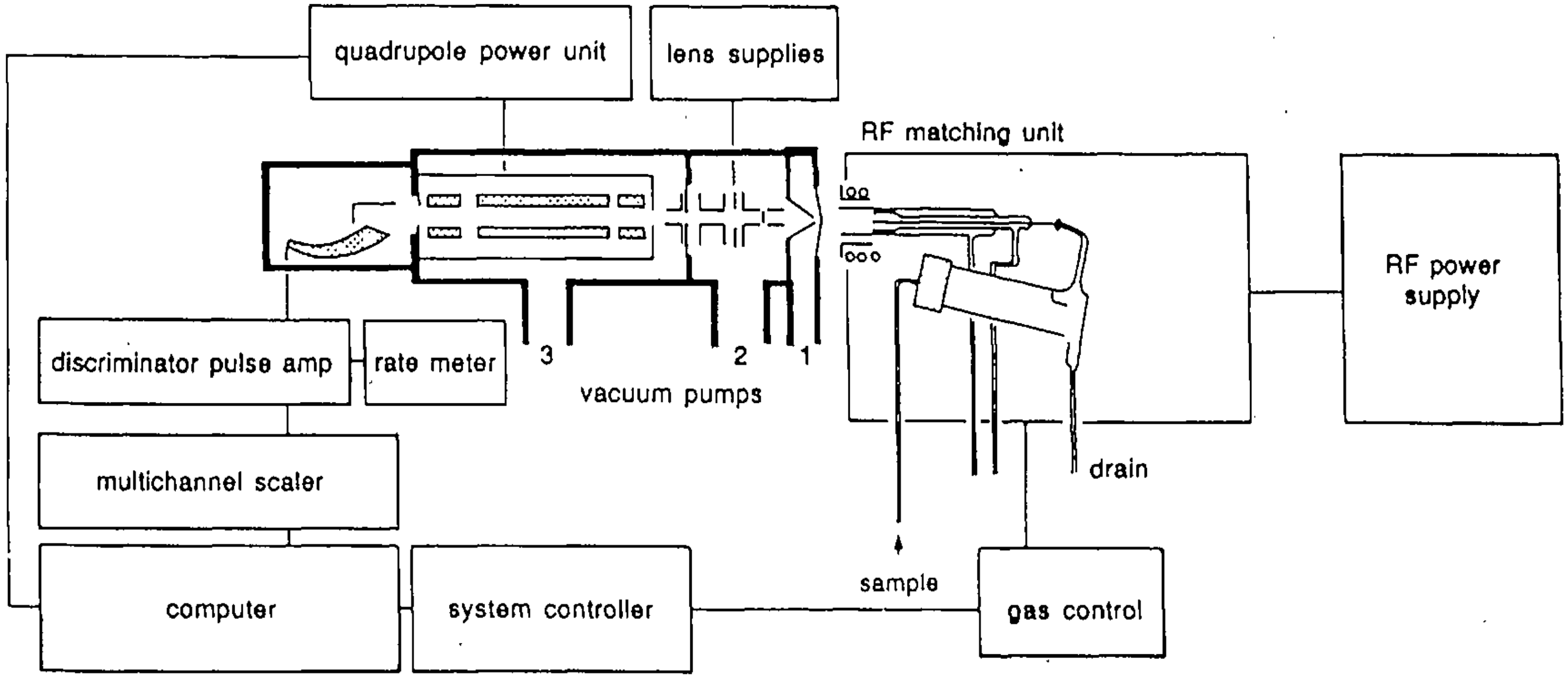
quadrupole power unit
lens supplies
RF matching unit
RF power supply
discriminator pulse amp
rate meter
3
2
1
vacuum pumps
multichannel scaler
drain
sample
computer
system controller
gas control

Figure 1.4 Schematic of the ICP-MS instrument[2].

Calibration ranges over 6 orders of magnitude and a multi-element capability allowing fully quantitative calibrations for elements across the mass range are also key advantages of ICP-MS over the single element technique of GFAAS. ICP-AES also offers a multi-element capability but this is limited by the monochromator or polychromator.

Sample introduction is also very flexible. Manufacturers such as Fisons and Perkin Elmer now offer flow injection (FI) and autosampling packages for liquid samples, laser ablation and electrothermal vaporisation (ETV) accessories for solid sample introduction and hydride generators for gaseous sample introduction. Due to excellent detection limits and the ability to accept samples as gas, liquid or solid, ICP-MS is also amenable to coupling with other techniques including liquid chromatography (LC) [26,27], gas chromatography (GC)[28,29] and FI[30,31]. ICP-AES and GFAAS can also be coupled with these procedures but limits of detection are generally poorer in the case of ICP-AES and sample loading is time consuming and difficult when using GFAAS.

Due to the advantages of ICP-MS over techniques such as ICP-AES and GFAAS, it has been rapidly accepted and applied to a wide range of fields. These include:

☐ Clinical applications, *e.g.* analysis of body fluids for vital trace elements or toxic metal levels[32,33].

☐ Environmental applications, *e.g.* analysis of environmentally sensitive elements such as Cd, As or Pb[34-36].

☐ Geological applications, *e.g.* analysis of potential ore materials or for isotope ratio measurements for dating rocks[37,38].

☐ Petrochemical applications, *e.g.* analysis of organic or inorganic species in fossil fuels[39,40].

Table 1.1 ICP-MS, ICP-AES and GFAAS detection limits (3 σ) for a range of elements found in environmental samples such as sea water.

Element	ICP-MS* ($ng\ ml^{-1}$)	ICP-AES+ ($ng\ ml^{-1}$)	GFAAS# ($ng\ ml^{-1}$)
Na	0.001 - 0.01	1.0	0.002
Ca	0.1 - 1.0	0.03	0.2
Mn	0.001 - 0.01	0.3	0.002
Fe	0.01 - 0.1	1.5	0.03
Ni	0.001 - 0.01	5.5	0.1
Co	<0.001	0.05	0.05
Cu	0.001 - 0.01	2	0.02
Zn	0.001 - 0.01	0.9	0.001
As	0.001 - 0.01	12.0	0.06
Mo	0.001 - 0.01	4	0.03
Cd	0.001 - 0.01	1.5	0.001
Hg	<0.001	8.5	1.0
Pb	<0.001	14.0	0.02
U	<0.001	18.0	---

* ICP-MS data from Fisons Elemental product literature (10 s integrations multi-element mode[23]

+ ICP-AES data from Varian literature[24]

# GFAAS data from Ebdon[25]

- ☐ Nuclear industry applications, *e.g.* analysis of radioactive materials[41,42].
- ☐ Water industry applications, where high sample throughput and multi-element capabilities make it well suited to the analysis of potable water.
- ☐ Certification and validation, *e.g.* Certification of Community Bureau of Reference (BCR) reference materials (now the Measurements and Testing Programme)[43,44].

There are some notable drawbacks to ICP-MS. It is expensive to purchase and maintain. An instrument typically costs up to £200K with running costs in the region of £5K per annum (about two to three times the cost of purchasing and running an ICP-AES or GFAAS). ICP-MS is also particularly prone to long term stability and sensitivity problems as a result of environmental temperature fluctuations and therefore needs to be kept in controlled laboratory environments (*e.g.* an air conditioned, clean room) in order to function at its best. However, the single largest shortcoming of the technique is the occurrence of spectroscopic and non-spectroscopic interferences. These are discussed below.

1.1.4 INTERFERENCES

Interferences which occur in ICP-MS are defined as either spectroscopic or non-spectroscopic. Spectroscopic interferences can be divided into four main areas:

(a) isobaric overlap,
(b) refractory oxide ions,
(c) doubly charged ions,
(d) polyatomic ion interferences.

Non-spectroscopic interferences (or matrix effects) are more complex, not specific to one particular element and not apparent in the spectrum. They can be divided into:

(a) suppression and enhancement effects.

(b) physical effects.

1.1.4.1 Spectroscopic interferences

(a) Isobaric Overlap

An isobaric overlap occurs when two elements have isotopes at the same nominal mass. The masses may differ by a small amount (0.005 m/z) which cannot be resolved by a conventional quadrupole mass analyser. In practice, however, most elements have at least one (*e.g.* Co), two (*e.g.* Sm) or even three (*e.g.* Sn) isotopes free from isobaric overlap. The exception to this is In which has an overlap at m/z 115 and 113 with ^{115}Sn and ^{113}Cd.

(b) Refractory Species

Interferences that occur either as a result of incomplete dissociation of the sample matrix, or from recombination in the plasma tail, are termed refractory species. For example, the level of oxide formation rarely exceeds 1.5 % for most elements. The level of MO^+ ions generated has been shown to be influenced by plasma operating conditions such as RF forward power and nebuliser gas flow rate[45,46].

(c) Doubly Charged Ion Interferences

Doubly charged ion interference formation in the plasma is controlled by the second ionisation energy of the element and the condition of the plasma[47]. Doubly charged ions are common for elements with a second ionisation energy lower than the first ionisation energy of argon. The alkaline earth elements, rare earth elements and elements such as U and Th are most likely to form M^{2+} species. The effect of a small proportion of doubly charged ions is two-fold. It results in a loss of sensitivity for the singly charged species due to a small loss of signal and generates a number of isotopic overlaps at one half of the mass of the parent element.

(d) Polyatomic Ion Interferences

The most serious interference problems are caused by the formation of polyatomic ions. The ions result from the short lived combination of two or more atomic species *e.g.* ArO^+ These are particularly troublesome below m/z 80[48-51] and interfere with elements in this mass range. Some common examples of polyatomic ion interferences are summarised in Table 1.2. These polyatomic ions can be introduced via precursor atoms in the argon support gas such as Ar, H or O, from atmospheric gases (*e.g.* N or O), from solvents or acids used during sample preparation (*e.g.* N, S, or Cl) or from the sample matrix.

Table 1.2 Common polyatomic ion interferences.

Mass	Element	Abundance (%)	Interfering ion
31	P	100	NOH^+
44	Ca	0.14	CO_2^+
48	Ti	73.7	POH
51	V	99.7	ClO^+
52	Cr	83.8	ArC^+, ArO^+
53	Cr	9.5	ClO^+
54	Fe, Cr	2.36, 5.8	ArN^+
55	Mn	100	$ArNH^+$
56	Fe	91.7	ArO^+
57	Fe	2.14	$ArOH^+$
63	Cu	69.0	$ArNa^+$
64	Zn	48.9	SO_2^+
66	Zn	27.8	SO_2^+
67	Zn	4.1	SO_2H^+
75	As	100	$ArCl^+$
80	Se	50.0	Ar_2^+

The most likely source of polyatomic ions was thought to be condensation reactions in the expansion region[52]. However Douglas and French[53] have calculated that the degree of ionisation in the expansion region is frozen and that little ion-molecule chemistry occurs. Other theories suggest that polyatomic ions are formed in collisional reactions in the boundary layer around the outside surface of the sampler[54,55] or through survival in the plasma, particularly with respect to refractory metal oxide ions[56,57].

Approaches to overcoming polyatomic ion interferences

The systematic error caused by polyatomic ion interferences needs to be overcome in order to obtain acceptable analytical results. Some reduction of these species, or the effects of these species, can be achieved by carefully setting the instrument parameters[50,58]. As with refractory oxides, those of most importance have been shown to be RF forward power and nebuliser gas flow rate.

Approaches to overcoming spectroscopic interferences include alternative sample preparation methods, *e.g.* the judicious choice of acids for digestion. Hence if V or As is to be determined then hydrochloric acid should be avoided in order to prevent the occurrence of Cl based polyatomic interferences. Commonly occurring interferences caused by nitric, sulphuric and hydrochloric acids, and water have been well documented[48,50]. An alternative approach to the dissolution of geological samples has been to prepare samples by finely grinding them and forming a suspension or slurry[59,60]. Precipitation and solvent extraction are useful methods of separating the analyte from the matrix component[61,62]. However, such procedures have only been performed in batch mode, are time consuming and impurities in the organic solvents or complexing agents can increase blank values[57]. On-line methods using chelation or ion exchange resins in FI manifolds[31,63] or chromatographic separations using LC[64,65] can be used both to preconcentrate the analytes of interest and remove the matrix, or to separate the analytes from the interference.

Desolvation techniques using Peltier coolers[20], membrane interfaces[18] or heater/condensers[17] reduce water vapour and hence oxide and hydroxide interferences. Desolvation can also increase the analyte signal by an order of magnitude due to the reduction in oxide, hydroxide and doubly charged ions[17,56]. Introducing the sample in a dry form using thermal vaporisation methods such as electrothermal vaporisation (ETV)[66], direct sample insertion (DSI)[67] or laser ablation[68] can result in a reduction of hydroxide and oxide interferences. However, thermal vaporisation techniques can contribute to, rather than reduce interferences, if a chemical modifier is used, and are difficult to optimise. Mathematical correction methods such as elemental equations (*e.g.* calculating the isotopic abundances of the interference precursors) and multivariate techniques have been used to correct for spectroscopic interferences[69,70]. For example, multiple linear regression (MLR), principle components regression (PCR) and partial least squares (PLS) have been successfully used to compensate for MoO^+, ZrO^+ and RuO^+ in the determination of low levels of Cd^+, In^+ and Sn^+ [70]. The separation of analytes and polyatomic ions with similar m/z ratios is possible using a high resolution double focusing magnetic sector mass spectrometer[71]. However, the scan speed is slower with high resolution (HR)-ICP-MS instruments and magnetic sector mass spectrometers are more cumbersome to use than quadrupole instruments. Although commercially available, (HR)-ICP-MS is also expensive (at least £500K) in comparison with quadrupole ICP-MS (£200K).

Mixed gas plasmas, using molecular or inert gases bled into, or replacing one of the three gas flows of the ICP-MS to facilitate the reduction of polyatomic ion interferences has recently been investigated by several groups. This is further discussed in Section 1.1.5.

1.1.4.2 Non-spectroscopic interferences

Non-spectroscopic interferences are characterised by a reduction or enhancement in analyte signal due to factors exerting an influence on sample transport, ionisation in the plasma, ion extraction and ion throughput in the resultant ion beam[57].

Sample introduction and transport is affected by the nebuliser design and nebuliser gas flow, and the viscosity, surface tension, density, evaporation rate and vapour pressure of the sample. It is therefore critical to matrix match samples and standards with respect to the solvent. The sample matrix can also affect the atomisation, excitation and ionisation characteristics by altering the plasma temperature[72]. However, an excess of heavy, easily ionisable elements in the matrix creates the most serious non-spectroscopic interferences[73-77]. A number of theories have been put forward to explain the role of easily ionisable elements in signal suppression or enhancement[74-76]. However, current explanations suggest that space charge effects in the ion beam are a major contributor[78]. Suppression of the analyte signal and long term stability problems can also result from the physical deposition of material on the sampler and skimmer cones and the subsequent restriction of the orifices[79].

Approaches to overcoming non-spectroscopic interferences

In order to overcome the effect of matrix suppression, removal of the matrix (or the effect of the matrix) is necessary. This can be achieved in a similar fashion to the removal of spectroscopic interferences, *e.g.* LC[64,65] or on-line preconcentration and matrix removal using FI can be used[31,63]. Similarly, internal standardisation[73], isotope dilution[80] or careful setting of the instrument parameters are all effective means of compensating for matrix effects. An example of the latter approach was investigated by Evans and Caruso[81] who Simplex-optimised the ion lens settings to yield zero analyte suppression due to

10000 μg g^{-1} of U on ^{115}In. Extraction lens voltage was found to be the most critical factor. Sample dilution using FI, where a discrete sample is injected into an aqueous carrier stream, has found considerable application in ICP-MS[82-87]. However, mixed gas plasmas, which have been successfully used for the suppression of spectroscopic interferences, have not been studied to the same degree for the suppression of matrix effects[88,89].

1.1.5 THE USE OF NITROGEN-ARGON PLASMAS FOR THE REMOVAL OF SPECTROSCOPIC AND NON-SPECTROSCOPIC INTERFERENCES

Alternative gases including nitrogen[88-98], helium[99], xenon[100], hydrogen[101,102], methane[103] and ethene[104] have been investigated by a number of groups. Nitrogen has been added to the nebuliser gas[90-95], auxillary gas[94,95] and coolant gas[94,95,97] flows. Evans and Ebdon[90,91] were the first to publish on the use of mixed gas plasmas. By introducing nitrogen to the nebuliser gas at a rate of 0.03 l min^{-1}, a reduction in the signal due to $ArCl^+$ of three orders of magnitude was achieved. Other interferences due to $ArAr^+$ and $ClCl^+$ were also significantly reduced. ^{75}As and ^{78}Se recovery was thus enhanced by 13.8 and 3.08 times respectively. Univariate searches of the nebuliser flow rate with and without nitrogen were also performed. Nitrogen addition was found to shift the optimum nebuliser flow rate to a lower value and reduce both the signal intensity for indium and the polyatomic ion interferences. In a follow up study[93] the method was successfully applied to the determination of As in urine.

Lam and co-workers investigated the addition of nitrogen to the coolant gas flow[97]. It was found that the addition of 5 % nitrogen to the outer gas resulted in the need for higher nebuliser gas flow rates to recover the analyte signal in the shrunken plasma. Polyatomic ions such as ArCl+, ClO+, ArO+ and MO+ were observed to decrease in conjunction with an increase in analyte ion signal. The same authors also examined the skimmer-sampler cone separation on the performance of all argon and 5 % nitrogen-argon plasmas. It was proposed that the addition of nitrogen changed the dimensions of the barrel shock and the position of the Mach disc in the interface region.

Addition of nitrogen to the coolant gas flow was investigated by Beauchemin and co-workers[88,89,96]. In this work the nebuliser flow rate was kept constant, with the percentage of nitrogen in the plasma gas (0-10 %) and the RF forward power (1.0-1.4 kW) as the only variables. Beauchemin and Craig[88] found that adding nitrogen to the coolant flow increased the sampling depth which in turn resulted in decreased sensitivity for Fe and Se. It was concluded that nitrogen changed the fundamental characteristics of the plasma, which could make argon-nitrogen plasmas more suitable as an ion source for MS than all argon plasmas. The same authors[96] examined the effect of concomitant elements (non-spectroscopic interferences) in ICP-MS by adding nitrogen to the coolant gas. The effect of 0.01 M potassium was eliminated with 10 % nitrogen for all elements examined except Al and Pb. However, the elimination of the effect of 0.1 M potassium could only be carried out on one analyte at a time by adjusting the nitrogen % on the given analyte. This work was later extended to include a study of matrix effects resulting from 0.1 and 0.01 M Na[89]. The effect of 0.01 M Na was eliminated across the whole mass range using 10 % N addition with only a slight degradation of sensitivity.

Using univariate searches of nitrogen added to either the nebuliser, auxiliary or coolant gas flows, Wang *et al.*[94] defined optimal parameters for the removal of $ArCl^+$ and ClO^+. These were 1 % addition to the outer gas and 3 % addition to the nebuliser gas. A certified reference material (SRM-2670 freeze-dried urine) was successfully analysed. Hill *et al.*[95] employed a more rigorous multivariate optimisation using a simplex procedure to facilitate the maximum possible removal of $ArCl^+$. When 4.5 % nitrogen was added to the nebuliser, the $ArCl^+$ interference was shown to be successfully removed in the presence of 1 % chloride. A comprehensive analysis of a range of certified reference materials (CRMs) was carried out by Laborda *et al.* [98], using both all argon and argon-nitrogen plasmas. A significant reduction in polyatomic ion interferences was attained by adding 8 % nitrogen to the nebuliser gas. Detection limits were 2-3 times worse with the mixed gas plasma but improvements in the measurement of ^{51}V, ^{53}Cr, ^{67}Zn, ^{68}Zn ^{75}As and ^{77}Se in five reference materials was achieved.

1.2 FI AND LC COUPLED WITH ATOMIC SPECTROMETRY

This section discusses FI and LC methods coupled with atomic spectrometric detectors such as AAS, ICP-AES and ICP-MS. Section 1.2.1 discusses on-line analyte preconcentration and matrix removal using solid phase reactors incorporated into FI manifolds for the determination of trace metals. Section 1.2.2 deals with the determination and speciation of trace metals using LC coupled with ICP-AES and ICP-MS with an emphasis on application to real samples.

1.2.1 FLOW INJECTION ANALYSIS

The term flow injection analysis (FIA) was first described by Ruzicka and Hansen[105] in 1975. It is characterised by its simplicity, inexpensive nature and rapidity of analysis. The versatility of FI allows the method to be readily adapted to meet a range of requirements without introducing complex technical changes.

1.2.1.1 Basic principles

FI is based on the injection of a liquid sample into a moving continuous carrier stream of a suitable reagent[106]. During its transport to the detector, the injected sample forms a zone which physically disperses and reacts with the components of the carrier stream. The detection system yields a transient signal which is recorded using a chart recorder, integrator or computer. The characteristics of the resulting peak reflect the concentration of the injected analyte and provide kinetic information of the chemical reactions taking place in the flowing stream. The simplicity of FI, together with saving of reagent and sample consumption, and time, has resulted in the adaption of many traditional, manual spectrophotometric procedures to the FI mode[107]. Other physical processes including solvent extraction, dialysis and gas diffusion have also been incorporated into FI manifolds. More recently atomic spectroscopic techniques (including ICP-MS) have been enhanced by the use of FI for on-line preconcentration, matrix removal and chemical conversion by means of solid phase reactors[31,108,109]. A single channel FI manifold is shown in Figure 1.5.

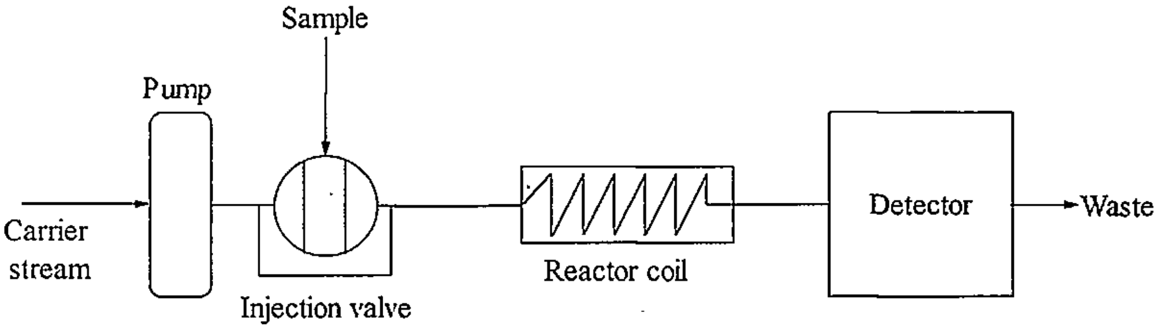

Figure 1.5 Schematic diagram of a simple single line FI manifold.

1.2.1.2 On-line sample treatment

Specific detectors such as ion-selective electrodes and atomic spectrometers, or separations using chromatographic techniques have historically been employed to determine analytes in the presence of specified interferents. However, such approaches are generally time consuming and limited in their applicability. Alternatively, selectivity enhancement using separation, matrix modification or conversion techniques can be accomplished rapidly and simply using FI procedures. This section outlines the most commonly used FI matrix modification techniques including on-line solid phase reactors. A more detailed description of these techniques can be found in monographs on FIA such as Ruzicka and Hansen[107], Karlberg and Pacey[110] and Valcarcel and Luque de Castro[111].

(a) Liquid-liquid extraction

The first liquid-liquid extraction paper based on the FI principle was published in 1978[112]. The basic principle involves the injection of a known volume of sample into an aqueous carrier stream. This stream is segmented with an immiscible solvent. The extraction procedure takes place in a coil of narrow bore PTFE tubing (typically 0.5 mm i.d.).The organic phase, containing the extracted analyte, is then separated from the aqueous phase, *e.g.* via a PTFE membrane and transported to the detector.

Preconcentration can be achieved by integrating two FI manifolds operating at different flow rates. The first manifold extracts the analyte from the matrix. A volume of the organic phase is then injected into the second manifold, which carries the analyte to the detector. This approach was used by Nord and Karlberg[113] to extract copper from an aqueous sample into isobutyl methyl ketone (IBMK) using ammonium pyrrolidinedithiocarbamate(APDC) as a complexation reagent. A portion of the separated IMBK phase was then injected into a slower flowing aqueous stream and detected using flame atomic absorption spectrometry (FAAS).

(b) Gas diffusion

A number of analytes such as ammonia, carbon dioxide and chlorine dioxide can be determined in the gas phase at room temperature and atmospheric pressure. The major advantage of the gas diffusion process is that it removes the analyte of interest from the sample matrix into a new matrix (the acceptor stream) which contains no chemical or physical interferents.

Gas diffusion membranes incorporated into FI manifolds have been used successfully in clinical determinations. Svensson and Anfalt[114] developed a method for the determination of ammonia in biological fluids, in which the sample was injected into a sodium hydroxide carrier stream. Liberated ammonia diffused across a PTFE membrane and was detected photometrically after mixing with an indicator in the acid form. Carbon dioxide in blood plasma has also been determined using a gas diffusion process. In this case the sample was injected into a sulphuric acid stream which yielded CO_2. The liberated CO_2 diffused across the gas diffusion membrane and was detected using a UV/vis spectrophotometer[115].

(c) Dialysis

Dialysis is a selectivity enhancement technique for the separation of the analyte of interest from the sample matrix. The same design considerations for gas diffusion hold true for dialysis. However, the membranes for dialysis are hydrophilic in nature, as opposed to hydrophobic gas diffusion membranes. As the efficiency of dialysis in FI systems is only 1-4 %[111], the dialyser essentially acts as a separator and dilutor. Hansen and Ruzicka[116] reported the first applications of FI dialysis for the determination of inorganic phosphate and chloride in blood serum. Dialysis has also been used for the determination of inorganic sulphate in urine, and the separation of proteins and other species prior to the determination of urea in blood serum[117,118].

(d) Solid-liquid extraction

Preconcentration, matrix removal and chemical conversion can be accomplished with the aid of reactors packed with a suitable solid phase, *e.g.* ion or chelation exchange resins[30,31,108,109], reducing agents[119], activated carbon filters[120,121] or immobilized enzymes[122].

The common characteristics of packed reactors are their small size (2.0 x 0.2 cm i.d. or less) and the coarse nature of the packing material (50 - 200 μm) which is necessary to prevent high back pressure. Packed reactors used for preconcentration also share the "all or nothing" principle[106], *i.e.* the distribution ratio of selected species is either >>100 or <<0.01. This results in either complete retention or complete release of the analyte from the solid surface.

The most widely used solid supports are surface modified silica, surface modified polymeric materials and controlled pore glass. Many of these materials are used as solid packings in pre-columns and guard columns for LC. The preconcentration of the analytes of interest and the removal of the matrix is accomplished by passing a known volume of sample through the packed reactor. The analytes are retained on the column whilst the matrix passes to waste. The analytes of interest can subsequently be eluted using a mineral acid, organic solvent or complexing agent. Solid phase reagents incorporated into FI manifolds with atomic spectrometric detection are discussed in more detail in Section 1.2.2.

1.2.2 FI COUPLED WITH ATOMIC SPECTROMETRY

FI techniques coupled with FAAS, ICP-AES and ICP-MS have generally involved some form of preconcentration of the analytes of interest and physical separation of the matrix using solid phase reactors packed with ion exchange or chelation exchange resins. The following section discusses the application of chelation exchange resins in FI manifolds coupled with atomic spectrometric techniques.

1.2.2.1 Preconcentration using chelation exchange resins

Multidentate ligands, *e.g.* ethylenediaminetetra acetic acid (EDTA) which is a hexadentate ligand, donate more than one electron pair to the same central metal ion to form a cyclic or ring structure which is termed a chelate, and the process is called chelation. Chelating compounds usually contain hydrogen, which can be replaced with a metal ion under appropriate conditions. Typical groups where this can occur are -OH, -COOH, $-NH_2$, =NOH, -SH and $-PO_3H_2$. Chelation exchange resins such as iminodiacetic acid (IDA) and quinolin-8-ol (8-hydroxyquinoline) are generally covalently bonded to a substrate, such as silica or polystyrene-divinylbenzene. The structures are shown in Figure 1.6. Chelex-100 is the most common chelating resin. It contains chemically bonded iminodiacetic acid chelating groups. These groups readily chelate transition metal ions and other cations (*e.g.* Pb). In general, the higher the cationic charge of the metal ion, the more strongly the metal ion is bound to the resin. Anionic species containing metals ions are not retained. The functional groups of chelating resins are weak acids (*e.g.* COOH) and weak bases (*e.g.* NH_2). Therefore, hydronium ions (H_30^+) compete strongly with metal ions for chelating sites. As a result, mineral acids such as HCl or HNO_3 are effective eluents. The IDA group is also present in a number of other chelating resins including Dowex A1, Muromac-A1 and Metpac-CC1.

1.2.2.2 Simultaneous preconcentration and matrix removal using chelation exchange resins

There have been many reports in the literature regarding the use of chelation or ion exchange columns coupled with FAAS[108,123-128], ICP-AES[109,129-131] and ICP-MS[31,63,132-138].

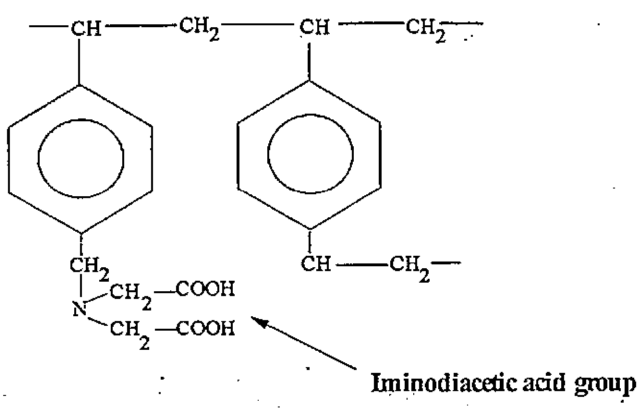

(a) Iminodiacetic acid (IDA)

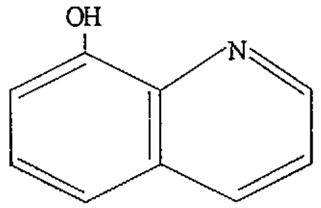

(b) 8-hydroxyquinoline (8-HQ)

Figure 1.6 Structures of two typical chelating compounds.

The first on-line preconcentration with atomic spectrometric detection was reported by Olsen *et al.*[123] who used Chelex-100 to preconcentrate Pb, Cd and Zn at μg l^{-1} levels from sea water. Several FI manifolds were examined, including a back-flushing system, and a fully automated system. Detection limits of 1 μg l^{-1} and a sampling rate of 30-60 samples per hour were achieved. Hartenstein *et al.*[109] also used Chelex-100 in an FI system coupled with ICP-AES. Detection limits were over 20 times better than for continuously aspirated systems. However, the efficiency of the column was only 55 % for aqueous standards. It was concluded that modifications such as more efficient resins, different buffers, or different flow rates were required.

The determination of eight trace metals in a coastal sea water certified reference material (CASS-2) was achieved by McLaren *et al.*[30] using standard additions or isotope dilution. In both cases off-line separation of the metals from the sea water by 8-hydroxyquinoline was carried out prior to ICP-MS detection. Good agreement with the certified values was achieved and detection limits were low enough to determine trace metals in open ocean samples. On-line methods for preconcentrating trace metals from sea water using 8-hydroxyquinoline have been developed by Fang and Welz[125] and Beauchemin and Berman[63]. The former method (coupled with FAAS) used conical ion-exchange columns, small bore conduits and three dimensionally disorientated reactors to limit dispersion and thus improve precision (RSD 1.2-1.8 %).The FI manifold was complicated but had a high concentration efficiency with an enrichment factor (EF) of 25-31 (concentration efficiency = 50 - 62 EF min^{-1}) although no detection limits were quoted. The latter method was coupled with ICP-MS. Detection limits of less than 1.0 μg l^{-1} for Mn, Co and Cu were achieved. The manifold was very straightforward, but the concentration efficiency was low (0.67 EF min^{-1}). More recently 8-hydroxyquinoline resin has been used off-line to preconcentrate Ti, Ga and In from sea water[136] and rare earth elements from natural waters[134] at sub ng l^{-1} levels.

Ebdon *et al.*[31] recently developed an on-line method using an IDA chelating resin, similar to Chelex-100, manufactured by Sigma. The sodium form of the resin was used to separate V, Cu, Zn, Cd and Pb from digested biological matrices prior to ICP-MS detection. The removal of the matrix (and particularly the chloride anion, which can cause severe polyatomic ion interferences) resulted in the interference free determination of the metals of interest. The method was validated by analysing a series of reference materials. Attempts to use the chelating column for Cr determinations proved unsuccessful because recovery was only 60 % and the precision was poor (RSD 15 %). It was also reported that Cr standards that produced a signal one day failed to do so the next day, indicating that Cr(III) complexes were slowly being formed.

The same group in a later publication[133] examined a commercially available chelating column (MetPac CC-1) from Dionex. This column contains an IDA resin that is similar to Chelex-100 but has a greater degree of cross-linking and is therefore less susceptible to swelling with changes in its ionic form, a significant drawback with Chelex-100. The FI system was complex and expensive, using Dionex inert switching valves and a Dionex auto ion controller. No limits of detection were quoted, although an open ocean certified reference material (NASS-3) was analysed and reasonable agreement with the certified values was achieved for Cu, Mo, U and Zn. Details of various applications of the use of on-line chelating resins in conjunction with atomic spectrometry are presented in Table 1.3.

Other solid phase reactors are also worthy of mention. For example, activated alumina has been used by several workers, *e.g.* Cox *et al.*[139] developed a rapid Cr speciation technique. A micro-column of activated alumina was used in a FI manifold to selectively preconcentrate Cr(III) from a mixture of Cr(III) and Cr(VI) in synthetic aqueous solutions and in two natural water certified reference materials, prior to ICP-AES detection. A similar procedure was developed by Ebdon *et al.*[140] to determine oxy-anions such as Cr, Se and V in biological matrices by ICP-MS without interference from polyatomic ions. Trojanowicz and Pyrzynska[141] also used alumina but in this case it was modified with 1-nitroso-2-naphthol-3,6-disulphonate for the on-line preconcentration of Co(II) prior to detection with FAAS.

Biochelating silicas utilising hydroxamate complexation have also been investigated[142]. This application showed promise for the preconcentration of Fe(III) and Cu(II) from large

Table 1.3 Examples of trace metal determinations using chelating resins.

Exchange medium	Detection	Analyte	Matrix	Ref
Chelex-100	on-line FI-AAS	Cd, Pb, Cu and Zn	Sea water	123
Muromac A-1	on-line FI-AAS	Cd, Zn, Cu, Mn, Pb Fe and Cr	Biological CRMs	108
8-Hydroxyquinoline	on-line FI-AAS	Cu, Cd and Pb	Sea water	125
8-Hydroxyquinoline	on-line FI-AAS	Al	River and sea water	124
Polyhydroxamic acid	on-line FI-AAS	Cr	Sea water	126
Chelex-100	on-line FI-ICP-AES	Ba, Be, Cd, Co, Cu,Mn Ni and Pb	Waters	109
Muromac A-1	on-line FI-ICP-AES	Cr,Ti, V, Fe and Al	Waters	130
Muromac A-1	on-line FI-ICP-AES	Cd	Waters and CRMs	131
8-Hydroxyquinoline	on-line FI-ICP-AES	Al, Cu, Cd, Fe and Mn	Human serum	129
8-Hydroxyquinoline		Mn, Co, Ni, Cu, Zn Cd and Pb	Sea water CRM	30
8-Hydroxyquinoline	on-line FI-ICP-MS	Mn, Co, Ni, Cu, Pb and U	Sea water CRMs	63
DTC chelating agent	on-line FI-ICP-MS	V, Cr, Ni, Co, Cu, Mo, Pt, Hg and Bi	Urine and sea water	135
Muromac A-1	on-line FI-ICP-MS	Fe, Zn, Cu, Ni and Cr	Waters	137
MetPac CC-1	on-line LC-ICP-MS	Transition metals and Pb	Sea water	138
IDA resin (Sigma)	on-line FI-ICP-MS	V, Mn, Cu, Zn, Cd and Pb	Biological CRMs	31
MetPac CC-1	on-line FI-ICP-MS	Cu, Mo, Ni, U and Zn	Concentrated brines	133
8-Hydroxyquinoline	off-line FI-ICP-MS	Ti, Ga and In	Sea water	136
8-Hydroxyquinoline	off-line FI-ICP-MS	Rare earth elements	Natural waters	134

volumes (1000 ml) of trace metal solution. Octadecyl groups (C_{18}) have been used to determine Cd, Cu and Pb[143]. The eluent used in this case was a dithiophosphate complex and detection limits in the μg l^{-1} range were obtained using FAAS. A particularly interesting method using immobilised algae covalently bonded onto controlled pore glass has been reported by Elmahadi and Greenway[144]. It was shown that each alga had unique binding properties. This was thought to be due to the presence of different binding sites on the cell walls. Using this procedure a FI system for the speciation of Cr(III) and Cr(VI) with FAAS detection was developed.

1.2.3 LIQUID CHROMATOGRAPHY

1.2.3.1 Basic principles

Chromatography is a technique for the separation of components in a mixture and their subsequent identification and quantification, based on their chemical or physical properties. In liquid chromatography (LC) the components are partitioned between a mobile liquid phase (commonly referred to as the eluent) and a microparticulate stationary phase with a large surface area. The sample, dissolved in a solvent, is injected into a flowing stream of eluent and transported to the column where the components of the mixture are separated by interaction with the stationary phase. As the components elute from the column transient signals for each component are detected at a flow through detector. A plot of detector response with time is called a chromatogram. A schematic diagram of the basic LC components is shown in Figure 1.7.

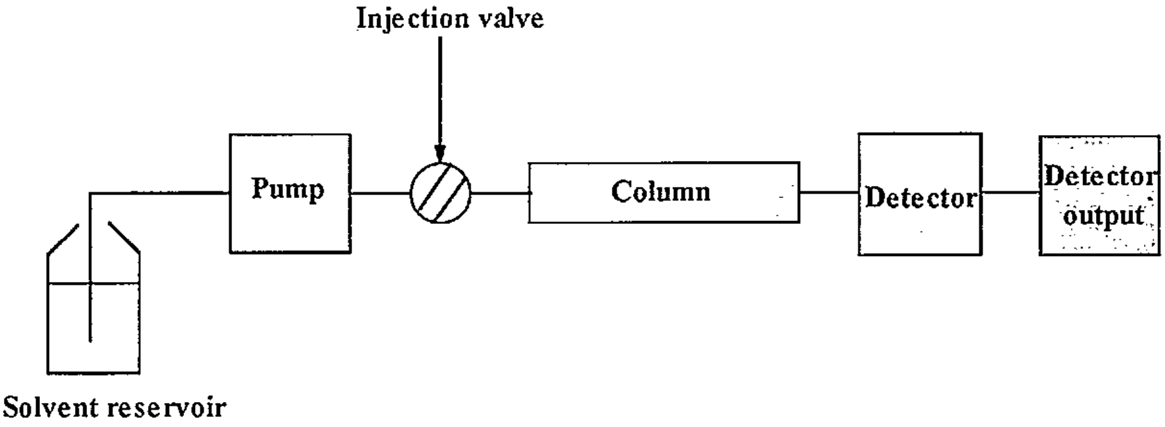

Figure 1.7 Schematic diagram of the basic LC system.

LC is a very versatile technique for the separation, speciation and determination of metal ions. Recent reviews by Robards[145] and Chau[146] on the determination of trace metals by LC highlight the advances in metal determination and speciation over the past decade. Several different modes of chromatography are available. These include adsorption, reversed or normal phase, ion exchange and size exclusion. A brief description of each is given in Table 1.4.

Table 1.4 Classification of modes of LC.

LC Mode	Description	Separation
Adsorption	Solid stationary phase *e.g.* silica or alumina. Non-polar organic mobile phase *e.g.* hexane	Adsorption
Liquid-liquid and bonded phase	Liquid physically adsorbed or chemically bonded to a solid support. Can either be normal phase or reversed phase.	Partition, adsorption
Ion exchange	Ion-exchange resin stationary phase; aqueous buffer mobile phase	Ion-exchange
Size exclusion	Porous stationary phase; aqueous or organic mobile phase	Partition, sieving

A wide range of techniques including ultraviolet/visible absorbance (UV/VIS), amperometry, fluorimetry and conductimetry are suitable for the detection of metal ions. However, detection based on the use of atomic spectrometry or mass spectrometry (including ICP-AES and ICP-MS) are of increasing importance, especially for high specificity and speciation studies.

1.2.3.2 Chromatographic parameters

In order to determine and compare the performance of different chromatographic columns, there are several fundamental parameters and factors that can be derived from the chromatogram, some of which are outlined below. More detailed descriptions of these parameters are given in chromatography texts such as those by Hamilton[147] and Meyer[148].

Phase preference can be expressed by the **distribution coefficient**, denoted by K. This gives the ratio of the concentration of solute in the stationary and mobile phase:-

$$K = \frac{Cs}{C_m}$$

Where Cs and Cm are the molar concentrations of a solute in the stationary phase and mobile phase respectively. The various components of the mixture in a chromatographic separation must have different distribution coefficients if the mixture is to be separated. The time taken for a component to elute to its maximum concentration is known as the **retention time**, denoted by t_R. Two compounds can be separated if they have different retention times. Figure 1.8, where t_0 is the dead time or retention time of an unretained solute, and t'_R is the net retention time, shows that:-

$$t_R = t_0 + t'_R$$

t_0 is identical for all eluted substances and represents the mobile phase residence time. t^1_R is the stationary phase residence time and is different for each separated compound.

A chromatographic column may be considered as a series of narrow layers known as **theoretical plates**. The ability of a column to minimise band broadening is termed the column efficiency and can be expressed as:-

$$N = \frac{L}{H}$$

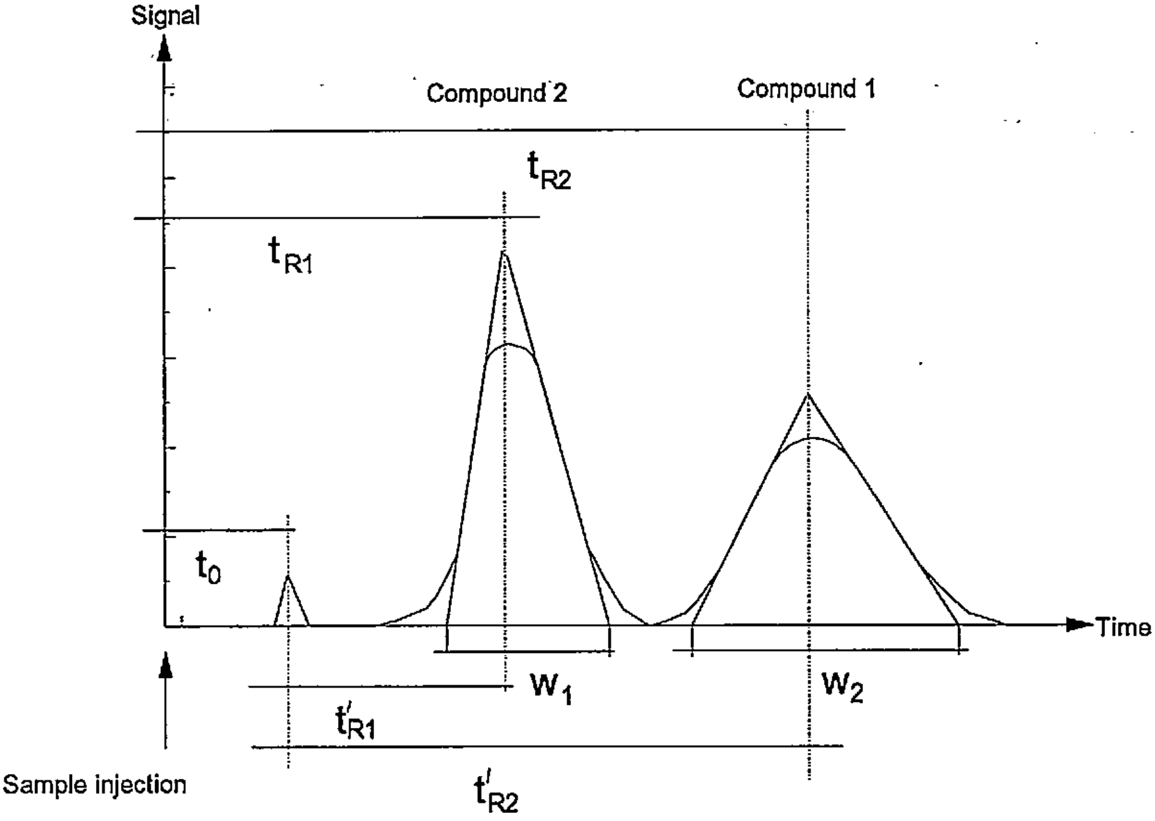
Signal
Compound 2
Compound 1
t_{R2}
t_{R1}
t_0
Time
W_1
W_2
t'_{R1}
t'_{R2}
Sample injection

Figure 1.8 Illustration of parameters for retention time and resolution.

where the number of theoretical plates is expressed as N, the length of the column packing is L and the height equivalent of the theoretical plate is H.

Resolution, R_s is a measure of the ability of a column to resolve two solutes. It is experimentally defined as the difference in retention times of two peaks, divided by the average peak width.:-

$$R_s = 2\,\frac{(t_R^{1} - t_R^{2})}{W_1 + W_2}$$

Where t_R^1 and t_R^2 are the retention times, and W_1 and W_2 are the base widths of the two peaks. This is illustrated in Figure 1.8. When R_s equals unity there is overlap of the two peaks (2 %) but it is clear that two components are present. At R_s=1.5 (0.03 %) the overlap is considerably reduced and values such as this are generally considered more suitable for trace metal analysis. The difference between the degrees of retention of the different solutes can be described by the **selectivity factor**, α, which is always calculated so that the value is greater than, or equal to, unity. If the value is unity, the components cannot be separated by that particular set of chromatographic conditions. The selectivity factor can be defined as:-

$$\alpha = \frac{K_B}{K_A}$$

where K_B is the partition coefficient for the more strongly retained solute and K_A the partition coefficient for the less strongly retained solute, which therefore moves more rapidly through the column.

1.2.4 LC COUPLED WITH ATOMIC SPECTROMETRY

This section on LC coupling covers both ICP-AES and ICP-MS detection as the nature of the coupling with both detectors is essentially the same, although the chromatography *e.g.*, mobile phase composition and concentration, may have to be modified for use with ICP-MS.

Although the various atomic spectrometric techniques offer the possibility of detecting the total concentration of a wide range of metals and non-metals there has been an increasing demand for qualitative and quantitative information on the physico-chemical form of elements (speciation) in a range of samples. Therefore trace metal speciation studies have increasingly coupled the separatory powers of chromatography with the sensitivity of atomic spectrometric detection. Two major reviews covering the direct coupling of gas chromatography (GC)-atomic spectrometry[149] and LC-atomic spectrometry[150] were published in the mid-1980s. One of the major advances in atomic spectrometry since that time has been the introduction in many laboratories of commercial ICP-MS systems. The use of ICP-MS as an element specific detector for LC offers exceptional sensitivity, multi-element capability and detection limits that allow the direct determination of trace metals of environmental samples. The ability of LC to remove troublesome matrix interferences on-line also offers a potential generic advantage for all ICP-MS applications.

Conventional LC-ICP couplings, *i.e.* direct connection between the end of the LC column and the nebulizer, can suffer from poor transport efficiency, particularly when pneumatic nebulizers are used. Such couplings also demonstrate low tolerance to many of the organic solvents commonly employed in mobile phases for LC. Investigations have therefore been performed to characterise the effects of mobile phase composition and flow rates on LC-ICP methods[151,152]. In addition, workers have reported studies on modified nebulizer and spray chamber arrangements in an attempt to maximise analytical performance, *e.g.* the effects of nebulization chamber position using both Meinhard[153,154] and fixed cross-flow nebulizers[10,155] for LC-ICP couplings. These studies revealed that, for aqueous eluents, peak broadening and distortion occurred when the chamber was placed inside the ICP gas box due to extended liquid transport. However, when the chamber was placed outside the gas box, a loss in signal commensurate with aerosol transport over an equivalent distance occurred, thus emphasising the importance of keeping the dead volume associated with the coupling to a minimum.

More recently a number of other workers have used ultrasonic nebulizers[9], thermospray vaporisers[10-12] and glass frit nebulizers[13] for sample introduction in LC-ICP-AES. In all cases improvements in sample transport efficiency were reported when compared with pneumatic nebulization, particularly for organic solvents. The solvent load of the plasma (important in terms of plasma stability) can be decreased by aerosol thermostatting[156-158], cooling of the spray chamber[158,159] and application of a condenser[160-162]. The amount of solvent introduced into the plasma can also be reduced by employing micro-LC systems for separation[163,164]. Lawrence *et al.*[165] described a total injection, micro-concentric nebulizer that was reported to yield up to 100 % nebulization and transport efficiency for LC-ICP-AES. Later, this group under Fassel extended the study and the direct injection nebulizer (DIN) was again used in LC-ICP-AES[13], although this time the range of organic solvents was expanded to include up to 100 % methanol, acetonitrile, IBMK and pyridine in the LC eluent. In addition, it was reported that detection limits using LC-DIN-ICP-AES for a number of elements including Se, As, Cr and S were better than those obtained using LC-ICP-AES with other nebulizer arrangements. For example the detection limit for selenium (42-57 μg l^{-1}) were 3 orders of magnitude better than that obtained using conventional nebulization by McCarthy *et al.*[166]

The coupling of LC with ICP-MS has also been investigated by a number of workers. In an early paper by Dean *et al.*[26] the characteristics of LC-ICP-MS couplings were investigated using the number of theoretical plates, peak tailing, rise time and wash-out time as criteria of merit. The LC flow rates used in this work were limited to 0.5 - 1.5 ml min^{-1} in order to remain compatible with the normal range of uptake rates of the cross flow nebulizer. It was found that the optimum coupling consisted of a short aerosol line with extended liquid transfer tubing.

Ideally the choice of mobile phase to achieve optimum chromatographic separation should not be compromised. However, problems can arise when using ICP-MS with mobile phases containing certain buffers or high concentrations of organic solvent. For example, Heitkemper *et al.*[27] reported that the phosphate buffer system, used in their work on the speciation of arsenic in urine, caused rapid clogging and erosion of the nickel sampler cone. After two hours the sampler cone became badly pitted and salt deposits started to clog the sampling orifice. In this case, a solution was found using an aluminium sampler with a 0.7 mm orifice, which was unaffected by the phosphate buffer solution.

The use of mobile phases with high concentrations of organic solvent *(e.g.* greater than 10 %) can be a bigger problem. This can result in elevated reflected powers, even at high RF forward powers, which can lead to generator cut-out with extended use. Furthermore, soot deposits on the faces of the sampler and skimmer cones within the ICP-MS interface region result in elevated noise and decreased signals. These problems can be overcome by introducing oxygen into the nebulizer gas[27,167] although the reflected power can still be greater than 100 W. An alternative approach is to replace the standard torch supplied with most commercial instruments with a low argon flow torch. This approach was applied by Branch *et al.*[64] to the speciation of Sn in waters. A Fassel torch design with 1.3 mm jets in the coolant and auxiliary gas flows and a configuration ratio of 0.82 was used; this contrasts with gas inlets of 6.0 mm and a configuration ratio of 0.78 in the standard Fassel torch. When operated at a total argon flow of 10.55 l min^{-1}, the reflected power was less than 25 W and no soot deposition was observed on the cones.

To reduce the amount of organic solvent from the mobile phase reaching the plasma, most workers reduce the temperature of the spray chamber[27,65], although more efficient desolvation can be achieved by passing the aerosol through a heating chamber prior to the cooling condenser[14]. A range of desolvation systems have been described, which are capable of removing a large percentage of the organic solvent (up to 80 %) prior to its reaching the plasma[15-19,162]. The advantages of such desolvation systems in terms of LC-ICP-MS are the increase in plasma stability and detection limits that are comparable to those obtained during aqueous operation.

1.2.4.1 Environmental applications of LC-ICP-MS

A number of reports describing off-line preconcentration of trace metals in matrices such as sea water[168] and the removal of matrix elements by ion exchange[169] using ICP-MS detection were published in the mid-1980s. However, the first use of ICP-MS as an on-line multi-element detector for LC was published by Thompson and Houk in 1986[170]. In the original study, ion-pair reversed-phase LC was used and sample introduction was achieved by ultrasonic nebulization with aerosol desolvation. The work concentrated on As and Se species and gave absolute detection limits of the order of 0.1 ng. This study also reported on the precision (<2 %) and accuracy (≅1 %) when using isotope ratio measurements, and concluded that LC-ICP-MS had considerable potential for speciation studies using stable tracer isotopes. Jiang *et al.*[171] also reported on isotope ratio experiments that quantified Cu, Zn and Cd in the presence of excess Ti and Mo interferents using an LC-ICP-MS procedure. The same paper also discussed the removal of ionisation interferences caused by U, by chromatographically separating the interferent as an N-methyl-furohydroxamic acid complex which was permanently retained on the LC column.

As with LC-ICP-AES, various forms of chromatography have also been employed with ICP-MS. These include reversed-phase, ion-pairing, ion-exchange, size-exclusion micellar and supercritical fluid chromatographic (SFC) methods. Micellar liquid chromatography has been used for example, in the speciation of alkyltin compounds[167]. Trimethyltin chloride, triethyltin bromide and tripropyltin chloride were separated with a 0.1 M sodium dodecyl sulphate micellar mobile phase and C_{18} stationary phase. Absolute detection limits for the three tin species were 27, 51 and 111 pg respectively. Other workers have used ion-exchange resins to separate organotins. Branch *et al.*[64] employed a column packed with Partisil SCX (10 µm) for the determination of tributyltin species in waters. The study also presented the results from a 'blind trial' of water samples spiked with tributyltin and concluded that LC-ICP-MS offered a sensitive and accurate method of determining the tributyltin ion. More recently, SFC coupled with ICP-MS has been reported[172,173] for the determination of organotins. Shen *et al.*[172] separated tetraalkyltin and trialkyltin compounds which gave absolute detection limits in the pg to sub-pg range (0.034 pg for tetrabutyltin and 1.5 pg for tributyltin). The method was linear over three orders of magnitude (1-1000 pg) and gave RSDs of better than 5 % for six replicate 10 pg tributyltin and triphenyltin mixtures.

Sensitivity was enhanced by Bushee[174] with the inclusion of post-column cold vapour (CV) generation for the determination of Hg in a marine CRM and thiomersal (thimerosal), a constituent of proprietary contact lens solutions. The spray chamber was replaced with a glass, gas-liquid separator. Three Hg species were determined: methylmercury(II) chloride; mercury(II) chloride; and ethylmercury(II) chloride. Detection limits for all three species were decreased by an order of magnitude using this system from 7-16 μg l^{-1} to 0.6-1.2 μg l^{-1}. Mercury speciation was also examined by Huang and Jiang[175] who demonstrated the merits of coupling LC with ICP-MS with ultrasonic nebulization. Comparable detection limits with LC-CV-ICP-MS were achieved.

Considering the relatively short period of time that ICP-MS has been available in many laboratories, there are a suprising number of publications (26) reporting a range of applications of LC-ICP-MS. These include mercury speciation in marine biological reference materials[165,175]; arsenic in various marine reference materials[176-178], seafoods[179,180] and natural waters[175]; tin in natural waters[64,167,181,182], harbour sediments[183] and fish[173]; metals in soil leachates[184]; and tellurium compounds in waste water streams[185]. Details of the various environmental and general applications of coupled LC-ICP-MS are presented in Table 1.5.

1.2.4.2 Clinical and Industrial Applications of LC-ICP-MS

In terms of clinical and industrial applications for LC-ICP-MS, arsenic has been one of the elements to receive most attention. This reflects both the interest in the wide ranging levels of toxicity exhibited by the various physico-chemical forms of this element, and the problems of determining arsenic species using more traditional methods of analysis. Whilst hydride generation is well suited to the reducible forms of arsenic, species such as arsenobetaine were not suited to this approach and so were often estimated by subtraction once the reducible forms and total arsenic had been determined. LC-ICP-MS methods overcome this problem, allowing both the reducible and non-reducible forms of arsenic to

Table 1.5 LC-ICP-MS applications (environmental).

Detector	Chromatography	Sample	Detection Limits	Comments	Ref.
VG PlasmaQuad 1.65kW FP. HPLC coupled to ICP via Teflon tubing into a standard neb.	Spherisorb ODS-2 column or Adsorbosphere SCX ion Exchange column	Speciation and detection of organotin compounds.	ICP-MS: 0.4-1.0 ng Sn ICP-AES 200-1700 ng Sn	Major tin isotope measured at 120.	167
VG PlasmaQuad ICP-MS 1.0-1.8 kW FP. HPLC coupled to ICP via silicon rubber tubing into a standard nebuliser.	Partisil STX column (250 x 4.6 mm i.d.). Mobile phase: 80/20 methanol water 0.1M ammonium acetate.	Monitoring TBT in waters.	Low flow torch: 500 ng ml^{-1} Standard torch: 25 ng ml^{-1}	Standard and low flow torches used.	64
Sciex Elan 250 ICP-MS 1.25 kW FP. HPLC effluent from column coupled to ICP-MS via an ultrasonic neb. Multiple ion monitoring mode.	Hamilton PRP-1 column (150 x 4.1 mm i.d.). Mobile phase: N-MFHA in de-ionised distilled water with 2% ethanol	Study of the retention of complexes of Mo (VI) & Ti(IV) in 1% HNO_3 in distilled water	Cu: 2 µg l^{-1} Zn: 1 µg l^{-1} Cd: 1 µg l^{-1}	-	171
Sciex-Elan 250 ICP-MS 1.2 kW FP. HPLC coupled to ICP-MS via stainless steel tubing into an ultrasonic nebuliser	Econosphere C18 column (250*4.6 mm i.d.). Mobile phase: 5% methanol in water, 0.005M PIC-135 pH 3.0.	Elemental speciation of 30 elements, particularly As and Se.	near 0.1 ng (as element) for 6 species of As and Se.	-	170
VG PlasmaQuad ICP-MS 1.35 kW FP. SFC coupled to ICP-MS via a stainless steel heated transfer line directly into the ICP injector.	SB-Octyl-50 capillary column housed in a gas chromatograph. Mobile phase: bone dry grade carbon dioxide.	Separation of tetraalkyltin compounds.	TBT: 0.034 pg TPT: 0.047 pg	-	172

Table 1.5 LC-ICP-MS applications (environmental) cont.

Detector	Chromatography	Sample	Detection Limits	Comments	Ref.
VG PlasmaQuad ICP-MS 1.3 kW FP. HPLC coupled to ICP via Teflon (FEP) tubing into nebuliser inlet.	Water Picotag C18 column. Mobile phase: 0.06 M ammonium acetate, 3% acetonitrile and 0.005% v/v mercaptoethanol pH 5.3-6.8.	Hg Speciation in HBS RM-50 Albacore tuna sample and thimerosal in contact lens solution.	LC-ICP-MS: 0.6-1.2 ng ml^{-1} DMM LC-cold vapour ICP-MS: 7-20 ng ml^{-1} DMM	(i) post column Hg cold vapour generation, spray chamber replaced with glass chamber. (ii) Optimised at mass 201 to minimise background at 202.	174
Sciex Elan 250 ICP-MS 1.4 kW FP. HPLC coupled to ICP via Teflon tubing into a standard neb. Single ion monitoring mode.	Pierce C18 column (300x4.6 mm i.d.). Mobile phase: 1.0 mM sodium dodecyl sulphate 5% methanol, 2.5% acetic acid.	Quantification of As species in dogfish muscle ref. material (DORM 1).	Arsenobetaine 300 pg of As	FIA-ICP-MS det. limits were compared: Arsenobetaine 30 pg of As.	176
Sciex Elan 250 ICP-MS 1.4 kW FP. HPLC coupled to ICP via Teflon tubing into a standard neb. Multi element analysis mode.	Columns either: anion pairing anion exchange cation pairing.	Determination of arsenic species in DORM 1.	Absolute detection limit: 50-300 pg	Anion pair found to be sensitive to the matrix. Anion exchange more tolerant.. Cation pairing more suitable for DMAA and AsB in biological samples with high salt content.	177
Yokogawa PMS100 ICP-MS 1.3 KW FP. HPLC coupled to ICP via Teflon tubing into a concentric neb.	Asahipak GS220 reversed-phase gel permeation column(500x7.6) Intersil ODS-2 reversed-phase column(250x4.6) Mobile phase: 1. anionic As: pH 7. 2. cationic As: alkylsulphonate pH 3.	Separation and detection of 15 arsenic compounds from natural samples including human urine after eating fish.	arsenobetaine (VIII) and cacodylate(IV) 20-50 pg As.	-	178

Table 1.5 LC-ICP-MS applications (environmental) cont.

Detector	Chromatography	Sample	Detection Limits	Comments	Ref.
VG PlasmaQuad ICP-MS 1.3 KW FP. HPLC coupled to ICP via Teflon capillary tubing into a standard concentric neb.	Spherisorb ODS-2 column (500x0.6mm id.). Mobile phase: Prepared by addition of the appropriate modifier to the stock solution and diluted with 3% v/v propanol.	Speciation of alkyl tin compounds.	TMT-Cl: 27 pg TET-Br: 51 pg TPrT-Cl: 111 pg MMT-TCl: 46 pg DMT-DCl: 26 pg	Micellar LC applied using 0.1 M or 0.02 M SDS micellar mobile phase.	181
VG PlasmaQuad ICP-MS 1.35 kW FP. SFC coupled to ICP via insulated copper tubing from the GC oven into the ICP torch.	Octyl-50 capillary column 2.5 x 50 mm i.d.) fitted into a Hewlett-Packard 5890 series II GC oven. Mobile phase: bone dry grade liquid CO_2.	Determination of ultra-trace levels of organotin compounds.	Tetrabutyltin: 0.034 pg. Tetraphenyltin: 0.047 pg.	-	182
Sciex Elan 500 ICP-MS 1.2 kW FP. Thermostatted nebuliser spray chamber.	Strong cation exchange column.	Determination of tributyltin and dibutyltin in the harbour sediment ref. material PACS-1.	Tributyltin: 5 ng g^{-1} Sn Dibutyltin: 12 ng g^{-1}Sn	-	183
Sciex Elan 500 ICP-MS. 1.2 kW FP. HPLC coupled to ICP-MS via 0.5 mm i.d. tubing into the nebuliser.	Superose-12 size exclusion column. Mobile phase: 0.2M ammonium acetate pH 3.6-5.2.	Determination of organic and inorganic Al, Mn, Fe, Ni, Cu, Zn, Cd, La in soil leachates.	Not reported	At a higher pH more organic material was dissolved, whereas the total metal concentration was usually lower.	184
Sciex Elan 500 ICP-MS 1.5 kW FP. HPLC coupled to ICP via PTFE tubing into a Meinhard type nebuliser.	Dionex ion chromatography AG4A+AS4A column. Mobile phase: eluent 1: 200 mg l^{-1} NaOH eluent 2: 500 mg l^{-1} Na_2CO_3 eluent 3: 500 mg l^{-1} $NaHCO_3$ Eluent 4: H_20.	Determination of tellurium compounds in wastewater streams.	Not reported	-	185

Table 1.5 LC-ICP-MS applications (environmental) cont.

Detector	Chromatography	Sample	Detection Limits	Comments	Ref.
Sciex Elan 250 ICP-MS 1.25kW FP. HPLC coupled to ICP via stainless steel tubing into an ultrasonic neb.	Hamilton PRP-1 or Vydal 201TP. Ion pairing reagent and mobile phase dependant on compound to be separated.	Detection of P and S compounds.	0.4-4.0 ng P 7.0 ng S	Analyte sensitivity decreases as organic modifier concentration in mobile phase increases.	194
Sciex Elan 500 ICP-MS.	Anion exchange chromatography using SGE 250GL- SAX columns (250 x 2 mm). Mobile phase: ammonium acetate buffer and acetonitrile.	Analysis of target and non-target pollutants in aqueous leachates, including Cl, other halogens, P, and S.	Not reported	Preliminary data presented on an anion exchange chromatography-based technique for the detection of the target compound 4-chlorobenzene sulphonic acid.	195
VG PlasmaQuad ICP-MS 1.3 kW FP. HPLC coupled to ICP-MS via Teflon FEP tubing into the nebuliser.	Waters PicoTag C_{18} column (Isocratic separation). Mobile phase: 0.4 M HIBA, 0.02 M octanesulphonic acid (pH 3.8). BakerBond WP C_{18} column (Gradient separation) Mobile phase: 0.05 M-0.4 M 2-hydroxy-2-methyl propanoic acid.	Determination of rare earth elements in SRM 1633a fly ash.	Ho: 0.4 ng ml^{-1} La: 5.0 ng ml^{-1}	Spray chamber cooled to 8°C.	196
Sciex Elan 250 ICP-MS 1.3 kW FP. HPLC coupled to ICP-MS via a direct injection nebuliser (DIN).	Metal free GLT column with Intersil ODS-2 (5μm). Mobile phase:5% or 25% methanol in water with ion pair reagent.	Charged species of tin and arsenic separated as ion pairs.	Tin: 16-20 μg l^{-1} Arsenic: 0.4-1.2 μg l^{-1}	The use of DIN improved the detection limit by 1-2 orders of magnitude.	197

Table 1.5 LC-ICP-MS applications (environmental) cont.

Detector	Chromatography	Sample	Detection Limits	Comments	Ref.
VG PlasmaQuad ICP-MS 1.3 kW FP. HPLC coupled to ICP-MS via Polyplex tubing into a concentric nebuliser.	Pharmacia PEP RPC HR 5/10 reversed phase colomn. Mobile phase: 5% methanol-95% 0.01 M orthophosphoric acid.	Determination of the growth promoter 4-hydroxy-3-nitrophenyl-arsenoic acid in chicken tissue.	7 - 25 µg kg^{-1}	-	191
All argon ICP-MS. HPLC coupled to ICP-MS via a Tefzel transfer line.	Dionex AS4A anion exchange column. Mobile phase 6mM ammonium sulphate or 10µM $HClO_4$ buffered to pH 9	Determination of hexavalent chromium.	Cr(VI): 0.4µg ml^{-1}	This method was compared with a method using the same ion chromatographic separation, coupled with colorimetry. Detection limits were comparable for both techniques.	198
All argon ICP-MS.	Ion pair reverse phase chromatography.	Lead speciation in a lead fuel reference material and a water quality control sample.	Inorganic lead: 0.37 ng TEL: 0.14 ng TPhL: 0.17 ng TTEL: 3.9 ng	-	199

be determined with good sensitivity. Heitkemper *et al.*[27] have used this technique to determine arsenic in urine. Four arsenic species were determined: arsenic; arsenate; dimethylarsinate; and monomethylarsonate, using an ion-exchange system. The determination of arsenite was however complicated by the presence of $^{40}Ar^{35}Cl$ ions (m/z=75) resulting from the correlation of chlorine containing species. In a later work the same group reduced the interference by employing ion chromatography to separate the chloride from the arsenic compounds[65]. A 20-fold dilution of the urine samples was necessary to avoid column overloading from chloride and subsequent $ArCl^+$ interferences. Mixed gas approaches (discussed in 1.1.5) could be combined with LC-ICP-MS in order to overcome the problem of matrix effects and spectroscopic interferences. For example, Hill *et al.*[95] have shown that the $ArCl^+$ interference can be eliminated by the addition of nitrogen to the coolant and nebulizer gas flows in the presence of 1 % m/v chloride.

LC-ICP-MS has been utilised for the study of metalloprotein species. Dean *et al.*[26] investigated the characteristics of LC-ICP-MS couplings for this type of application using the number of theoretical plates, peak tailing, rise time and wash-out time as criteria of merit. They found that a short aerosol connection line was optimal and, when compared with on-line UV monitoring, ICP-MS gave a comparable number of theoretical plates. In another study on metalloproteins, Mason *et al.*[186] used size-exclusion LC coupled with ICP-MS and concluded that the technique had considerable potential for the rapid quantitative analysis of metals associated with cytosolic metal-binding ligands. The greatest limitation encountered was the ability to effectively separate the various metal binding moieties, although it was suggested that this might be overcome using tandem LC systems, *e.g.* size-exclusion followed by ion-exchange.

Other clinical and industrial applications include the determination of lead and other trace element species in blood by size-exclusion LC-ICP-MS[187], the determination of cadmium species in kidney[188], the determination of gold-based drug metabolites in human blood[189], the use of reversed-phase LC for the separation of zinc species and growth promoter in chicken tissue[190,191], the determination of thimerosal in biological products[192], and, in one of the few industrial applications, the determination of rare earth impurities[193]. Details of these applications are presented in Table 1.6.

Table 1.6 LC-ICP-MS applications (clinical and industrial)

Detector	Chromatography	Sample	Detection Limits	Comments	Ref.
VG PlasmaQuad ICP-MS 1.35 kW FP. HPLC coupled to ICP-MS via PTFE tubing into crossflow neb. Single ion monitoring mode.	Superose-12 SEC column capable of separating proteins of relative molecular mass 1000-300000 u. Mobile phase: 0.12 M Tris HCl pH 7.5.	Study of metallo-proteins in gel filtration Std. and solutions of metallo-thionein and ferritin.	Not reported	Physical coupling was studied in detail particularly involving minimum liquid transport & extended aerosol transport, and vice versa.	26
VG PlasmaQuad ICP-MS 1.5 kW FP. HPLC coupled to ICP via Flexon HP tubing into a concentric neb.	Weak anion exchange column (250x4.6 mm id.). Mobile phase: 30% methanol-15 mM $NH_4H_2PO_4$- 1.5 mM CH_3COONH_4 pH 5.75.	Speciation of As in urine.	20-91 pg in aqueous media 36-96 pg in urine	Determination of As^{3+} complicated by interference from co-elution of Cl containing species forming $ArCl^+$ ions.	27
VG PlasmaQuad ICP-MS 1.35 KW FP. HPIC coupled to ICP-MS via polyplex tubing.	Wescan anion R-IC column (250x4.1 mm id). Mobile phase 5 mM phthalic acid.	Elimination of $AgCl^+$ interference from arsenic speciation in urine samples.	As(III): 340 pg As(V): 420 pg DMA: 700 pg	-	65
VG PlasmaQuad Ar-ICP-MS 1.35 KW FP. He-ICP-MS 1.55 KW FP. Type C-1 concentric nebuliser	Wescan anion R-IC column (250x4.1 mm id). Gradient programme using 2% propan-1-ol and 50 mM carbonate buffer	As in urine	As(III): 5.0 µg l^{-1} As(V): 6.0 µg l^{-1} DMA: 1.2 µg l^{-1} MMA: 3.6 µg l^{-1} (100 ml injection)	Paper also contains results for As speciation in club soda and wine	200
VG PlasmaQuad ICP-MS 1.25 kW FP. HPLC coupled to ICP via Teflon capillary tubing into a standard concentric neb.	Spherogel TSK SW 2000 size exclusion column (600 x 7.5 mm). Mobile Phase: 0.06 M Tris-HCl, 0.05% NaN_3 pH 7.5.	Separation and elemental analysis of metallo-proteins in biological samples.	Absolute: 240-350 pg of protein (calculated from the peak areas of the Cd signal).	The techniques' versatility was demonstrated by quantitative multi-element analysis of cytosolic metal binding proteins separated from a species of polychaete worm.	186

Table 1.6 LC-ICP-MS applications (clinical and industrial)

Detector	Chromatography	Sample	Detection Limits	Comments	Ref.
Sciex Elan 250 ICP-MS 1.3 kW FP. HPLC coupled to ICP via PTFE tubing into a cross flow nebuliser.	TSK G 3000 SW size exclusion column). (300x7mm Mobile phase: 0.1 M Tris/HCl pH 7.2.	Determination of lead and other trace element species in blood.	Pb in protein fraction: 0.15 µg l^{-1} to 0.05 µg l^{-1}.	-	187
VG PlasmaQuad ICP-MS 1.3 kW FP. HPLC coupled to ICP via Teflon tubing into a crossflow neb. Single ion monitoring mode.	Superose-12 SEC column. Mobile phase: 0.12 M Tris HCl pH 7.5.	Investigation of cadmium speciation in Kidney.	Not reported	-	188
Sciex Elan 250 ICP-MS 1.3 KW FP. HPLC coupled to ICP via PTFE tubing into a concentric neb. Multi element mode.	(a)Altech anion WAX300 exchange column. Mobile phase: 15 min. gradient from 20 mM to 200 mM Tris buffer. (b)TSK 250 SEC column. Mobile phase: Aq. 25 mM Tris buffer.	Determination of gold drug metabolites in human blood.	Cu 3.0 pg Cd 7.0 pg Zn 8.0 pg Au 10.0 pg	-	189
VG PlasmaQuad PQ2 Turbo Plus ICP-MS. 1.35 KW FP. HPLC coupled to ICP-MS via a V7 manual valve into a de Galan nebuliser.	Both Size exclusion and reverse phase chromatography.	Size exclusion chromatography was used to separate known proteins. Reverse phase chromatography was used to separate Zn containing species in chicken meat.	Not reported	-	190

Table 1.6 LC-ICP-MS applications (clinical and industrial)

Detector	Chromatography	Sample	Detection Limits	Comments	Ref.
VG PlasmaQuad ICP-MS. Procedure as per reference 82.	Waters Picotag C18 column. Procedure as per reference 82.	Determination of thimerosal and biological products.	Not reported	Spray chamber cooled to 8°C	192
Yokogawa PMS200ICP-MS 1.4 kW FP. HPIC coupled to ICP via ETFE tubing into a Meinhard concentric neb.	Yokogawa Excel-pak ICS-C35 (150x4.6mm) and ICS-C15 (125 x 4.9) ion chromatography columns. Mobile phase: either, lactic acid or hydroxy-isobutyric acid. Both adjusted to pH 4.3.	Determination of rare earth elements as impurities in other rare earth materials.	1.0 to 5.0 pg ml^{-1} for 14 rare earth elements.	-	193
All argon ICP-MS.	Gel permeation liquid chromatography.	Determination of iron containing proteins	Ferritin: 0.01 µg Haemoglobin: 1.0 µg Myoglobin: 0.7 µg Cytochrome c: 0.4 µg	-	201
Sciex Elan 250 ICP-MS 1.4 kW FP. HPLC coupled to ICP via a narrow bore tubing into a direct injection nebuliser (DIN).	PEEK micro-bore column packed with reverse phase C_{18} material. Mobile phase: ammonium salts of S5, S7 and S12.	Speciation of mercury and lead compounds in human urine.	MePb: 0.2 pg Pb. EtPb: 0.2 pg Pb MeHg: 18pg Hg	A DIN system was used.	202

1.3 TRACE METALS IN SEA WATER

The high dissolved solids loading of sea water (3 % m/v) makes it a difficult matrix, both physically and chemically, for ICP-MS. Continuous nebulization results in the physical deposition of material on the sampler and skimmer cones and the subsequent restriction of the orifices, which causes a reduction in sensitivity and long term stability. The chemical composition of the sea water matrix also causes a number of polyatomic ion interferences and non-spectroscopic interferences, particularly for the determination of the first row transition elements, which can considerably degrade the analytical capabilities of the instrument in this mass range.

1.3.1 SEA WATER COMPOSITION

Of all water in the surface zone of the earth, 97 % (1370 million cubic kilometres) is in the oceans[203]. Sea water can be described as a complex mixture of chemical, physical and biological parameters. Three fundamental properties of sea water are salinity, temperature and density. These are inter-linked and the equation of state of sea water[204] is a mathematical expression of the relationship between these properties. Salinity is of particular importance in the determination of trace metals in sea water by ICP-MS. It is a measurement of the 'saltiness' of sea water and is a function of the weight of the total dissolved solids in a quantity of sea water. The major ions in sea water are listed in Table 1.7. The major polyatomic ion interferences caused by the composition of sea water are summarised in Table 1.2 (Section 1.1.4.1)

Although the salt content may vary (*e.g.* from precipitation, evaporation, land run-off and the melting or formation of ice) these constituents are almost always present in the same

Table 1.7 The major ions of sea water[205].

Ion	Concentration (g kg^{-1}) at 35 S
Cl^-	19.354
SO_4^{2-}	2.712
Br^-	0.0673
F^-	0.0013
B	0.0045
Na^+	10.77
Mg^{2+}	1.290
Ca^{2+}	0.4121
K^+	0.399
Sr^{2+}	0.0079

relative proportions. This is termed the constancy of composition. The major elements that contribute to salinity are described as being conservative, that is, under most conditions their concentration ratios remain constant and total concentrations can only be changed by physical processes. A number of general trends can be identified, including:

(a) Surface ocean water salinity usually ranges between 32 and 37 S.

(b) Higher values are encountered in semi-enclosed seas such as the Mediterranean (37-39 S) where evaporation exceeds precipitation and run-off.

(c) Lower values are found in coastal waters, where run-off can result in decreased surface salinities (*e.g.* < 32 S).

1.3.2 METAL SPECIATION AND COMPLEXATION

Trace elements are conventionally considered to be those which exist at concentrations of 1 mg l^{-1}. In sea water they are present at concentrations in the range from pg l^{-1} to mg l^{-1} levels. Such low concentrations have historically resulted in significant analytical problems. For example, an inter-laboratory comparison carried out by Brewer and Spencer in 1970[206]

found that the data for Zn ranged from 0.02 to 21.2 µg l^{-1} for subsamples of the same original sample, and concluded that it was imprudent to draw conclusions from weak regional trends that may be apparent in data from disparate sources. However, improvements in both analytical and sample collection techniques, especially with regard to the elimination of sample contamination, have resulted in updated trace element concentration data including the certification of marine reference materials (e.g. the National Research Council of Canada series of CRMs).

There has also been an increasing demand for qualitative and quantitative information on the physico-chemical form of elements in sea water which has been reflected in current environmental legislation. The speciation of trace metals has, for many years, focused on environmentally sensitive metals such as Hg, Sn and As[64,174,176]. However, there has also been an interest in a wide range of trace elements (including the first row transition elements) in order to determine the effect of speciation on trace metal particle reactivity and bioavailability, and the processes that are involved in trace metal removal from sea water[205]. A selection of speciation and concentration data for trace elements in unpolluted sea water is given in Table 1.8.

It should be stressed that the details on speciation presented in Table 1.8 are for inorganic species only. However, complexation with humic and fulvic acids (and other organics and clays etc.) is thought to be an important mechanism for removing metal ions from a solid phase to a solution phase[207].

The average time an element spends in the sea before being removed into the sediment sink is termed the residence time. In a steady state system, it is assumed that the imput of an

Table 1.8 Speciation and concentration data for

selected trace elements in sea water[208].

Element	**Main species in oxygenated sea water**	**Range of concentrations at 35 S**
Se	$Se(OH)_3$	8 - 20 pmol kg^{-1}
V	HVO_4^{2-}, $H_2VO_4^-$, $NaHV0_4^-$	20 - 35 nmol kg^{-1}
Cr	CrO_4^{2-}, $NaCrO_4^-$	2 - 5 nmol kg^{-1}
Mn	Mn^{2+}, $MnCl^+$	0.2 - 3 nmol kg^{-1}
Fe	$Fe(OH)_3$	0.1 - 2.5 nmol kg^{-1}
Co	Co^{2+}, $CoCO_3$, $CoCl^+$	0.01 - 0.1 nmol kg^{-1}
Ni	Ni^{2+}, $NiCO_3$, $NiCl^+$	2 - 12 nmol kg^{-1}
Cu	$CuCO_3$, $CuOH^+$, Cu^{2+}	0.5 - 6 nmol kg^{-1}
Zn	Zn^{2+} $ZnOH^+$, $ZnCO_3$, $ZnCl^+$	0.05 - 9 nmol kg^{-1}
As	$HAsO_4^{2-}$	15 - 25 nmol kg^{-1}
Mo	MoO_4^{2-}	0.11 μmol kg^{-1}
Cd	$CdCl_2$	0.001 - 1.1 nmol kg^{-1}
Sn	$SnO(OH)_3^-$	1 - 12 pmol kg^{-1}
Hg	$HgCl_4^{2-}$	2 - 10 pmol kg^{-1}
Pb	$PbCO_3$, $Pb(CO_3)_2^{2-}$, $PbCl^+$	5 - 175 pmol kg^{-1}

element per unit time is balanced by its output. However, a more useful concept is that of mean oceanic residence time (MORT), which is defined as the total quantity of an element present in the oceans divided by its imput rate or its output rate. A number of general trends regarding the residence times of elements in sea water can be identified:

(a) Residence time values span a range of six orders of magnitude from Al (3.7×10^2 yr) to Na (7.4×10^7 yr).

(b) The lower atomic number alkali and alkaline earth metals have the longest residence times due to the lack of reactivity of their aqueous ions in sea water.

(c) Trace metals such as Zn, Mn, Co and Cu have intermediate residence times (10^3 - 10^4 yr).

(d) Refractory elements such as Al, Ti, Cr and Fe have the shortest residence times, generally less than the mixing times for oceanic water masses (less than 1000 yr).

1.3.3 MERCURY SPECIATION

A specific example of the dynamic nature of trace metals in sea water is the cycling of Hg (MORT 8 x 10^4 yr). Different Hg species occur in the atmosphere, hydrosphere and geosphere and at the interfaces between each phase. The concentration and physico-chemical form of Hg in sea water is affected by natural (Hg^0) and anthropogenic inputs from the atmosphere (Hg^0, CH_3HgCH_3 and CH_3Hg^+), surface run-off ($HgCl_2$), and the organic content of the water (Hg_2^+, Hg_2^{2+} and CH_3Hg^+). The removal of Hg from the hydrosphere is influenced by the pH of the sea water and the biomass present. The nature of the sediment will also have an effect on the solubility of Hg and will determine whether it passes back into the water column as a soluble form (CH_3Hg^+)or remains in the sediment as an insoluble form (HgS and CH_3HgCH_3). This cycle is shown in Figure 1.9.

It is also well established that inorganic mercury, whether from anthropogenic sources or natural geological activities, is converted into the more toxic organomercury compounds by aquatic organisms [209]. After the Minamata mercury poisoning tragedy in the late 1960s various methods for mercury determination have been reported[210,211]. As organomercury(II) compounds such as methylmercury are more toxic to human beings than inorganic mercury, speciation of the chemical forms in environmental samples is necessary. The technique most widely used for the speciation of mercury involves gas chromatography (GC) coupled to microwave-induced plasma atomic emission spectrometry (MIP-AES) or FAAS[212,233]. In the last 10 years LC procedures have also been developed[174,214,215]. This topic will be discussed in more detail in Chapter 5 which describes an LC-ICP-MS method for the speciation of Hg in sea water samples.

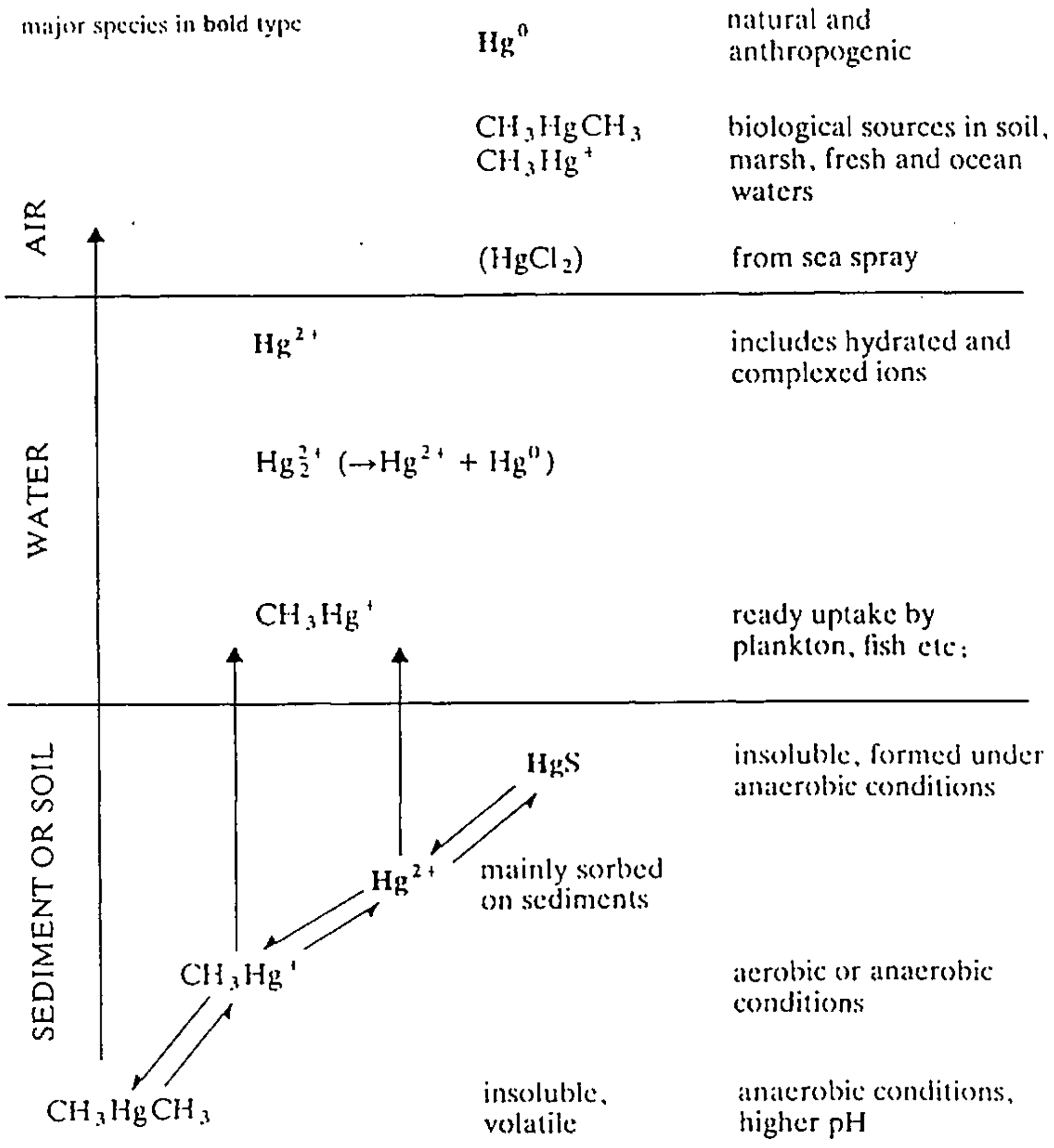
major species in bold type
Hg^0
natural and anthropogenic
CH_3HgCH_3
CH_3Hg^+
biological sources in soil, marsh, fresh and ocean waters
AIR
$(HgCl_2)$
from sea spray
Hg^{2+}
includes hydrated and complexed ions
WATER
Hg_2^{2+} $(\rightarrow Hg^{2+} + Hg^0)$
CH_3Hg^+
ready uptake by plankton, fish etc;
SEDIMENT OR SOIL
HgS
insoluble, formed under anaerobic conditions
Hg^{2+}
mainly sorbed on sediments
CH_3Hg^+
aerobic or anaerobic conditions
CH_3HgCH_3
insoluble, volatile
anaerobic conditions, higher pH

Figure 1.9 Cycling of mercury in the environment[203].

1.4 RESEARCH OBJECTIVES

The use of inductively coupled plasma-mass spectrometry as a method of trace metal analysis is now well established. It offers significant advantages over other rival techniques such as ICP-AES and GFAAS, including excellent sensitivity, multi-element capability, detection limits in the range 0.001-0.1 μg l^{-1} for many elements, linear calibration ranges over five orders of magnitude and relative freedom from chemical interferences. However, it suffers from a range of spectral and non-spectral interferences that occur when determining trace metals in complex matrices such as sea water. The primary aim of this research was to develop a portfolio of analytical methods with ICP-MS detection to remove or reduce these interference effects for the determination and speciation of trace metals in sea water.

Specific aims of this research were:

1. An investigation of nitrogen-argon plasmas for the removal of the $ArNa^+$ polyatomic ion interference at m/z = 63 and non-spectroscopic interferences affecting other masses in sea water, for the determination of ^{63}Cu, Cr, Mn, Ni, Co, Zn and Pb.

2. The study of on-line FI-ICP-MS matrix elimination and analyte preconcentration methods using solid phase reactors for the determination of trace levels (between <0.1 μg l^{-1} and >10 μg l^{-1}) of metals such as Mn, Ni, Co, Cu, Zn and Pb in sea water.

3. The optimisation of on-line FI procedures with cold vapour generation (CVG) coupled with atomic fluorescence spectrometry (AFS), ICP-AES and ICP-MS to determine mercury in sea water at ng l^{-1} levels.

4. An investigation of mercury speciation in sea water and concentrated brines using coupled LC-ICP-MS.

CHAPTER 2

Determination of Trace Metals in Sea Water Using Mixed Gas Plasmas

CHAPTER 2: DETERMINATION OF TRACE METALS IN SEA WATER USING MIXED GAS PLASMAS

Introduction

The formation of polyatomic species below m/z = 80 cause spectroscopic interferences in ICP-MS by overlapping with the analytes at the m/z value of interest. Such polyatomic ions can be introduced via precursors in the argon support gas or atmospheric gases. However, the most important source of polyatomic interferences come from the reagents used (*e.g.* acids) and the sample matrix itself, and can cause a systematic error that needs to be overcome in order to obtain acceptable analytical results. The major polyatomic interferences are shown in Table 1.2.

The high dissolved salt content of sea water (typically 3 %), in combination with the very low concentrations of many of the elements of interest, usually precludes direct analysis. Even if the problem of salt deposition on the sampler and skimmer is avoided by the use of FI instead of continuous nebulization, 10-fold dilutions of the matrix are necessary in order to reduce suppression of sensitivity due to the high salt concentration. This results in placing the concentrations of all but a few elements of environmental interest too low for accurate determination. The chemical composition of sea water is presented in Tables 1.7 and 1.8.

The magnitude of such interfering effects can be reduced or eliminated by optimisation of the instrument conditions but this is usually achieved to the detriment of sensitivity[50,58,76,89]. If the interferent is present in the sample matrix, it can be eliminated by separating the analyte from the interfering matrix component using off-line precipitation and solvent extraction procedures[61,62] or on-line approaches such as FI or LC[31,65]. An alternative way to facilitate the removal of polyatomic interferences is the use of molecular or inert gases added to, or replacing one of the three gas flows of the ICP-MS.

The use of mixed gas plasmas for the removal of polyatomic ion interferences and non-spectroscopic interferences in ICP-MS has primarily concentrated on nitrogen addition[88-98]. The introduction of nitrogen into the nebulizer gas flow has been shown to dramatically reduce polyatomic ions such as $ArCl^+$ and $ClCl^+$ [90-95]. However, little work has been carried out on the removal of interferences from real samples such as sea water.

This chapter discusses the effect of sea water on the analytical performance of ICP-MS. Initial studies were carried out using a single channel FI manifold. This included the univariate investigation of the addition of nitrogen to the nebulizer gas flow of the ICP-MS for the reduction of the $ArNa^+$ polyatomic ion interference at $m/z = 63$ on the Cu signal. This was followed up with a multivariate simplex optimisation for the removal of the $ArNa^+$ polyatomic ion interference at $m/z = 63$ and non-spectroscopic interferences affecting other masses in sea water, for the determination of Cu, Cr, Mn, Ni, Co, Zn and Pb.

2.1 EXPERIMENTAL

2.1.1 INSTRUMENTATION

All analyses were performed using either a VG PlasmaQuad PQ2 ICP-MS or a Fisons PlasmaQuad PQ2 Turbo + ICP-MS (Fisons Elemental, Winsford, Cheshire, U.K.). Minor modifications were carried out to both instruments. The sample introduction system was modified by the inclusion of a high solids nebulizer (Ebdon Type, PS Analytical, Sevenoaks, Kent) with an enlarged gas orifice of 300 μm to allow for higher gas flows. Addition of nitrogen to the nebulizer was achieved using either the second mass flow controller on each instrument, or a gas blender. Further details of this are given in Section 2.1.2. The spray chamber was cooled using water circulated using a conventional pump (NesLab RTE 100). The ICP-MS scan parameters and standard operating conditions are given in Tables 2.1 and 2.2

2.1.2 GAS ADDITION

The nebulizer gas line of the PQ2 instrument was fitted with a second mass flow controller, the purpose of which is to add oxygen to the nebulizer gas in order to prevent the deposition of carbon on the cones when analysing organic samples. This facility can be used for any gas at a flow rate between 0.03-0.2 l min^{-1} and was used for the initial nitrogen addition studies. However, this method did not give accurate and reproducible gas addition and therefore a gas blender was used (Signal Instrument Company, Camberley, Surrey, UK.) for all subsequent experiments. The gas blender relied on applying a constant differential pressure across an orifice in order to obtain a constant flow of gas. The output flow from the blender comprised of two streams, the second stream (the added or span stream) had a variable orifice enabling varying gas flows to be mixed with the first stream (the argon diluent gas). The standard argon line was replaced by the output of the gas blender. This was metered using a 2.0 l min^{-1} argon mass flow controller which allowed the total gas flow and the percentage mix gas to be controlled independently. A calibration of the percentage mix gas (nitrogen) added through the Signal gas blender is shown in Figure 2.1.

2.1.3 REAGENTS

High purity de-ionised water purified by a Milli-Q analytical reagent grade water purification system (Millipore, Chester, Cheshire UK.) was used throughout. All reagents

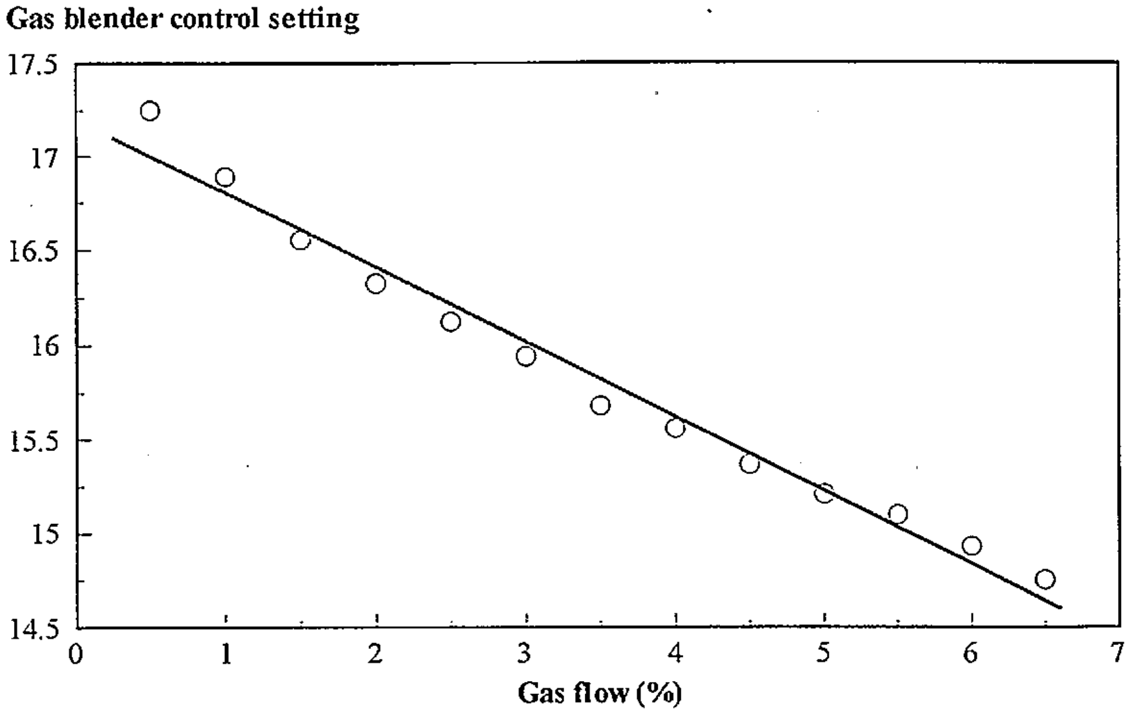

Figure 2.1 Calibration of the percentage mix gas added through the Signal gas blender.

Table 2.1 ICP-MS scan parameters.

(a) Time resolved scan parameters for FI	
Mass range (a.m.u.)	56.93-210.11
Channels	1024
Scan sweeps	10
Dwell time (µs)	160
Points per peak	5
Peak jump sweeps	20
Collector type	Pulse

(b) scan parameters for simplex optimisation	
Mass range (a.m.u.)	57.93 - 65.35
Channels	512
Scan sweeps	1600
Dwell time (µs)	80
Points per peak	5
Peak jump sweeps	50
Collector type	Pulse

Table 2.2 Standard operating conditions for the ICP-MS.

ICP system	
Forward power (W)	1500
Reflected power (W)	5
Nebulizer gas flow (l min^{-1})	0.97
Auxiliary gas flow (l min^{-1})	0.75
Coolant gas flow (l min^{-1})	15.0
Spray chamber ($^{\circ}$C)	Glass, Water cooled 6.5

Interface	
Sample cone aperture (mm)	1.00
Skimmer cone aperture (mm)	0.75

Default ion lens settings	
Extraction	1.00
Collector	7.70
Lens 1	7.70
Lens 2	5.40
Lens 3	5.0
Lens 4	3.85
Pole Bias	5.50

Vacuum pressures	
Expansion region (torr)	2.8
Intermediate region (torr)	$< 10^{-4}$
Analyser region (torr)	2.3×10^{-6}

used were Aristar grade. Stock solutions of Co, In, V, Fe, As, Se, Cu, Ni, Zn, Pb, Mn, and Cr (100 $\mu g\ l^{-1}$) were prepared from 1000 $\mu g\ l^{-1}$ commercial stock solutions (Merck, Poole, Dorset, UK). Standard solutions were prepared daily by appropriate dilution of the stock solutions with 2 % v/v nitric acid (2 parts concentrated HNO_3 and 98 parts Milli-Q) or a synthetic sea water solution (Corrosion test mixture, Merck). Stock solutions were stored in acid-washed (10 % v/v HNO_3) polypropylene containers. Standard solutions were made up in acid washed volumetric flasks (100 ml, Grade A). The nitrogen gas (99.999 %) was supplied by Air Products Ltd (Walton-on-Thames, UK).

2.1.4 SIMPLEX OPTIMISATION

The key operating conditions in ICP-MS are the nebulizer and auxiliary gas flows, forward RF power and any added gas flow and the optimisation of these variables must take into account their inter-dependence. Simplex optimisation has been used to reduce interferences and improve detection limits in ICP-AES[216,217], for the analysis of organics in ICP-MS[14] and for the addition of mixed gases such as nitrogen, methane and ethene to the plasma[95,103,104]. In these studies the lens settings were manually tuned after each iteration to optimise the plasma conditions. The ion optics have also been successfully optimised using simplex to reduce the effects of a 10000 $\mu g\ ml^{-1}$ U matrix solution[81].

Multivariate approaches such as simplex optimisation can be used to achieve the simultaneous optimisation of two or more interdependent variables[218,219]. Simplex optimisation works by locating the 'summit' (the optimal conditions) of the response surface defined by the parameters of the optimisation. A simplex is a geometrical figure with n+1 vertices with respect to n parameters *i.e.* for two parameters the simplex is a triangle. If a fixed step size system with two parameters X and Y is considered (Figure 2.2), the initial simplex is defined by three points which represent three sets of experimental conditions. The response is measured at each of these points. The point associated with the worst response (point 1) is reflected through the centroid of the other points (points 2 and 3). The response is then measured for the new set of experimental conditions (points 2, 3 and 4) and the triangle is reflected away from the new worst point (in this case point 2). The process is repeated and the simplex migrates towards the optimum.

One problem with the fixed step size simplex is that if the step size is too small the optimisation is very slow, and if it is too big the optimisation is coarse and imprecise. To improve this situation the basic simplex method can be modified[220] such that the step size is variable, within certain boundaries, throughout the optimisation.

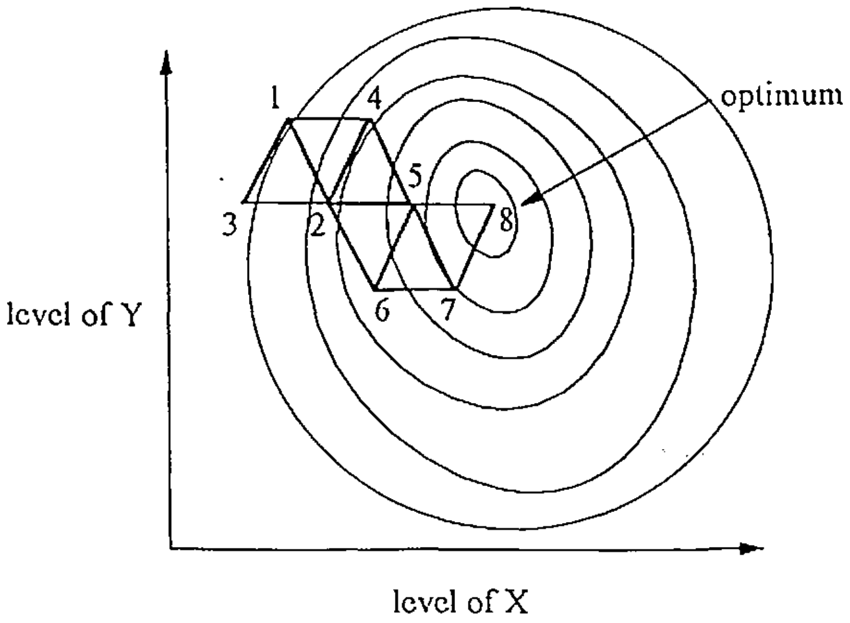

Figure 2.2 **Fixed step size simplex optimisation with two variables, X and Y.**

The choice of initial step size is a significant factor for a simplex procedure, as it is important to search all of the factor space. The choice of the figure of merit is also critical as it will determine the progress and direction of the optimisation. This may be raw counts, net counts, signal to background (S/B), signal to noise (S/N) or interference to analyte ratio. In ICP-MS it is considered best to use a figure of merit that incorporates a ratio as this will compensate for instrument drift.

Initial studies using univariate searches were employed in order to examine the effect of adding nitrogen to the nebulizer gas on the removal of Na based polyatomic interferences from 1 % v/v synthetic sea water solutions spiked with copper (100 μg l^{-1}). This involved assessing the effect of nitrogen addition whilst the forward power, nebulizer, coolant and auxiliary gas flows were kept constant. However optimum conditions for maximum interference removal could not be defined using univariate searches due to the inter-dependence of the above variables. Therefore a multivariate procedure using a modified simplex was applied. A variable step size simplex optimisation procedure with the ratio of the signals for Co^+ at m/z = 59 to $ArNa^+$ at m/z = 63 as the criterion of merit was used for optimisation of the instrument conditions for the removal of $ArNa^+$. The start conditions for the simplex are summarised in Table 2.3.

Table 2.3 Simplex optimisation start conditions for 1 % v/v synthetic sea water.

Factor	Unit	Lower limit	Upper limit	Start	Resolution
Nebulizer	l min^{-1}	0.5	1.5	1.1	0.3
Power	Watts	1200	1800	1500	150
Nitrogen	%	0.0	8.0	0.0	2.0
Auxiliary	l min^{-1}	0.5	2.0	1.0	0.3

The simplex was completed when the n+1 highest ratios agreed to within 5 %, and from these ratios the optimal conditions were defined. Confirmation of the position of the optimum parameters was tested by univariate searches, where n-1 parameters were held constant, whilst the remaining parameter was changed.

2.1.5 FLOW INJECTION MANIFOLD

The effect of sea water on the analytical performance of the ICP-MS was investigated by either continuously nebulizing the sample or by injecting discrete volumes (200 µl) of the sample into the instrument using a simple single channel FI manifold. A schematic diagram of the manifold is shown in Figure 2.3. A 2 % v/v HNO_3 solution was used as the carrier stream in all the FI experiments.

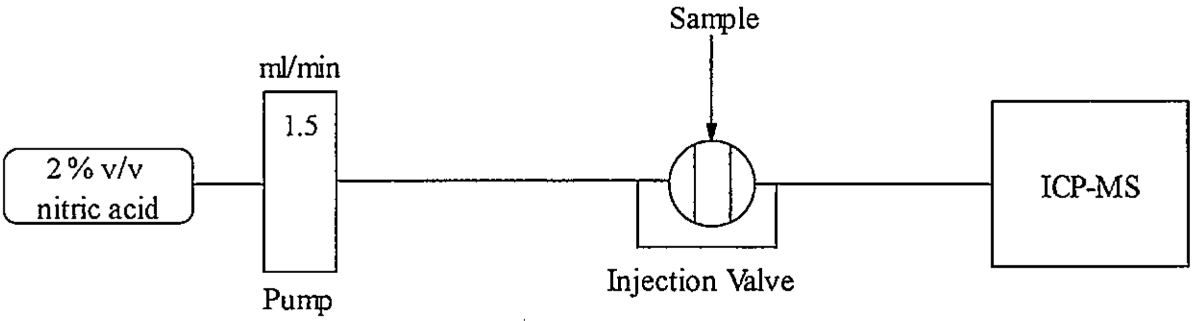

Figure 2.3 Schematic diagram of the FI manifold.

2.2 RESULTS AND DISCUSSION

2.2.1 DETERMINATION OF TRACE METALS IN SALINE AND NON-SALINE MATRICES BY ICP-MS

In Table 2.4, detection limits for a range of trace metals in 2 % v/v nitric acid and 10 % v/v synthetic sea water using continuous nebulization are compared. The interferences resulting from the 10 % synthetic sea water matrix have a significant effect on the sensitivity of the instrument with detection limits between one and three orders of magnitude poorer than those for the 2 % v/v nitric acid matrix. The signals for Cu and Zn standard solutions in 10 % v/v sea water were not detectable below 50 µg l^{-1} due to matrix interferences at m/z = 63 ($ArNa^+$) and at m/z = 64 (S_2^+/SO_2^+) respectively. The precision also deteriorated. Relative standard deviations (RSDs) for the metals of interest (n = 5, 1.0 µg l^{-1}) in 2 % v/v nitric acid were <7 % compared with 7 - 42 % for the equivalent analytes in 10 % v/v sea water. Enhancement and suppression of the signal resulting in elevated intercept values and lower gradient values was apparent for all the analytes in the 10 % v/v sea water solution (V, Cr, Fe, Ni, Mn, Co, Cu, Zn and Pb). This suggested that not only were there significant spectroscopic interferences present (*e.g.* $ArNa^+$ at m/z = 63) but also that physical deposition of material on the sampler and skimmer cones and an excess of easily ionizable elements in the matrix were causing non-spectroscopic matrix effects.

A simple and effective approach to overcoming matrix effects is the on-line dilution of the sample using FI[82-87]. Detection limits for four of the metals of interest in 2 % v/v nitric acid and 10 % v/v synthetic sea water using the FI approach are shown in Table 2.5. When 2 % v/v nitric acid was used as the diluent the detection limits for FI were poorer than by continuous nebulization (*e.g.* the detection limit for Ni was 0.74 µg l^{-1} compared with 0.11 µg l^{-1} for continuous nebulization). However, a noticeable improvement in the detection limits for Cu and Zn in 10 % v/v synthetic sea water was achieved using on-line dilution of the sample (*e.g.* FI detection limits for Cu and Zn standard solutions in 10 % v/v sea water were 10 µg l^{-1} compared with >50 µg l^{-1} using continuous nebulization).

Figure 2.4 shows the effect of varying the sea water concentration on the signal for ^{63}Cu. Enhancement of the blank signal occurs as the concentration of sea water increases due to

Table 2.4 Limits of detection (3 σ) for the metals of interest in 2 % nitric acid and a 10 % synthetic sea water matrix using continuous nebulization.

Analyte	2 % nitric acid matrix ($\mu g\ l^{-1}$)	10 % synthetic sea water matrix ($\mu g\ l^{-1}$)
^{51}V	0.01	0.59
^{52}Cr	0.04	0.26
^{54}Fe	1.64	2.45
^{58}Ni	0.11	1.11
^{55}Mn	-	50.86
^{59}Co	-	12.99
^{63}Cu	0.02	>50
^{64}Zn	0.11	71.8
^{208}Pb	0.01	0.28

Table 2.5 Limits of detection (3σ) for the metals of interest in 2 % nitric acid and a 10 % synthetic sea water matrix using flow injection (200 μl sample loop).

Analyte	2 % nitric acid matrix ($\mu g\ l^{-1}$)	10 % synthetic sea water matrix ($\mu g\ l^{-1}$)
^{58}Ni	0.74	3.96
^{63}Cu	0.04	>10
^{64}Zn	0.13	>10
^{208}Pb	0.02	0.32

increasing polyatomic ion interference from $ArNa^+$. Suppression of the signal, poor precision (RSD = 28 %, n = 3 for 5 μg l^{-1} in 25 % v/v sea water) and lack of linearity ($r^2 = 0.3570$, 25 % v/v sea water) for spiked Cu standard solutions also occurred as the sea water concentration increased. This effect was due to non-spectroscopic interferences, such as salt build-up on the cones, deterioration in nebulizer function as a result of changes in the sample viscosity, and high concentrations of easily ionizable elements, *e.g.* Li, Na, K, Cs, Mg, Ca, B and Al in the matrix. These effects have been reported previously by Beauchemin and co-workers[73] who found that some concomitant elements (Na, K, Cs, Mg, Ca) induce enhancement of the analyte signal whilst others (B, Al, U) cause a suppression.

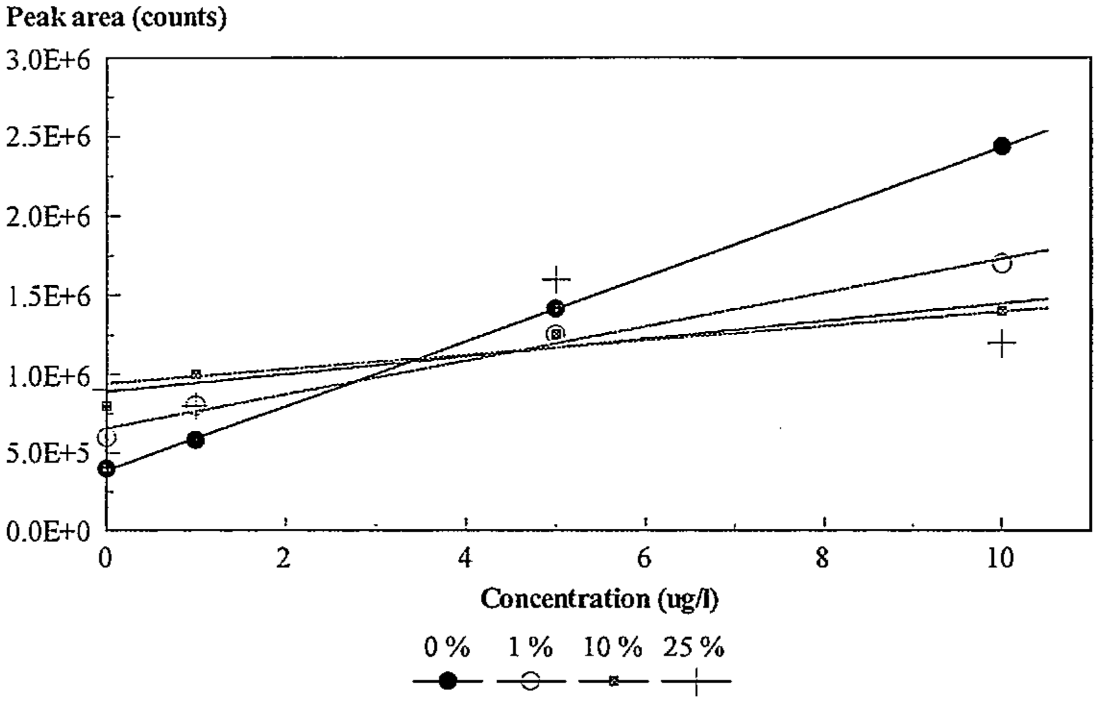

Figure 2.4 Effect of increasing sea water concentration on the ^{63}Cu signal.

It can be concluded from this initial study that although introducing discrete sample volumes though an FI manifold resulted in some improvement in the figures of merit, spectroscopic and non-spectroscopic interferences resulting from the complex nature of the synthetic sea water matrix still had a serious effect on the analytical performance of the ICP-MS. In previous studies[82-87] improvements in the figures of merit using on-line dilution procedures were more significant because the analyte levels are higher and the matrix was considerably less complex than sea water. For example, Stroh *et al.*[87] improved the detection limit for Ga in a 3 % Ni solution from 85 μg l^{-1} using continuous nebulization to 2 μg l^{-1} with 200 μl sample injections. However, because of the low levels of trace metals in sea water (see Table 1.8) and the complexity of the matrix (see Table 1.7) the improvement in the figures of merit using FI were less pronounced. Further reduction of matrix effects would be possible by diluting the sea water matrix (*e.g.* below 1 % v/v) but this would also degrade the detection limits due to the high dilution factor.

2.2.2 PRELIMINARY UNIVARIATE SEARCH

The effect of nitrogen addition to the nebulizer gas flow can be seen in Figure 2.5. When no nitrogen is added to the nebulizer gas, the apparent signal for copper at m/z = 63 increases dramatically with increasing sea water concentration. In 1 % and 10 % v/v sea water, the apparent increase in signal for Cu at m/z = 63 was 119 times and 440 times greater than the Cu signal in 2 % v/v HNO_3. With the addition of 4 % nitrogen to the nebulizer gas flow, the increase in signal at m/z = 63 was only 1.6 times in 1 % v/v sea water and 57 times in 10 % v/v sea water.

From this experiment it was apparent that the addition of nitrogen to the nebulizer flow was effective in removing the polyatomic interference at m/z = 63. However, the addition of nitrogen has also been shown to reduce the analyte intensity by previous workers[88,89].

In order to investigate this effect, nitrogen was added to the nebulizer gas at concentrations between 0 and 8 %. At each concentration of nitrogen, signal-to-background ratios for

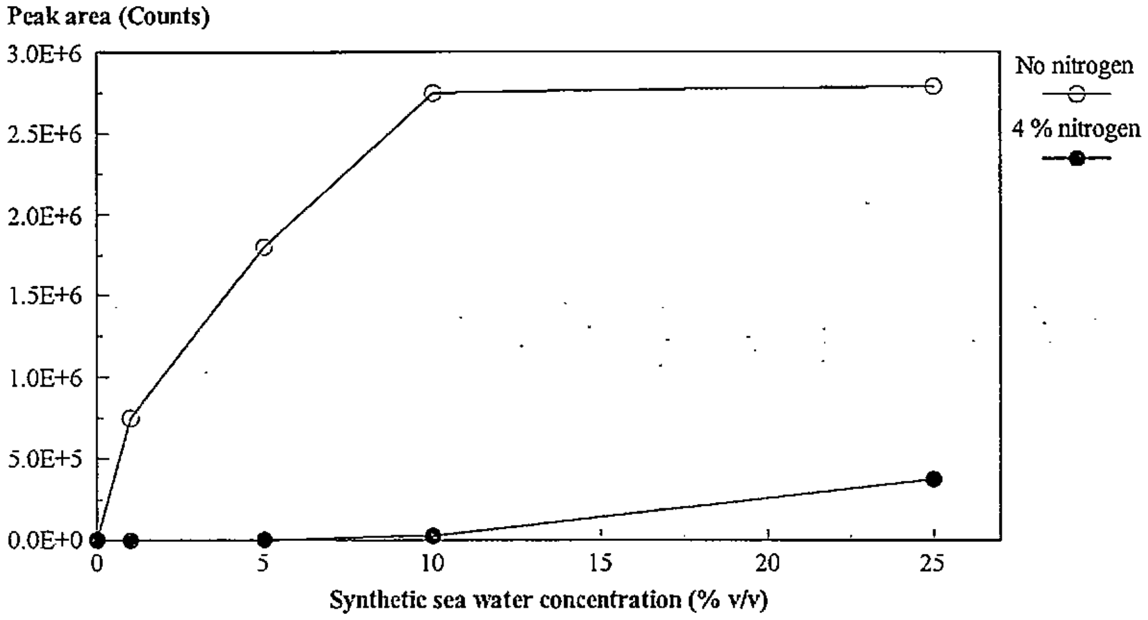

Figure 2.5 Effect of sea water concentration on the signal at m/z = 63 with and without nitrogen addition to the nebulizer gas flow.

Table 2.6 The effect of nitrogen addition on the signal-to-blank ratio (S/B) for 100 µg l^{-1} copper.

% Nitrogen addition	Nebulizer flow rate ($l\ min^{-1}$)	S/B ratio	Indium 100 µg l^{-1} (counts)
0	0.90	8.8	6.0×10^5
1.0	0.82	11.1	6.25×10^5
2.5	0.78	16.9	6.0×10^5
4.0	0.77	13.8	5.5×10^5
6.0	0.75	5.4	4.8×10^5
8.0	0.75	3.9	3.0×10^5

copper (100 μg l^{-1}) in 10 % v/v sea water were determined after the ion optics had been tuned with 100 μg l^{-1} indium. The results are summarised in Table 2.6. A decrease in the sensitivity for 100 μg l^{-1} indium from 6.0 x 10^5 to 3.0 x 10^5 counts per second was observed when re-optimising the tuning of the instrument after increasing the concentration of nitrogen. The most significant change in the instrument operating conditions, apart from fine tuning the ion optics, was the nebulizer gas flow rate. In order to achieve the maximum In signal, the nebulizer flow rate needed to be decreased (from 0.9 l min^{-1} to 0.75 l min^{-1}). Xiao and Beauchemin[89] suggested that a significant decrease in sensitivity when adding nitrogen to the outer gas was a result of a shift in the initial radiation zone when the nebulizer gas flow was kept constant. Therefore decreasing the nebulizer flow maintained the optimum sampling depth. However, in this work this was not the case. Although optimising the nebulizer flow rate after increasing the nitrogen concentration improved the In signal, the maximum signal obtained was still less than when no nitrogen was added (*e.g.* at 6 % nitrogen the In signal was 3.0x10^5 compared with 6.0x10^5 when no nitrogen was added) and it was noticed that the sampling depth still increased after optimising the nebulizer flow rate. The central channel was also much wider than when no nitrogen was added, resulting in a more diffuse central channel.

It was concluded that altering RF forward power or sample uptake rate would have improved this situation. The S/B ratio for copper at m/z = 63 increased by a factor of two (from 8.8 to 16.9) when the nitrogen concentration was increased from 0 - 2.5 %. Above 2.5 % nitrogen the S/B ratio decreased to a lower level than with no nitrogen again, a result of the increasingly diffuse central channel. This initial data indicated that the inter-dependence of the ICP-MS operating conditions needed to be taken into account and therefore a multivariate optimisation technique was used to investigate the addition of nitrogen.

2.2.3 SIMPLEX OPTIMISATION OF OPERATING CONDITIONS FOR THE REMOVAL OF $ArNa^+$ WITH NITROGEN ADDITION TO THE NEBULIZER GAS FLOW USING AN FI SAMPLE INTRODUCTION PROCEDURE

The optimal conditions for the addition of nitrogen to the nebulizer gas are given in Table 2.7. The synthetic sea water concentration was 10 % v/v. The ICP-MS survey acquire programme was used rather than the time resolved software, which required the manual integration of each peak between simplex iterations. The survey acquire programme was manipulated in such a way that only two masses were measured, using the peak jumping mode, with a scan time of 90 s per injection. The net intensities were calculated using the computer software for each mass (m/z = 59 and 63) reducing the operating time of the instrument and thus reducing the probability of long term instrument drift. The scan parameters are given in Table 2.1(b). However, the time per experiment (10 min) which included injection of the sample, calculation of the response ratios and tuning of the instrument between simplex steps still resulted in an overall experiment time of over 9 h (55 iterations). Univariate searches of the 4 variables were carried out in order to determine whether the optimum values were the same as the conditions defined by the simplex. This involved assessing the effect of changing each variable whilst the other parameters were held constant.

From Figure 2.6a - 2.6d it is apparent that the univariate searches do not agree with the simplex defined optimum conditions. The most likely explanation for this was the length of analysis time to perform the simplex (9 h). Over this time period there were drifts in the stability of the instrument as a result of temperature fluctuations in the immediate environment, and a build up of salt on the cones. It was also likely that the high concentration and complex nature of the matrix was causing significant matrix effects that were destabilising the plasma.

Table 2.7 Simplex optimum conditions for the removal of ArNa+ interference with nitrogen addition (10 % v/v synthetic sea water) using FI.

Parameter	Value
Nebulizer gas flow (l $\mathrm{min^{-1}}$)	1.0
Auxiliary gas flow (l $\mathrm{min^{-1}}$)	0.9
Forward power (W)	1600
Nitrogen (%)	2.6
Number of iterations	55

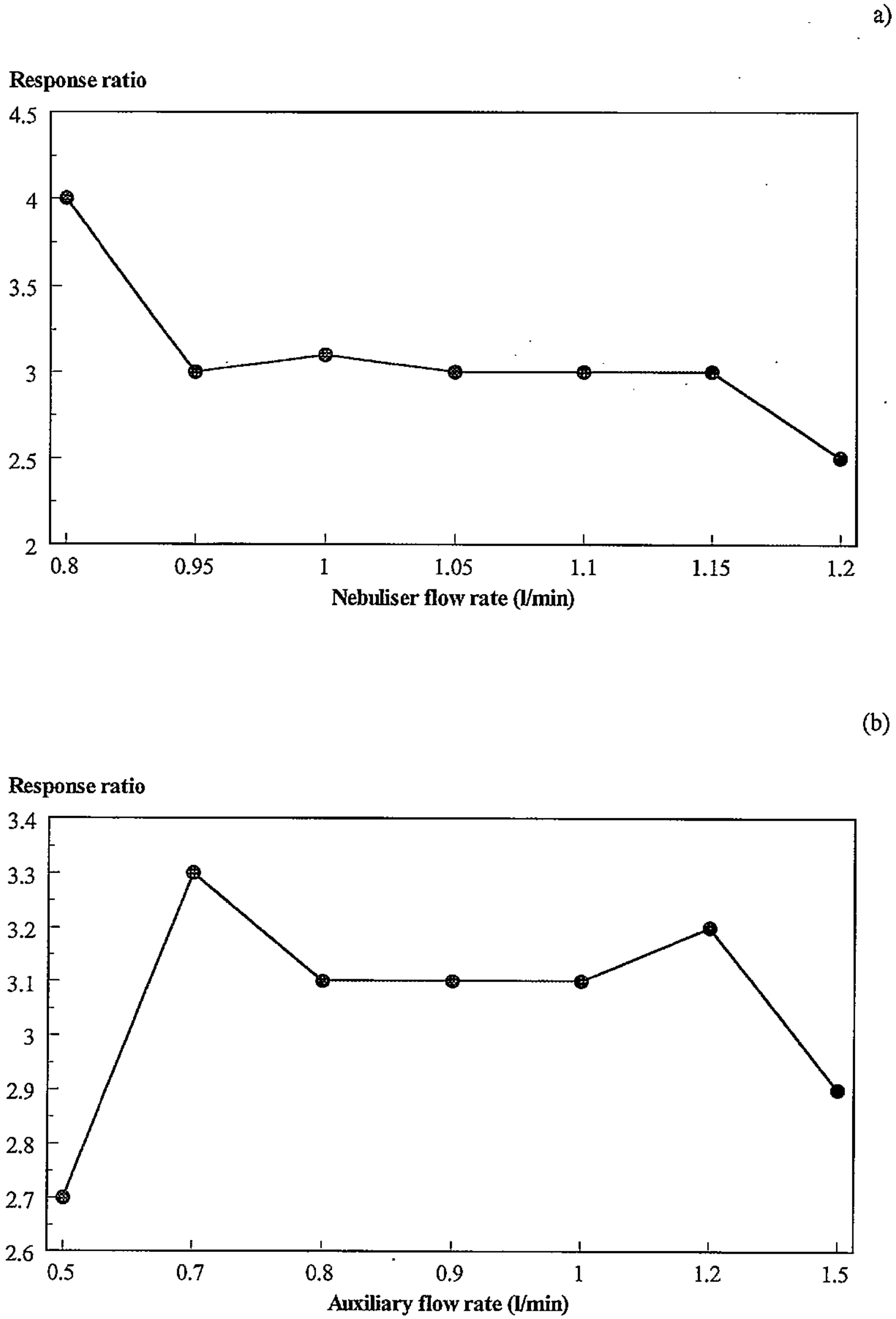

Figure 2.6 Univariate searches of the effect of (a) nebulizer gas and (b) auxiliary gas on the $Co^+/ArNa^+$ ratio.

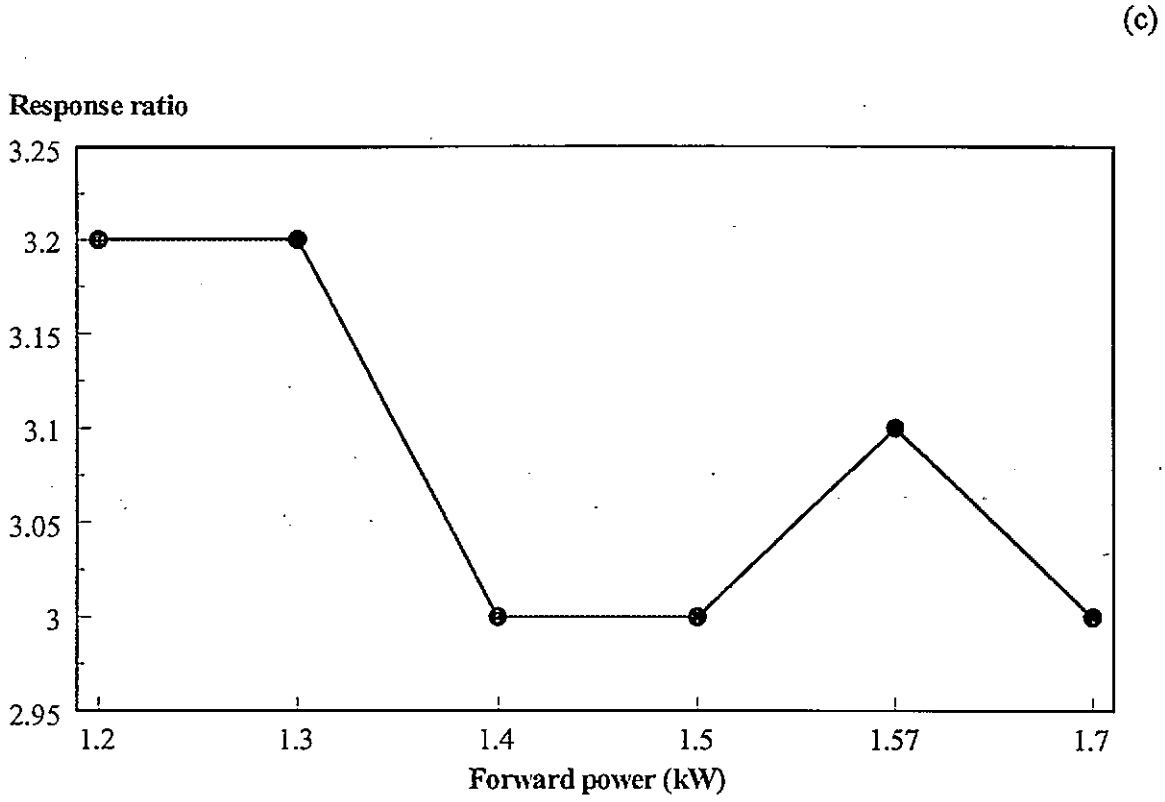

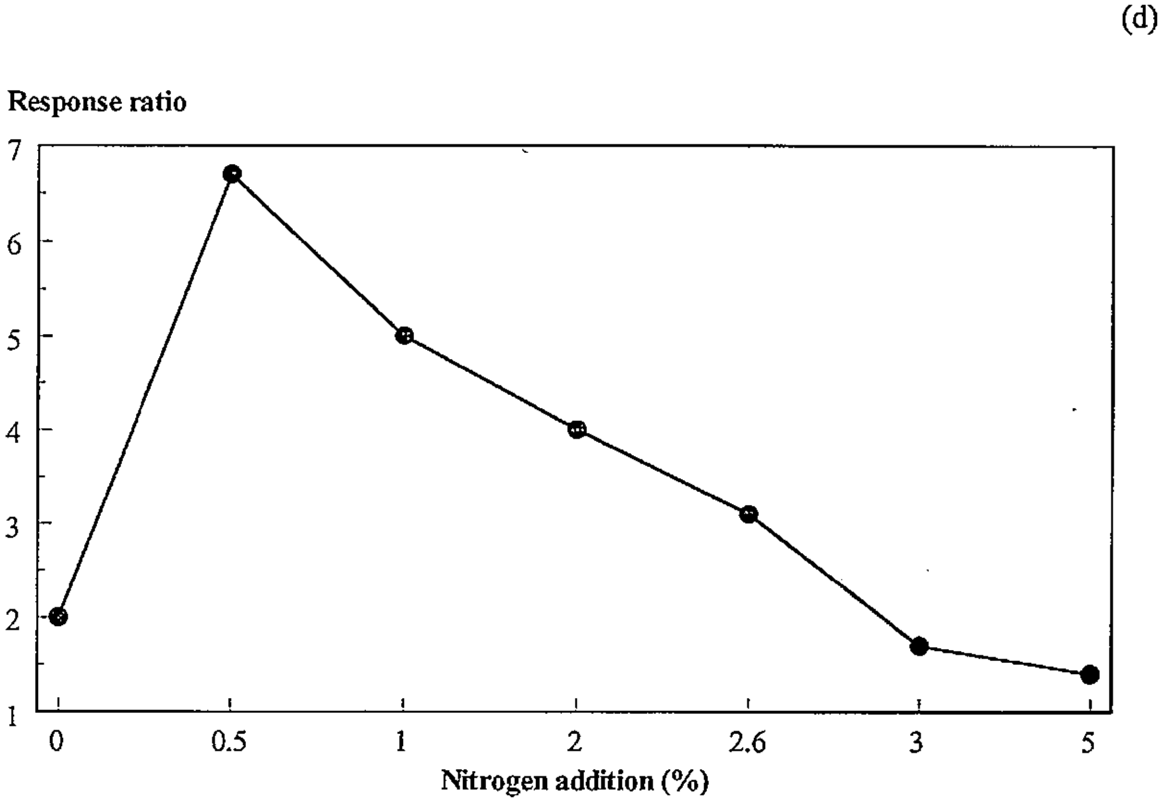

Figure 2.6 Univariate searches of the effect of (c) forward power and (d) nitrogen addition on the $Co^+/ArNa^+$ ratio.

2.2.4 SIMPLEX OPTIMISATION OF OPERATING CONDITIONS FOR THE REMOVAL OF $ArNa^+$ WITH NITROGEN ADDITION TO THE NEBULIZER GAS FLOW USING A CONTINUOUS NEBULIZATION SAMPLE INTRODUCTION PROCEDURE

Due to the failure of the procedure described in Section 2.2.3, it was necessary to reduce both the operating time and the concentration of the matrix. Reduction in operating time would reduce the likelihood of instrument stability problems due to temperature changes and salt build-up on the cones. Dilution of the matrix would also reduce salt build-up on the cones and matrix effects from easily ionizable elements which were effecting the stability of the plasma. Therefore the instrument was used in the conventional continuous nebulization mode and the sea water concentration was decreased to 1 % v/v. The optimal conditions for this procedure are given in Table 2.8 and the simplex history is shown in Figure 2.7.

The simplex was stopped after 53 iterations and the time taken to reach this point was 3 h 30 min. The optimum conditions using continuous nebulization were considerably different from the FI optimisation described in Section 2.2.3 and the optimum concentration of nitrogen (0.8 %) was much lower than previous reports in the literature[90,91,93,95,98] of between 3.5 - 8.0 %. This is because previous workers have concentrated specifically on chloride as opposed to sodium interferences and have optimised the operating parameters using the Ar^+Cl^- interference at m/z = 75 and 77, rather than the $ArNa^+$ interference at m/z = 63.

The reduction in the sensitivity for Co^+ from 3872 to 1674 CPS was far less severe than the reduction in $ArNa^+$ response which was virtually eliminated (from 1173 to 29 CPS). The optimum parameters for forward power and nebulizer flow rate were in general agreement with those reported by Gray and Williams[49] who, when discussing the optimisation of argon

Table 2.8 Simplex optimum conditions for the removal of ArNa+ interference with nitrogen addition (1 % v/v synthetic sea water) under continuous nebulization.

Parameter	Value
Nebulizer gas flow (l min^{-1})	1.26
Auxiliary gas flow (l min^{-1})	0.9
Forward power (W)	1350
Nitrogen (%)	0.8

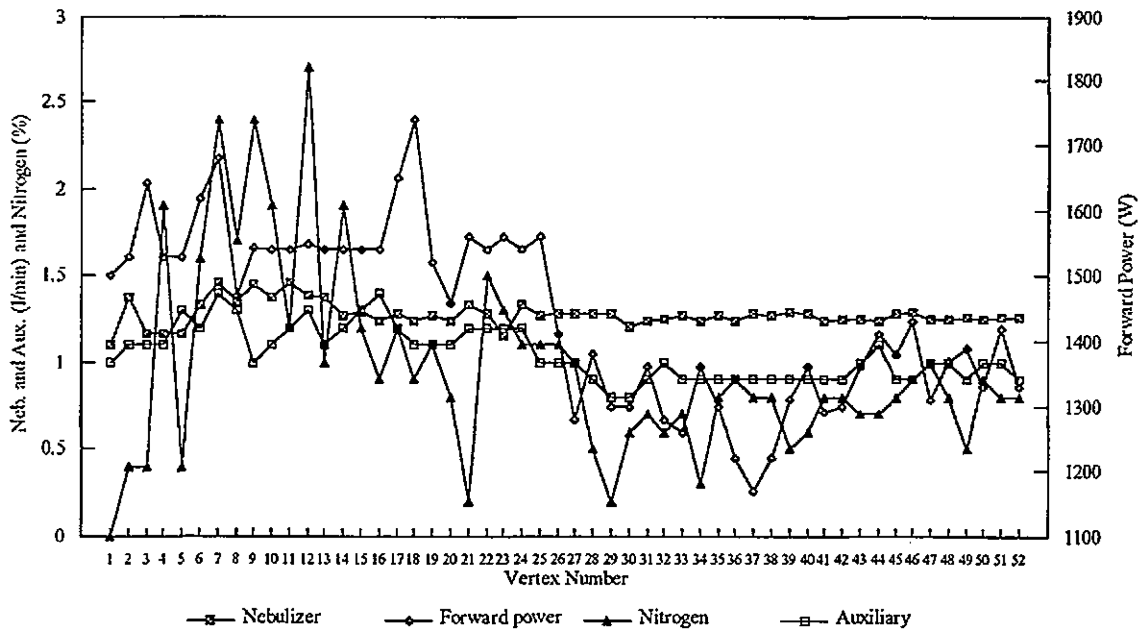

Figure 2.7 Simplex history.

only plasmas, found that low power (1100 W) and high nebulizer flow rates (>1.0 l min^{-1}) were the most important factors for suppressing polyatomic ion interferences.

Univariate searches at the optimal simplex conditions are given in Figures 2.8a - 2.8d and show that the optimum values were the same as the conditions defined by the simplex (Table 2.8). It can be seen that although an all argon plasma, low nebulizer flow rates (<1.0 l min^{-1}) and high forward power levels (>1600 W) generally gave the largest signals for the analyte of interest, these conditions also gave the poorest $Co^+/ArNa^+$ response ratios, due to high background levels. The addition of nitrogen to the nebulizer gas improved the ratio of $Co^+/ArNa^+$ from 2 without nitrogen to nearly 60 with 0.8 % nitrogen, a 30-fold increase in the response ratio.

In Table 2.9 limits of detection (3σ) for a range of metal ions in 1 % v/v synthetic sea water, using the optimised continuous nebulization conditions described above, are compared with those obtained using standard operating conditions (shown in Table 2.2). The detection limit for copper at m/z = 63 was significantly improved (from 12.19 μg l^{-1} to 0.06 μg l^{-1}) due to the removal of the polyatomic interference at that mass. Precision was enhanced with RSD values (1.0 μg l^{-1}, n = 5) of 2.6 % compared with 16.8 % with an all-argon plasma operating under standard operating conditions (Table 2.2). Linearity was also improved over the range 0-10 μg l^{-1} with correlation coefficients of 0.9996 with the optimised operating conditions, compared with 0.9322 for the standard operating conditions. The figures of merit for Zn at m/z = 64 were also dramatically improved, due to the removal of the S_2^+/SO_2^+ interference at this mass. Detection limits were improved from 16.63 μg l^{-1} to 0.22 μg l^{-1} and precision increased from 9.2 % to 4.3 % (1.0 μg l^{-1} , n = 5). Suprisingly, a very large increase in sensitivity was also achieved for Mn at m/z = 55.

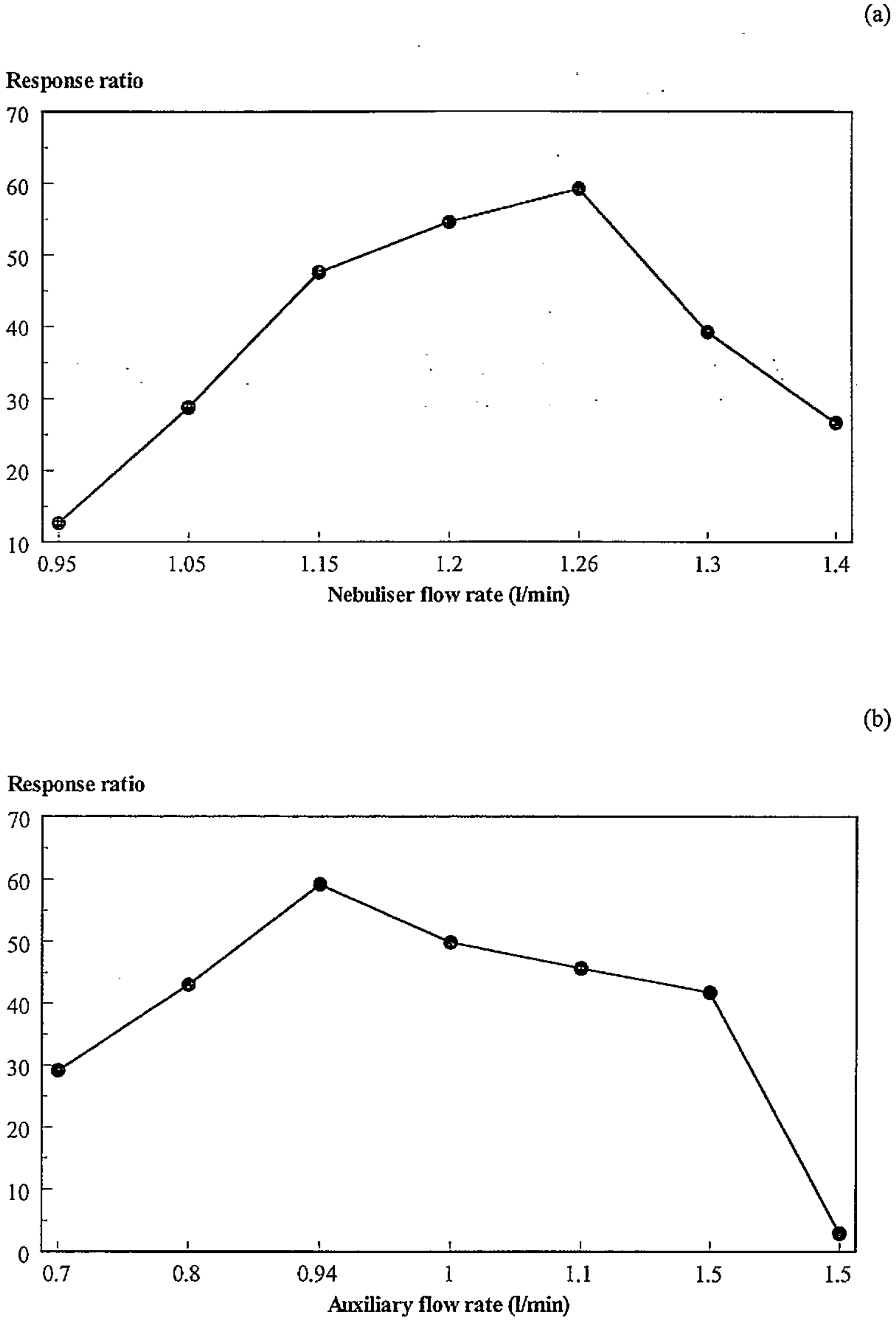

Figure 2.8 Univariate searches of the effect of (a) nebulizer gas and (b) auxiliary gas on the $Co^+/ArNa^+$ ratio.

(c)

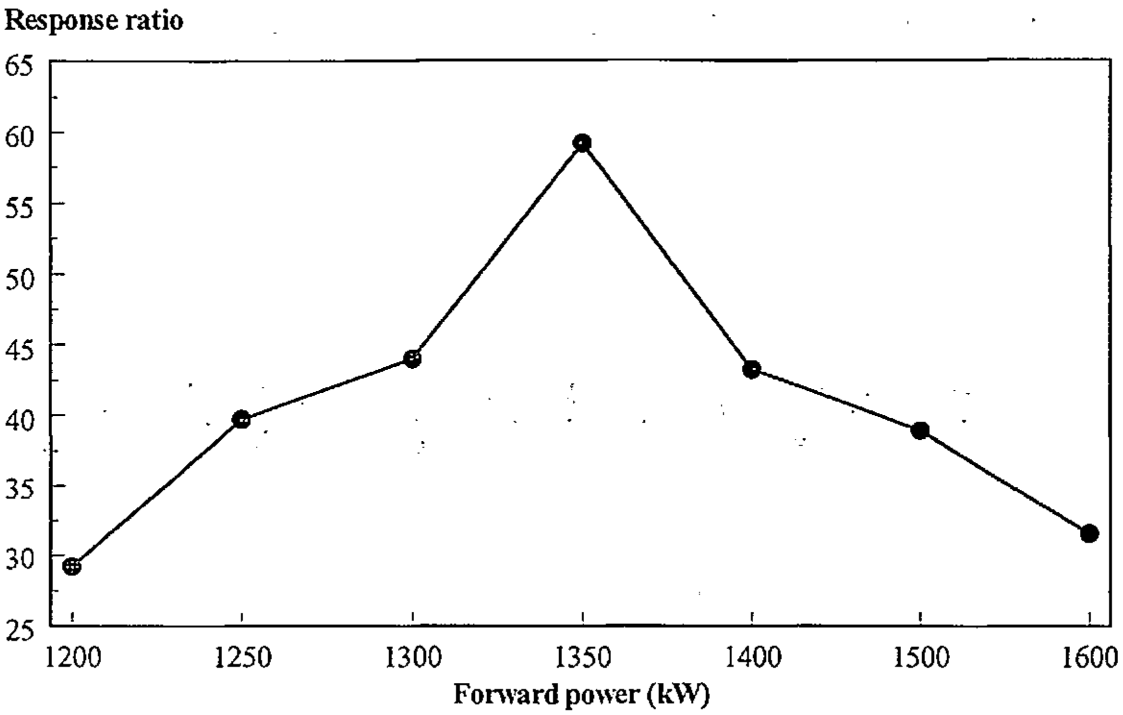

(d)

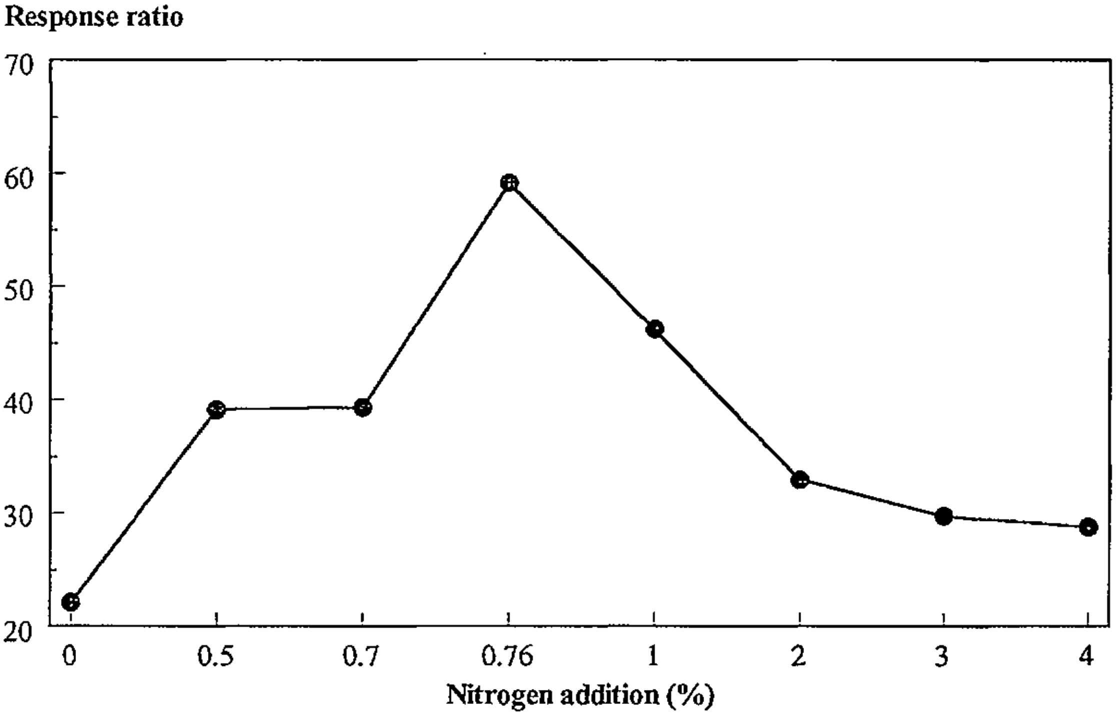

Figure 2.8 Univariate searches of the effect of (c) forward power and (d) nitrogen addition on the $Co^+/ArNa^+$ ratio.

The polyatomic interference at this mass is $ArNH^+$ and it would have been assumed that nitrogen added to the plasma would reduce the sensitivity at this mass. The instrument optimisation at m/z = 63 and particularly the optimisation of the nebulizer flow rate resulted in a decrease in signal enhancement and/or suppression due to the partial removal of concomitant or matrix interferences. Tan and Horlick[76] suggested that matrix effects are strongly dependent on nebulizer flow rate. This improved the detection limits for Co (from 9.22 to 1.32 μg l^{-1}), Ni (from 0.37 to 0.28 μg l^{-1}) and Pb (from 0.08 to 0.05 μg l^{-1}).

A degradation in the detection limit for vanadium when using the optimised conditions occurred (0.23 μg l^{-1} for the standard operating conditions compared with 0.77 μg l^{-1} for the simplex optimised conditions), as a result of NCl^+ interference at m/z = 51. This is not in accordance with results reported by Hill *et al.*[95] who found that 3.41-8.11% nitrogen resulted in values of 100 μg l^{-1} vanadium within 10 % of that expected for all N ratios and levels of Cl. However the improvement achieved was due to the optimisation of the operating parameters using the Ar^+Cl^- interference at m/z = 75, rather than the $ArNa^+$ interference at m/z = 63.

The addition of nitrogen to the nebulizer gas flow caused a significant interference for iron at m/z = 54 due to the ArN^+ dimer. This resulted in a degradation in detection limits from 1.0-4.0 μg l^{-1} for the standard operating conditions to 287.5 μg l^{-1} for the simplex optimised conditions.

Table 2.9 Comparison of limits (3σ) of detection for the analytes of interest under simplex optimised conditions and standard operating conditions.

	Optimised operating conditions	**Standard operating conditions**
Analyte	1 % v/v synthetic sea water matrix (µg l^{-1})	1 % v/v synthetic sea water matrix (µg l^{-1})
^{51}V	0.8	0.2
^{52}Cr	0.2	0.2
^{54}Fe	300	2.0
^{58}Ni	0.3	0.4
^{55}Mn	1.7	180
^{59}Co	1.3	9.2
^{63}Cu	0.06	12.1
^{64}Zn	0.2	16.6
^{208}Pb	0.05	0.08

2.3 CONCLUSIONS

The addition of nitrogen to the nebulizer gas flow was effective in removing polyatomic ion interferences for copper at m/z = 63. Multivariate simplex optimisation of the ICP-MS virtually eliminated $ArNa^+$ interference at m/z = 63. A decrease in the analyte intensity was apparent but a greater reduction in background intensity resulted in significantly improved detection limits for copper from 12.9 µg l^{-1} using standard ICP-MS operating conditions to 0.06 µg l^{-1} for simplex optimised conditions. Concomitant interference at other masses, notably ^{58}Ni, ^{59}Co, ^{55}Mn and ^{208}Pb, were also reduced using the optimised conditions for ^{63}Cu, although not as dramatically as for $^{63}Cu^+$.This resulted in improved detection limits for these elements, *e.g.* Mn at m/z = 55 was improved from 180 µg l^{-1} to 1.72 µg l^{-1}.

Concentrations of >10 % v/v presented problems in terms of instrument stability due to the salt loading of the sea water matrix. Therefore, when simplex optimisation of the instrument was being carried out, a maximum of 1 % v/v synthetic sea water was used. However, in terms of detection limits, a 1 % dilution of the original sample will not achieve the detection levels required for the elements of interest in real sea water samples without preconcentration. For example the limit of detection calculated in a 1 % v/v sea water solution (0.06 µg l^{-1}) equates to 6.0 µg l^{-1} in undiluted sea water, whereas mean copper concentrations in sea water are generally below 0.5 µg l^{-1}. As a method to overcome this problem, a FI procedure is a potentially attractive option. However, the use of FI when simplex optimising the ICP-MS presented problems due to long term instrument drift.

In summary, although this method is not applicable for the determination of trace metals in sea water, it would be suitable for the analysis of high salinity industrial brines and discharge waters.

CHAPTER 3

On-line Removal of Matrix Interferences in Sea Water by Flow Injection with Inductively Coupled Plasma Mass Spectrometric Detection

CHAPTER 3: ON-LINE REMOVAL OF MATRIX INTERFERENCES IN SEA WATER BY FLOW INJECTION WITH INDUCTIVELY COUPLED PLASMA-MASS SPECTROMETRIC DETECTION

Introduction

ICP-MS is widely used for trace metal analysis but the formation of polyatomic ions (particularly below m/z = 80) can cause serious interferences[48]. Such species can be introduced via atmospheric gases, the sample matrix or impurities in the argon support gas, and cause a systematic error.

The determination of trace metals in sea water using ICP-MS can be problematic due to the high dissolved solids loading of the matrix (3 % m/v). This can result in the physical deposition of material on the sampler and skimmer cones which can subsequently restrict the orifices, resulting in a reduction in sensitivity and long term stability. The nature of the sea water matrix also results in a number of polyatomic ion interferences from elements such as Na, Ca, Cl and S which can considerably degrade the analytical capabilities of the instrument. Polyatomic interferences are summarised in Table 1.2 (Chapter 1). Reduction of these interferences can be achieved by diluting the matrix but this process reduces the sensitivity. This is important in sea water analysis, since trace metal levels are often below 0.5 μg l^{-1}. Table 1.8 in Chapter 1 summarises the concentration of selected elements in sea water, *e.g.* a limit of detection for copper at m/z = 63 in sea water of >10 μg l^{-1} can be expected, as opposed to <10 ng l^{-1} in a non-saline matrix. Reported detection limits for a range of trace metals are presented in Tables 2.3 and 2.4 (Chapter 2).

Some reduction of the interfering ions or the effects of the interfering ions can be achieved by careful setting of the instrument parameters[58]. However, in order to facilitate a more complete removal of polyatomic interferences, further procedures are generally required. The addition of molecular gases such as nitrogen has been shown to dramatically reduce polyatomic ions such as $ArNa^+$, $ArCl^+$ and ClO^+ [91,93,95,98], *e.g.* in Chapter 2, $ArNa^+$ response was virtually eliminated (from 1173 to 29 CPS). Precision and accuracy can also be significantly improved by using internal standardisation or isotope dilution[80]. Overcoming matrix interference problems can also be accomplished by separating the analytes from the matrix and various liquid chromatographic approaches including anion exchange[65], reverse phase[174] and size exclusion chromatography[178] have been used successfully.

Chelation exchange resins containing iminodiacetate (IDA) or quinolin-8-ol functional groups have been used extensively to separate first row transition metals from complex matrices such as sea water and biological samples[127,130,221-223]. Historically such techniques have been performed off-line but this approach is slow, requires large sample volumes and is susceptible to contamination due to increased sample handling. In contrast on-line micro-columns with dimensions of 2.0 x 0.2 cm or less incorporated into flow injection (FI) manifolds can provide rapid, low volume, contamination free procedures[31,109,123]. This was discussed in detail in Section 1.2.2.

This chapter discusses an on-line FI-ICP-MS matrix elimination method for the determination of trace metals such as Mn, Co, Cu, Zn and Pb in sea water. It involves chelation of the analytes onto either Chelex-100 IDA resin packed into Omnifit columns or a Dionex MetPac IDA based resin in a pre-packed micro-column, with the simultaneous removal of indirectly interfering matrix species such as Na and Cl ions. Results showing how the effects of the interferences are overcome, together with validation of the method by the analysis of open ocean, coastal and estuarine certified reference materials are reported.

3.1 EXPERIMENTAL

3.1.1 INSTRUMENTATION

Initial studies were carried out using a flame atomic absorption spectrometer (I.L. 151, Thermo Electron, Warrington, Cheshire). Subsequent analyses were performed on either a standard VG PlasmaQuad PQ2 ICP-MS or a standard Fisons PlasmaQuad PQ2 Turbo+ ICP-MS (Fisons Elemental, Winsford, Cheshire, U.K.). Both instruments were operated in the time resolved analysis monitoring mode. The sample introduction system was modified by the inclusion of an Ebdon nebulizer (PS Analytical, Sevenoaks, Kent, U.K.). Full instrument details (FAAS) are given in Table 3.1. Typical ICP-MS operating conditions are presented in Table 2.1 (Chapter 2). The ICP-MS time resolved analysis parameters together with the isotopes used for each element are given in Table 3.2.

3.1.2 FLOW INJECTION MANIFOLD

A schematic diagram of the FI manifold is shown in Figure 3.1. The reagents were pumped at a flow rate of 0.8 ml min^{-1} using peristaltic pumps (Ismatec Mini-S 820, Ismatec, Switzerland) and PVC peristaltic pump tubing. The switching valves (PS Analytical, Sevenoaks, Kent, U.K.) were pneumatically operated using argon gas (20 psi). The procedure by which injections were made was as follows;

(1) The sample loop (100-1000 μl) on valve 1 was filled with the sample via peristaltic pump 2.

(2) Valve 1 was switched so that the contents of the loop were eluted onto the column in a carrier stream of ammonium acetate buffer via peristaltic pump 2.

Table 3.1 FAAS Operating conditions for the determination of copper.

Copper	
Wavelength (nm)	324.7
Spectral Bandpass (nm)	1.0
Lamp Current (mA)	5
Slit Width (µm)	320
Burner Head	Single Slot

Table 3.2 ICP-MS time resolved analysis parameters and isotopes used for each element.

Time resolved scan parameters	
Channels per AMU	2048
PC Dwell Time	320 µs
Sweeps	100
Collector Type	PC
Mass Range	5.5 - 239.5 AMU

Selected isotopes		
Element	**Mass**	**Abundance (%)**
Copper	63	69.1
Nickel	58	67.8
Zinc	64	48.9
Chromium	52	83.8
Manganese	55	100
Vanadium	51	99.7
Lead	208	52.4

(3) Valve 2 was orientated such that the solution emerging from the end of the column went to waste.

(4) After 3-4 minutes valve 2 was switched to direct the flow to the detector.

(5) The sample loop on valve 3 was then filled with the nitric acid eluent (2.0 M) from peristaltic pump 3, which on switching valve 3, eluted the analyte from the column into the detector.

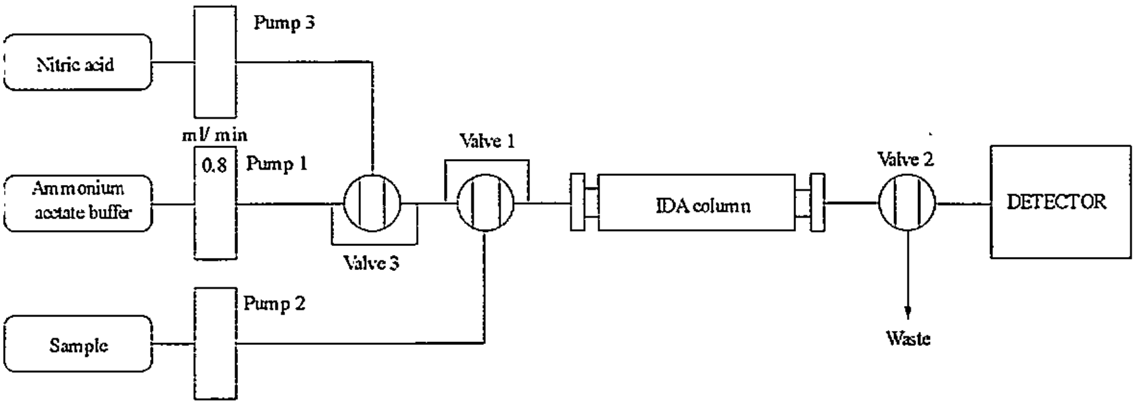

Figure 3.1 A schematic diagram of the FI manifold.

3.1.3 REAGENTS

High purity de-ionised water purified by a Milli-Q analytical reagent grade water purification system (Millipore) was used throughout. All reagents were Aristar grade and purchased from Merck (Poole, Dorset, UK.), apart from the nitric acid used in the analysis of the CRM's (Romil double sub boiling distilled nitric acid, Romil Chemicals Ltd). Stock solutions of ammonium acetate buffer (3.0 M) were prepared by mixing appropriate amounts of acetic acid with ammonia solution and diluting to volume. Nitric acid eluent (2.0 M) was prepared by diluting nitric acid with water. Stock solutions of the analytes of interest (10 mg l^{-1}) were prepared from commercial stock solutions (1000 mg l^{-1}, SpectrosoL, Merck). Standard solutions were prepared daily by dilution of the stock solutions with appropriate volumes of synthetic sea water solution (Corrosion test solution, Merck). Stock solutions were stored in acid washed (10 % v/v nitric acid, Aristar grade) polypropylene containers. Standard solutions were made up in acid washed volumetric flasks (25 or 100 ml, grade A).

3.1.4 CERTIFIED REFERENCE MATERIALS

Reference materials have been available for more than 70 years but the importance in validating analytical measurements was not fully recognised until about 20 years ago[224]. The recent increase in reference materials has led to the need for international agreement in nomenclature, certification and methods of use. The Council Committee of Reference Materials of the International Organisation for Standardisation (ISO-REMCO) were the first to formally define such materials (ISO guide 30-1981[E]):

Reference material (RM) A material or substance one or more properties of which are sufficiently well established to be used for the calibration of a method, or for assigning values to materials.

Certified reference material (CRM) A reference material one or more of whose property values are certified by a technically valid procedure, accompanied by or traceable to a certificate which is issued by a certifying body.

There are 3 approaches used for the certification of a reference material:

1. Definitive method, usually undertaken by a single laboratory employing a method that is based on first principles.

2. Independent measurement method, usually undertaken by one laboratory using two or more reliable independent methods.

3. Interlaboratory consensus method, where 5 - 20 laboratories analyse in replicate one or more units of the material being evaluated.

CRMs are used for four main purposes:

(a) Calibration and verification of measurement processes under routine conditions.
(b) Internal quality control and quality assurance schemes.
(c) Verification of the correct application of standardised methods.
(d) Development and validation of new methods of measurement.

Three CRMs were analysed in this experiment. These were an open ocean sea water (NASS-3), a coastal sea water (CASS-2) and an estuarine water (SLEW-1). NASS-3 was collected at the 1300 metre level, southeast of Bermuda (32° 10'S, 64° 30'W). It is representative of a North Atlantic open ocean water (35.1S). CASS-2 (29.2S) was collected at the 5 metre level 10 km south of Halifax, Nova Scotia, Canada. SLEW-1 (11.6S) was gathered in the St. Lawrence River estuary at the 5 metre level. All 3 CRMs were filtered through 0.45 μm porosity filters, acidified immediately with nitric acid to pH 1.6, re-filtered through 0.2 μm porosity filters and bottled in 2 litre polyethythene containers. Table 3.3. shows the thirteen metals for which certified values have been established in the NASS-3 CRM.

Table 3.3 Thirteen metals for which certified values have been established in the NASS-3 CRM.

Element	$\mu g.l^{-1}$
As	1.65 ± 0.19
Cd	0.029 ± 0.004
Cr	0.175 ± 0.010
Co	0.004 ± 0.001
Cu	0.109 ± 0.011
Fe	0.327 ± 0.022
Pb	0.039 ± 0.006
Mn	0.022 ± 0.007
Mo	11.5 ± 1.9
Ni	0.257 ± 0.027
Se	0.024 ± 0.004
U	3.0 ± 0.15
Zn	0.178 ± 0.025

3.2 RESULTS AND DISCUSSION

3.2.1 PRECONCENTRATION OF TRACE METALS USING CHELEX-100

3.2.1.1 Properties of Chelex-100

Chelex-100 is a microporous polystyrene divinylbenzene (PS-DVB) polymer containing paired IDA ions which act as chelating groups in binding polyvalent metal ions. Its selectivity for divalent ions over monovalent ions is approximately 5000:1 and it has a strong preference for transition metals such as Cu and Zn over cations such as Na and K, even in highly concentrated salt solutions. This makes it well suited to a range of applications, including removing, concentrating or analysing trace metals in natural waters[222], reagents[225] and biological solutions[226]. IDA resins such as Chelex-100 differ from ion exchangers not only in their high selectivity for metal ions but also in their much higher bond strengths, of the order of 63 - 105 kJ mol^{-1} compared to 8 - 13 105 kJ mol^{-1} for monovalent ion exchangers, and their slower kinetics which are governed by second order kinetics rather than by diffusion.

The quantitative measurement of the affinity that Chelex-100 displays for a particular cation is termed the selectivity factor and is compared with its affinity to a reference cation (Zn). A list of selectivity factors for several divalent cations is given in Table 3.4.

The quantity of metal cations retained by Chelex-100 is a function of pH. Below pH 2.0 the resin acts as an anion exchanger and adsorption of metal cations does not occur. Above pH 4.0 maximum adsorption occurs and the metal cations removed from solution replace an equivalent amount of cations on the resin (e.g. $[NH_4]^+$). The capacity of the sodium form of the resin is 0.4 meq ml^{-1} (defined as $Cu(NH_3)_4^{2+}$ uptake).

Table 3.4 Selectivity for divalent cations.

Element	Selectivity factor
Hg	1060
Cu	126
UO	5.70
Ni	4.40
Pb	3.88
Zn	1.00
Co	0.615
Cd	0.390
Fe	0.130
Mn	0.024
Ba	0.016
Ca	0.013
Sr	0.013
Mg	0.09
Na	1×10^{-7}

The most effective eluting agents are mineral acids, although complexing agents, *e.g.* thiourea, can also be used. The regeneration of the sodium form of the resin loaded with copper is a two step process:

$$\text{Resin-Cu} + 2\text{HCl} \longrightarrow \text{Resin-H} + \text{CuCl}_2$$

$$\text{Resin-H} + \text{NaOH} \longrightarrow \text{Resin-Na} + \text{H}_2\text{O}$$

A volume change occurs with Chelex-100 when its ionic form is altered or the external medium is changed. This can result in up to a 100 % increase in volume when going from the hydrogen to a monovalent salt form and is a major drawback of this resin when incorporated into FI manifolds, resulting in high back-pressure.

3.2.1.2 Optimisation of the FI procedure

A slurry of Chelex-100 resin (Biorad, Hemel Hempstead, Herts. UK.) (sodium form, 50-100 mesh, 0.4 meq/ml, 0.3 g) was introduced into an Omnifit column (30 mm x 5 mm i.d.) with a syringe. Once loosely packed, the column was washed with nitric acid (3.0 M, 20 ml) in order to elute interfering sodium ions and allow the resin to shrink and settle. The procedure was repeated until no voids were visible. The column was finally rinsed with de-ionised water.

The effect of various concentrations of a synthetic sea water matrix on the breakthrough of 5 mg l^{-1} Cu on the resin was examined. The results are shown in Figure 3.2. It can be seen that increasing sea water concentration above 25 % v/v increased the breakthrough of Cu which was inversely related to the peak height of the analyte eluted with acid. This trend was also observed for Ni and Zn. It was also noticed that the FAAS flame glowed orange on elution of the Cu which indicated that sodium was being retained on the column.

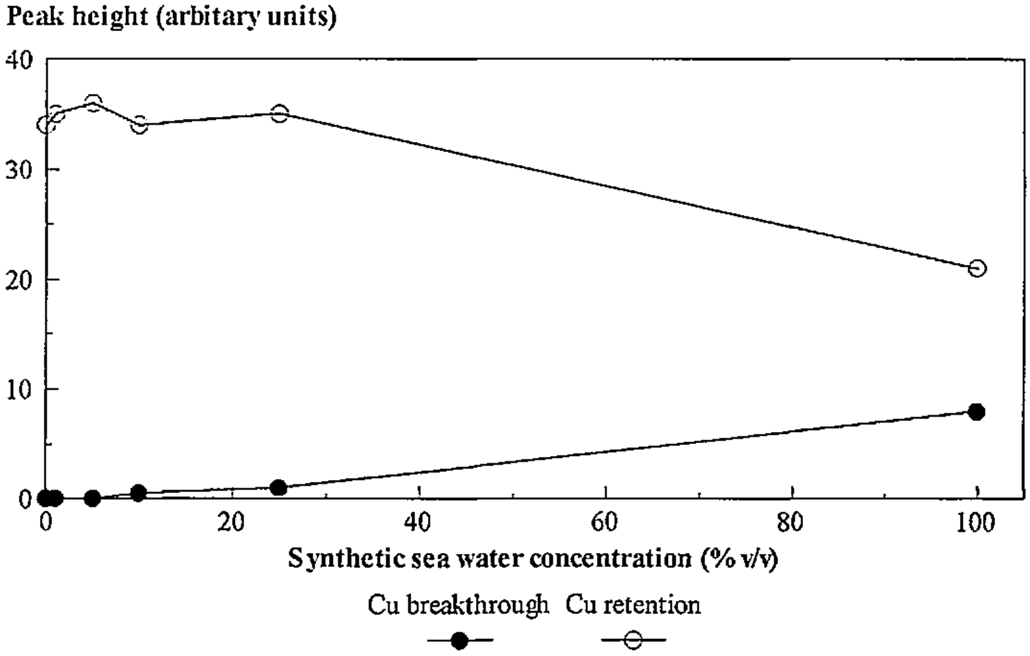

Figure 3.2 Effect of synthetic sea water concentration on the breakthrough of copper (carrier stream, 1.5 M ammonium acetate buffer; acid eluent, 3.0 M nitric acid).

The remaining optimisation experiments were carried out using a 10 % v/v sea water concentration as this was the highest concentration (least dilution) at which no breakthrough of copper was observed.

The buffer concentration and pH of the carrier stream was also examined. The results are shown in Figure 3.3. At ammonium acetate concentrations of between 0.5 and 2.5 M, there was no breakthrough of Cu. However, it was again observed that the flame changed to a sodium orange colour upon elution of the analyte. This colour change was greater at lower buffer concentrations (below 1.0 M) suggesting that the buffer was inadequate at preventing sodium from being retained on ion exchange sites in the resin. The optimum pH range was very wide (pH 4.5 - 8.0). Within this range no breakthrough of copper was observed.

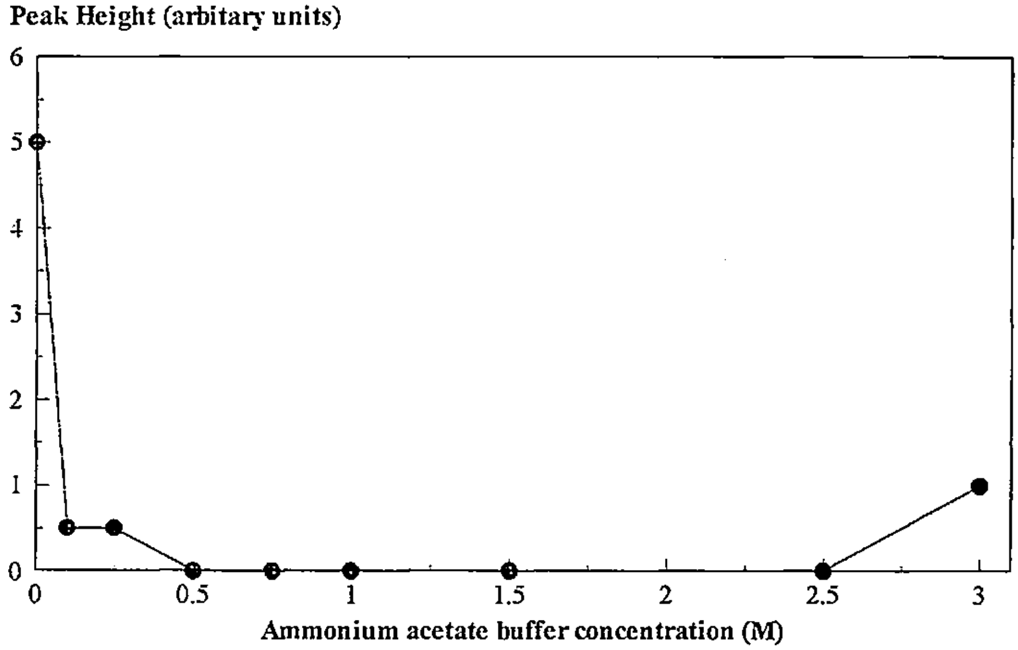

Figure 3.3 Effect of ammonium acetate buffer concentration on the breakthrough of Cu in 10% v/v synthetic sea water.

The continued presence of sodium when eluting the analyte of interest was investigated. If sodium was retained on the column when determining trace levels of the metals of interest in sea water with ICP-MS detection, it would be likely that spectroscopic and non-spectroscopic interferences resulting from this element would considerably degrade the sensitivity of the instrument. By measuring the sodium emission line at 589 nm (Figure 3.4) it can be seen that sodium was indeed being retained on the column and that removal of this element was only achieved after three successive injections of the nitric acid (3.0 M) eluent.

This effect was overcome by increasing the buffer concentration from 1.0 M to 2.0 M. However, this approach resulted in severe swelling, under basic conditions, of the resin due to the low cross linking of the (gel type) microporous polystyrene divinylbenzene supporting polymer. The increased swelling meant that the FI manifold leaked due to increased back pressure.

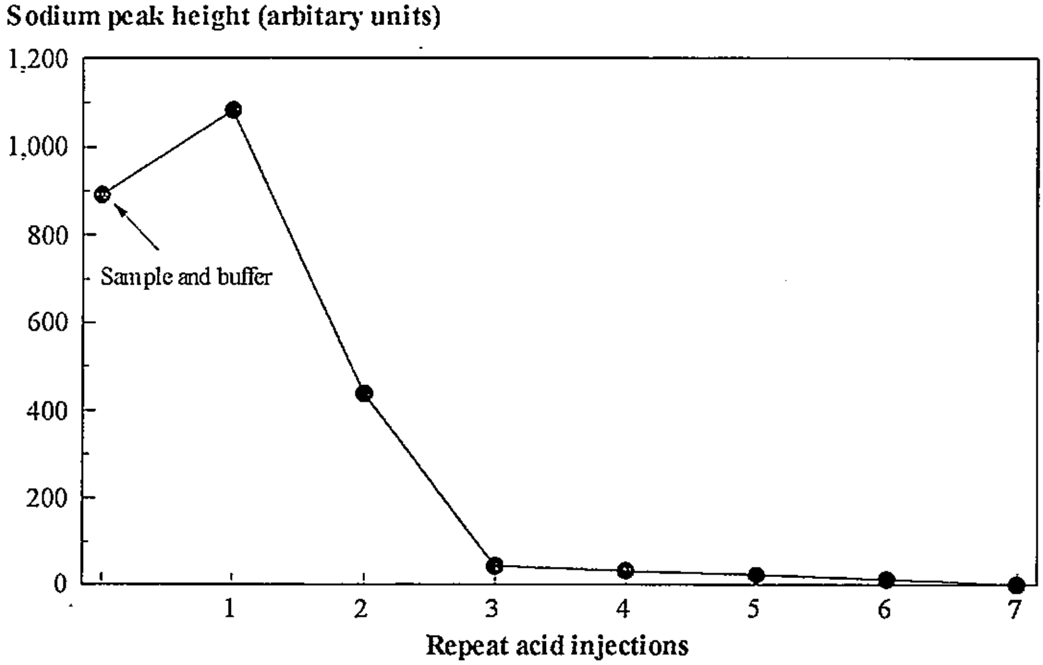

Figure 3.4 Investigation of the retention of sodium on Chelex-100.

The investigation of successive discrete injections of buffer (2.0 M, 200 µl) onto the column after the sample had been injected was also examined. A de-ionised water carrier stream was used instead of ammonium acetate buffer (1.0 M). Although the second injection of ammonium acetate buffer resulted in the elution of a large proportion of the sodium, retention due to non-selective ion exchange processes, still occurred. This retained sodium was again removed with nitric acid (3.0 M).

It was concluded that Chelex-100 was unsuitable for the concentration of trace metals in sea water due to problems associated with non-selective retention of potential interferents such as sodium and substantial volume changes in acidic and basic solutions due to the low cross-linking of the support polymer.

3.2.2 PRECONCENTRATION OF TRACE METALS USING METPAC CC-1

3.2.2.1 Properties of MetPac CC-1

Due to the problems associated with Chelex-100, another approach was needed. A more highly cross-linked macroporous PS-DVB containing the IDA functional group was supplied by the Dionex Corporation pre-packed into 50 mm x 4.0 mm i.d. columns, with a theoretical column capacity of 0.45 milliequivalents (0.7 meq ml^{-1}). The relative selectivity of the resin is the same as that for Chelex-100 (see Section 3.2.1.1.). As with Chelex-100, the higher the cationic charge of the metal ion, the more strongly bound the metal ion is to the resin. The structure of MetPac CC-1 is shown in Figure 3.5. Mineral acids such as hydrochloric or nitric acid at 0.5 - 2.0 M are effective eluents. Below pH 2.5 MetPac CC-1 does not concentrate metals. In the pH range 5.0 - 6.0, resin selectivity is optimised for transition and lanthanide metals relative to alkali and alkaline-earth metals.

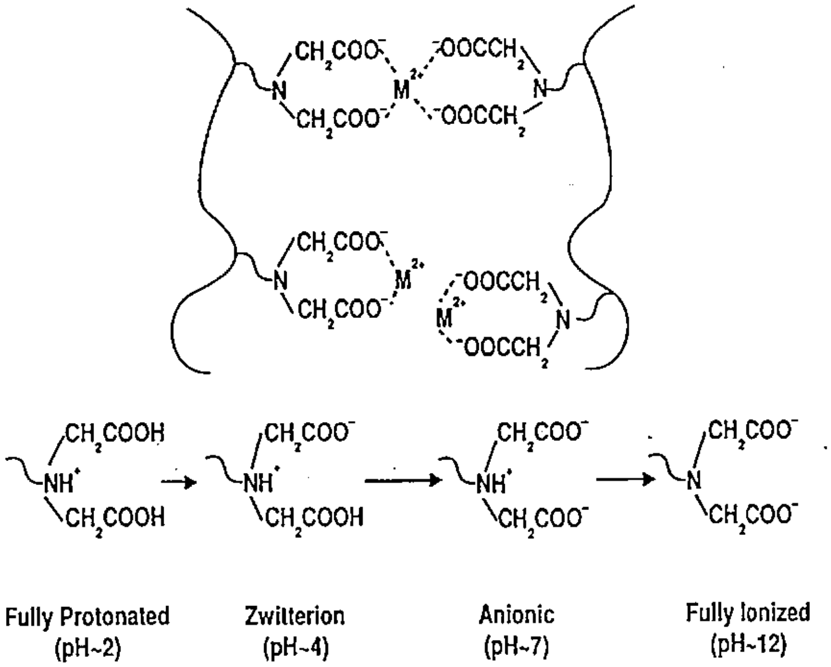

Figure 3.5 The structure of MetPac CC-1 chelating resin[227].

3.2.2.2 Optimisation of the FI procedure

A univariate investigation of a number of variables in the FI procedure was carried out, with flame AAS and flame AES detection, in order to ascertain the optimum conditions for the retention of copper and the elimination of the matrix (as sodium). These variables were ammonium acetate buffer concentration (0 - 1.0 M) and pH (4.3 - 7.3), sea water concentration (1 - 100 % v/v) and pH (3.0 - 8.0), and nitric acid eluent concentration (0.5 - 3.0 M). The sodium emission line at 589.0 nm and the copper absorption line at 324.7 nm were used to monitor sodium ion and copper ion retention respectively. These species were investigated because sodium ions are precursors of the $ArNa^+$ polyatomic ion interference at m/z = 63 which considerably degrades the ICP-MS analytical signal for copper at this mass.

Table 3.5 shows the effect of various concentrations of a synthetic sea water matrix (1 - 100 % v/v, diluted with appropriate volumes of Milli-Q) on the retention of sodium ions on the MetPac column in a 0.25 M buffer carrier stream. No retention of sodium was observed at any sea water concentration. This was noticeably different from the previous results using Chelex-100. It was concluded that although the IDA functionality was identical in both resins, the physical stability of the substrate of the MetPac resin prevented swelling and therefore allowed the matrix to be eluted to waste. From this data undiluted sea water was used in all subsequent experiments in order to eliminate any loss of sensitivity associated with sample dilution.

From Table 3.6 it can be seen that at the normal pH of the synthetic sea water (8.0) there was complete retention of the 5.0 mg l^{-1} copper spike but the efficiency of retention decreased as the pH of the matrix was lowered. However, sea water samples are generally acidified to pH 1.0 on collection in order to maintain the integrity of the sample with respect to total trace metal concentration. It may also be important to lower the pH of the matrix in order to release any bound organic complexes which might not be selectively chelated onto the column. It is therefore essential that samples are buffered to pH 8.0 prior to analysis.

Table 3.5 Effect of synthetic sea water concentration on the retention and elution of sodium.

Synthetic sea water concentration (% v/v)	Sodium eluted to waste (arbitary units.)	Sodium retained on column (arbitary units)
1	281	2
5	428	2
10	798	2
50	1167	3
100	1219	3

Table 3.6 Effect of synthetic sea water pH on the breakthrough and retention of 5.0 mg l^{-1} copper.

Sea water pH	Copper breakthrough (arbitary units)	Copper retention (arbitary units)	Copper retention precision (RSD %, n = 3)
3.0	0.6	0.09	7.8
4.0	0.6	0.09	8.2
5.0	0.6	0.14	6.4
6.0	0.2	0.20	5.3
8.0	0	0.22	4.7

Results from the investigation of ammonium acetate buffer concentration and pH are shown in Table 3.7 and Figure 3.6. When water was used as the carrier stream, there was significant retention of sodium ions due to non-selective ion-exchange processes. At buffer concentration of 0.01 M or higher however, there was no sodium ion retention because the ion exchange effect was dominated by ammonium ions. The buffer concentration had no significant effect on the retention of copper (5 mg l^{-1}) and copper showed quantitative retention at all buffer concentrations (0-1.0 M). The optimum buffer concentration should be kept as low as possible in order to minimise the blank signal due to impurities in the reagent. Therefore 0.01 M ammonium acetate was used for all subsequent experiments. Previous workers have used higher buffer concentrations[31,123,228,229]. For example, Heithmar *et al.*[228] and Siriraks *et al.*[229] used 2.0 M ammonium acetate. Heithmar and co-workers. discussed the problem of the reagent blank and suggested that stringent clean up procedures should yield lower blanks. Ebdon *et al.*[133] washed the preconcentration column with dilute solutions of ammonium acetate following preconcentration of brine (1.2 ml). It was found that washing the column with the buffer had very little effect in removing sodium. It was concluded that during preconcentration the resin was returned to the sodium form and that no amount of washing would remove the sodium until acid was

Table 3.7 Effect of buffer concentration on the retention and breakthrough of copper (5.0 mg l^{-1}) and sodium (100 % v/v synthetic sea water).

Buffer concentration (M)	Sodium retention (arbitary units)	Copper retention (arbitary units)	Copper breakthrough (arbitary units)
0	298	0.15	0
0.01	5	0.14	0
0.05	5	0.14	0
0.1	5	0.14	0
0.25	5	0.14	0
0.5	5	0.14	0
1.0	5	0.15	0

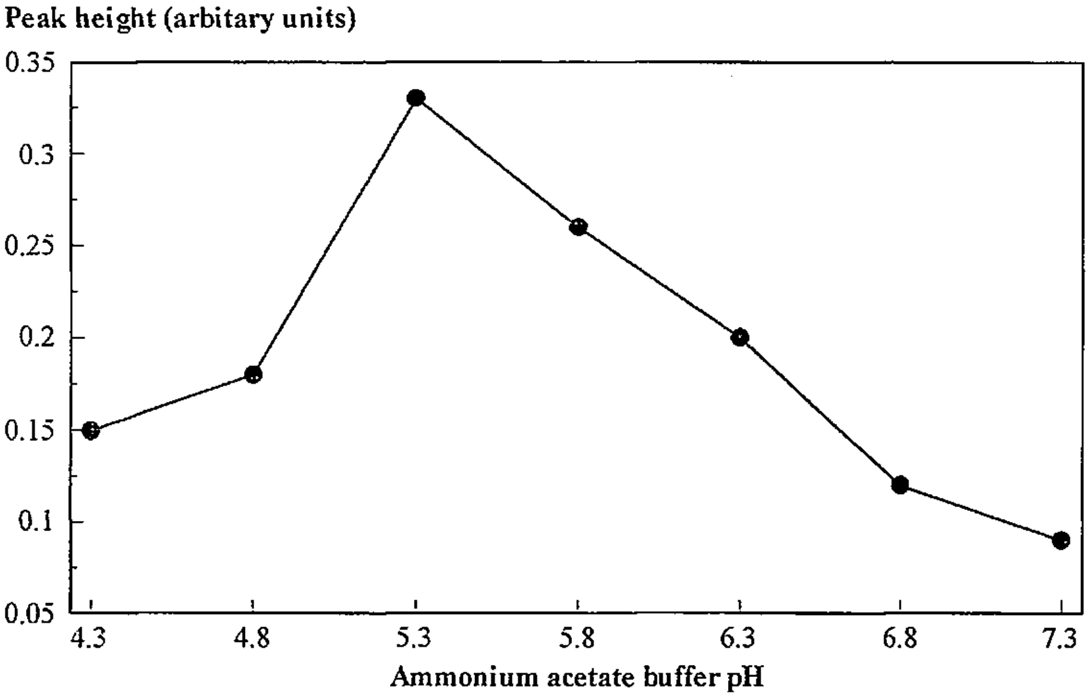

Figure 3.6 Effect of buffer pH on the retention of 5 mg l^{-1} copper.

passed through the column. The relationship between 0.01 M ammonium acetate buffer pH and the retention of copper is shown in Figure 3.6. The optimum pH for quantitative retention was 5.3 which is in accordance with literature values [31,227].

Figure 3.7 shows the relationship between the nitric acid eluent concentration and the eluted copper peak shape. An increase in the nitric acid concentration from 0.5 to 2.0 M resulted in sharper peaks. Although eluent concentrations of 3.0 M nitric acid gave a further improvement in peak shape, prolonged use of such concentrations would rapidly degrade the column by destroying the cross linked PS-DVB substrate. Therefore a 2.0 M HNO_3 eluent was used for all subsequent experiments. The optimum FI conditions are shown in Table 3.8.

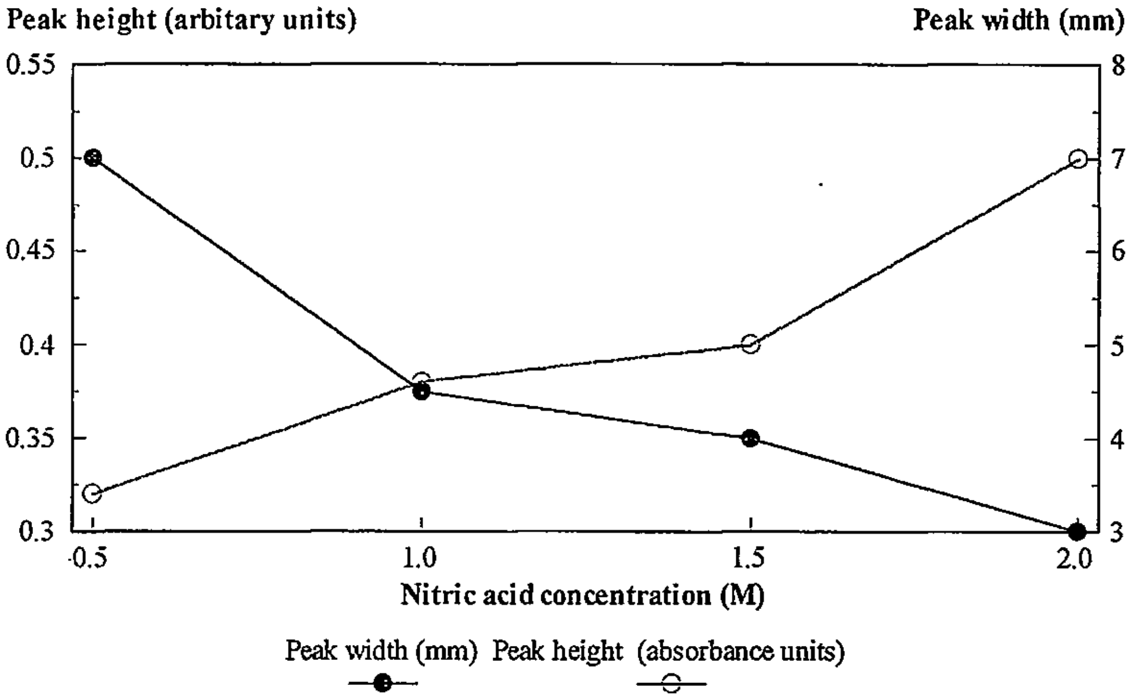

Figure 3.7 Effect of nitric acid concentration on the elution characteristics for 5 mg l^{-1} copper.

Table 3.8 Optimum FI conditions.

Parameter	Optimum condition
Sea water concentration	100 %
Sea water pH	8.0
Buffer concentration	0.01 M ammonium acetate
Buffer pH	5.3
Eluent concentration	2.0 M HNO_3

3.2.2.3 Preconcentration of copper from sea water

Using the optimised conditions shown in Table 3.8, various sample loop sizes (50 - 2000 μl) were evaluated to determine the effect of increased sample volume on the retention/breakthrough of copper (1.0 mg l^{-1}) and the removal of the matrix (100 % v/v synthetic sea water). Increasing the sample volume from 200 μl to 2000 μl was linear (r^2=0.9854) and resulted in an 8 fold increase in response with respect to a 1 mg l^{-1} copper spike (Figure 3.8). A 3 fold increase in the reagent blank signal also occurred and was attributed to an increase in the analysis time from 3 min to 9 min, and thus an increase in the volume of ammonium acetate buffer passing through the column.

Figures of merit for copper in synthetic sea water (100 % v/v), using both 200 and 2000 μl sample loops, are shown in Table 3.9. Typical peak profiles for 1.0 mg l^{-1} copper (RSD = 4.4 %, n = 9) are shown in Figure 3.9.

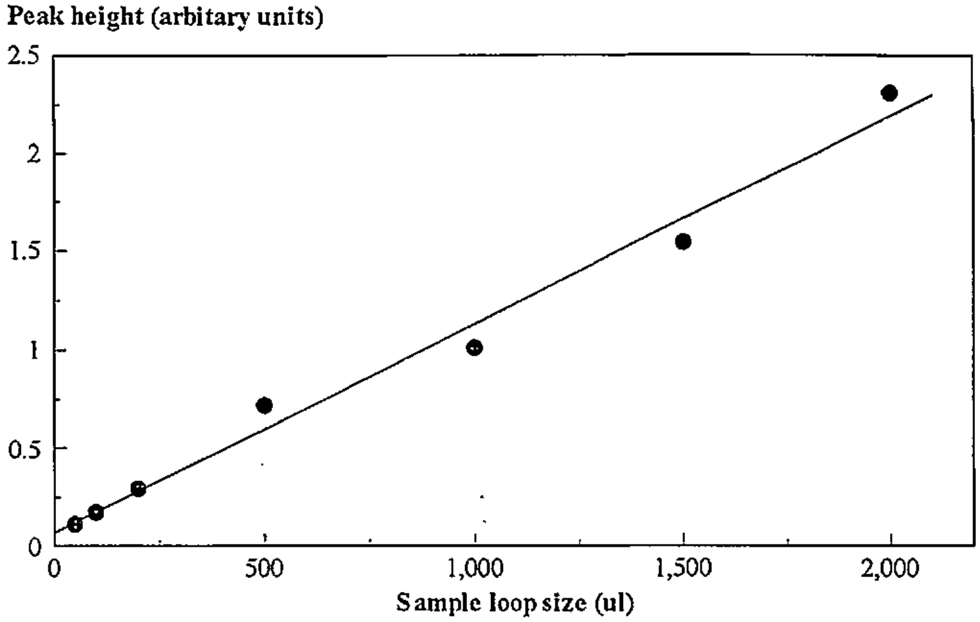

Figure 3.8 Effect of sample loop size on the quantitative retention of 1.0 mg l^{-1} copper.

Calibration data for the AAS procedure was linear over the range 25 to 5000 µg l^{-1} for 200 and 2000 µl sample volumes (r^2 of 0.9983 and 0.9961 respectively). The precision was 4.4 % and 9.9 % respectively (n = 5) for 50 µg l^{-1} standards and the limits of detection (3σ) were 22 and 9 µg l^{-1} respectively. However, the limit of detection would not be sufficient for the determination of trace metals in sea water. For example, the certified value for copper in the NASS-3 CRM is 0.109 µg l^{-1}. (see Table 3.3). The method was therefore adapted for ICP-MS detection.

Table 3.9 Figures of Merit for 200 and 2000 µl Sample Injections for Cu over the range 10 - 100 µg l^{-1}.

Figure of Merit	200 µl Sample Loop	2000 µl Sample Loop
Gradient	0.071	0.372
Intercept	1.009	2.999
Linearity (r^2)	0.9983	0.9961
RSD % (50 µg l^{-1}, n = 5)	4.4	9.9
Limit of Detection (3 σ)	22 µg l^{-1}	9 µg l^{-1}

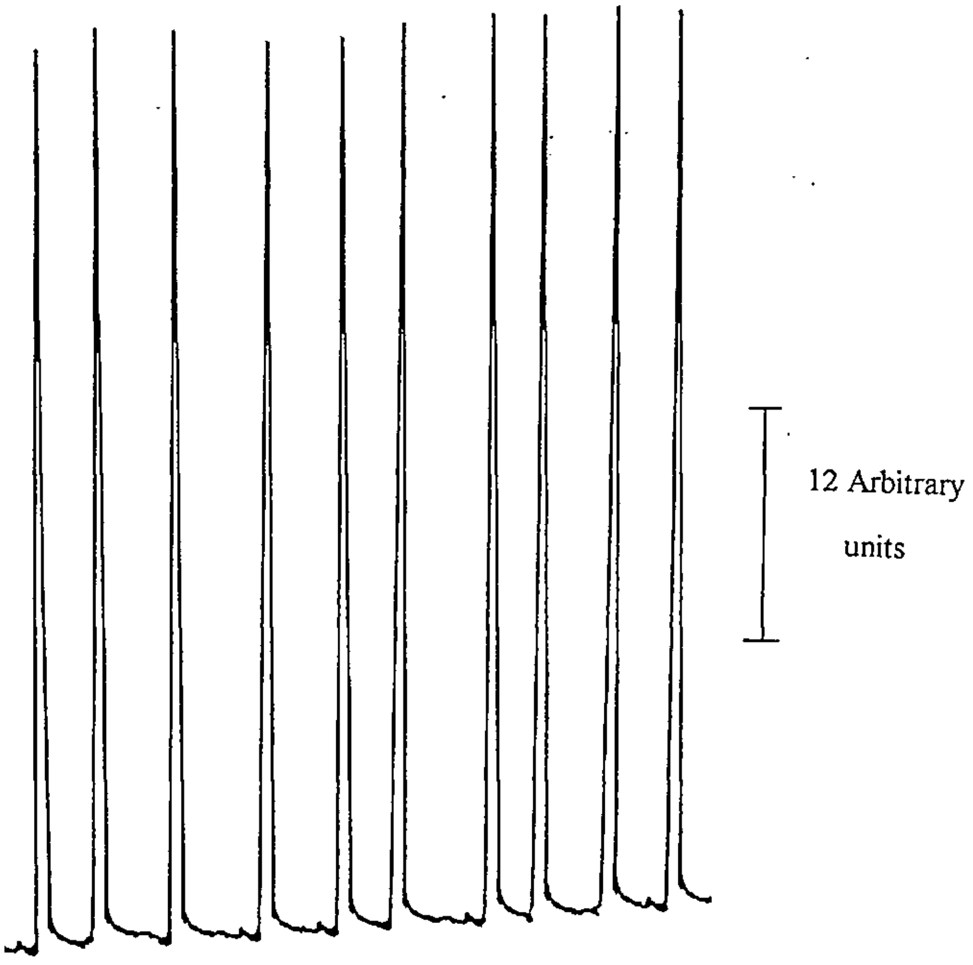

Figure 3.9 Replicate injections (n = 10) of 1.0 mg l^{-1} copper in 100 % v/v synthetic sea water.

3.2.3 COUPLING OF FI METPAC CC-1 PRECONCENTRATION WITH ICP-MS DETECTION

3.2.3.1 Reagent purity

Preliminary experiments showed that trace metal impurities in the ammonium acetate buffer seriously degraded detection limits for Cu, Zn and Pb when using ICP-MS detection. For example, 0.015 µg of copper was retained on the column when 0.01 M ammonium acetate was pumped through the manifold for seven minutes. This is equivalent to a higher concentration of copper than is present in the NASS-3 CRM. In order to minimise this reagent blank problem the following clean-up protocol was developed.

Two gravity fed glass columns (25.0 x 1.5 cm) were filled with 10 cm of sodium form, 50-100 mesh, 400 meq ml^{-1} iminodiacetate resin (Sigma Chemicals etc). Each column was then washed with 10 % v/v nitric acid (250 ml) followed by Milli-Q water (250 ml). The reservoir (1.0 l) of the first column was filled with ammonium acetate buffer solution (1.0 M) and the pH of the eluent was monitored until it reached pH 5.3. The eluted buffer was then collected in a 1.0 l polythene container and passed through the second column using the same procedure. The collected fraction was then diluted to 0.01 M with Milli-Q. Using the purified buffer, a limit of detection (3σ) for copper in Milli-Q of 0.09 µg l^{-1} was achieved.

3.2.3.2 Analysis of synthetic sea water

Initial analysis of spiked synthetic sea water standards over the range 0 - 10.0 µg l^{-1} indicated that this matrix contained higher levels of the trace metals of interest than the CRM. From Table 3.10 it was apparent that the matrix was a limiting factor when trying to achieve acceptable limits of detection and was not considered suitable as a diluent for metal ion standard solutions. However, the results showed that the FI-FAAS method was readily adapted to ICP-MS detection and could achieve the sensitivity necessary to analyse sea water CRMs.

Table 3.10 Figures of merit for the Merck corrosion test mixture.

Analyte	Precision (RSD %, n=3)	Regression (r^2)	Limit of detection µg l^{-1} (3 σ)	NASS-3 certified value (µg l^{-1})
^{52}Cr	< 9.6	0.9999	0.34	0.175
^{58}Ni	< 6.2	0.9928	0.43	0.257
^{63}Cu	< 2.9	0.9923	0.13	0.109
^{64}Zn	< 9.7	0.9904	1.3	0.178
^{208}Pb	< 10.6	0.9999	0.55	0.039

3.2.3.3 Standard additions

Standard additions, as the name suggests, is a calibration method in which the analyte standards are added to the sample to be analysed. The sample is thus divided into aliquots, to which are added equal volumes of standard solutions of different concentrations. To one aliquot (the blank), no standard solution is added. Figure 3.10 shows the plotted results. The y-axis represents the instrumental signal in the usual way and the x-axis represents the concentration of added standard solution. Therefore the first point on the graph, x = 0 (A), represents the test aliquot to which no standard solution has been added. The slope, *b*, and intercept, *a*, can be determined using the equations used in conventional calibration experiments:

$$b = \frac{\Sigma\,(x_i - \overline{x})\,(y_i - \overline{y})}{\Sigma\,(x_i - \overline{x})^2}$$

$$a = \overline{y} - b\overline{x}$$

The concentration of determinand in the sample is obtained by extrapolating the line to y = 0, the value then being the x-axis intercept, which is given by the ratio *a/b* (C).

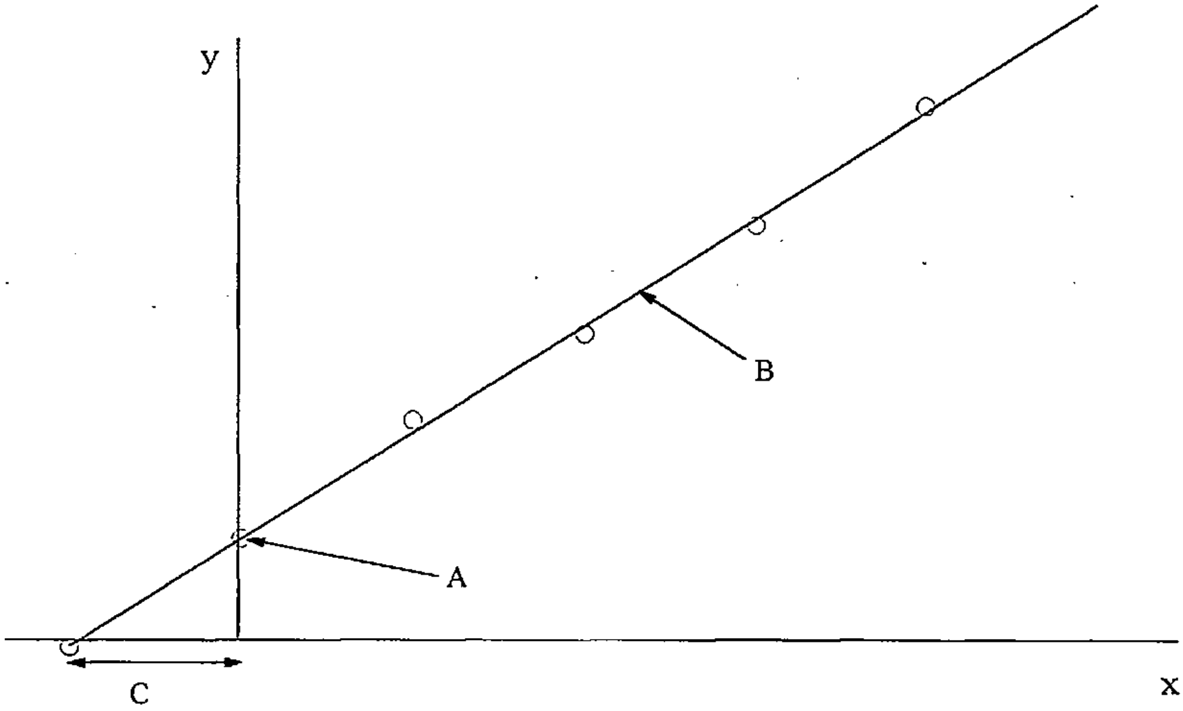

Figure 3.10 Standard additions calibration graph.

3.2.3.4 Validation of the procedure

In order to validate the proposed method, three CRMs (NASS-3, CASS-2 and SLEW-1) of varying analyte concentrations (0.03 - 13.0 μg l^{-1}) and salinities (11.6 - 35.1 S) were analysed by standard additions using the multi-element time resolved software on the ICP-MS instrument (see Tables 2.1 and 3.2 for operating conditions). This was done by spiking a series of 4 volumetric flasks (25 ml) with μl volumes of multi-element (Mn, Co, Cu, Zn and Pb) standards and diluting with the CRM's. For example, NASS-3 was spiked with copper and zinc at 0.1 - 0.4 μg l^{-1}, and manganese cobalt and lead at 0.01 - 0.04 μg l^{-1}. In order to prevent contamination from the environment, all the procedures described were carried out in an air-conditioned clean room.

The standard addition calibration graphs for these metals showed good linearity *e.g.* regression for NASS-3 was in the range 0.9934 - 0.9999 for the five elements over the concentration range 0.1 - 0.4 μg l^{-1}. The precision of the method (n = 5) for the five elements was in the range 2.3 - 6.9 % for NASS-3 spiked with a 0.1 μg l^{-1} multi-element standard. The results for the three CRM's are given in Tables 3.11 - 3.13. Good agreement with the certified values was achieved for all of the elements determined except for Co in NASS-3 which gave a positive bias. Recovery tests were performed by spiking volumetric flasks (25 ml) with 0.2 μg l^{-1} (NASS-3), 1.0 μg l^{-1} (CASS-2) and 2.0 μg l^{-1} (SLEW-1) of a Mn, Co, Cu, Zn, and Pb multi-element standard and diluting with the appropriate CRM. The mean results (n = 3) are given in Tables 3.11-3.13 and show good recoveries (94 - 105 %) for Mn, Cu, Zn and Pb. The recovery for Co was good for SLEW-1 but high for NASS-3 and CASS-2 (137 and 131 % respectively) due to ng l^{-1} concentrations of this element in the reagents used for preconcentration and elution. Typical peak profiles for replicate injections of spiked NASS-3 samples (Cu, Zn and Pb, 0.2 μg l^{-1}) are shown in Figure 3.11.

The value of stringent clean up protocols and the availability of clean room conditions is apparent in the above results. Previous workers have encountered difficulties in analysing zinc due to high background levels attributed to laboratory contamination[228], and Co[133,230] and Mn[133] due to the extremely low concentration of these analytes in CRMs such as NASS-3. However analysis of nickel proved difficult in this work. Recoveries were >120% in all 3 CRM's, precision was poor (>8 %, n = 5) and the calculated values were all above the certified values. This was due to nickel being (non-quantitatively) ablated from the nickel sampler and skimmer cones by the 2.0 M nitric acid eluent and not from sample contamination.

Table 3.11 NASS-3 open ocean sea water certified reference material results.

The uncertainties represent 95 % confidence limits for an individual subsample (n=3).

Analyte	Calculated Value $\mu g\ l^{-1}$	Certified Value $\mu g\ l^{-1}$	Recovery %
Mn	0.039 ± 0.017	0.022 ± 0.007	105
Co	0.029 ± 0.011	0.004 ± 0.001	137
Cu	0.119 ± 0.008	0.109 ± 0.011	97
Zn	0.167 ± 0.011	0.178 ± 0.025	100
Pb	0.039 ± 0.016	0.039 ± 0.006	105

Table 3.12 CASS-2 near shore sea water certified reference material results.

The uncertainties represent 95 % confidence limits for an individual subsample (n=3).

Analyte	**Calculated Value** **$\mu g\ l^{-1}$**	**Certified Value** **$\mu g\ l^{-1}$**	**Recovery** **%**
Mn	1.84 ± 0.17	1.99 ± 0.15	99
Co	0.032 ± 0.016	0.025 ± 0.006	131
Cu	0.672 ± 0.096	0.675 ± 0.039	94
Zn	1.98 ± 0.24	1.97 ± 0.12	100

Table 3.13 SLEW-1 estuarine water certified reference material results.

The uncertainties represent 95 % confidence limits for an individual subsample (n=3).

Analyte	Calculated Value $\mu g\ l^{-1}$	Certified Value $\mu g\ l^{-1}$	Recovery %
Mn	12.6 ± 0.7	13.1 ± 0.8	95
Co	0.046 ± 0.014	0.046 ± 0.007	99
Cu	1.73 ± 0.05	1.76 ± 0.09	104
Zn	0.89 ± 0.19	0.86 ± 0.15	101

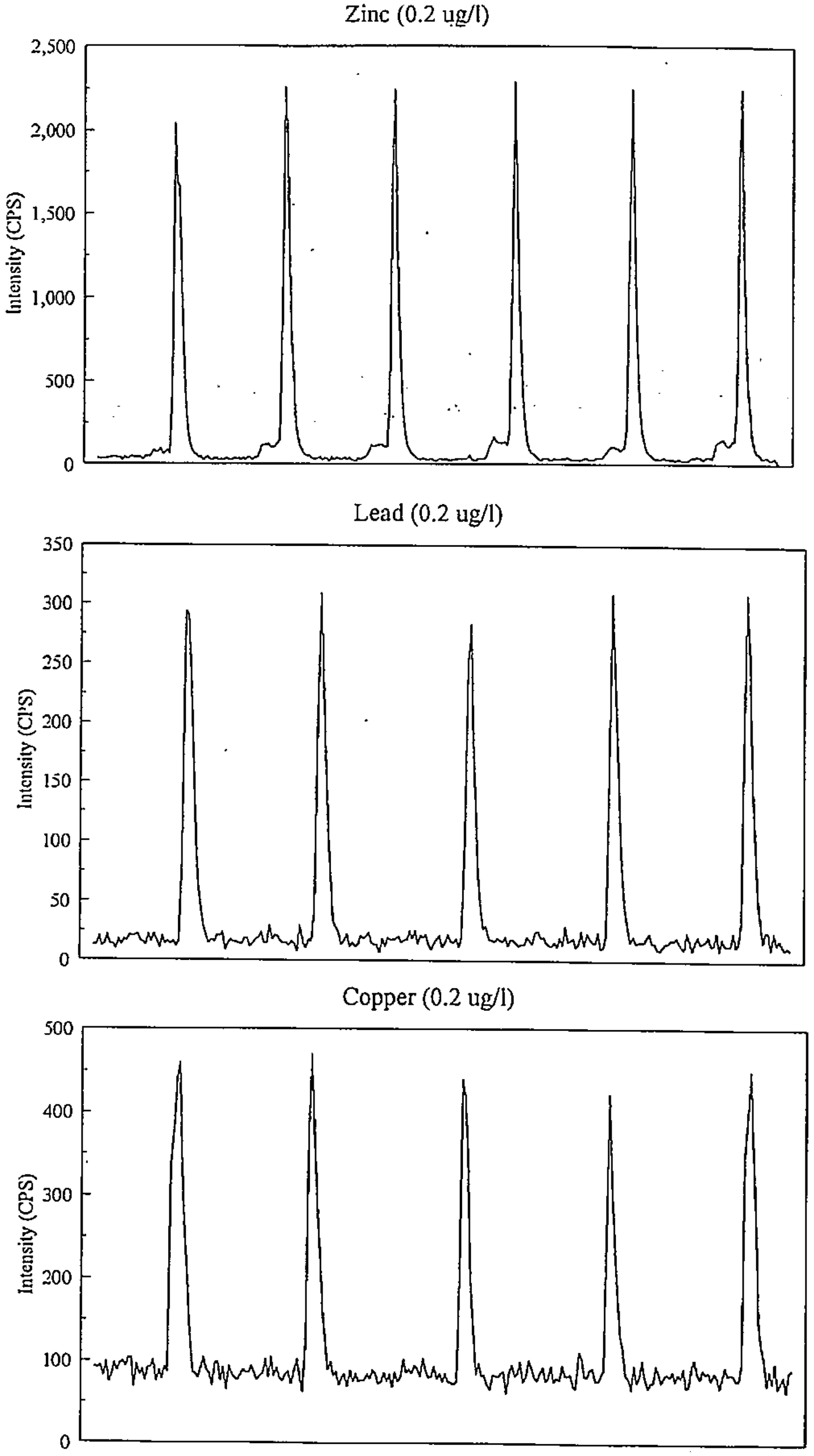

Figure 3.11 Typical peak profiles for replicate injections of spiked NASS-3 samples.

3.3 CONCLUSIONS

Two IDA resins have been evaluated for the determination of trace metals in saline matrices when incorporated into an FI manifold. Chelex-100 was found to be unsuitable because the resin retained sodium ions at low buffer concentrations. When the buffer concentration was increased, the resin (with a low cross-link microporous PS-DVB supporting polymer) swelled, physically preventing the matrix from being eluted to waste. The second resin (MetPac-CC1), with a more highly cross-linked macroporous PS-DVB substrate overcame this problem.

Using this resin, an on-line FI matrix elimination method, with ICP-MS detection was developed for the determination of trace metals (Mn, Co, Cu, Ni, Zn and Pb) in sea water. It involved the chelation of the analytes onto the IDA based resin in a micro-column with the simultaneous removal of indirectly interfering matrix species such as Na and Cl ions. In 100 % v/v synthetic sea water sodium was completely separated from the metals of interest which were quantitatively retained on the column when using a 0.01 M ammonium acetate buffer concentration. Sensitivity was degraded by the ammonium acetate buffer solution but a clean-up protocol enabled a reduction of the blank signal which resulted in significantly improved detection limits (e.g. from 2.0 $\mu g\ l^{-1}$ to 0.09 $\mu g\ l^{-1}$ for copper).

The procedure was validated using open ocean (NASS-3), coastal (CASS-2) and estuarine (SLEW-1) CRMs. The results obtained were in good agreement with the certified values and the procedure is therefore applicable over a wide range of analyte concentrations and matrix salinities.

CHAPTER 4

Determination of Total Mercury in Sea Water by Flow Injection with Atomic Spectrometric Detection

CHAPTER 4: DETERMINATION OF TOTAL MERCURY IN SEA WATER BY FLOW INJECTION WITH ATOMIC SPECTROMETRIC DETECTION

Introduction

Mercury is a non-essential metal found in minerals, soil, oceans, lakes and air. Over the last 100 years mercury has been used extensively by industry in the production of pesticides, electrical apparatus, paints and dental applications. However, the single largest use of mercury has been in the manufacture of sodium hydroxide and chlorine by the electrolysis of brine. About half of the anthropogenic input of mercury to the environment has come from this source (approximately 150-250 g Hg per tonne of Cl_2). However, since a peak in annual world production in the early 1970s (10,600 tonnes) it has steadily declined due to the discovery of the dangers to human health, increased recycling and concern about environmental pollution (*e.g.* biomagnification through the food chain)[231,232].

A substantial proportion of the total annual production of mercury (estimated to be 7000 t yr^{-1} worldwide) eventually enters the natural environment. Although natural inputs of mercury into the environment occur on a larger scale (*e.g.* 25,000-150,000 t yr^{-1} from degassing of the earths crust) these occur on a global scale. Anthropogenic inputs however tend to be more localised (*e.g.* the Minamata Bay accident), causing biomagnification in the food chain[232].

The marine distribution of mercury is of considerable interest because of concern over mercury poisoning and accumulation of methylmercury in fish. The concentration of mercury in open ocean water has been reported to be between 1.0 ng l^{-1} [205] and 20 ng l^{-1} [206]. Concentrations of mercury in coastal waters tend to be higher due to anthropogenic discharges and levels of 2 - 100 ng l^{-1} are typical[233]. Due to the low concentrations of mercury in sea water, sensitive techniques are required for analysis. Historically, the most extensively used method for the measurement of mercury has been cold vapour-FAAS[234-236]. However the analysis of sea water samples using this method is limited by the short linear calibration range, spectral interferences and lack of sensitivity. Therefore in recent years cold vapour generation-atomic fluoresence spectrometry (CVG-AFS) have been adopted for the determination of mercury in such matrices.

This chapter compares FI approaches coupled with AFS, ICP-AES and ICP-MS detectors for the determination of total mercury. Initial studies compare figures of merit for FI (conventional pneumatic nebulisation) and FI-CVG coupled with ICP-AES and ICP-MS. Detection limits for total mercury were further improved by developing simple on- or off-line preconcentration procedures using the MetPac CC-1 micro-column incorporated into a FI manifold with conventional pneumatic nebulisation. An AFS detector was then used in the development of a method for the determination of total mercury with an on-line bromide/bromate oxidation step.

4.1 ATOMIC FLUORESENCE SPECTROMETRY

The determination of mercury using AFS was pioneered by Thompson *et al.* in the 1970s[237]. The instrument described was a dispersive system based on a modified FAAS and offered a detection limit of 0.02 μg l^{-1}. Non-dispersive AFS has also been investigated[238]. However the increased light gathering power of non-dispersive systems is often offset by background scatter from the flame atom cell. This was overcome by Godden and Stockwell[239] who developed a filter fluorimeter that took advantage of the fact that mercury is atomic at room temperature and therefore does not require a flame to generate atomic species. A detection limit for mercury of less than 0.02 μg l^{-1} was achieved. Further specific instrumental details are given in Section 4.2.1.

In CVG systems the mercury in the sample is typically oxidised to mercury(II) using a suitable oxidant and then reduced to elemental mercury by adding an excess of reducing agent. Due to the appreciable vapour pressure of elemental mercury at room temperature (14 mg Hg m^{-3}), mercury vapour is rapidly volatilised when a carrier gas (usually argon) is bubbled through the solution containing inorganic mercury and tin(II) chloride. The liberated mercury purged from the solution is subsequently delivered to a detection system. The two most common reduction schemes utilised for the generation of gaseous mercury are tin(II) chloride and sodium tetrahydroborate. The reduction of mercury(II) with tin(II) is shown below:

$$\mathrm{Hg(II)} + \mathrm{Sn(II)} \longrightarrow \mathrm{Hg}^0 + \mathrm{Sn(IV)}$$

In order to determine total mercury concentrations, it is necessary to oxidise mercury compounds prior to the reduction process. The most favoured method for aqueous samples is the off-line oxidation of bromide with acid bromate. This procedure is effective at room temperature and almost complete breakdown of organomercury compounds (>95 %) occurs after several minutes[240]. Prior to analysis, free bromine is removed using hydroxylammonium chloride as excess bromine can cause interference due to quenching (non-radiative loss of energy)[241,242].

Sodium tetrahydroborate reduction generates large amounts of hydrogen which causes agitation within the reaction vessel encouraging the release of mercury vapour from solution. Tin(II) chloride reduction is less vigorous resulting in the majority of the mercury remaining in solution, and it is therefore necessary to provide forced agitation of the liquid to release the mercury. This is accomplished with a gas liquid separator as illustrated in Figure 4.1.

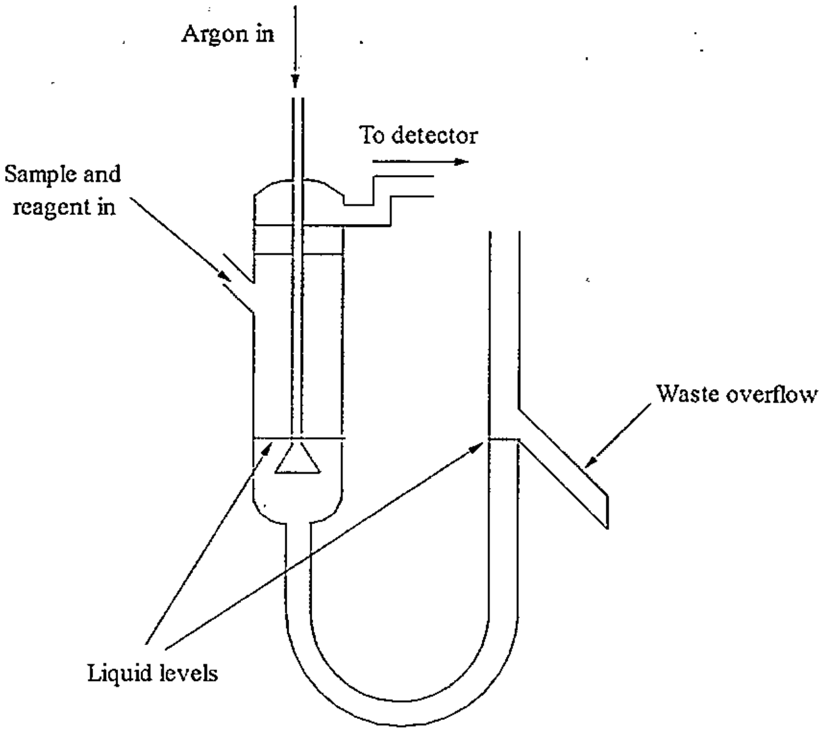
Argon in
To detector
Sample and reagent in
Waste overflow
Liquid levels

Figure 4.1 Gas-liquid separator for the tin(II) chloride scheme.

4.2 EXPERIMENTAL

4.2.1 INSTRUMENTATION

ICP-AES

A standard Varian Liberty 200 ICP-AES was used to obtain the initial mercury calibration data. This instrument uses a conventional sequential scanning Czerny-Turner monochromator with holographic gratings. The RF generator is a solid-state crystal control locked type with direct serial coupling (DISC). This directly couples the RF tuning circuitry to the load coil and ensures that the tuning circuit responds to load changes in the shortest possible time. One of the advantages of this system is that it allows high concentrations of organic solvents to be nebulized without extinguishing the plasma.The operating conditions are given in Table 4.1.

Table 4.1 Varian Liberty 200 operating conditions.

ICP operating conditions	
RF power (W)	1500
Plasma gas (l min^{-1})	15.0
Nebulizer gas (l min^{-1})	0.8
Auxiliary gas (l min^{-1})	1.5
Nebulizer type	Meinhard concentric
Snout purge	High

Spectrometer conditions	
Viewing height (mm)	3
Search window (mm)	0.06
Integration (sec)	1
Order	1
PMT (V)	650
Wavelength (nm)	184.98

ICP-MS

Mercury analyses using conventional nebulisation and CVG were performed on a Fisons PlasmaQuad PQ2 Turbo+ ICP-MS (Fisons Elemental, Winsford, Cheshire, U.K.). Modifications to the system when coupling with CVG are discussed in Section 4.2.4.2. The instrument was operated in the time resolved analysis monitoring mode. Typical ICP-MS operating conditions are presented in Table 2.1 (Chapter 2). The ICP-MS time resolved analysis parameters are given in Table 3.2 (Chapter 3). The ^{202}Hg isotope (abundance 29.7 %) was monitored in this study because it is the most abundant isotope of mercury. The instrument was tuned at m/z = 202 and then stabilised for one hour prior to use in order to minimise the background signal due to mercury memory effects.

AFS

Mercury vapour was detected using a PSA 10.023 Merlin atomic fluoresence detector (PS Analytical Ltd, Sevenoaks, Kent, UK.). A schematic diagram of the instrument is shown in Figure 4.2. The lamp source is a specific high intensity mercury vapour discharge lamp. A series of lenses focus and collect light from the source which is collimated over the chimney interface. The mercury vapour is fed into the central core of the chimney interface at 0.5 l min^{-1}. A further argon flow (0.2 l min^{-1}) sheaths the sample, which effectively constrains the mercury vapour to a laminar flow past the fluoresence head of the monitor. Fluoresence emission was filtered with a 254 nm interference filter to achieve wavelength isolation and detected using a side window photomultiplier tube (PMT). The detector can operate in either the emission or the ratio mode. The latter compensates for lamp drift by dividing the signal by the response of the reference cell. The operating conditions are given in Table 4.2. The output from the PMT was recorded on a strip chart recorder (Chessell BD40, Kipp and Zonen, Holland) and the response was measured manually as peak height.

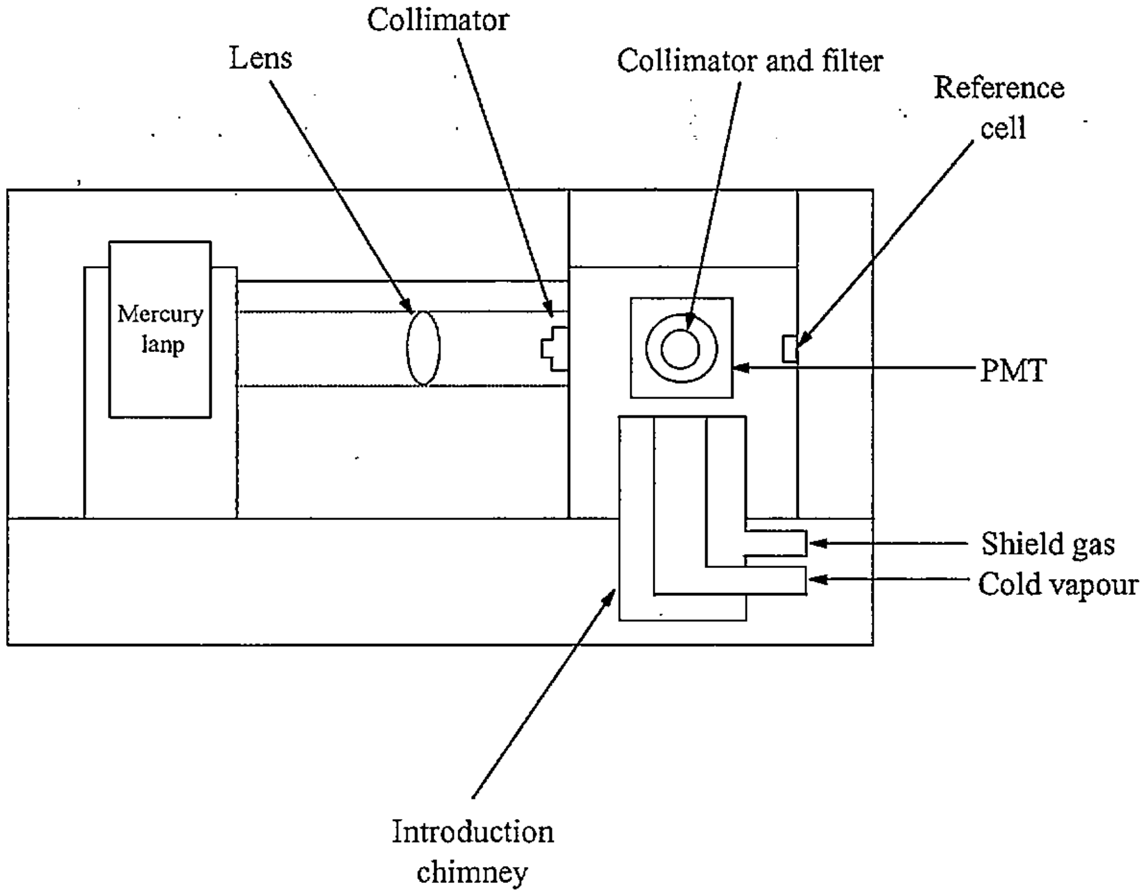
Collimator
Lens
Collimator and filter
Reference cell
Mercury lanp
PMT
Shield gas
Cold vapour
Introduction chimney

Figure 4.2 Schematic diagram of the PS Analytical Merlin atomic fluoresence detector.

The CVG system necessary to convert aqueous mercury to an elemental vapour is discussed in section 4.2.4.4.

Table 4.2 Merlin AFS detector operating conditions.

Wavelength	254 nm
Read mode	Running
Integration	1/4 sec
Calibration range gain settings	1 - 1000
Fine gain	0 - 10
Mode	Ratio
Argon carrier gas flow rate (l min^{-1})	0.5
Argon shield gas flow rate (l min^{-1})	0.2

4.2.2 REAGENTS

High purity de-ionised water purified by a Milli-Q analytical reagent grade water purification system (Millipore, Chester, Cheshire, UK.) was used throughout. All reagents used were purchased from Merck (Poole, Dorset, UK.) and were AnalaR grade unless otherwise stated.

Conventional nebulisation and cold vapour generation ICP-AES and ICP-MS

The carrier stream (hydrochloric acid, 2.0 M) was made up daily by appropriate dilution from 36 % m/m concentrated hydrochloric acid (Aristar grade). Tin(II) chloride solutions (3 % m/v in 15 % v/v hydrochloric acid) were prepared by dissolving tin(II) chloride dihydrate (15 g) in concentrated hydrochloric acid (75 ml) and making up to 500 ml with Milli-Q. Fresh solutions were prepared daily. Traces of mercury were removed by purging the solution with argon gas (2.0 l min^{-1}) for 20 min.

Cold vapour generation AFS

The hydrochloric acid carrier stream (2.0 M) and tin(II) chloride reductant (3 % m/v in 15 % v/v hydrochloric acid were prepared as above. Potassium bromate and potassium bromide were heated overnight at 280°C in a muffle furnace to remove traces of mercury. After cooling, each reagent (1.4 g and 5.0 g respectively) was dissolved in Milli-Q (1000 ml) and stored in borosilicate bottles. The 0.14 % m/v and 0.5 % m/v stock solutions were prepared weekly. The bromide/bromate reagent was prepared daily by mixing equal volumes of the above stock solutions. Hydroxylammonium chloride solution (6.0 % m/v) was prepared daily by dissolving spectroscopy grade hydroxylammonium chloride (Merck) and diluting to 500 ml in Milli-Q in a volumetric flask.

On-line preconcentration with FI-ICP-MS

The carrier stream was prepared by disolving thiourea (1.0 g) in Milli-Q to produce a 0.1 % m/v solution. The eluent (2.0 M hydrochloric acid, 2 % m/v thiourea) was prepared by diluting concentrated hydrochloric acid (167 ml) with Milli-Q deionised water (500 ml), adding thiourea (20 g) and diluting to 1000 ml in a volumetric flask with Milli-Q de-ionised water. Both the carrier stream and the eluent were prepared daily.

Mercury(II) chloride salt was obtained from Alfa Products (Johnson Matthey, Royston, Herts., UK.) and was used without further purification. A stock solution (1000 mg l^{-1}) was prepared by dissolving the above reagent grade compound in Milli-Q. Methylmercury chloride (1000 mg l^{-1}) was also obtained from Alfa Products as a stock solution. Standard solutions were prepared daily by appropriate dilution of the stock solutions with either Milli-Q or a synthetic sea water solution (Corrosion test mixture, Merck Ltd, Poole, Dorset, UK.). All glassware was soaked in 20 % v/v nitric acid for at least 24 h prior to use, and then rinsed four times with deionised water. Stock mercury solutions were stored in acid washed (20 % v/v hydrochloric acid) amber glass bottles. Standard solutions were made up in acid washed volumetric flasks (25 or 100 ml, Grade A).

4.2.3 ANALYSIS OF TORT-1 LOBSTER HEPATOPANCREAS

Samples (0.25 g) of the certified reference material TORT-1 lobster hepatopancreas (National Research Council of Canada, Ottawa, Canada) were accurately weighed into PTFE digestion bombs (Savillex, Minnetonka, Minnesota, USA). Hydrogen peroxide (1.0 ml) and nitric acid (3.0 ml) were added and the mixture was left to digest for 1 hour. The bomb was securely tightened and the digestion was completed using a domestic microwave oven for 2 min at medium power. The mixture was left to cool for 20 min and the pressure in the bomb was slowly released. The microwave step was repeated until the digest was green/blue in colour. The digests were then transferred quantitatively to acid washed volumetric flasks and diluted to the mark with Milli-Q. For the preconcentration procedure, the digest was buffered to pH 8.0 with concentrated ammonia solution (Aristar grade, Merck, Poole, Dorset, UK.).

4.2.4 FI PROCEDURES

4.2.4.1 Single channel FI manifold for ICP-AES and ICP-MS detection

A simple single channel FI manifold similar to that described in Figure 2.1 was used to inject discrete volumes (500 μl) of the sample into the ICP-AES and ICP-MS instruments. The manifold served two purposes, firstly the matrix was diluted, minimising non-spectroscopic interferences such as salt build-up on the cones and an excess of easily ionisable elements and secondly, significant wash out times between injections reduced memory effects from the mercury. In this mode, the spray chamber which acts as a mercury sink, (*e.g.* relatively low levels of mercury (50 mg l^{-1}) can produce a significant lingering memory in ICP-MS) is not exposed to mercury for prolonged periods and is continuously washed between injections. A 2.0 M hydrochloric acid solution was used as the carrier stream. The acid carrier stream also prevented the build up of mercury on the ICP glassware (*e.g.* the nebuliser, spray chamber, angle bend and torch).

4.2.4.2 Cold vapour generation FI manifold for ICP-AES and ICP-MS detection

The FI manifold, shown in Figure 4.3, consisted of a peristaltic pump (Gilson Minipuls 2, Anachem, Luton, Beds. UK.), rotary injection valve (Rheodyne, HPLC Technology, Macclesfield, Cheshire, UK.) and gas-liquid separator (PS Analytical, Sevenoaks, Kent, UK.). The reagents were pumped at 1.5 ml min^{-1} using PVC peristaltic pump tubing. A tin(II) chloride reduction scheme was used throughout. The sample (500 µl) was injected into a flowing carrier stream of hydrochloric acid (2.0 M) which subsequently merged with the tin(II) chloride reductant stream (3 % m/v tin(II) chloride, 15 % v/v hydrochloric acid). The sample and reductant passed into the gas-liquid separator where Hg^0 was purged from the liquid with argon (0.5 l min^{-1}). The mercury vapour then passed into a silicon tubing transfer line (10 cm) coupled directly into the ICP torch.

4.2.4.3 FI preconcentration manifold for ICP-MS detection

The preconcentration manifold (Figure 4.4) was adapted from the system described in Section 3.1.2. The column, discussed in more detail in Sections 1.2.2 and 3.2.2, was a MetPac CC-1 column containing a macroporous IDA chelating resin. The major difference between the manifold previously described for the preconcentration of trace metals such as Cu, Zn, Mn, Co and Pb and the manifold described here for the preconcentration of mercury was the incorporation of a backflushing procedure. This was required due to the high selectivity of the MetPac resin for mercury (selectivity factor of 1060 compared

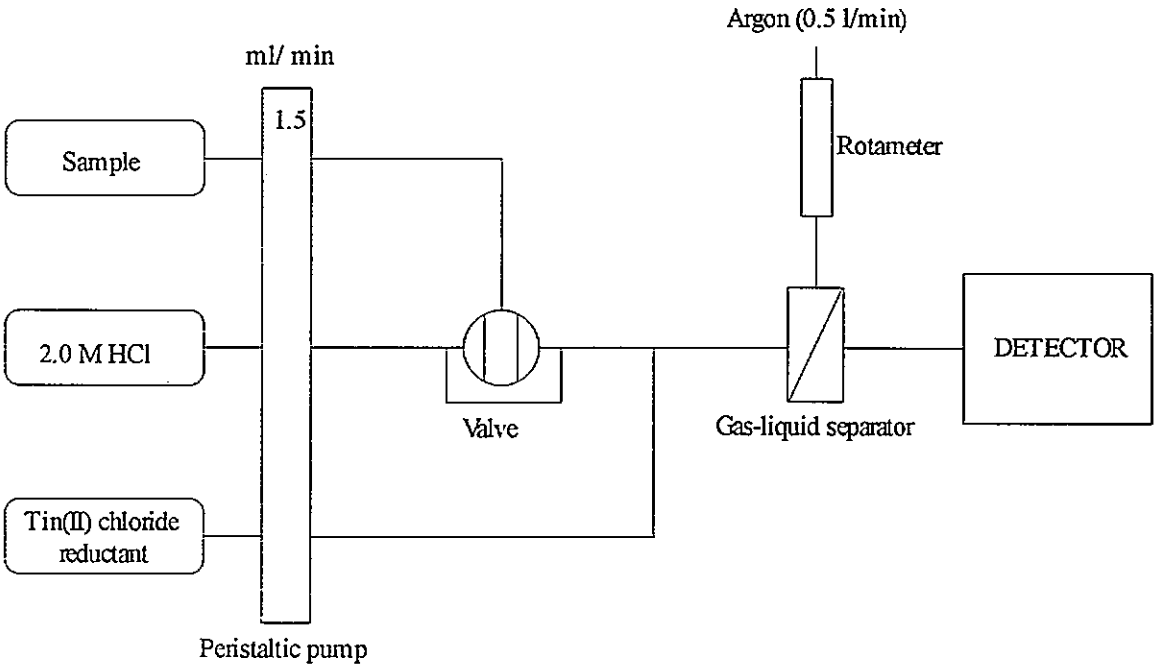
Argon (0.5 l/min)
ml/ min
1.5
Rotameter
Sample
2.0 M HCl
DETECTOR
Valve
Gas-liquid separator
Tin(II) chloride reductant
Peristaltic pump

Figure 4.3 Schematic diagram of the cold vapour generation FI manifold for ICP-AES and ICP-MS detection.

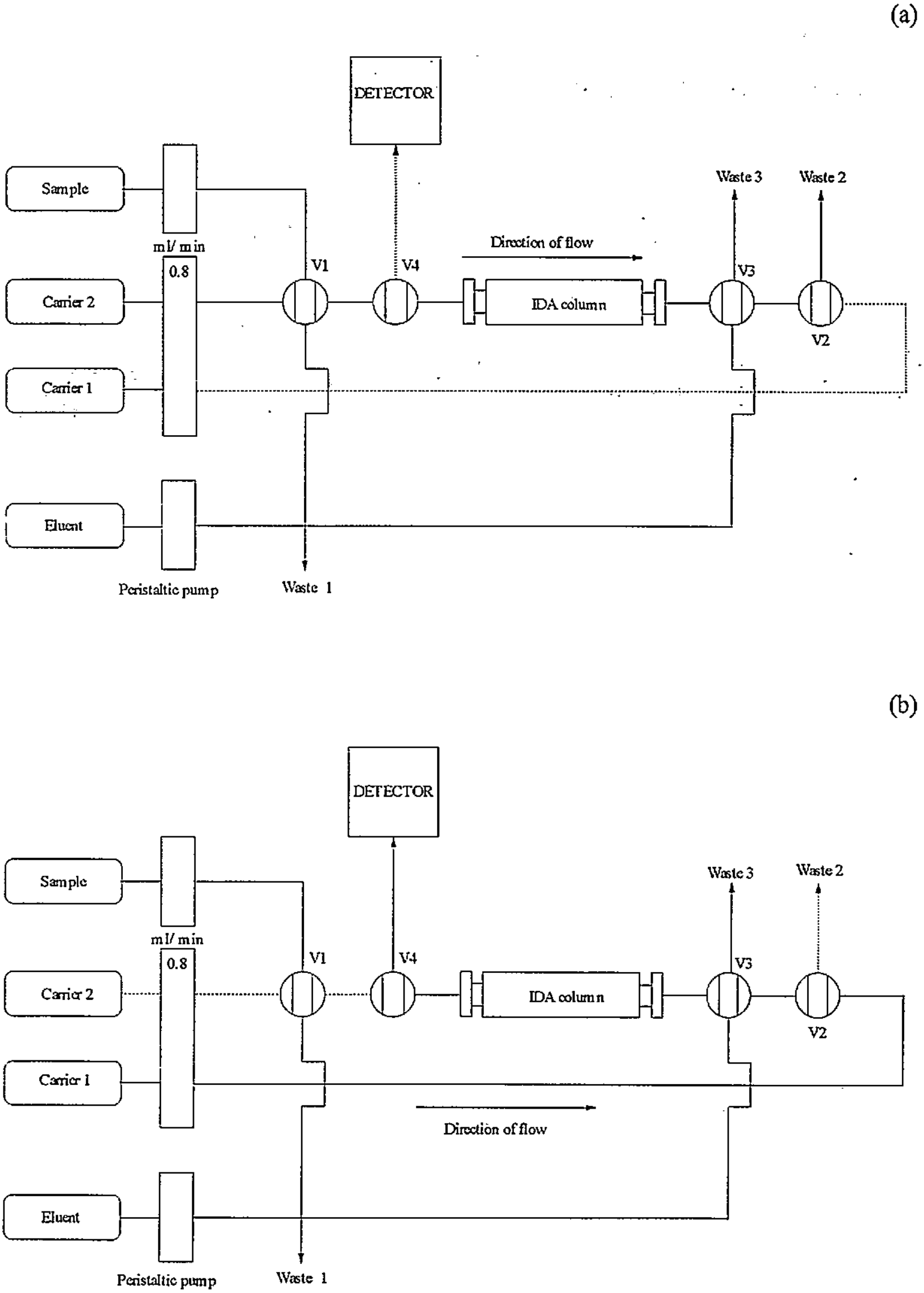
(a)
DETECTOR
Sample
Waste 3
Waste 2
ml/ min
Direction of flow
0.8
V1
V4
V3
Carrier 2
IDA column
V2
Carrier 1
Eluent
Peristaltic pump
Waste 1
(b)
DETECTOR
Sample
Waste 3
Waste 2
ml/ min
V1
V4
V3
0.8
Carrier 2
IDA column
V2
Carrier 1
Direction of flow
Eluent
Peristaltic pump
Waste 1

Figure 4.4 Schematic diagram of the FI preconcentration manifold with ICP-AES or ICP-MS detection. (a)Mercury preconcentration step; (b) Mercury elution step.

with 1 for zinc). This resulted in significant interaction between the IDA resin and the mercury passing through the column when eluted with acid, thus producing broad peak shapes. Back-flushing allowed the mercury to be removed from the back of the column and therefore little contact was made with the majority of the resin.

The reagents were pumped at a flow rate of 0.8 ml min^{-1} using peristaltic pumps (Ismatec Mini-S 820, Ismatec, Switzerland) and PVC peristaltic pump tubing. The switching valves (PS Analytical, Sevenoaks, Kent, U.K.) were pneumatically operated using argon gas (20 psi). The procedure by which injections were made was as follows:

(1) The sample loop (100-2000 µl) on valve 1 (V1) was filled with the sample.

(2) Valve 1 was switched so that the contents of the loop were eluted onto the column in carrier stream 2, whilst carrier stream 1 was stopped.

(3) Valve 2 was orientated such that the solution emerging from the end of the column went to waste (Figure 4.4a).

(4) After 3-4 min (Figure 4.4b) carrier 2 was stopped and valve 4 switched to direct the flow to the detector, whilst valve 2 was switched such that the eluent passed through the column from the opposite direction.

(5) Carrier 2 was then switched such that the sample loop (V3) filled with acid-thiourea eluted the analyte from the column into the detector.

4.2.4.4 Cold vapour generation FI manifold for AFS detection

The cold vapour FI manifold for AFS detection shown in Figure 4.5 was adapted from the manifold described in Section 4.2.4.2 However, the manifold discussed here was modified such that the on-line oxidation of bound humic species and organic species of mercury could be achieved. This involved the addition of two extra channels, one for the oxidation

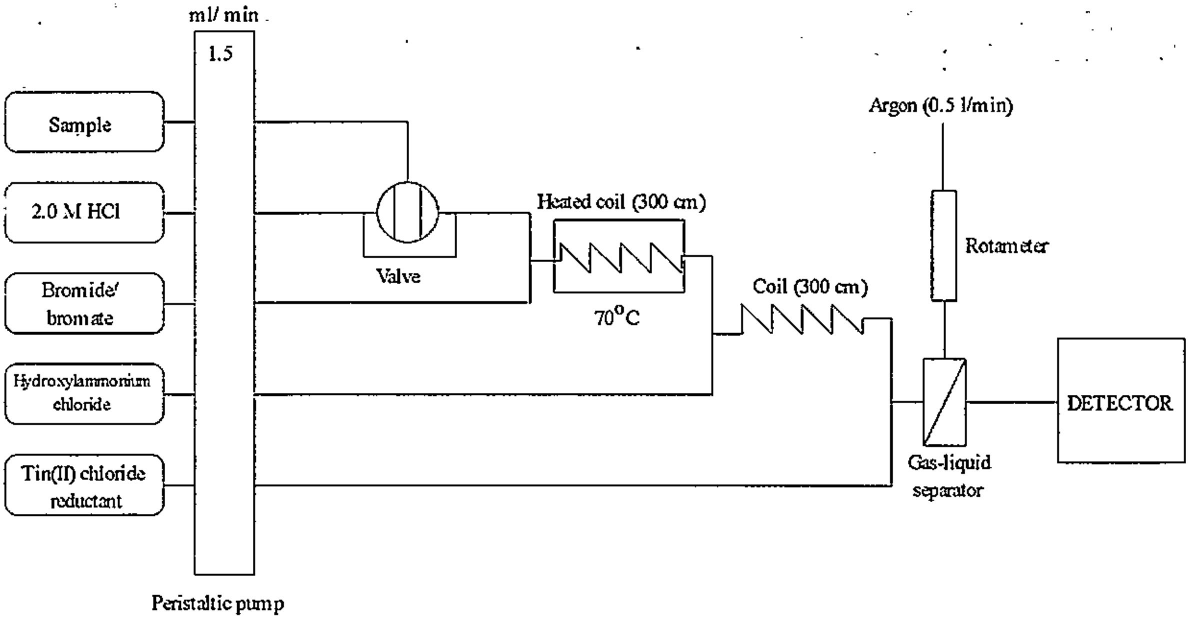
ml/ min
1.5
Sample
2.0 M HCl
Bromide/ bromate
Hydroxylammonium chloride
Tin(II) chloride reductant
Peristaltic pump
Valve
Heated coil (300 cm)
70°C
Coil (300 cm)
Argon (0.5 l/min)
Rotameter
Gas-liquid separator
DETECTOR

Figure 4.5 Schematic diagram of the cold vapour generation FI manifold for AFS detection.

step using bromide/bromate (0.5 % m/v / 0.14 % m/v) and a hydroxylammonium chloride stream (6 % m/v) to remove free bromine prior to the reduction step. All the reagent streams were pumped at a flow rate of 1.5 ml min^{-1}.

4.3 RESULTS AND DISCUSSION

4.3.1 DETERMINATION OF INORGANIC MERCURY IN SALINE AND NON-SALINE MATRICES BY ICP-AES AND ICP-MS

4.3.1.1 FI-ICP-AES

Figure 4.6 and Table 4.3 compare calibration data and figures of merit for the determination of mercury in de-ionised water and synthetic sea water (100 % v/v) using the single channel manifold (conventional pneumatic nebulisation) and the FI CVG manifold with ICP-AES detection. The results obtained using the single channel FI manifold show that the sea water matrix significantly affected the sensitivity of the instrument. Detection limits were 4.5 times higher for mercury in synthetic sea water (110 μg l^{-1}) than in de-ionised water (24 μg l^{-1}) and linearity was poorer (r^2 of 0.9910 compared with 0.9999) over the range 0-1.0 μg l^{-1}. This was due to changes in the matrix characteristics (such as density and viscosity) exerting an influence on sample introduction and transport, or matrix effects affecting the atomisation and excitation characteristics and thus altering the plasma temperature[72]. Potassium also interferes with the mercury line at 184.95 nm. However at the typical concentrations of potassium expected in sea water (60 μg l^{-1}), it was unlikely that this was causing significant interference.

The CVG manifold significantly improved the detection limits (3 σ) in both matrices to 4 μg l^{-1} from 110 and 24 μg l^{-1} respectively. This was as expected, due to the increased transport efficiency of mercury to the plasma from approximately 1 % using continuous nebulisation to approaching 100 % with CVG. The removal of potassium, which results in interfence overlap at 184.95 nm and non-spectroscopic effects due to separation of the mercury vapour from the matrix, also improved the detection limits for mercury in sea water.

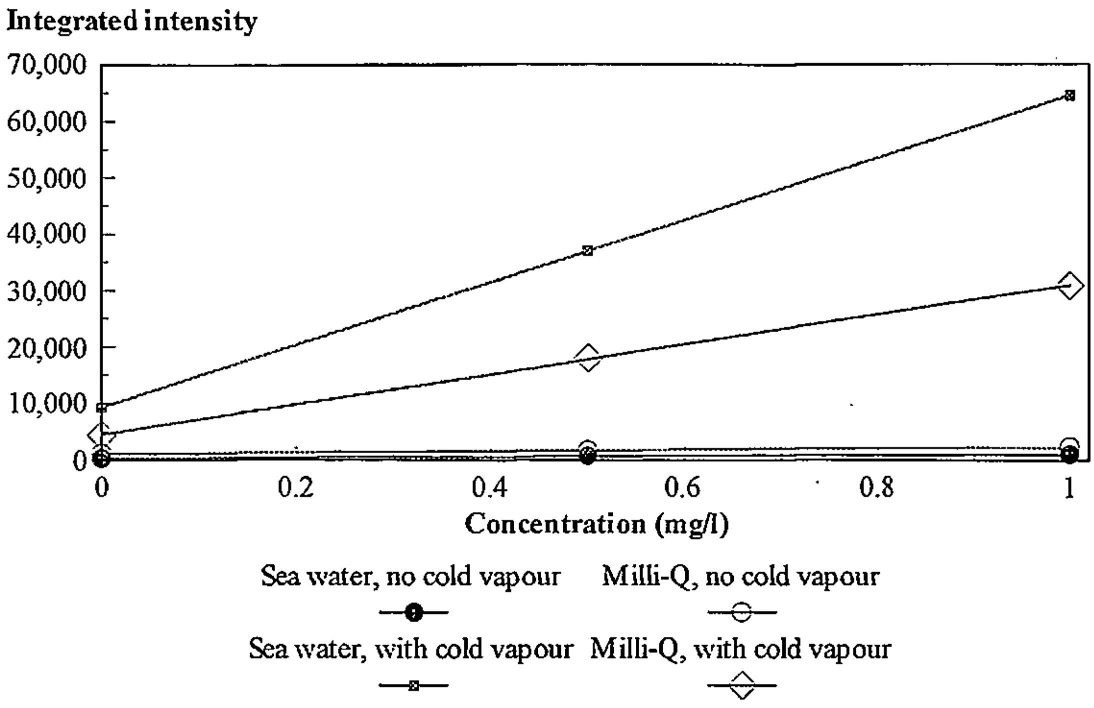

Figure 4.6 Calibration graphs for de-ionised water or synthetic sea water using either conventional (Meinhard) nebulization or cold vapour generation.

Table 4.3 Figures of merit using either conventional (Meinhard) nebulization or cold vapour generation.

Milli-Q matrix			
	Limit of detection ($\mu g\ l^{-1}$, 3 σ)	Precision (RSD %, 0.5 $\mu g\ l^{-1}$, n = 5)	Linearity (r^2), 0 - 1 $mg\ l^{-1}$
Conventional nebulisation	24	4.1	0.9999
Cold vapour generation	4	3.2	0.9999
Synthetic sea water matrix			
	Limit of detection ($\mu g\ l^{-1}$, 3 σ)	Precision (RSD %, 0.5 $\mu g\ l^{-1}$, n=5)	Linearity (r^2), 0 - 1 $mg\ l^{-1}$
Conventional nebulisation	110	2.7	0.9910
Cold vapour generation	4	1.1	0.9998

However, the increase in sensitivity also resulted in an increase in background (*e.g.* the background intensity for synthetic sea water increased from 1948 to 9230). This was attributed to mercury impurities in the tin(II) chloride and hydrochloric acid.

4.3.1.2 FI-ICP-MS

When the CVG system was initially coupled with the ICP-MS the carrier gas flow from the gas-liquid separator (0.5 l min^{-1}) was not sufficient to effectively punch the plasma and the resulting mercury peak (5.0 μg l^{-1}) was only just visible above the background (S/B = 5). Increasing the carrier flow to 0.7 l min^{-1} did punch the plasma but the increased flow also resulted in increased pressure to the gas-liquid separator. This pressure change produced larger, more irregular bubbles and lowered the liquid level in the separator, resulting in a significant increase in the background and noise with a resultant S/B ratio for mercury (5.0 μg l^{-1}) of 2.

A suitable solution to this problem was to bleed a separate argon flow into the transfer line prior to the torch assembly. It was also necessary to modify the gas-liquid separator by blanking off the existing waste overflow in order to compensate for the pressure change. The waste was removed with a peristaltic pump, allowing the liquid level in the gas-liquid separator to reach an equilibrium such that the argon purger was submerged. The modified gas-liquid separator (a) and the nebulizer flow split (b) are schematically represented in Figure 4.7. Various combinations of nebuliser and carrier gas flow rates were examined and the results are shown in Figure 4.8. Significant improvements in the S/B ratio were achieved by balancing the flow from the two streams, such that enough pressure was present to punch the plasma but not alter the gas-liquid separator level. Using this approach it was possible to improve the S/B ratio for mercury (5 μg l^{-1}) from 2 to 56

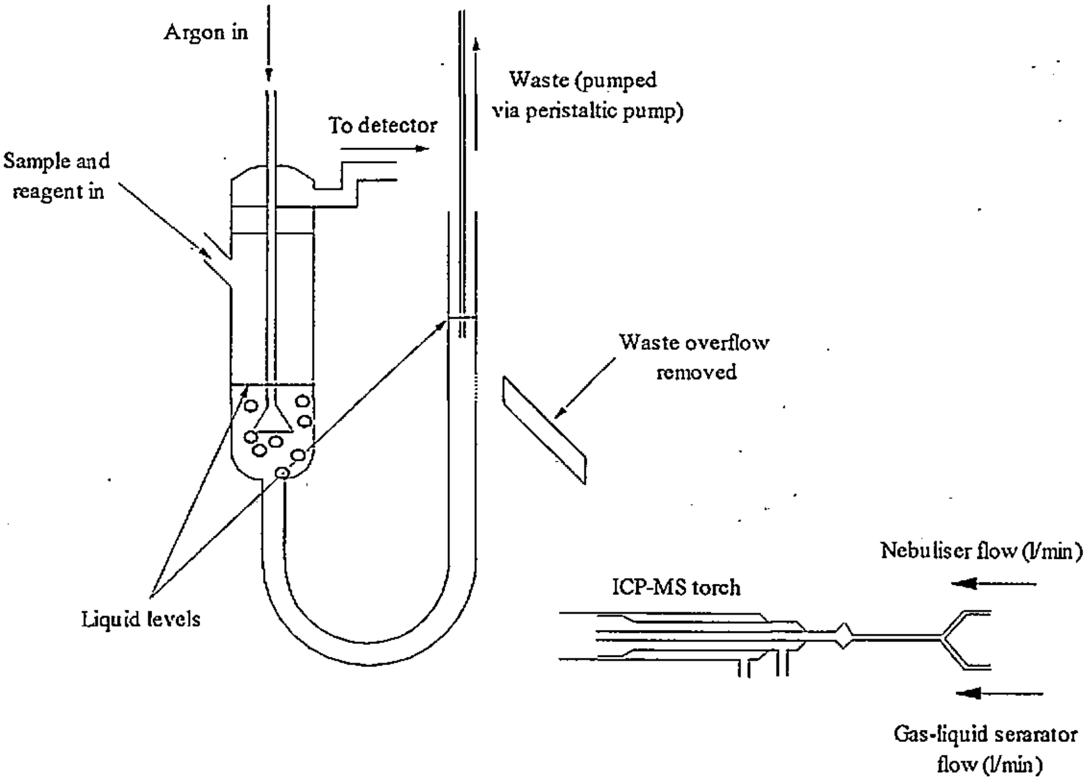
Argon in
To detector
Waste (pumped via peristaltic pump)
Sample and reagent in
Waste overflow removed
Liquid levels
ICP-MS torch
Nebuliser flow (l/min)
Gas-liquid serarator flow (l/min)

Figure 4.7 Modified gas-liquid separator for the tin(II) chloride reduction system.

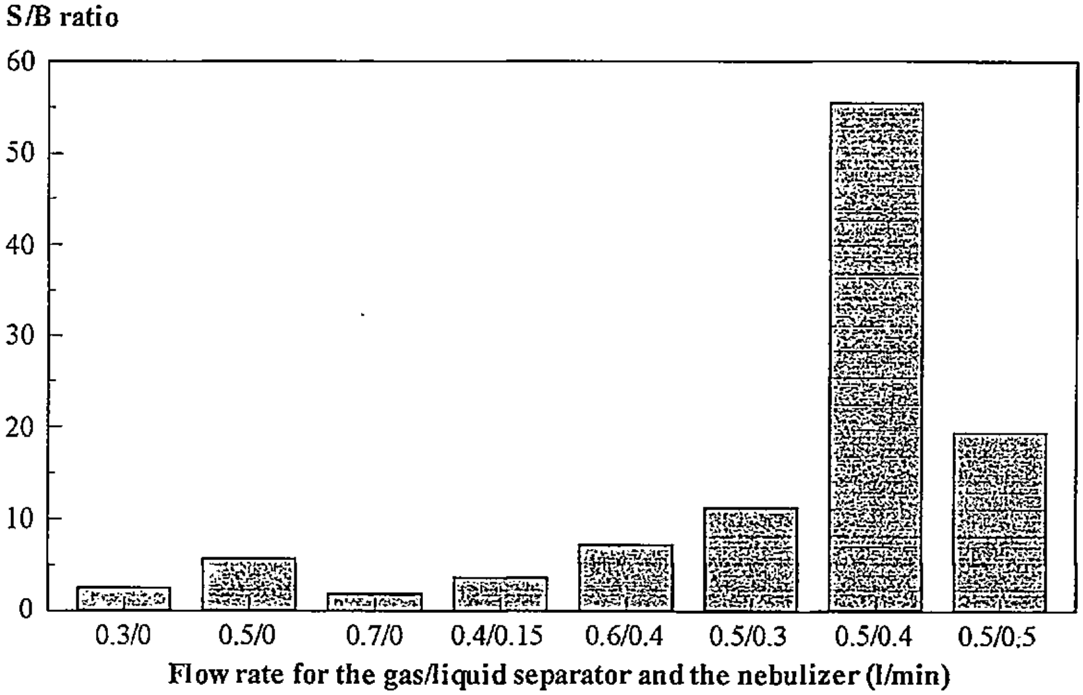

Figure 4.8 Effect of modified gas-liquid separator and nebulizer flow rates on the signal to background ratio for mercury(II) chloride.

with an argon flow rate of 0.5 l min^{-1} for the carrier gas flow and 0.4 l min^{-1} for the nebuliser gas flow. Calibration data and figures of merit for the single channel FI manifold and the CVG manifold with ICP-MS detection are presented in Figure 4.9 and Table 4.4. There was less difference between the detection limits for mercury in de-ionised water (0.5 µg l^{-1}) and the synthetic sea water (1.8 µg l^{-1}) using the single channel manifold than there was with ICP-AES detection. If the sample was continuously nebulised, it would be expected that the analysis of mercury in sea water would be problematic due to non-spectroscopic interferences. However, the injection of discrete samples through the FI manifold prevented both the excessive build up of salt on the sampler and skimmer cones and an excess of easily ionisable elements such as Na, P and Cl. The Quadrupole ion lens stack was tuned for mercury at m/z = 202 and it was also likely that mass bias at m/z = 201 precluded many of the ions at lower masses (*e.g.* Na, P, Cl etc.) that produce non-spectroscopic interferences affecting the ion beam. Precision was poor for both matrices (RSDs of 14.9 and 18.0 % respectively, 0-1.0 µg l^{-1}) because of memory effects from the glass spray chamber, even though dicrete volumes of sample (500 µl) were injected with a 2 min wash-out time between injections. Increasing the wash out time (*e.g.* 10 minutes between injections) improved the precision (6.4 % RSD, 1.0 µg l^{-1}, n = 3). However, a longer wash-out time would reduce the speed of analysis and remove one of the intrinsic advantages of FI. Linearity was also degraded for mercury in the synthetic sea water (from 0.9995 to 0.9796) due to salt build-up on the cones and/or memory effects from mercury.

When the modified CVG manifold was coupled with ICP-MS, the precision improved from 18.0 % to 4.1 % RSD for mercury in synthetic sea water (1.0 µg l^{-1}, n = 5). This again suggested that significant plating of mercury on the ICP-MS glassware was occurring when using the single channel manifold with conventional pneumatic nebulisation.

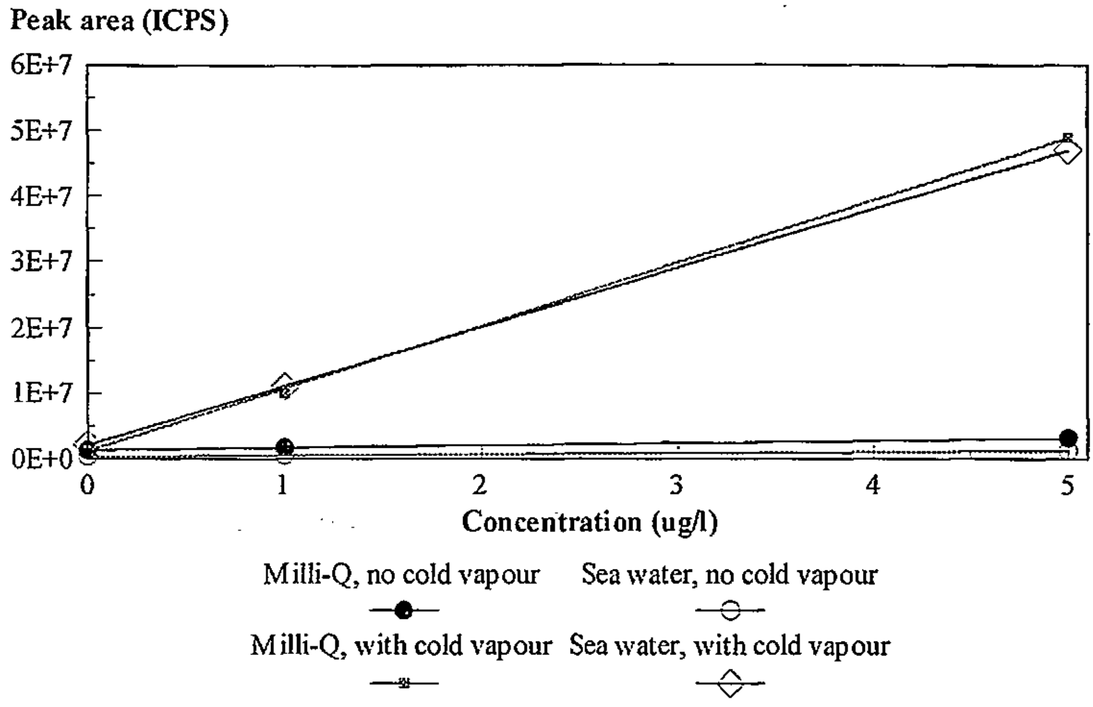

Figure 4.9 Calibration graphs for de-ionised water or synthetic sea water using either conventional (Meinhard) nebulization or cold vapour generation.

Table 4.4 Figures of merit using either conventional (Meinhard) nebulization or cold vapour generation.

Milli-Q matrix			
	Limit of detection (ng l^{-1}, 3 σ)	Precision (RSD %, 1.0 μg l^{-1}, n = 5)	Linearity (r^2), 0 - 5 μg l^{-1}
Conventional nebulisation	500	14.9	0.9995
Cold vapour generation	40	2.9	0.9993
Synthetic sea water matrix			
	Limit of detection (ng l^{-1}, 3 σ)	Precision (RSD %, 1.0 μg l^{-1}, n=5)	Linearity (r^2), 0 - 5 μg l^{-1}
Conventional nebulisation	1800	18.0	0.9796
Cold vapour generation	40	4.1	0.9999

Detection limits were improved by 45 times (from 1800 to 40 ng l^{-1}) when determining mercury in spiked synthetic sea water. Methylmercury chloride (1 μg l^{-1}) was also determined after off-line oxidation to mercury(II) chloride with 2 ml of potassium bromide/potassium bromate solution (0.5 % v/v bromide/0.14 % v/v bromate (2 ml) in 33 % v/v hydrochloric acid (15 ml)). The recovery was 97 % (n = 4) when compared with the results for an equivalent concentration of mercury(II) chloride (1 μg l^{-1}).

Although the detection limits described above would be acceptable for many biological matrices (*e.g.* marine biological CRMs such as TORT-1 contain over 300 μg l^{-1} total mercury), it would be difficult to determine mercury at natural levels in sea water samples (typically less than 20 ng l^{-1})[206]. A preconcentration method for the determination of total mercury in sea water was therefore developed.

4.3.2 ON-LINE PRECONCENTRATION OF TOTAL MERCURY WITH ICP-MS DETECTION

4.3.2.1 Optimisation of the procedure

Initial studies using the FI system developed for the preconcentration of trace metals such as Mn, Co, Cu, Zn and Pb from sea water suggested that the procedure would require considerable modification for the preconcentration of mercury. At high masses such as m/z = 202 spectroscopic ion interferences do not occur and non-spectroscopic effects appeared to be less significant. Therefore it was decided that ammonium acetate buffer (used to exclude Na from the column) was not necessary and initial studies used Milli-Q deionised water as the carrier stream. By analysing the efluent from the column prior to the elution step it was found that the column retained 100 % of the mercury. However, 2.0 M hydrochloric acid (500 µl) was not sufficient to quantitatively remove the retained mercury and it was necessary to carry out at least 3 successive 500 µl elutions to remove all mercury from the column. The same effect was observed using higher concentrations of hydrochloric acid (3.0 M). However, when the FI manifold was backflushed with 3.0 M hydrochloric acid (500 µl), mercury was quantitatively removed from the column (*e.g.* no mercury was observed upon a second elution of hydrochloric acid). Although mercury was eluted from the column, prolonged use of such concentrations of acid would rapidly degrade the column by destroying the PS-DVB substrate (Section 3.2.2.2) and therefore an alternative approach for the elution of mercury was required.

Although complexing agents such as thiourea and thiocyanate form stable complexes with mercury (with stability constants, $\alpha_{M(L)}$, of 22.4 and 16.9 respectively), 1.0 M solutions of these complexing agents (500 µl) were not capable of eluting mercury from the column, suggesting that the IDA-Hg complex was more stable than 2-mercaptoethanol or thiourea. However, previous workers used acidic-thiourea solutions (pH 1.0)[243] to quantitatively elute mercury from dithiocarbamate resin and this approach was examined using the IDA based MetPac column.

A univariate investigation of a number of variables in the FI procedure was carried out with ICP-MS detection, in order to ascertain the optimum conditions for the preconcentration and subsequent elution of mercury(II) chloride and methylmercury chloride. These variables were hydrochloric acid eluent concentration (0 - 2.5 M), thiourea eluent concentration (0 - 2.5 % m/v), thiourea carrier concentration (0 - 2 % m/v) and sample volume (50 - 2000 µl) and were optimised to give the maximum peak height.

Eluent concentration

The eluent concentration was optimised in the following manner. The thiourea concentration was kept constant at 1.0 % m/v whilst the hydrochloric acid concentration was varied. The process was then reversed such that the hydrochloric acid concentration was kept constant at 2.0 M whilst the thiourea concentration was varied. The results are given in Figures 4.10 and 4.11. Figure 4.10 shows that increasing the hydrochloric acid concentration increased the peak height for mercury (1.0 µg l^{-1}). With no hydrochloric acid, a small broad peak was observed (height = 5 x10^5 counts per second, CPS) and examining the peak area revealed that mercury was being retained on the column. This was substantiated when hydrochloric acid (2.0 M) was pumped through the column and a second broad mercury peak observed. With any acid concentration above 0.5 M complete elution of mercury was achieved (determined from the peak area for mercury at each hydrochloric acid concentration) although peak tailing occurred. Above 2.0 M HCl the increase in peak height was negligable (height = 3.1 x 10^6 CPS at 2.0 M compared with 3.2 x 10^6 CPS at 2.5 M).

Varying the thiourea concentration also had a significant effect on the peak height for the mercury spike. Figure 4.11 shows an optimum at 2 % m/v thiourea. At concentrations above 2 % m/v the dissolved solids content was such that there was a reduction in peak height (from 3.3 x 10^6 CPS at 2.0 % m/v to 1.9 x 10^6 CPS at 3.0 % m/v) due to matrix effects, including an observed build-up of solids on the cones. When no thiourea was present in the eluent there was retention of mercury on the column which again could only be removed with successive elutions of 2.0 M hydrochloric acid. Significant peak tailing was still occuring.

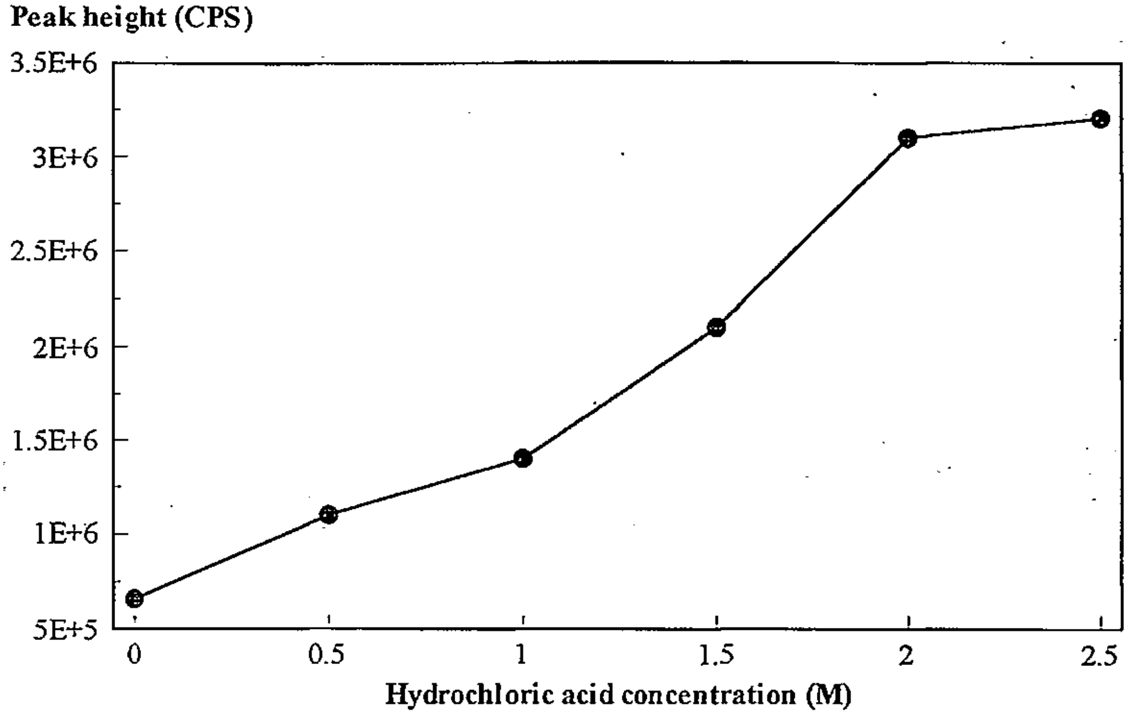

Figure 4.10 Optimisation of hydrochloric acid eluent concentration

(thiourea concentration maintained at 1.0 % m/v).

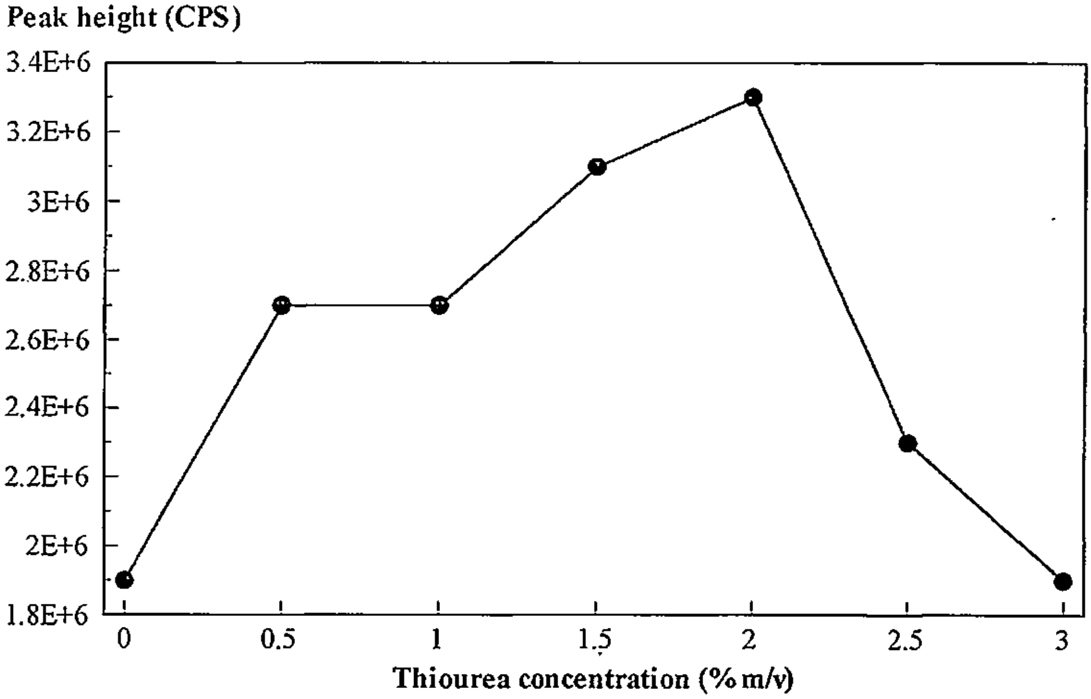

Figure 4.11 Optimisation of thiourea concentration

(hydrochloric acid concentration maintained at 2.0 M).

Carrier stream concentration

Thiourea was added to the carrier stream to see whether it would reduce peak tailing and improve peak shape. The results are shown in Figure 4.12. With a de-ionised water carrier stream the result was similar to that described above (Figure 4.11). The addition of 0.1 % m/v thiourea to the carrier stream resulted in a dramatic increase in peak height and a reduction in peak tailing. Beyond this concentration, the peak shape deteriorated, due to increased dissolved solids loading in the plasma. The thiourea in the carrier improved the peak shape because the equilibrium within the column was altered, such that the IDA-mercury complex was less stable than in de-ionised water and the eluent could thus compete more effectively with mercury ions for the chelating sites.

Sample volume

The effect of sample volume on the detection of mercury was also examined. Figure 4.13 shows that increasing the sample volume did not give a linear detector response due to mercury contamination from the argon gas or the reagents. Another effect of increasing the sample volume was an improvement in precision. With a 200 µl sample loop the precision for 1 µg l^{-1} mercury was 8.1 % RSD (n = 4). When the sample volume was increased to 2000 µl the precision was improved to 5.8 % RSD (n = 4). This was again attributed to the greater concentration of mercury entering the plasma.

4.3.2.2 Figures of merit

Linear calibrations and figures of merit for mercury(II) chloride and methylmercury chloride in 100 % v/v synthetic sea water are presented in Figure 4.14 and Table 4.5. The preconcentration procedure was effective for both mercury species over the range 50 -

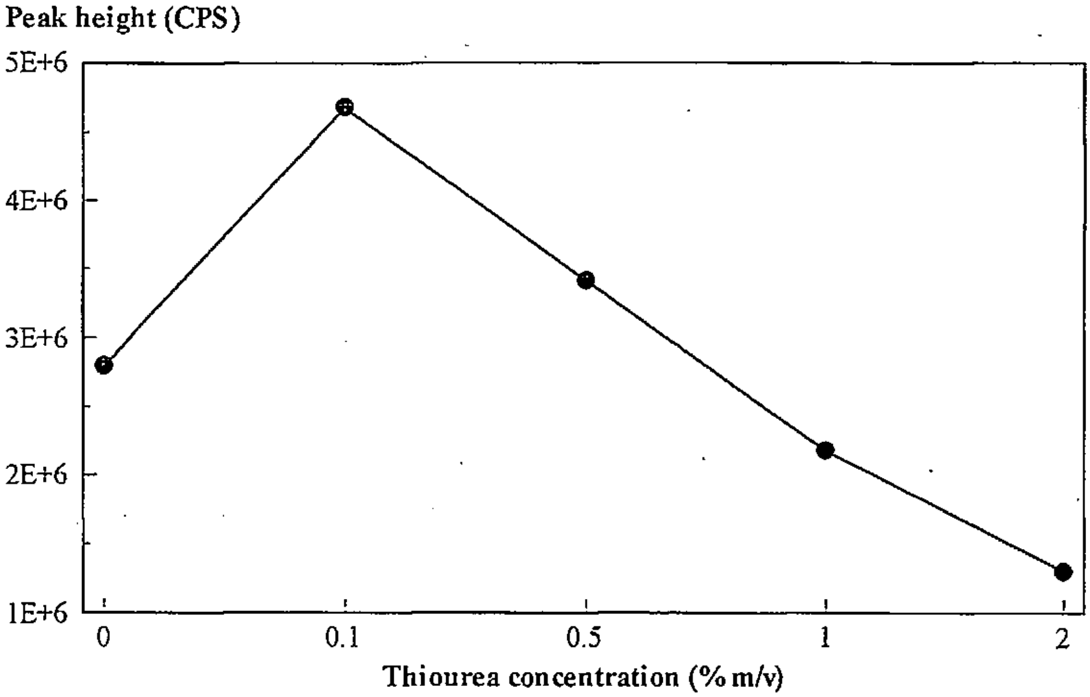

Figure 4.12 Optimisation of thiourea concentration in carrier stream.

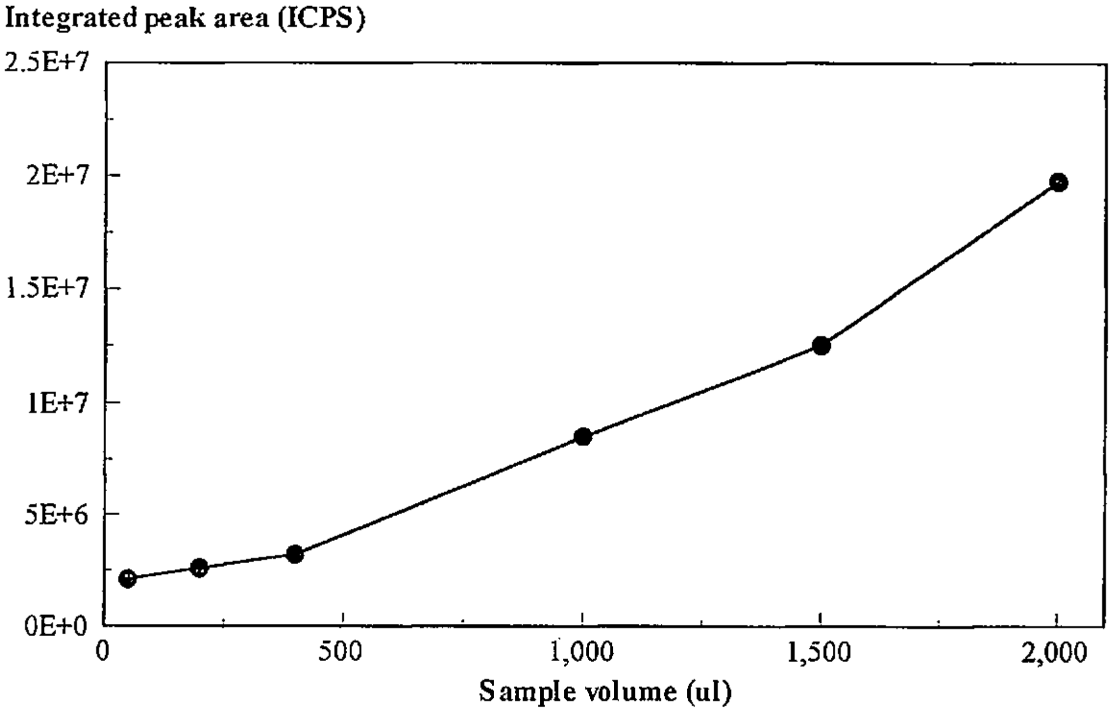

Figure 4.13 Effect of sample volume on the response for mercury(II) chloride (5.0 µg l^{-1}).

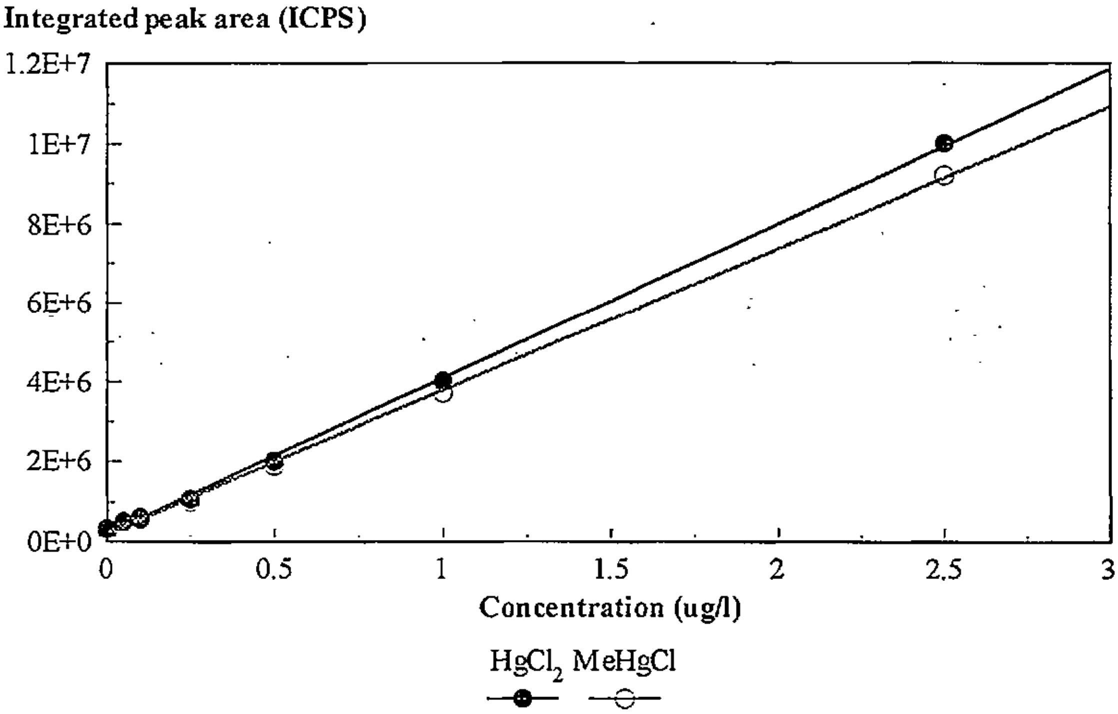

Figure 4.14 Calibration graph for mercury(II) chloride and methylmercury chloride in 100 % v/v synthetic sea water.

Table 4.5 Figures of merit for the on-line preconcentration of mercury.

	Mercury(II) chloride	Methylmercury chloride
Limit of detection, ng l^{-1} (3 σ)	11	14
Precision (RSD %, 50 ng l^{-1}, n=4)	1.2	3.5
Linearity (r^2, 50-2500 ng l^{-1})	0.9992	0.9985

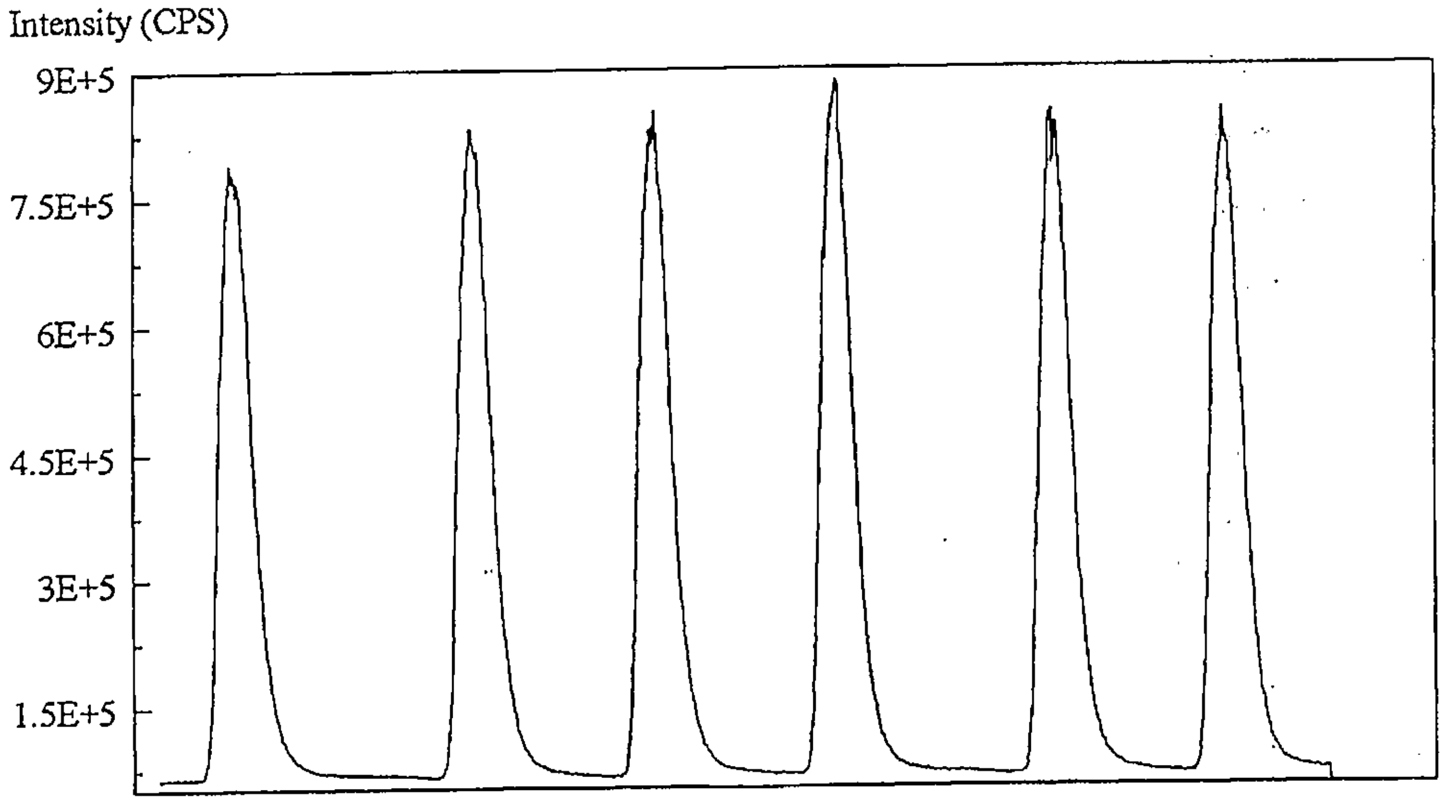

Figure 4.15 Replicate 100 ng l^{-1} mercury peaks.

2500 ng l^{-1} (r^2 = 0.9992 and 0.9985 respectively) and precision was excellent (1.2 % and 3.5 % RSD respectively, 50 ng l^{-1}, n = 4). The resultant detection limits of 11 ng l^{-1} for mercury(II) chloride and 14 ng l^{-1} for methylmercury chloride were considerably better than those achieved using the CVG system (40 ng l^{-1} for mercury(II) chloride) and are similar to, or better than, those achieved using FI-CVG and FI preconcentration procedures coupled with AFS (10 - 200 ng l^{-1}), FAAS (10 - 100 ng l^{-1}), ICP-AES (0.2 - 2.0 µg l^{-1}), and ICP-MS (4 ng l^{-1})[244-249]. Replicate injections of 100 ng l^{-1} mercury are shown in Figure 4.15.

4.3.2.3 Validation using TORT-1 CRM

At present, a natural water CRM with a certified value for mercury is not available. Therefore in order to validate the method a marine biological reference material TORT-1, which has a certified value for total mercury of 330 µg l^{-1}, was analysed. The lobster hepatopancreas digest was buffered to pH 8 with ammonia solution and diluted to 0.825 µg l^{-1} with Milli-Q. Mercury standards in the range 0 - 1.0 µg l^{-1} were also prepared in Milli-Q. The results are shown in Table 4.6. The calibration graph for mercury showed good linearity (r^2 = 0.9994), precision was excellent (1.5 % RSD, 0.5 µg l^{-1}, n = 4) and reasonable agreement with the certified value was achieved.

Table 4.6 TORT-1 certified reference material results.

	Calculated value (µg l^{-1})	Certified value (µg l^{-1})
TORT-1	348 ± 33	330 ± 60

4.3.2.4 Analysis of a Sutton Harbour sample

The FI preconcentration procedure described above was further modified for the determination of mercury in real sea water samples. The preconcentration step was performed off-line by pumping the sample through the column using an HPLC pump (Altex

110A) at a flow rate of 9 ml min^{-1}. This enabled a 500 ml sample to be concentrated on the column in less than 1 hour. After the preconcentration step the column was washed with Milli-Q for 5 min and then coupled with the ICP-MS in the FI manifold described in Section 4.2.4.3. Using this procedure duplicate mercury standards (0, 1, 10, 30 and 100 ng l^{-1}) made up in Milli-Q (500 ml) were preconcentrated on the MetPac column and eluted into the ICP-MS detector. The results are shown in Table 4.7 The preconcentration procedure was linear between 1 and 100 ng l^{-1} Hg, indicating that breakthrough of mercury was not occuring in this concentration range. The detection limit was further improved (6 ng l^{-1} compared with 11 ng l^{-1} for the on-line preconcentration procedure described above). However, considering the increased preconcentration factor (1000 compared with 4 for the on-line system) the improvement was less than expected. This was due to an elevated blank value (x 10008 ICPS, 22.0 % RSD compared with 16090 ICPS for 10 ng l^{-1}) resulting from background levels of mercury in the synthetic sea water or the acidic-thiourea eluent.

Table 4.7 Figures of merit for the off-line total mercury preconcentration procedure.

Limit of detection, ng l^{-1} (3 σ)	6.0
Precision (RSD %, 10 ng l^{-1}, n=3)	13.3
Linearity (r^2, 1 - 100 ng l^{-1})	0.9957

The off-line preconcentration step was then applied to the analysis of two coastal sea water samples. The samples were collected in 1.0 l acid-washed (20 % hydrochloric acid) amber glass bottles from Sutton Harbour, Plymouth and acidifed to pH 2.0 on collection. The sampling locations are shown in Figure 4.24. Prior to preconcentration, the pH of each sample was adjusted to pH 8.0 with ammonia solution and divided into 500 ml aliquots. The preconcentration system was fitted with an on-line filter (45 μm) to remove any

suspended solids. The levels determined in each sample are shown in Table 4.8 and are compared with the FI-CVG-AFS technique in Table 4.13.

Table 4.8 Total mercury concentrations in two environmental samples.

Sutton Harbour SH2 surface water	37 ng l^{-1}
Sutton Harbour SH3 surface water	41 ng l^{-1}

The levels were slightly elevated from typical total mercury concentrations in sea water (< 30 ng l^{-1}) However, Sutton harbour, a busy fishing and yachting marina located near the Naval dockyards at Devonport, has recently undergone considerable development, including the construction of a tidal barrage. The considerable industrial activity in the area combined with an estimated increase in flushing times for the water present in the harbour from 25 (spring)-62 hours(neap) to 136 (spring)->300 hours (neap)[250], due to the barrage, may explain why the concentration of heavy metals such as mercury are elevated.

4.3.3 FI-CVG-AFS

The CVG manifold discussed in Section 4.2.4.2 was coupled with AFS detection for comparative purposes. No modification to the system was required. Detection limits for this procedure were 15 ng l^{-1} (3 σ). Using this manifold as a starting point, an on-line oxidation step using the bromide/bromate scheme to convert organic or complexed mercury to the mercury(II) form was developed. A schematic diagram of the manifold is shown in Figure 4.5. Historically this procedure has been performed off-line prior to the reduction step, although recently on-line oxidation using potassium persulphate has been successfully employed for the determination of total mercury in urine[245].

4.3.3.1 Optimisation of the procedure

Using reagent concentrations similar to those used for the off-line oxidation of organic mercury species (0.5 % m/v bromide/0.14 % m/v bromate; 2 % m/v hydroxylammonium chloride), initial experiments showed that although inorganic mercury was being detected, organic mercury was not. This was due to insufficient time for the oxidation of the sample to take place, prior to the removal of excess bromine with the hydroxylammonium chloride (HAC). From the results shown in Figure 4.16, increasing the reaction coil length increased the peak height for methylmercury chloride from 27 arbitary units with a 100 cm coil to 110 arbitary units with a 300 cm coil. A further increase in reaction coil length resulted in increased dispersion of the sample and a resultant broadening of the peak. From this figure it was also apparent that the organic mercury peak (100 $\mu g\ l^{-1}$) was approximately half that of the inorganic peak (100 $\mu g\ l^{-1}$).

Increasing the oxidising agent from 0.5/0.14% to 0.75/0.21% bromide/bromate resulted in a reduction in peak height for both species (100 $\mu g\ l^{-1}$), suggesting that bromine was quenching the fluoresence. Increasing the HAC concentration did not improve the situation. Figure 4.17 and Table 4.9 show how the effect of increasing or decreasing these two reagents affected the detection of organic and inorganic mercury. The general rule shown in Figure 4.17 was that increasing the oxidising agent concentration increased quenching of the fluoresence, and increasing the HAC concentration to remove the excess bromine resulted in poorer mixing with the bromination reagents due to changes in the HAC viscosity, which again resulted in bromine reaching the detector. It is also apparent from Figure 4.17 that the organic mercury signal was consistently half that of the inorganic signal, indicating that the conversion of the organic mercury form to the mercury(II) form was incomplete.

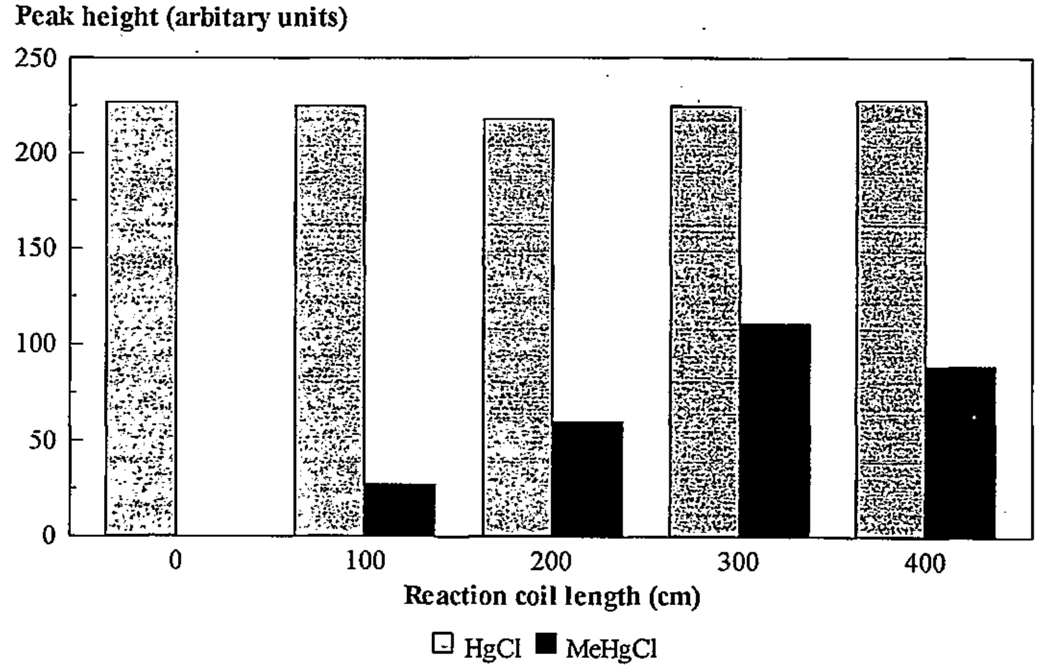

Figure 4.16 Effect of bromide/bromate reaction coil length on the detection of mercury(II) chloride and methylmercury chloride.

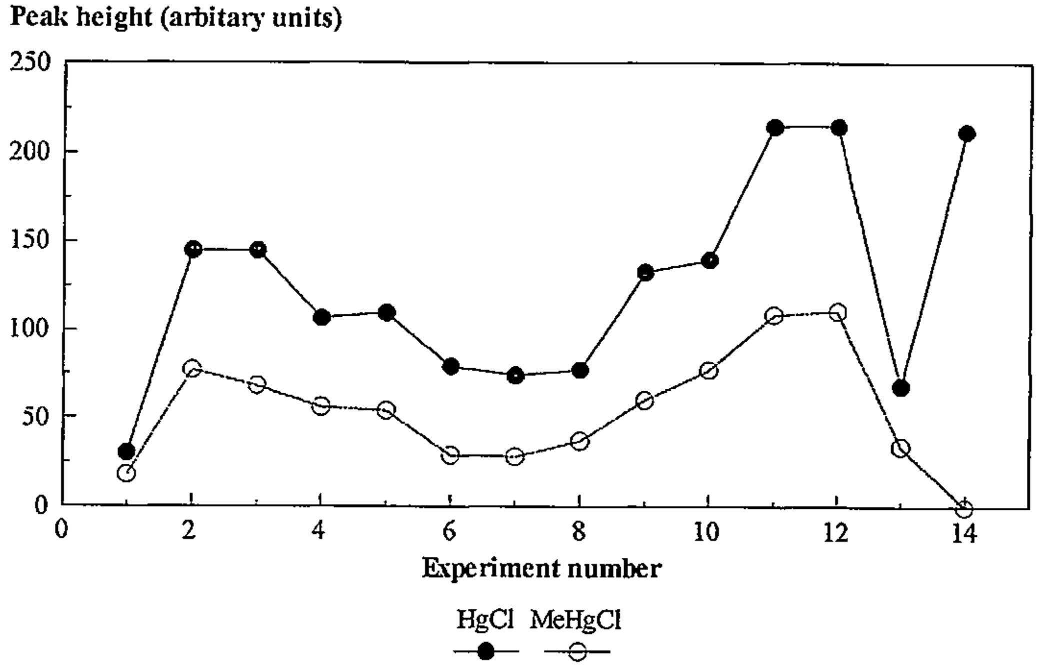

Figure 4.17 Effect of bromide/bromate and hydroxylammonium chloride concentration on the determination of mercury(II) chloride and methylmercury chloride (see Table 4.9).

Table 4.9 Bromide/bromate and hydroxylammonium chloride concentrations.

Experiment no.	Bromide/bromate concentration (% m/v)	Hydroxylammonium chloride concentration (% m/v)
1	0.56/2.38	12
2	0.28/1.0	10
3	0.28/1.0	8
4	0.28/1.0	6
5	0.28/1.0	4
6	0.21/0.75	4
7	0.21/0.75	2
8	0.14/0.5	12
9	0.14/0.5	10
10	0.14/0.5	8
11	0.14/0.5	6
12	0.14/0.5	4
13	0.14/0.5	0
14	0	0

Since altering the reagent concentrations was not successful in converting organic mercury to inorganic mercury, another approach to increase the kinetics of the conversion was needed. A stopped-flow method was considered but the operator would need to time each injection accurately in order to determine when the reagents were mixed, and when the oxidation process was over. A more elegant method was to incorporate a heated reaction coil (100 cm, Tecator, Perstorp Analytical, Bristol, UK.) in the FI manifold. Using this coil together with a 200 cm un-heated coil, the results shown in Figure 4.18 were obtained.

The reagent concentrations were kept at the following levels: 0.5 % m/v bromide/ 0.14 % m/v bromate; 6 % m/v hydroxylammonium chloride and 3 % tin(II) chloride as these concentrations gave the best response for inorganic mercury. A 200 cm HAC reaction coil was also incorporated to thoroughly mix the two reagent streams. At 30^{0}C the organic mercury peak height (80 arbitary units) was approximately half that for the inorganic mercury peak height (170 arbitary units). However as the temperature increased, the difference in peak height between the species decreased to a point where both species give similar responses (70^{0}C) but the increase in peak height for methylmercury chloride (101 arbitary units) resulted in a decrease in peak height for mercury(II) chloride (from 168 arbitary units to 100 arbitary units). The reduction in mercury(II) chloride sensitivity was again due to the fluoresence being quenched, although in this instance as a result of an increase in excess bromine from the more efficient heated oxidation step.

In order to remove the excess bromine, the HAC reaction coil length was investigated. The results are shown in Figure 4.19. Increasing the reaction coil length from 200 cm to 300 cm resulted in an increase in peak height for both species (211 arbitary units for mercury(II) chloride and 198 arbitary units for methylmercury chloride). This was comparable with the peak height for inorganic mercury when no oxidation step was involved (205 arbitary units)

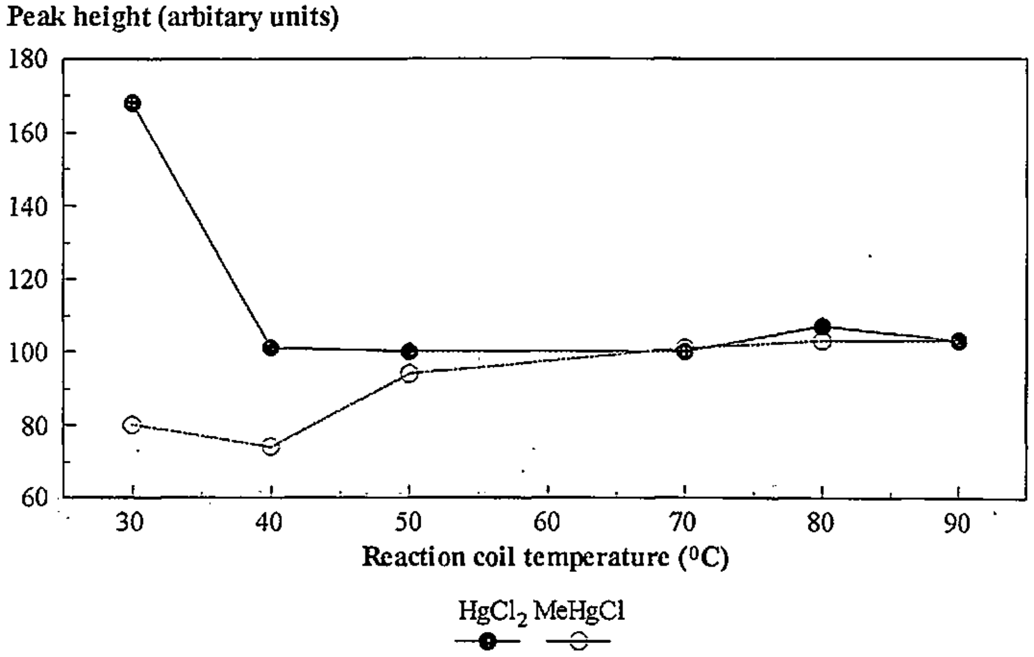

Figure 4.18 Effect of Bromide/bromate reaction coil temperature on the determination of mercury(II) chloride and methylmercury chloride.

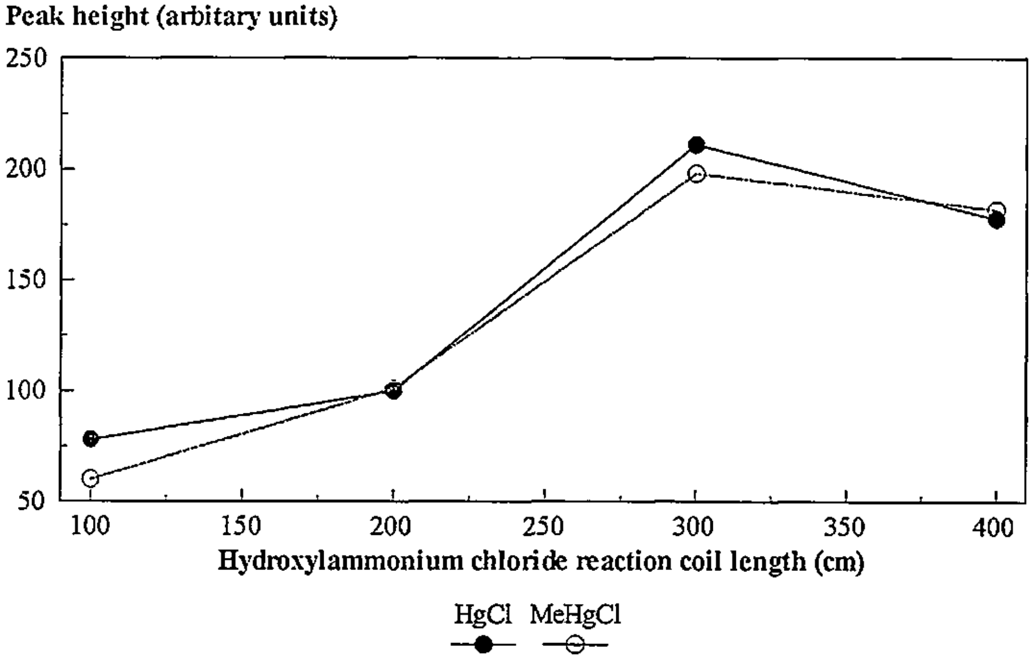

Figure 4.19 Effect of hydroxylammonium chloride reaction coil length on the determination of mercury(II) chloride and methylmercury chloride.

(Figure 4.17, experiment 7). The conversion of mercury(II) to the elemental form can be considered to be approaching 100 % efficient and therefore the recoveries for each species when the oxidation step was on-line were 103 % (3.9 % RSD) and 97 % (4.6 % RSD) respectively. Increasing the coil length further resulted in increased dispersion and a decrease in peak height (175 arbitary units) for both species. The final FI-CVG conditions used are given in Table 4.10.

Table 4.10 FI-CVG-AFS conditions for the on-line oxidation of organic mercury species.

Tin(II) chloride	3.0 % in 15.0 % hydrochloric acid
Potassium bromide/bromate	0.5 %/0.14 %
Hydroxylammonium chloride	6.0 %
Hydrochloric acid carrier stream	2.0 M
Oxidation reaction coil length	300 cm (100 cm heated)
Oxidation reaction coil temperature	70°C
Hydroxylammonium chloride reaction coil length	300 cm
Sample volume	200 µl

Using the conditions described in Table 4.10, the effect of increasing the sample volume was investigated. Increasing the sample volume from 100 µl to 2000 µl (Figure 4.20) resulted in a non-linear increase in peak height for mercury(II) chloride. However the peak height for methylmercury chloride did not increase by the same magnitude, resulting in a decrease in the ratio between the peak heights of two species from 99 % to 38 %. This was because larger sample volumes were not getting sufficiently mixed with the hydrochloric acid carrier stream and the bromide/bromate stream which resulted in only partial oxidation of the methylmercury chloride. This phenomenon is demonstrated in Figure 4.21 where a 2000 µl methylmercury chloride standard (100 µg l^{-1}) was injected into the manifold. The two peaks represent the front and back of the injected sample.

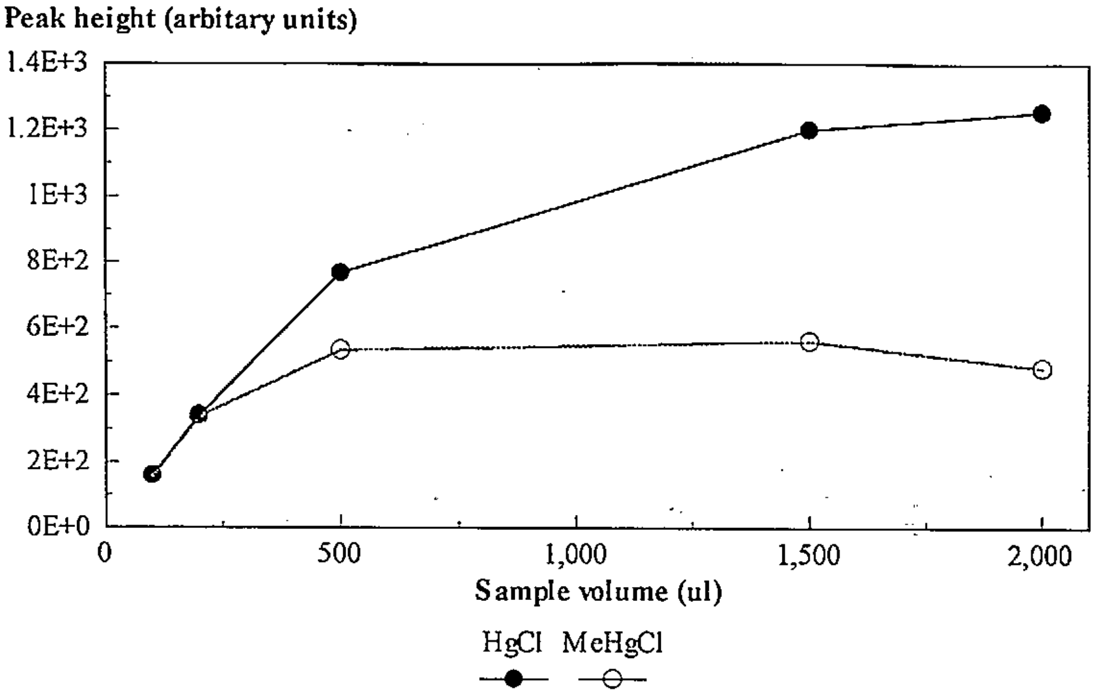

Figure 4.20 Effect of sample volume on the determination of mercury(II) chloride and methylmercury chloride.

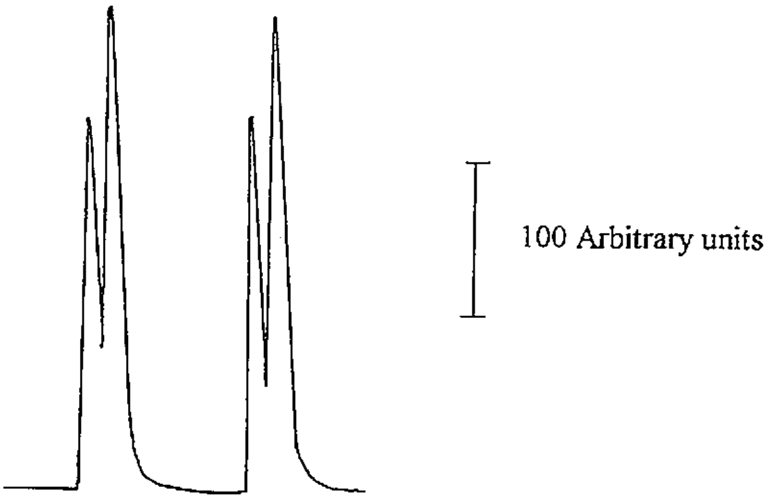

Figure 4.21 The effect of incomplete oxidation of methylmercury when injecting 2000 µl sample volumes.

4.3.3.2 Figures of merit

Figures of merit, calibration data and typical peak profiles for the FI-CVG AFS procedure are given in Table 4.11 and Figure 4.22 and 4.23. The procedure was linear to 200 ng l^{-1} for both species (r^2 = 0.9963 and 0.9957 for mercury(II) chloride and methylmercury chloride respectively) and the precison was good (3.8 % and 1.0 % RSD respectively, 50 ng l^{-1}, n = 3). Detection limits for both species were also good (25 and 23 ng l^{-1} respectively, 3 σ) and were comparable with those achieved using the manifold without the oxidation step (15 ng l^{-1}) and the on-line preconcentration procedure using the MetPac column (11-14 ng l^{-1}).

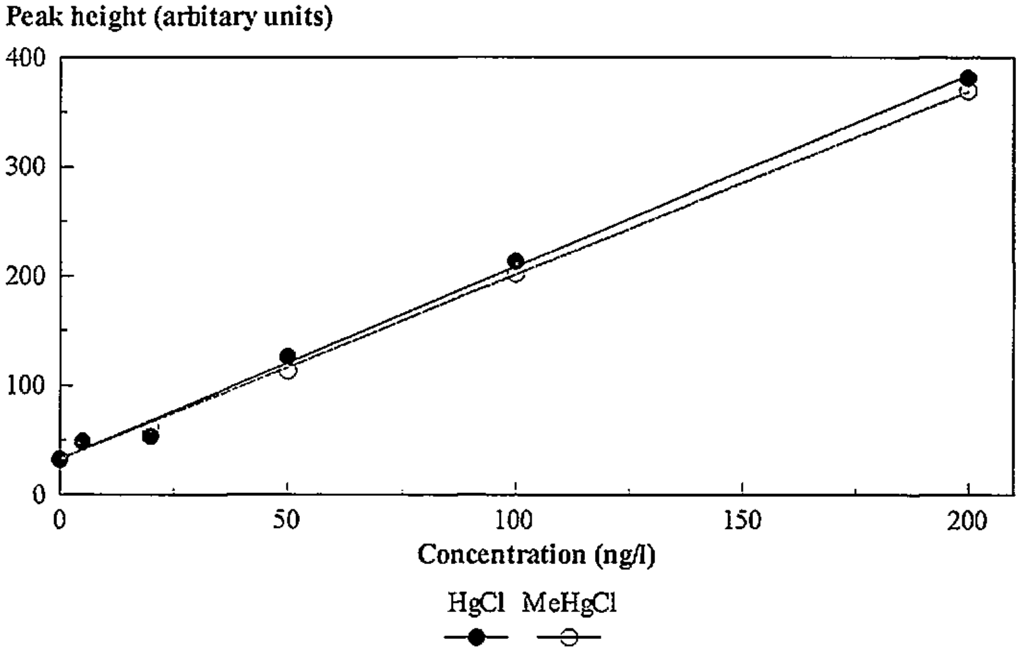

Figure 4.22 Calibration graph for mercury(II) chloride and methylmercury chloride in 100 % v/v synthetic sea water.

Table 4.11 Figures of merit for the on-line determination of mercury(II) chloride and methylmercury chloride in 100 % v/v synthetic sea water (200 μl sample volume).

	Mercury(II) chloride	Methylmercury chloride
Limit of detection, ng l^{-1}(3 σ)	25	23
Precision (RSD %, 50 ng l^{-1}, n=4)	3.8	1.0
Linearity (r^2)	0.9963	0.9957

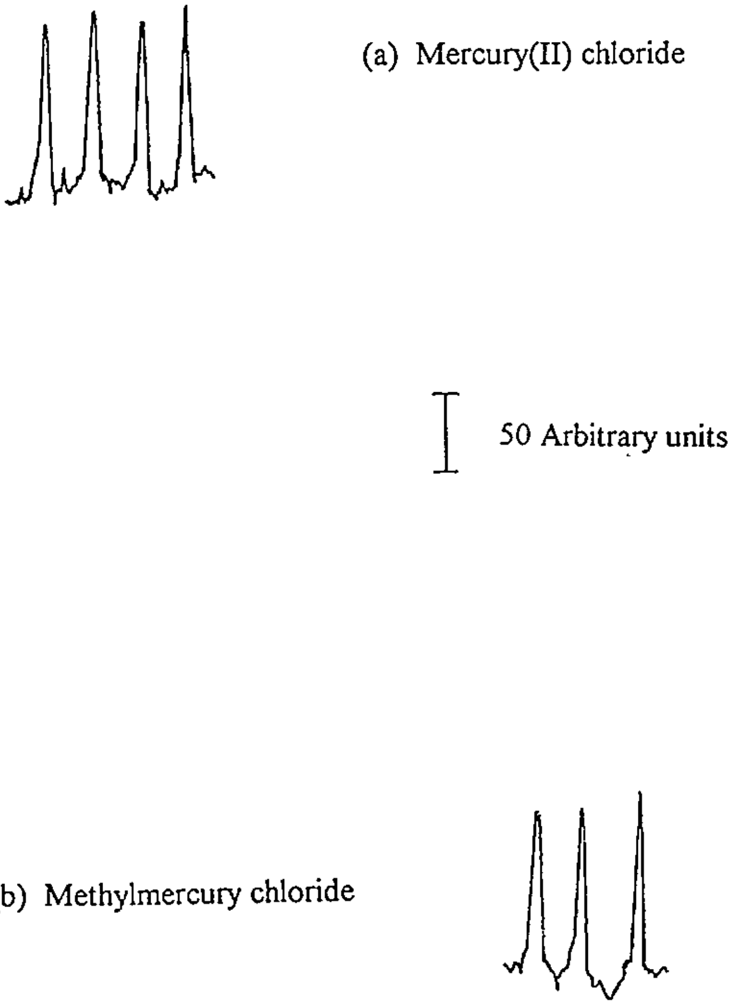

Figure 4.23 Replicate injections of 50 ng l^{-1} mercury(II) chloride (a); and methylmercury chloride (b) in 100 % v/v synthetic sea water.

4.3.3.3 Validation using TORT-1 CRM

The method was validated by analysing the marine biological reference material TORT-1 (described in section 4.2.3 and 4.3.2.3) which had a certified value for total mercury of 330 μg l^{-1}. The lobster hepatopancreas digest was diluted to 0.825 μg l^{-1} with Milli-Q de-ionised water. Mercury(II) chloride standards in the range 0 - 3.0 μg l^{-1} were prepared in a 2 % v/v nitric acid solution. The results are shown in Table 4.12. The calibration for mercury was linear between 0 - 3.0 μg l^{-1} ($r^2 = 0.9989$) and the precision was good (1.5 % RSD, 0.5 μg l^{-1}, n = 4). Reasonable agreement with the certified value was achieved. The result (353 ± 64 μg l^{-1}) was comparable with that calculated for the on-line preconcentration procedure in section 4.2.2.3 (348 ± 33 μg l^{-1}).

Table 4.12 TORT-1 Certified reference material results.

	Calculated value (μg l^{-1})	Certified value (μg l^{-1})
TORT-1	350 ± 60	330 ± 60

4.3.3.4 Analysis of Sutton Harbour samples

The FI-CVG-AFS technique was applied to the analysis of a series of coastal sea water samples. Eight samples were collected in 1.0 l acid-washed (20 % hydrochloric acid) amber glass bottles from either the bottom or the surface of Sutton Harbour, Plymouth and acidified to pH 2.0 upon collection. The sampling locations are shown in Figure 4.24. Prior to analysis, a sub-sample of each water (100 ml) was removed from the collected sample and filtered (45 μm). The total mercury levels determined in each sample are shown in Table 4.13 along with the results obtained for the off-line preconcentration technique using the MetPac column.

Table 4.13 Sutton Harbour total mercury concentrations.

Sample	**Surface** $ng\ l^{-1}$	**Bottom** $ng\ l^{-1}$	**Surface (off-line preconcentration)** $ng\ l^{-1}$
SH 1	24	38	-
SH 2	31	33	37
SH 3	52	54	41
SH 4	33	48	-

The results in Table 4.13 show that there was reasonable agreement between the two techniques. The total mercury levels in the analysed samples are at, or slightly above, expected coastal levels (typically <30 ng l^{-1}) due to the enclosed nature of the harbour, particularly since the completion of the tidal barrage (see Section 4.3.2.4). There was little variation between the sample sites. The exception was at SH3 where the elevated levels can be attributed to considerable construction activity, including land reclamation, close to the sample point. The samples collected at the bottom of the harbour are all elevated in relation to the surface levels. This was expected, as mercury is more strongly adsorbed onto particulate matter than in water and therefore mercury levels in sediments are generally much higher than in water (typically 0.5 - 30.0 mg kg^{-1}).

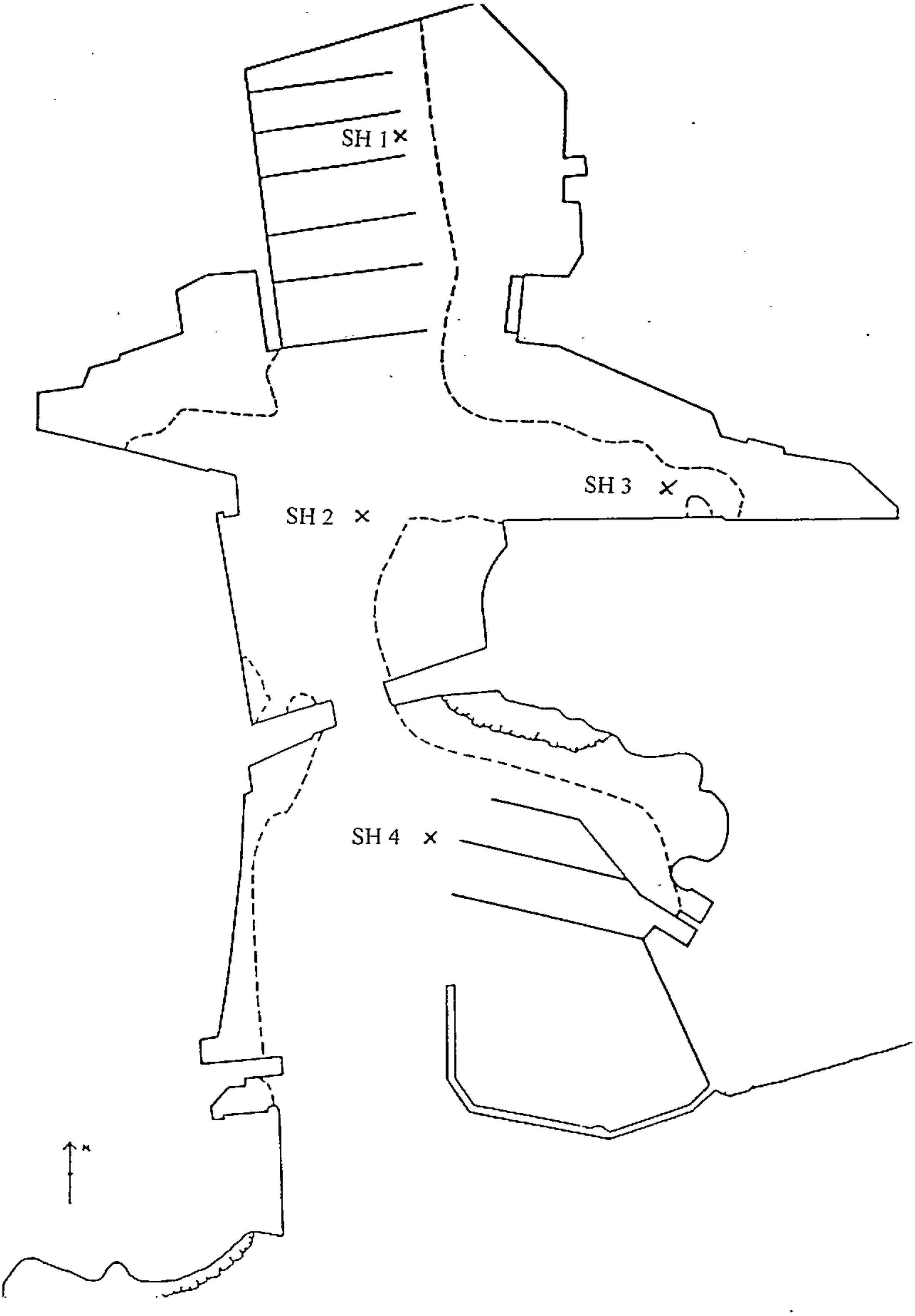
SH 1
SH 2
SH 3
SH 4
N

Figure 4.24 Location of sampling positions in Sutton Harbour.

4.4 CONCLUSIONS

Seven FI procedures coupled with ICP-AES, ICP-MS and AFS were compared for the determination of total mercury at ultra-trace (<1.0 μg l^{-1}) levels. The limits of detection for these methods are shown in Table 4.14. Initial studies comparing the figures of merit for FI (conventional pneumatic nebulization) and FI-CVG coupled with ICP-AES indicated that although the detection limit for mercury could be improved from 110000 ng l^{-1} to 4000 ng l^{-1} in synthetic sea water CVG-ICP-AES was not sensitive enough for the determination of mercury in real samples. Detection limits for total mercury were further improved by coupling the FI and FI-CVG manifolds with ICP-MS detection (*e.g.* the LOD for the FI-CVG-ICP-MS system was 40 ng l^{-1} for mercury in Milli-Q or synthetic sea water standards). However, in order to achieve these levels, the CVG system required modification which involved the addition of a second argon flow to the transfer line to increase the nebulizer gas flow (from 0.5 l min^{-1} to 0.9 l min^{-1}) and thus enable penetration of the plasma.

A simple on- or off-line preconcentration procedure (similar to that described in Chapter 3) using the MetPac CC-1 micro-column incorporated into a FI manifold with conventional pneumatic nebulization (rather than CVG) was then developed. Using this procedure, detection limits for total mercury of 11 ng l^{-1} (on-line, 2.0 ml sample volume) and 6 ng l^{-1} (off-line 500 ml sample volume) were achieved. The method was validated using TORT-1 (lobster hepatopancreas CRM) and the calculated value (348 μg l^{-1} ± 33 μg l^{-1}) was shown to be in good agreement with the certified value (330 μg l^{-1} ± 60 μg l^{-1}). The off-line procedure was then used to preconcentrate mercury from Sutton Harbour sea water samples. Levels of mercury between 37 - 41 ng l^{-1} were determined.

An AFS detector was used to develop an FI-CVG method, with an on-line bromide/bromate oxidation step, for the determination of total mercury. Complete oxidation of the organic species was achieved using a heated reaction coil (100 cm, 70°C). Detection limits for mercury(II) chloride and methylmercury chloride of 25 ng l^{-1} and 23 ng l^{-1} respectively indicated that the method was sufficiently sensitive to analyse real samples collected from Sutton Harbour. Levels of between 24 and 54 ng l^{-1} were determined. The procedure was also validated using TORT-1. Good agreement with the certified value was achieved (348 ng l^{-1} $\pm$ 33 ng l^{-1} compared with 330 ng l^{-1} $\pm$ 60 ng l^{-1}).

The methods described above show the versatility of FI and CVG coupled with atomic spectrometry. Simple and rapid analyses of total mercury can be carried out at the ng l^{-1} level and the preconcentration technique could be easily adapted for *in situ* preconcentration of mercury. However, such methods only provide information on the total concentration of mercury. In order to carry out speciation studies, separation of the physico-chemical forms is required. Chapter 5 discusses an LC-ICP-MS system for the speciation of mercury(II) chloride and methylmercury chloride in sea water and concentrated brines.

Table 4.14 Comparison of detection limits (3 σ).

	Milli-Q matrix		Synthetic sea water matrix	
Method	Mercury(II) chloride (ng l^{-1})	Methylmercury chloride (ng l^{-1})	Mercury(II) chloride (ng l^{-1})	Methylmercury chloride (ng l^{-1})
FI-ICP-AES	24000	-	110000	-
FI-CVG-ICP-AES	4000	-	4000	-
FI-ICP-MS	500	-	1800	-
FI-CVG-ICP-MS	40	-	40	-
On-line preconc ICP-MS	-	-	11	14
Off-line preconc ICP-MS	-	-	6	6
FI-CVG-AFS	-	-	25	23

CHAPTER 5

Speciation of Mercury in Sea Water by Liquid Chromatography with Inductively Coupled Plasma Mass Spectrometric Detection

CHAPTER 5: SPECIATION OF MERCURY IN SEA WATER BY LIQUID CHROMATOGRAPHY WITH INDUCTIVELY COUPLED PLASMA MASS SPECTROMETRIC DETECTION

Introduction

It is well established that inorganic mercury, whether from anthropogenic sources or natural geological activity, is converted into the more toxic organomercury compounds by aquatic organisms[209]. Public attention was focused on this effect after the Minamata mercury poisoning tragedy in the 1950s. The town of Minamata, Japan, was dependent on two sources of income; fishing in the bay and the production of vinyl chloride and acetaldehyde. In 1953 an illness affecting only fishermen and their families was reported but it was not diagnosed as mercury poisoning until 1956. In all, 2000 cases were recognised; of these 46 died and 700 were left with various severe permanent disabilities. Initially the poisoning was attributed to natural methylation of mercury in the Minamata Bay area and subsequent biomagnification up the food chain. This resulted in world-wide concern regarding the release of inorganic mercury into the environment which it was thought could be rapidly methylated in marine sediments and pass into the human food chain via seafood. However, in 1960 the source of the methylmercury was discovered to be the effluent from the vinyl chloride factory discharged into the bay near the affected community. Total mercury levels in sediment from Minamata Bay were as high as 200 mg l^{-1} and fish examined contained 10-55 mg kg^{-1} (dry weight) mercury, most of which was methylated[232].

Following the Minamata Bay disaster there was a greater appreciation of the risk of mercury poisoning from eating contaminated seafood. This resulted in numerous methods for the determination of total mercury being reported, including FAAS[234-236], AFS[237,239,244] FI-FAAS[247], ICP-AES[246] and ICP-MS[249].

Organomercury(II) compounds such as methylmercury are more toxic to human beings than inorganic mercury and therefore speciation of the physico-chemical forms in environmental samples is important. Although atomic spectrometric techniques can detect the total concentration of mercury alone, they do not provide the often vital physico-chemical information. However, interfacing chromatography with element specific detectors can provide discrimination of the various species. CVG-FAAS has been extensively coupled with LC for the determination of mercury[251-254] but lacks the sensitivity for ultra-trace (sub $\mu g\ l^{-1}$) analysis. ICP-AES detection has also been used[255-256] but detection limits of 30 - 400 $\mu g\ l^{-1}$ are not adequate for trace-level analysis. In recent years ICP-MS has been used successfully as an element specific detector coupled with LC for the speciation of mercury at levels as low as 0.5 $\mu g\ l^{-1}$ [174,175,192].

This chapter discusses an LC-ICP-MS method for the speciation of Hg in sea water samples. The method involves the separation of mercury(II) chloride, methylmercury chloride and ethylmercury chloride on a C_{18} ODS stationary phase with an ammonium acetate/acetonitrile/2-mercaptoethanol mobile phase. In order to achieve the necessary detection limits required for the determination of mercury in real sea water samples (< 50 ng l^{-1}), an off-line preconcentration method using a dithiocarbamate resin was used.

5.1 EXPERIMENTAL

5.1.1 INSTRUMENTATION

A Fisons PlasmaQuad PQ2 Turbo+ ICP-MS (Fisons Elemental, Winsford, Cheshire, U.K.) was used. The instrument was operated in the time resolved analysis monitoring mode. Typical ICP-MS operating conditions are presented in Table 2.1 (Chapter 2). The ICP-MS time resolved analysis parameters are given in Table 3.2 (Chapter 3). The ^{202}Hg isotope (abundance 29.7 %) was monitored in this study because it is the most abundant isotope of mercury. The instrument was tuned at m/z = 202 and then stabilised for one hour prior to use in order to minimise the background signal due to mercury memory effects.

The chromatographic system consisted of a reciprocating pump (Altex 110A) and a rotary injection valve (Rheodyne 7010, HPLC Technology, Cheshire, UK.) fitted with a 100 µl sample loop. Separation was achieved using a stainless steel column (150 x 3.2 mm i.d.) packed with Spherisorb S5 ODS2 (5 mm, Phenomenex, Macclesfield, Cheshire, UK.). The mobile phase consisted of 0.06 M ammonium acetate, 1.0 % v/v acetonitrile (ACN) and 0.005 % v/v 2-mercaptoethanol and was pumped at a flow rate of 1.0 ml min^{-1}. Stainless steel tubing was used for the connections between the LC pump and the column. The LC column was coupled directly into the nebulizer using narrow bore PTFE tubing (50 cm length x 0.15 mm i.d.).

5.1.2 REAGENTS

High purity de-ionised water purified by a Milli-Q analytical reagent grade water purification system (Millipore, Chester, Cheshire, UK.) was used throughout. Ammonium acetate (HiPerSolv), acetonitrile (AnalaR) and 2-mercaptoethanol (AnalaR) were purchased from Merck (Poole, Dorset, UK.). The LC mobile phase was prepared daily and degassed using an ultrasonic bath (Bransonic, Aldrich, Gillingham, Dorset, UK.) for 20 min immediately before use.

Mercury(II) chloride and ethylmercury chloride salts were obtained from Alfa Products (Johnson Matthey, Royston, Herts.,UK.) and were used without further purification. Stock solutions (1000 mg l^{-1}) were prepared by dissolving the above reagent-grade compounds in Milli-Q. Methylmercury chloride (1000 mg l^{-1}) was also obtained from Alfa Products as a stock solution. Standard solutions were prepared daily by appropriate dilution of the stock solutions with either Milli-Q or a synthetic sea water solution (Corrosion test mixture, Merck Ltd, Poole, Dorset, UK.). All glassware was soaked in 20 % v/v nitric acid for at least 24 h prior to use, and then rinsed four times with Milli-Q. Stock mercury solutions were stored in acid washed (20 % v/v hydrochloric acid) amber glass bottles. Standard solutions were made up in acid washed volumetric flasks (25 or 100 ml, Grade A).

5.1.3 ANALYSIS OF TORT-1 LOBSTER HEPATOPANCREAS

The certified reference material TORT-1 lobster hepatopancreas (National Research Council of Canada, Ottawa, Canada) was digested as described in Section 4.2.3.

5.1.4 OFF-LINE PRECONCENTRATION PROCEDURE

In section 4.3.2.4 an off-line preconcentration procedure using the MetPac CC-1 column was described. However, this method required a strong acid-complex eluent to elute mercury, and this was considered unsuitable for the preconcentration of mercury species prior to chromatographic separation because the low pH would break the organomercury bond. A more appropriate approach was developed using a commercially available dithiocarbamate resin (Metalfix Dithiochel, Fluka, Gillingham, Dorset, UK.). The physical properties of the resin are shown in Table 5.1.

Table 5.1 Physical properties of Metalfix Dithiochel resin.

Capacity (as Mn^{2+}):mmol g^{-1} dry resin	1.0
mmol g^{-1} hydrated resin	0.2
Water content of hydrated resin (%)	80
Particle size (µm)	40 - 80
pH range for use	7-12
Maximum temp. (°C at pH 7.0)	60

Dithiochel has a high selectivity for metals forming insoluble sulphides whilst not retaining alkali and alkaline earth metals. Elution of the retained metals is achieved using thio compounds such as thiourea, thioacetamide or thiocyanate. In this work 2-mercaptoethanol was used and was found to be an excellent eluent.

A slurry of Dithiochel resin was introduced into an empty Dionex guard column (50 mm length x 4 mm i.d.) with a syringe. Once packed the column was washed with the mobile phase solution (20 ml) and then rinsed with Milli-Q (20 ml). The preconcentration step was performed off-line by pumping the sample through an HPLC pump (Altex 110A) at a flow rate of 9 ml min^{-1}. This enabled a 1000 ml sample to be concentrated on the column in less than 2 h. After the preconcentration step the column was washed with Milli-Q for 5 min. The retained mercury was then eluted with 2-mercaptoethanol (0.15 % v/v, 10.0 ml). The collected eluate was then diluted to 20.0 ml with Milli-Q prior to analysis.

5.2 RESULTS AND DISCUSSION

5.2.1 OPTIMISATION OF ACETONITRILE CONCENTRATION

Figure 5.1 illustrates the chromatographic separation of methylmercury chloride, mercury(II) chloride and ethylmercury chloride in Milli-Q using a mobile phase with 3.0 % v/v ACN. Each species was injected at the 10 $\mu g\ l^{-1}$ level. It can be seen from Figure 5.1 that the methylmercury and mercury(II) chloride peaks are not completely separated (resolution of 1.2). Decreasing the organic component of the mobile phase to 2 % and 1 % v/v resulted in increased retention times for all three species, although the methylmercury form was more strongly retained than the mercury(II) chloride form resulting in an improved separation. The retention times for each ACN concentration are given in Table 5.2. Using 1 % v/v ACN rather than 3 %, improved the resolution from 1.20 to 1.58. This was because inorganic mercury had more affinity than methylmercury for the less polar acetonitrile component of the mobile phase (the polarity parameter, P', for acetonitrile is 5.8 compared with 10.2 for water). Therefore reducing the ACN concentration lessened the affinity of mercury(II) chloride for the mobile phase, increasing the retention time of this species. The chromatographic separation of the three mercury species using 1 % ACN is shown in Figure 5.2.

Table 5.2 Retention data for mercury(II), methylmercury and ethylmercury chloride (10 μg l^{-1}) using a 0.06 M ammonium acetate, 0.005 % v/v 2-mercaptoethanol mobile phase with varying concentrations of ACN.

ACN concentration	MeHgCl	$HgCl_2$	EtHgCl	MeHgCl/$HgCl_2$ resolution (R)
3.0 % v/v	3 min 40 sec	4 min 20 sec	9 min	1.20
2.0 % v/v	4 min	5 min	10 min 50 sec	1.26
1.0 % v/v	4 min 20 sec	5 min 40 sec	12 min 30 sec	1.58

Although reducing the ACN concentration from 3 % v/v to 1 % v/v improved the resolution between the methylmercury and mercury(II) chloride peaks it was at the expense of considerable peak tailing of the ethylmercury chloride peak. Again this was due to the reduction in affinity of this species for the more polar mobile phase at lower ACN concentrations. A degree of tailing can also be seen for the other two peaks although the trade-off in peak tailing was necessary in order to achieve base line separation for quantitative analysis. The fact that there was considerable peak tailing in the case of ethylmercury chloride is not important in the analysis of sea water because ethyl mercury chloride is not found in such an environment.

Figure 5.1 The chromatographic separation (eluting from left to right) of mercury(II), methylmercury and ethylmercury chloride ($10\ \mu g\ l^{-1}$) using a 0.06 M ammonium acetate, 0.005 % 2-mercaptoethanol mobile phase with 3 % ACN.

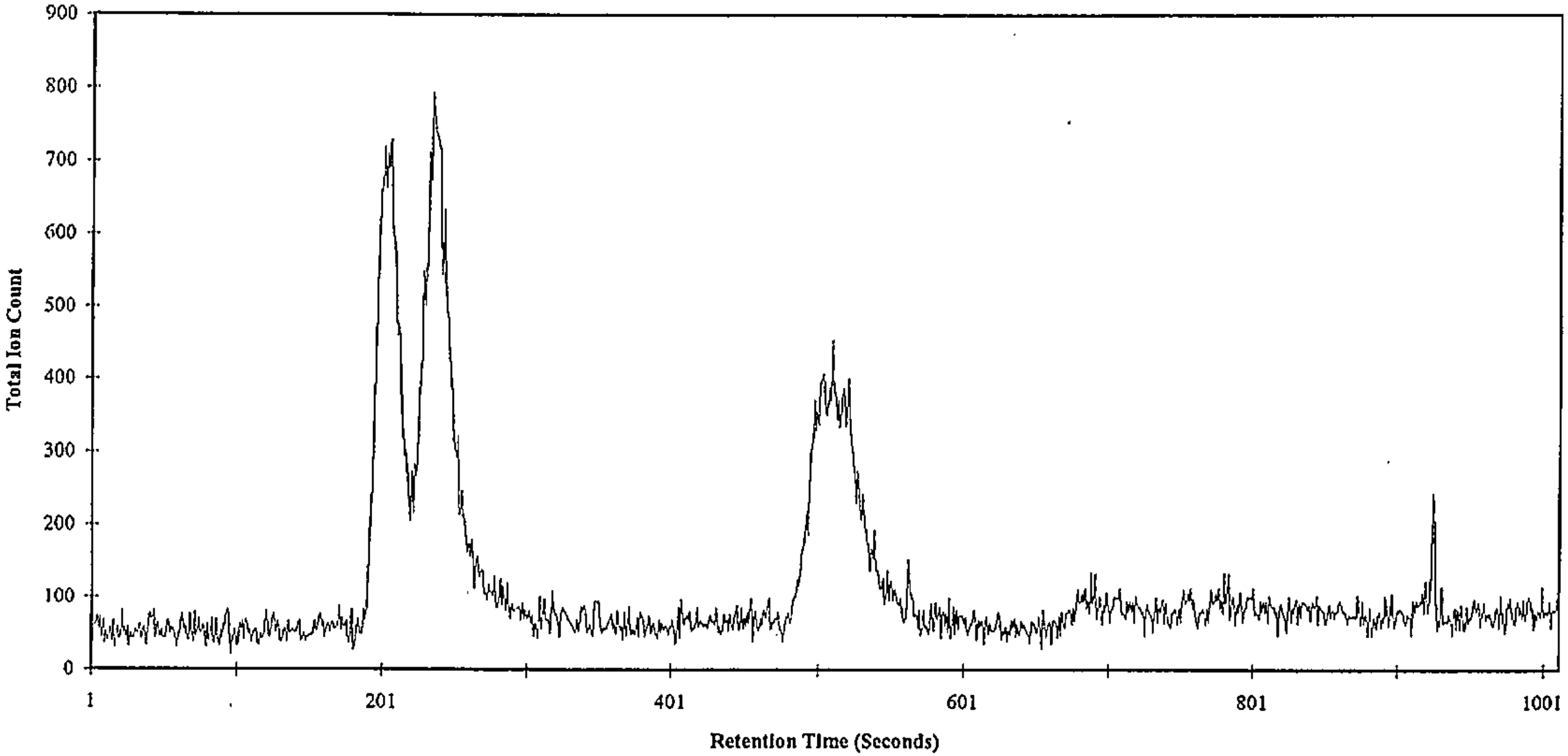

Figure 5.2 The chromatographic separation (eluting from left to right) of mercury(II), methylmercury and ethylmercury chloride (10 µg l^{-1}) using a 0.06 M ammonium acetate, 0.005 % 2-mercaptoethanol mobile phase with 1 % ACN.

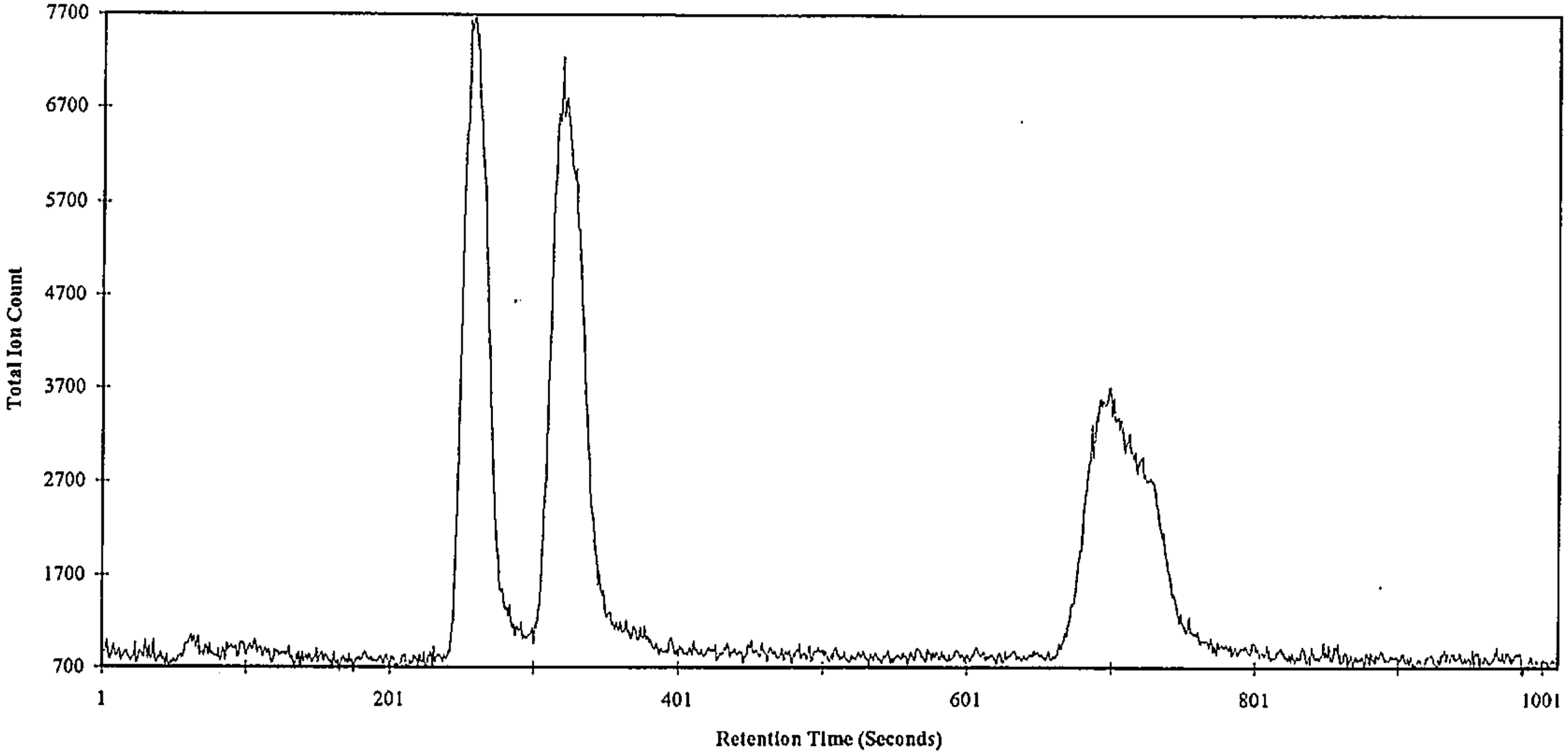

5.2.2 EFFECT OF SYNTHETIC SEA WATER ON THE CHROMATOGRAPHIC SEPARATION

From the chromatogram shown in Figure 5.3 it is apparent that the chromatography is sufficiently robust to effectively separate methylmercury chloride, mercury(II) chloride and ethylmercury chloride in synthetic sea water using a mobile phase containing 1.0 % v/v ACN. Each species was injected at the 10 μg l^{-1} level. Good baseline separation between methylmercury and mercury(II) chloride was achieved (R= 1.62) and the retention times were unaltered (see Table 5.2). The suppression in signal at 1.0 min corresponds to the solvent front of the chromatogram and is due to non-spectroscopic interferences from the sea water matrix. The capacity factors, k', for methylmercury and mercury(II) chloride (4.5 and 6.0 respectively) were good. Capacity factors of <1 would have indicated that the level of separation was inadequate. The k' value for ethylmercury chloride was 13.0. Capacity factors of >5 generally indicate an excessively long analysis time.

5.2.3 FIGURES OF MERIT

Figure 5.4 and Table 5.3 compare calibration data and figures of merit for de-ionised water and synthetic sea water (100 %) spiked with the three mercury species. Figure 5.4 and Table 5.3 show that there is virtually no difference in the calibration data for methylmercury and mercury(II) chloride in Milli-Q and synthetic sea water. The gradients for both species are similar (between 15696 and 16085) and linearity is excellent (*e.g.* the r^2 was 0.9999 for $HgCl_2$ in synthetic sea water over the range 0-50 μg l^{-1}). The results for ethylmercury in Milli-Q are also identical to the other species (gradient 16070) but the results in synthetic sea water were lower than expected (gradient 11977), due to the broad nature of the ethylmercury chloride peak. Detection limits (based on a 2:1 signal-to-noise ratio) were better for methylmercury and mercury(II) chloride in synthetic sea water (0.25 μg l^{-1}) than in Milli-Q

Figure 5.3 The effect of synthetic sea water on the separation of methylmercury, mercury(II) and ethylmercury chloride (10 ug/l) using a mobile phase containing 1.0 % ACN.

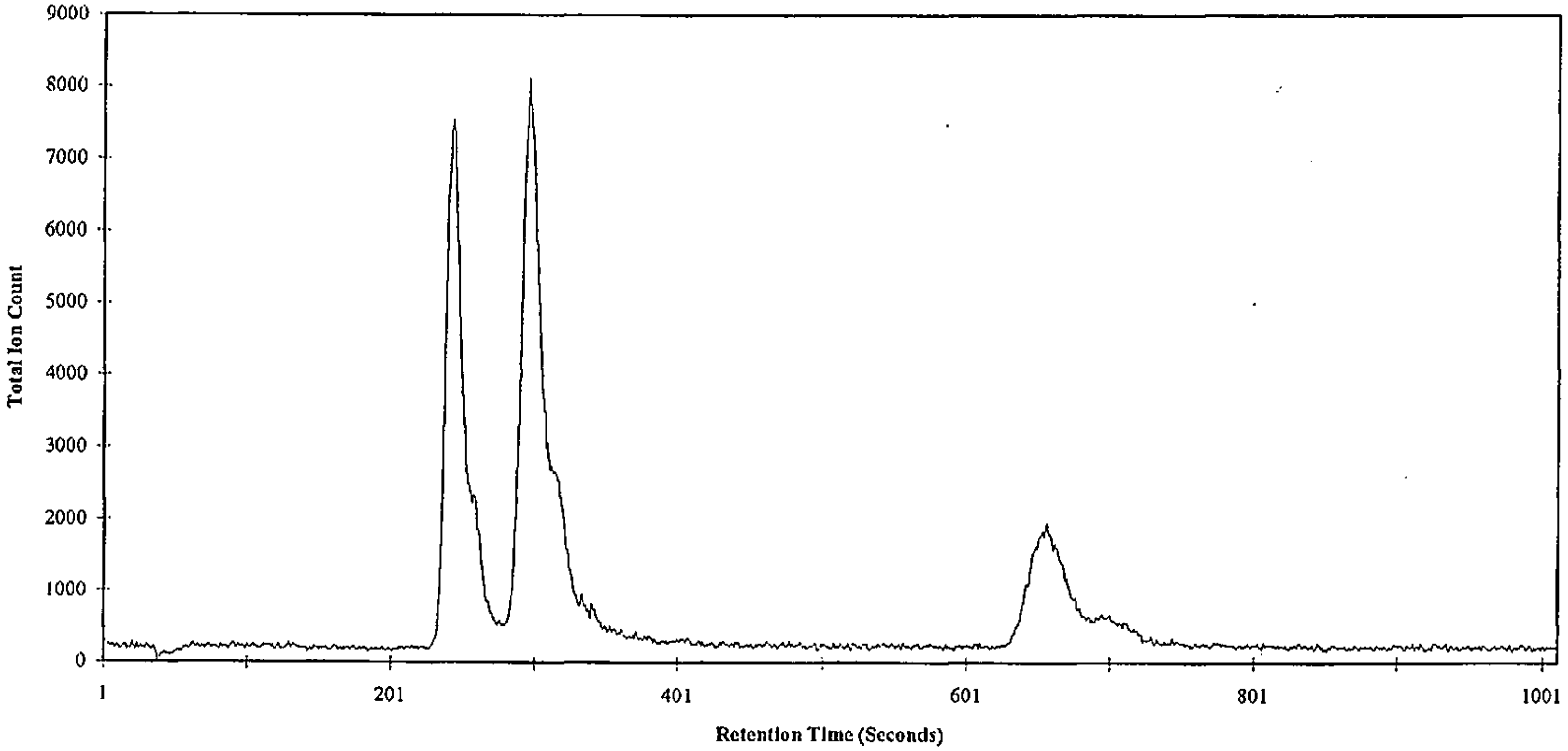

(0.50 µg l^{-1}) although this was a result of slightly elevated background and noise for the mercury spiked Milli-Q standards, due to memory effects after tuning the instrument. Detection limits for ethylmercury chloride in synthetic sea water (0.75 µg l^{-1}) and de-ionised water (1.0 µg l^{-1}) were poorer due to the broader nature of the peak. The detection limits using this chromatographic approach coupled with a standard ICP-MS with conventional nebulization were significantly better than previous reports. For example Bushee[174] achieved detection limits of 7 - 16 µg l^{-1} using conventional nebulization and 0.6 - 1.2 µg l^{-1} using a CVG system. More recently, Huang and Jiang[175] developed an LC-ICP-MS system with direct injection nebulization and achieved detection limits of 0.4 - 0.8 µg l^{-1}. A chromatogram for each mercury species, in synthetic sea water, injected at the 0.25 µg l^{-1} level is shown in Figure 5.5.

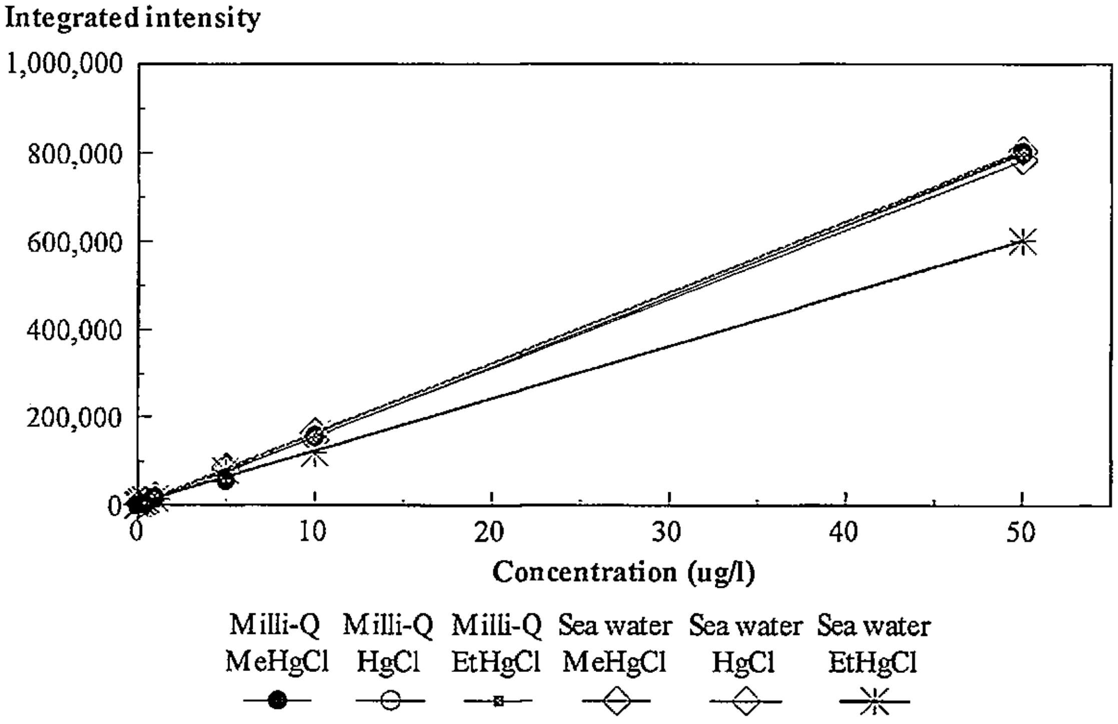

Figure 5.4 Calibration graph for mercury(II), methylmercury and ethylmercury chloride spiked in Milli-Q de-ionised water and synthetic sea water.

Table 5.3 Figures of merit for mercury(II), methylmercury and ethylmercury chloride spiked in Milli-Q de-ionised water and synthetic sea water.

	Milli-Q de-ionised water			Synthetic sea water		
	MeHgCl	$HgCl_2$	EtHgCl	MeHgCl	$HgCl_2$	EtHgCl
Gradient (b)	16029	16085	16070	15696	16087	11977
Linearity (r^2), 0 - 50 mg l^{-1}	0.9999	0.9991	0.9990	0.9998	0.9999	0.9991
Precision (RSD %, 1.0 μg l^{-1}, n = 3)	3.8	2.5	6.1	4.5	3.8	5.5
Detection Limit (μg l^{-1}, S/N 2)	0.5	0.5	1.0	0.25	0.25	0.75

5.2.4 VALIDATION USING TORT-1 LOBSTER HEPATOPANCREAS CRM

In order to validate the method the marine biological reference material TORT-1 (with certified values for total mercury and methylmercury of 330 μg l^{-1} and 128 μg l^{-1} respectively) was analysed (see section 4.2.3 and 4.3.2.3). The lobster hepatopancreas digest was buffered to pH 7.0 with ammonia solution and diluted to 8.25 μg l^{-1} with Milli-Q. Mercury(II) chloride standards of 0, 1.0 and 5.0 and 10 μg l^{-1} were prepared in Milli-Q. The results are shown in Table 5.4. No speciation data was obtained due to the nitric acid/hydrogen peroxide digestion procedure used, which oxidised the organic mercury to the inorganic form. However, good agreement with the total certified value was achieved. The result (350 ± 62 μg l^{-1}) was comparable with that calculated for the on-line preconcentration procedure (Section 4.3.2.3) and the on-line CVG-AFS procedures (Section 4.3.3.3) which also gave values (340 ± 30 μg l^{-1} and 350 ± 60 μg l^{-1} respectively) in good agreement with the certified value (330 ± 60 μg l^{-1}).

Figure 5.5 Chromatogram of methylmercury, mercury(II) and ethylmercury chloride (0.25 ug/l) in synthetic sea water (100 % v/v).

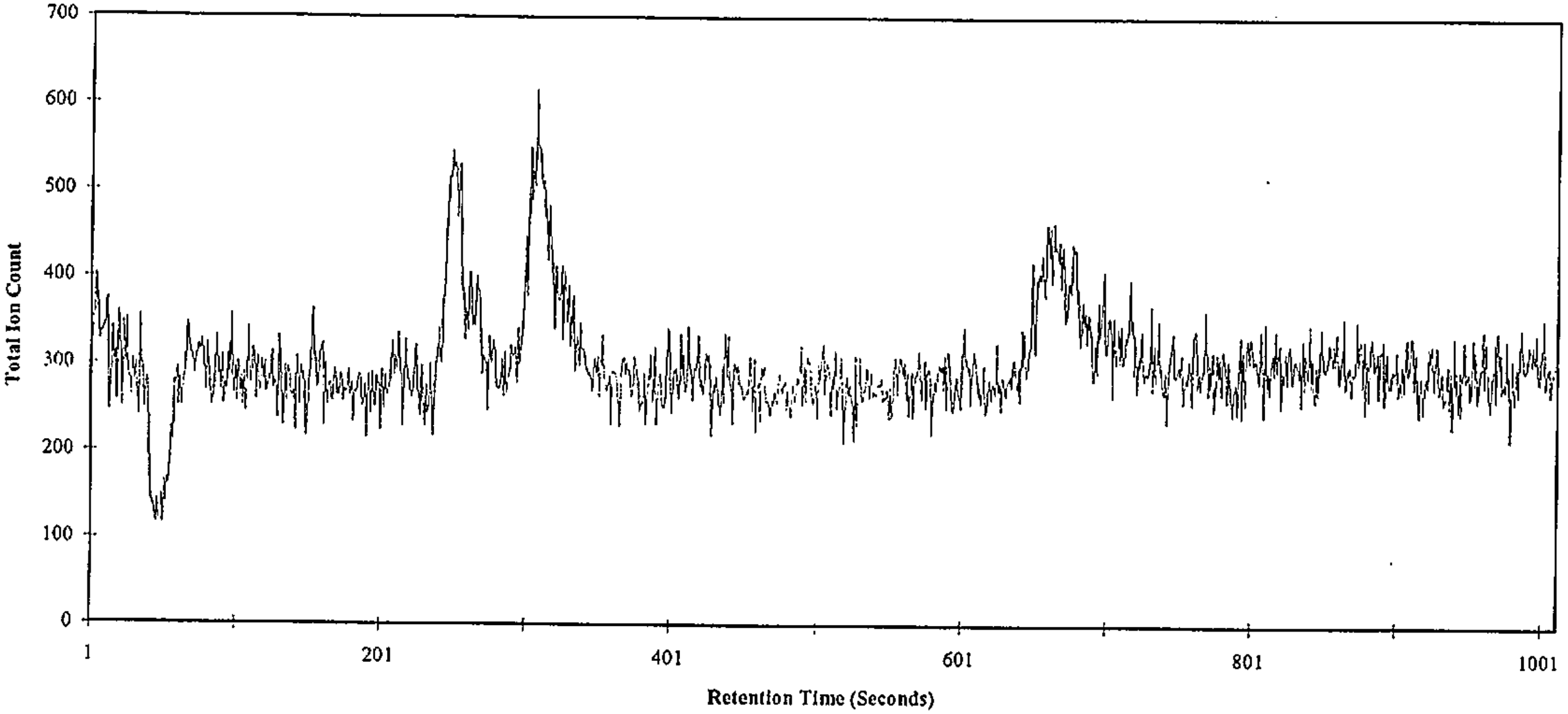

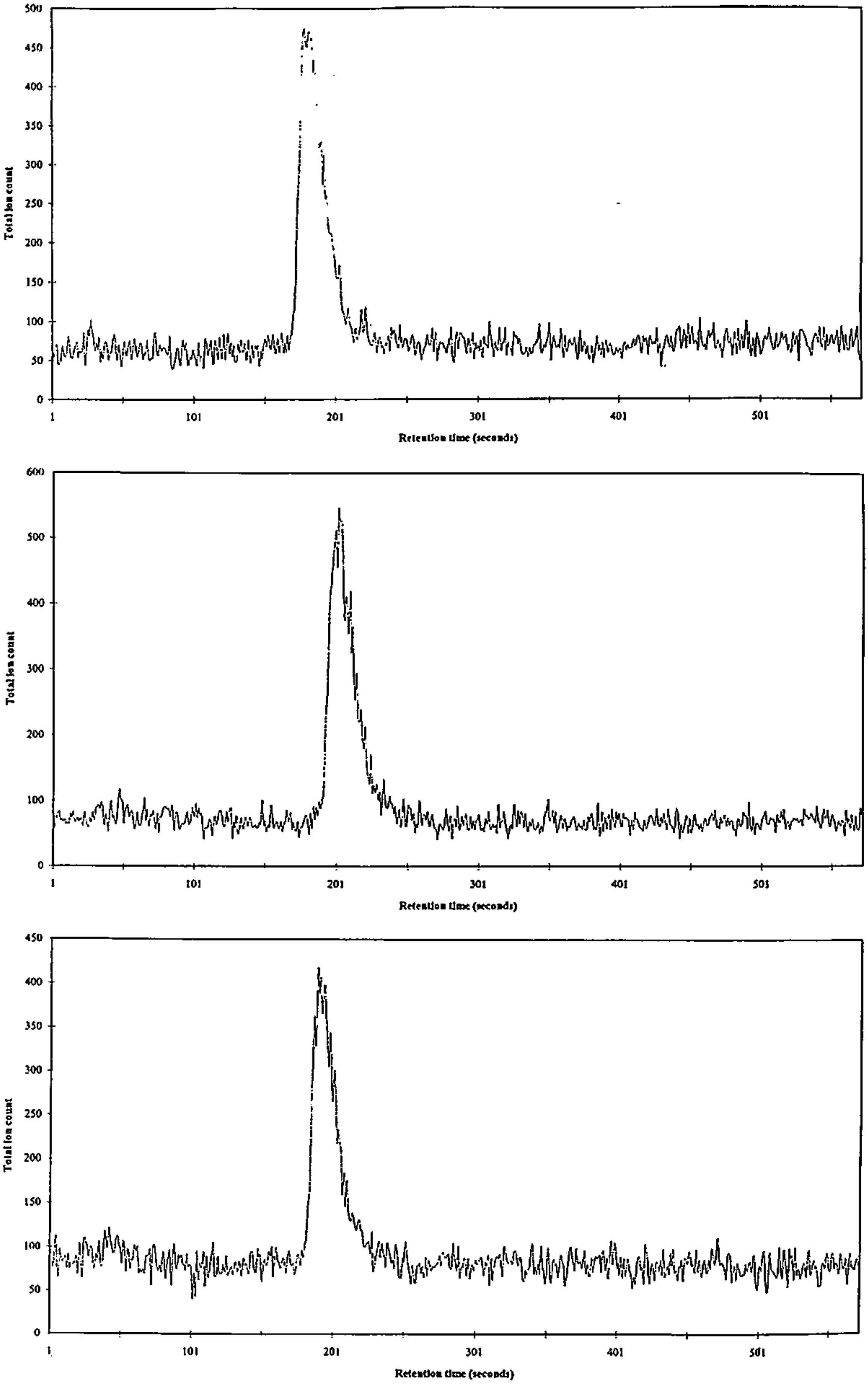

Figure 5.6 Replicate injections of TORT-1 lobster hepatopancreas extract.

Table 5.4 TORT-1 Certified reference material results.

	Calculated value ($\mu g\ l^{-1}$)	Certified value ($\mu g\ l^{-1}$)
TORT-1	350 ± 60	330 ± 60

The between run variability for the method was 8.9 % RSD (n = 3). This is illustrated in Figure 5.6 which shows replicate injections of the lobster hepatopancreas extract.

5.2.5 DETERMINATION OF MERCURY IN DISCHARGE WATER SAMPLES

North Sea discharge water samples with high salt content (9 - 32 g l^{-1} Na) were analysed by LC-ICP-MS. Previous analysis of the samples by vacuum distillation/cold cell AAS had revealed concentrations of total mercury between 0.17 and 0.4 $\mu g\ l^{-1}$. However the results in Table 5.5 indicate that the mercury measured in the discharge waters by the cold cell AAS method was between 8 and 22 times lower than the LC-ICP-MS method (*e.g.* using the LC-ICP-MS procedure, 5.8 $\mu g\ l^{-1}$ mercury was measured in sample 1 compared with 0.26 $\mu g\ l^{-1}$ using the cold cell AAS method). This indicated that poor recoveries were obtained from the vacuum distillation process. From Figure 5.7b it can be seen that the mercury present in the samples was in the inorganic form. Figure 5.7a compares a Milli-Q de-ionised water sample spiked with 5 $\mu g\ l^{-1}$ of the three mercury species.

Table 5.5 Comparison of mercury concentrations in North Sea discharge waters using LC-ICP-MS and vacuum distillation/cold cell AAS.

Sample no.	Na concentration ($g\ l^{-1}$)	Inorganic Hg concentration ($\mu g\ l^{-1}$, n = 3) LC-ICP-MS method	Total Hg concentration ($\mu g\ l^{-1}$) Vacuum distillation/cold cell AAS
1	10.4	5.8	0.26
2	9.4	7.5	0.4
3	32.5	2.6	0.17
4	10.5	3.1	-
5	10.1	2.0	0.25

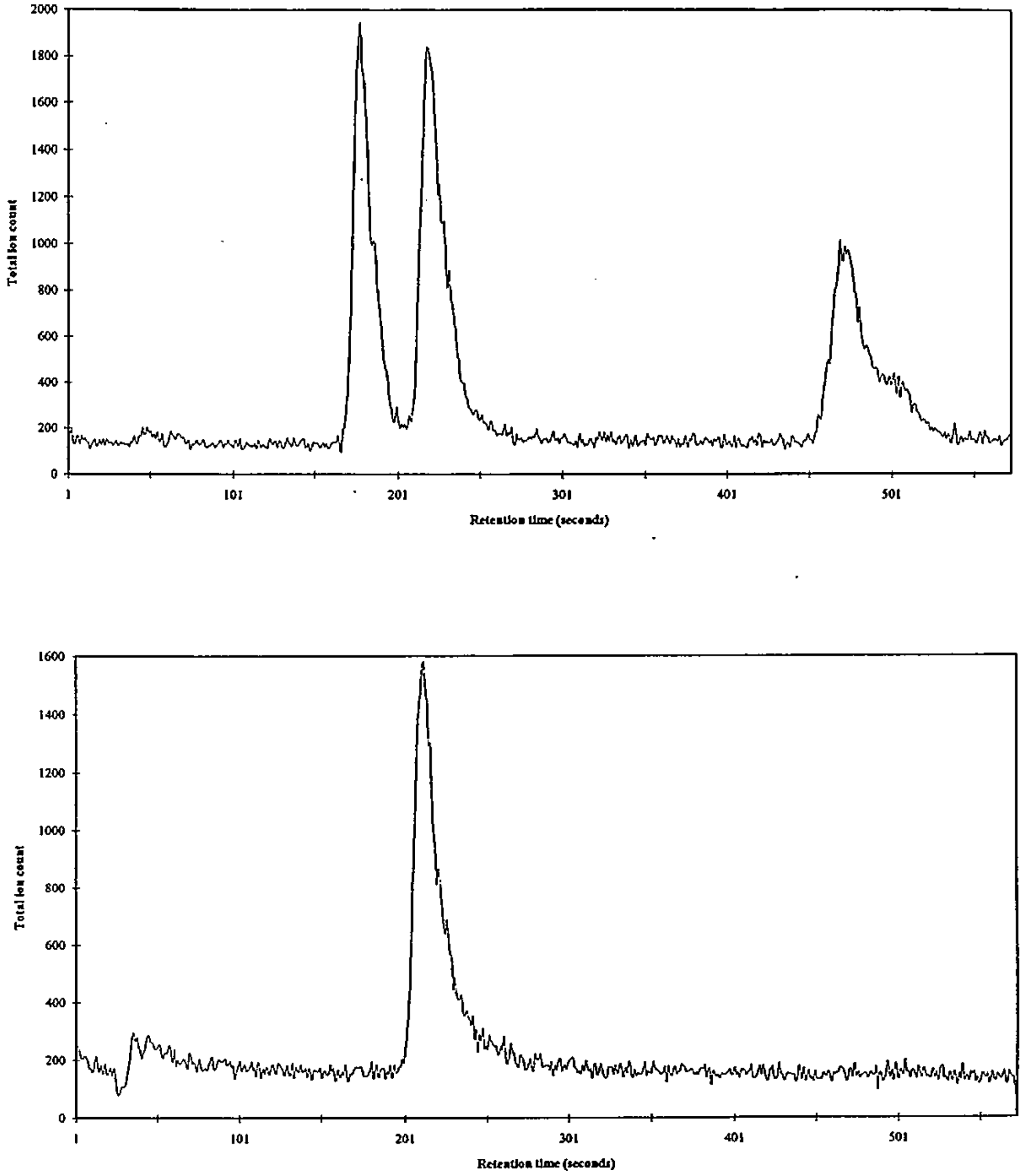

Figure 5.7 Chromatogram of (a) Milli-Q spiked with mercury(II), methylmercury and ethylmercury chloride (5 µg l^{-1}) and (b) a North Sea discharge water.

5.2.6 ANALYSIS OF PLYMOUTH SOUND SEA WATER SAMPLES

Although the detection limits quoted in Section 5.2.3 were good (*e.g.* 250 ng l^{-1} for methylmercury chloride), the speciation of mercury in real sea water samples could not be achieved due to the very low levels of mercury in sea water (typically <30 ng l^{-1}). In order to achieve the necessary detection limits an off-line preconcentration method using a dithiocarbamate resin was investigated.

Using the preconcentration procedure described in Section 5.1.4, recovery tests were carried out in order to determine whether breakthrough of the mercury species was occurring. Three Milli-Q samples (1000 ml) spiked with methyl-, ethyl-, and mercury(II) chloride (50 ng l^{-1}) were preconcentrated on the column at a flow rate of 9 ml min^{-1}. This enabled a concentration factor of 50 (1000 ml sample into 20 ml eluent) which resulted in 2.5 μg l^{-1} of each species injected onto the LC column. The recovery, calculated as the % difference between the preconcentrated sample and a Milli-Q standard spiked with 2.5 μg l^{-1} of the three mercury standards, was 70 %, 71 % and 70 % respectively (n = 2). Although low, the reproducibility for methylmercury and mercury(II) chloride was good with RSD values of 3.2 and 1.6 % (n = 3) respectively. The reproducibility of ethylmercury chloride was poorer (RSD 10.1 %) as a result of the less well defined peak profile.

The calibration for methylmercury and mercury(II) chloride in Milli-Q shown in Figure 5.8 was linear between 20 and 100 μg l^{-1} (r^2 values of 0.9916 and 0.9948 respectively). The limits of detection (based on the blank signal plus 3 standard deviations) were 16 ng l^{-1} for methylmercury chloride and 17 ng l^{-1} for mercury(II) chloride. These results are 15 times better than direct injection of the sample into the LC-ICP-MS system (250 ng l^{-1}, S/N = 2).

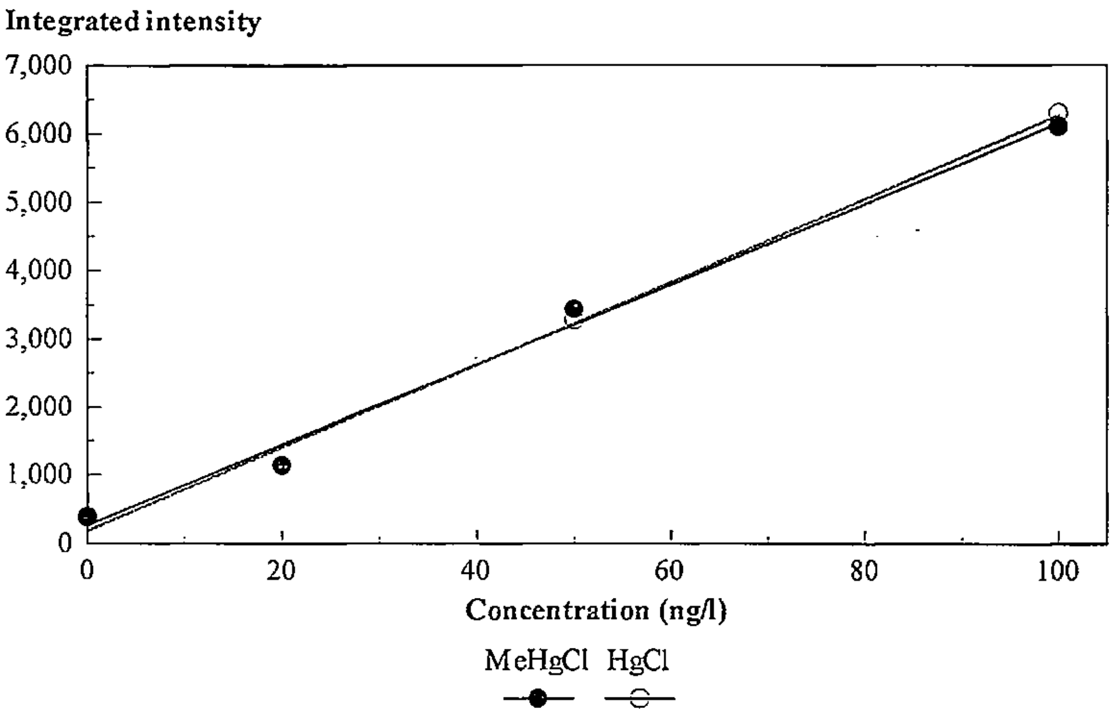

Figure 5.8 Calibration graph for methylmercury and mercury(II) chloride in Milli-Q after preconcentration on dithiocarbamate resin.

Table 5.6 Methylmercury and mercury(II) chloride concentrations in two Plymouth Sound samples.

Plymouth Sound sample	Methymercury chloride (ng l^{-1})	Mercury(II)chloride (ng l^{-1})
1	not detected	21
2	not detected	28

The off-line preconcentration step was then applied to the preconcentration of two coastal sea water samples. The samples were collected in 1.0 l acid washed (20 % v/v hydrochloric acid) amber glass bottles from Plymouth Sound, Plymouth. The samples were not acidified on collection. The preconcentration system was fitted with a filter (45 μm) to remove any undissolved solids. The levels determined in each sample are shown in Table 5.6.

The levels of mercury(II) chloride detected (21 and 28 ng l^{-1}) were similar to those expected in coastal sea water (30 ng l^{-1}). A small peak for methylmercury chloride was observed at 4 min 20 sec but was below the detection limit of the present system. Quantification of the methylmercury chloride fraction could be achieved if the detection limits were improved (*e.g.* by increasing the recovery from the preconcentration step by optimising the flow rate, sample volume, or eluent volume). It was also likely that volatile organomercury species (*e.g.* methylmercury chloride) present in Plymouth Sound were being lost between collection and analysis because the samples were not stabilised by acidification with a mineral acid (as this process would convert any organomercury species present to the inorganic form). One approach to overcoming this problem would be to preconcentrate the sample *in situ*, thus negating the need to acidify the sample upon collection, and therefore maintaining its physico-chemical integrity.

5.3 CONCLUSIONS

An LC-ICP-MS method for the speciation of mercury in high salinity discharge waters and sea water has been developed. The LC system used a mobile phase with low dissolved solids (< 0.5 %) and a low organic content (1 % v/v ACN) which had no significant effect on the plasma. Mercury(II), methylmercury and ethylmercury chlorides were fully resolved and the separation was complete in < 12 minutes. Although the detection limits achieved (*e.g.* 250 ng l^{-1} for methylmercury chloride) were comparable with, of better than, those achieved with more complex sample introduction devices (*e.g.* ultrasonic nebulization or CVG), they were not low enough to determine mercury in real sea water samples (typically <30 ng l^{-1}). Preconcentration of the sample using a dithiocarbamate resin packed into a micro-column improved detection limits (from 250 ng l^{-1} to 17 ng l^{-1} for mercury(II) chloride) and enabled the determination of mercury species in sea water to be carried out, although recoveries from the preconcentration step were low (70 %). Inorganic mercury was determined in Plymouth Sound sea water samples at levels consistent with typical coastal levels (< 30 ng l^{-1}) although methylmercury could not be detected. However, if methylmercury were present it was possible that it was being converted to the inorganic form between sampling and analysis. This was because no sample preservation step (*e.g.* acidification with a mineral acid) was carried out (as mineral acids would oxidise methylmercury to inorganic mercury). A logical method to overcome this problem would be to develop field sampling procedures for direct preconcentration.

CHAPTER 6

General Conclusions and Future Work

CHAPTER 6: GENERAL CONCLUSIONS AND FUTURE WORK

6.1 GENERAL CONCLUSIONS

In addition to the specific conclusions at the end of each chapter, the following general conclusions can be drawn from the work described in this thesis;

(1) Spectroscopic and non-spectroscopic interferences from sea water seriously degrade the analytical performance of ICP-MS. For example the detection limit for copper at m/z = 63 was >2500 times poorer in 10 % v/v synthetic sea water (>50 μg l^{-1}) than in 2 % v/v nitric acid (0.02 μg l^{-1}). Introducing discrete sample volumes though an FI manifold resulted in some improvement in the figures of merit but spectroscopic and non-spectroscopic interferences resulting from the complex nature of the synthetic sea water matrix still had a serious effect on the analytical performance of the ICP-MS. Reduction of matrix effects is possible by diluting the sea water matrix (*e.g.* below 1 % v/v) but the high dilution factor also degrades the limit of detection.

(2) The addition of nitrogen to the nebulizer gas flow and the simplex optimisation of instrument operating conditions led to the reduction of the $ArNa^+$ polyatomic interference to background levels, and thus allowed the detection limit for Cu to be improved over those obtained using standard conditions. However, the detection limits calculated (0.06 μg l^{-1}, 1% v/v sea water) were not sufficient for the analysis of real sea water samples, due to the dilution factor. FI was considered but the procedure was problematic due to long term (> 8 h) instrument drift.

(3) Solid phase reactors incorporated into FI manifolds coupled with ICP-MS provide sensitive and rapid procedures that are relatively contamination free. Traditional chelating resins such as Chelex-100 were found to be unsuitable for this approach due to volume changes which resulted in the physical retention of the matrix. However, Dionex MetPac CC-1 (a more highly cross-linked macroporous resin) did not suffer from this shortcoming. A FI method coupled with ICP-MS, using the MetPac column, was developed that was capable of detecting Mn, Co, Cu, Zn and Pb at sub $\mu g\ l^{-1}$ levels in sea water. The value of stringent clean-up protocols and the availability of clean room conditions was noted. Reagent purity required particular scrutiny, and involved the clean up of the stock ammonium acetate buffer on Chelex-100 prior to use. Double sub-boiling distilled nitric acid was used as the eluent to minimise potential contaminants.

(4) Seven FI procedures coupled with ICP-AES, AFS and ICP-MS were compared for the determination of total mercury at ultra-trace levels ($<1.0\ \mu g\ l^{-1}$). The methods described showed the versatility of FI coupled with atomic spectrometry for the analysis of mercury at the ng l^{-1} level. The detection limits for mercury using FI-CVG coupled with AFS and ICP-MS were comparable (27 and 40 ng l^{-1}). Further improvements in the detection limit was achieved by developing an on- or off-line preconcentration method with ICP-MS detection. This method did not require a CVG step, and therefore reduced the complexity of the procedure. Detection limits of 11 and 6 ng l^{-1} respectively were achieved. Further improvements in the detection limit would be possible if the procedure were carried out in a clean-room.

(5) The importance of the physico-chemical forms of mercury in determining its environmental impact is well established. However, the quantitative speciation of mercury in sea water is difficult due to the very low levels present (typically <30 ng l^{-1}). An off-line

preconcentration step using a dithiocarbamate resin was developed that resulted in the preconcentration of mercury(II) and methylmercury chloride (preconcentration factor of 50) prior to the chromatographic separation. An LC-ICP-MS method using a low dissolved solids, low organic content mobile phase was developed that separated the mercury species in less than 15 min. Inorganic mercury was determined in a real sea water sample at levels consistent with typical coastal waters (<30 ng l^{-1}).

6.2 FUTURE WORK

Future work arising from this research can be divided into five areas;

(1) The mixed gas method discussed in Chapter two was successful in virtually eliminating the $ArNa^+$ polyatomic ion interference at m/z = 63. However, the sea water matrix required dilution to 1 % v/v in order to prevent the deposition of salt on the sampler and skimmer cones. In order to improve the detection limits in sea water, the injection of higher concentrations of the matrix (*e.g.* >10 % v/v) is required. This could be achieved by injecting discrete sample volumes through an FI manifold. However, procedures would need to be investigated that would minimise the time taken to introduce the sample and manipulate the data and therefore reduce the time needed for the completion of the simplex optimisation (reducing the effect of long term instrument drift).

(2) In Chapters three and four, on- and off-line preconcentration methods using solid phase reactors incorporated into FI manifolds were discussed. However, a limitation of such techniques is the contamination or chemical alteration of the sample between collection and analysis. In order to minimise this effect, the continued development of off-line *in situ*

preconcentration procedures prior to ICP-AES or ICP-MS detection needs to be examined. This would include the preconcentration of environmentally sensitive metals such as Hg, Pb, Cd, Sn and As (*e.g.* using battery powered peristaltic pumps).

(3) In Chapter three, two iminodiacetate chelating resins were investigated. It was found that although Chelex-100 was efficient at preconcentrating copper, it was not suitable for FI, because of problems associated with volume changes of the resin. A second, more highly cross linked resin (MetPac CC-1) did not suffer from this effect and was used to develop a method for the determination of trace metals (*e.g.* Mn, Co, Cu, Zn, Pb) at the $\mu g\ l^{-1}$ level in sea water. It is therefore apparent that there is a need to characterise the applicability of a range of solid phase reactors for FI. This would include the investigation and development of basic analytical data (*e.g.* analyte retention, matrix elimination, % recovery) on a range of materials including, ion exchange and chelation exchange media (*e.g.* iminodiacetate, 8-hydroxyquinoline), and activated alumina.

(4) In Chapter five, the relative toxicity of different species of the same element was discussed. For example, the organic species of Hg are more toxic than the inorganic species. The separation of the different physico-chemical forms of an element has historically been performed using LC or GC whereas preconcentration procedures such as those described in Chapters three and four have been used to separate total metal species from the sample matrix. The development of FI methods for the separation of inorganic/organic species (*e.g.* inorganic and organic Hg)or species with different oxidation states (e.g. Cr(III) and Cr(VI) needs to be undertaken. This could be achieved by utilising existing LC stationary phases (*e.g.* ODS stationary phase for the separation of the organic and inorganic fractions of Hg) or by using existing solid phase reactors that concentrate either anionic or cationic forms (*e.g.* activated alumina for the separation of toxic Cr(VI) and non-toxic Cr(III) species).

(5) The LC-ICP-MS method discussed in Chapter five successfully separated Hg species in a synthetic sea water matrix at the µg l^{-1} level. The analysis of Hg in real sea water samples was achieved by preconcentrating Hg on a dithiocarbamate resin prior to the LC separation step. Recoveries of only 70 % were achieved. Therefore the preconcentration step requires modification to increase the recovery and ultimately improve the detection limits (*e.g.* by increasing the sample volume, optimising the preconcentration flow rate or increasing the eluent volume). On-line preconcentration also requires investigation to reduce the risk of contamination or sample loss. An alternative method would be to carry out the preconcentration step *in situ*, which would overcome the possibility of changes in the sample integrity between collection and analysis.

CHAPTER 7

References

CHAPTER 7: REFERENCES

1. Date, A.R., and Gray, A.L., Editors, "Applications of Inductively Coupled Plasma Mass Spectrometry", Blackie, Glasgow, 1989.
2. Jarvis, K.E., Gray, A.L., and Houk R.S., "Handbook of Inductively Coupled Plasma Mass Spectrometry", Blackie, Glasgow, 1992.
3. Houk, R.S., Fassel, V.A., Flesch, G.D., Svec, H.J., and Gray, A.L., *Anal.Chem.*, 1980, **52**, 2283.
4. Date, A.R., and Gray, A.L., *Analyst*, 1981, **106**, 1255.
5. Douglas, D.J., Rosenblatt, G., and Quan, E.S.K., *Trace Subst. Environ. Health*, 1983, **17**, 385.
6. Gray, A.L., *Spectrochim. Acta*, 1985, **40B**, 1525.
7. Gray, A.L., *J. Anal. At. Spectrom.*, 1986, 1, 403.
8. Date, A.R., and Gray, A.L., *Spectrochim. Acta*, 1983, **38B**, 29.
9. Wang, S.R. and Jiang, S.J., *J. Chinese Chem. Soc.*, 1991, **38**, 327.
10. Laborda, F., De Loos-Vollebregt, M.T.C. and De Galan, L., *Spectrochim. Acta*, 1991, **46B**,1089.
11. Roychowdhury, S.B. and Koropchak, J.A., *Anal. Chem.*, 1990, **62**, 484.
12. Elgersma, J.W., Balke, J. and Maessen, F.J.M.J., *Spectrochim. Acta*, 1991, **46B**, 6.
13. LaFreniere, K.E., Fassel, V.A. and Eckels, D.E., *Anal. Chem.*, 1987, **59**, 879.
14. Hill, S., Hartley, J. and Ebdon, L., *J. Anal. At.Spectr.*, 1992, 7, 23.
15. Uchida, J., Masamha, W.R., Uchida, T., Smith, B.W. and Winefordner, J.D., *Appl. Spectrosc.*, 1989, **43**, 425.
16. Brotherton, T.J., Pfannerstill, P.E., Creed, J.T., Heitkemper, D.T., Caruso, J.A. and Pratsinis, S.E., *J. Anal. At. Spectrom.*, 1989, **4**, 341.
17. Tsakahara, R. and Kubota, M., *Spectrochim. Acta.*, 1990, **45B**, 581.

18. Gustavsson, A., *Spectrochim. Acta.*, 1988, **43B**, 917.

19. Backstrom, K., Gustavsson, A. and Hietala, P., *Spectrochim. Acta.*, 1989, **44B**, 1041.

20. Weir, D.G.J. and Blades, M.W., *Spectrochim. Acta*, 1990, **45B**, 615.

21. Dean, J.R., Parry, H.G.M., Massey, R.C., and Ebdon, L., *ICP Newsletter*, 1990, **15**, 569.

22. Hutton, R.C., Bridenne, M., Coffre, E., Marot, Y., and Simondet, F., *J. Anal. At. Spectrom.*, 1990, **5**, 463.

23 Instrument Literature, Fisons PlasmaQuad II, Fisons Instruments, Winsford, Cheshire, UK, 1992.

24. Instrument Literature, Varian Liberty, Varian, Warrington, Cheshire, UK, 1993.

25. Ebdon, L., "An Introduction to Atomic Absorption Spectroscopy", Heyden, London, 1982.

26. Dean, J.R., Munro, S., Ebdon, L., Crews, H.M. and Massey, R.C., *J. Anal. At. Spectrom.*, 1987, **2**, 607.

27. Heitkemper, D., Creed, J., Caruso, J. and Fricke, F.L., *J. Anal. At. Spectrom.*, 1989, **4**, 279.

28. Kato, T., Uehiro, T., Yasuhara, A. and Morita, M., J. *Anal. At. Spectr.*, 1992, **7**, 15.

29. Kim, A., Hill, S.J., Ebdon, L. and Rowland, S.J., *High Res. Chromatogr.*, 1992, **15**, 665.

30. McLaren, J.W., Beauchemin, D., and Berman, S.S., *J. Anal. At. Spectrom.*, 1987 **2**, 277.

31. Ebdon. L., Fisher, A.S., Worsfold, P.J., Crews, H., and Baxter, M., *J. Anal. At. Spectrom.*, 1993, **8**, 691.

32. Viczian, M., Lasztity, A., and Barnes, R.M., *J. Anal. At. Spectrom.*, 1990, **5**, 293.

33. Mulligan, K.J., Davidson, T.M., and Caruso, J.A., *J. Anal. At. Spectrom.*, 1990, **5**, 301.

34. Lu, P.-L., Huang, K.-S., and Jiang, S.-J., *Anal. Chim. Acta,* 1993, **284**, 181.

35. Gregoire, D.C., *J. Anal. At. Spectrom.*, 1990, **5**, 623.

36. Gomez, J., Roehl, R., Paper given at Winter Conference on Plasma Spectrochemistry, San Diego, USA, 1994.

37. Date, A.R., and Hutchison, A., *Spectrochim. Acta,* 1986, **41B**, 175.

38. Jarvis, K.E., *J. Anal. At. Spectrom.*, 1989, **4**, 563.

39. Skelton, R.J., Chang, H.-C.K., Farnsworth, P.B., Markides, K.E. and Lee, M.L., *Anal. Chem.*, 1989, **61**, 2292.

40. Kim, A., Foulkes, M.E., Ebdon, L., Hill, S.J., Patience, R.L., Barwise, A.G. and Rowland, S.J., *J. Anal. At. Spectr.*, 1992, **7**, 1147.

41. Boomer, D.W., and Powell, J., *Anal. Chem.*, 1987, **59**, 2810.

42. Igarashi, Y., Kawamura, H., Shiraishi, K., and Takaku, Y., *J. Anal. At. Spectrom.*, 1989, **4**, 571.

43. Sturgeon, R.E., McLaren, J.W., Willie, S.N., Beauchemin, D., and Berman, S.S., *Can. J. Chem.*, 1987, **65**, 961.

44. Moens, L., Vanhoe, H., Vanhaecke, F., Goossens, J., Campbell, M., and Dams, R. *J. Anal. At. Spectrom.*, 1994, **9**, 187.

45. Gray, A.L., and Williams, J.G., *J. Anal. At. Spectrom.*, 1987, **2**, 81.

46. Horlick, G., Tan, S.H., Vaughan, M.A., and Rose, C.A., *Spectrochim. Acta,* 1985, **40B**, 1555.

47. Jarvis, K.E., Gray, A.L., and McCurdy, E., *J. Anal. At. Spectrom.*, 1989, **4**, 743.

48. Tan, S.H., and Horlick, G., *Appl. Spectrosc.*, 1986, **40**, 445.

49. Gray, A.L., and Williams, J.G., *J. Anal. At. Spectrom.*, 1987, **2**, 599.

50. Vaughan, M.A., and Horlick, G., *Appl. Spectrosc.*, 1986, **40**, 434.

51. Lyon, T.D.B., Fell, G.S., Hutton, R.C., and Eaton, A.N., *J. Anal. At. Spectrom.*, 1988, **3**, 601.

52.. Gray, A.L., *Spectrochim. Acta*, 1986, **41B**, 151.

53. Douglas, D.J., and French, J.B., *J. Anal. At. Spectrom.*, 1988, **3**, 743.

54. Gray, A.L., and Date, A.R., *Analyst*, 1983, **108**, 1033.

55. Vaughan, M.A., and Horlick, G., *Spectrochim. Acta*, 1990, **45B**, 1289.

56. Olivares, J.A., and Houk, R.S., *Anal. Chem.*, 1985, **57**, 2674.

57. Evans, E.H., and Giglio, J.J., *J. Anal. At. Spectrom.*, 1993, **8**, 1.

58. Hutton, R.C., and Eaton, A.N., *J. Anal. At. Spectrom.*, 1987, **2**, 595.

59. Ebdon, L., Foulkes, M.E., Parry, H.G.M., and Tye, C.T., *J. Anal. At. Spectrom.*, 1988, **3**, 753.

60. Hartley, J.H.D., Hill, S.J., and Ebdon, L., *Spectrochim. Acta*, 1993, **48B**, 1421.

61. Lyon, T.D.B., Fell, G.S., Hutton, R.C., and Eaton, A.N., *J. Anal. At. Spectrom.*, 1988, **3**, 265

62. Palmieri, M.D., Fritz, J.S., Thompson, J.J., Houk, R.S., *Anal. Chim. Acta*, 1986, **184**, 187.

63. Beauchemin, D., and Berman, S.S., *Anal. Chem.*, 1989, **61**, 1857.

64. Branch, S., Ebdon, L., Hill, S. and O'Neill, P., *Anal. Proc.*, 1989, **26**, 401.

65. Sheppard, B., Shen, W. -L., Caruso, J.A., Heitkemper, D.T. and Fricke, F.E., *J. Anal. At. Spectrom.*, 1990, **5**, 431.

66. Ediger, R.D., and Beres, S.A., *Spectrochim. Acta*, 1992, **47B**, 907.

67. Boomer, D.W., Powell, M., Sing, R.L.A., and Salin, E.D., *Anal. Chem.*, 1986, **58**, 976.

68. Denoyer, E.R., Fredeen, K.J., and Hager, J.W., *Anal. Chem.*, 1991, **63**, 445A.

69. Munro, S., Ebdon, L., and McWeeny, D.J., *J. Anal. At. Spectrom.*, 1986, **1**, 211.

70. Ketterer, M.E., Reschl, J.J., and Peters M.J., *Anal. Chem.*, 1989, **61**, 2031.

71. Morita, M., Ito, H., Uehiro, T., and Otauka, K., *Anal. Sci.*, 1989, **5**, 609.

72. Blades, M.W., and Caughlin, B.L., *Spectrochim. Acta*, 1985, **40B**, 579.

73. Beauchemin, D., McLaren, J.W., and Berman, S.S., *Spectrochim. Acta*, 1987, **42B**, 467.

74. Olivares, J.A., and Houk, R.S., *Anal. Chem.*, 1986, **58**, 20.

75. Gregoire, D.C., *Spectrochim. Acta*, 1987, **42B**, 895.

76. Tan, S.H., and Horlick, G., *J. Anal. At. Spectrom.*, 1987, **2**, 745.

77. Wang, J., Shen, W.-L., Sheppard, B.S., Evans, E.H., Caruso, J.A., and Fricke, F.L., *J. Anal. At. Spectrom.*, 1990 **5**, 445.

78. Gilson, G.R., Douglas, D.J., Fulford, J.E., Halligan, K.W., and Tanner, S.D., *Anal. Chem.*, 1988, **60**, 1472.

79. Williams, J.G., and Gray, A.L., *Anal. Proc.*, 1988, **25**, 385.

80. McLaren, J.W., Beauchemin, D., Berman, S.S., *Anal. Chem.*, 1987, **59**, 610.

81. Evans, E.H., and Caruso, J.A., *Spectrochim. Acta*, 1992, **47B**, 1001.

82. Beauchemin, D., Sui, K.W., and Berman, S.S., *Anal. Chem.*, 1988, **60**, 2587.

83. Dean, J.R., Ebdon, L., Crews, H.M., and Massey, R.C., *J. Anal. At. Spectrom.*, 1988, **3**, 349.

84. Wang, J., Evans, E.H., and Caruso, J.A., *J. Anal. At. Spectrom.*, 1991 **6**, 605.

85. Hutton, R.C., and Eaton, A.N., *J. Anal. At. Spectrom.*, 1988 **3**, 547.

86. Richner, P., *J. Anal. At. Spectrom.*, 1993 **8**, 927.

87. Stroh, A, Vollkopf, U., and Denoyer, E.R., *J. Anal. At. Spectrom.*, 1992 **7**, 1201.

88. Beauchemin, D., and Craig, J.M., *Spectrochim. Acta*, 1991, **46B**, 603.

89. Xiao, G., and Beauchemin, D, *J. Anal. At. Spectrom.*, 1994, **9**, 509.

90. Evans, E.H., and Ebdon, L., *J. Anal. At. Spectrom.*, 1989, **4**, 299.

91. Evans, E.H., and Ebdon, L., *J. Anal. At. Spectrom.*, 1990, **5**, 425.

92. Lam, J.W., and Horlick, G., *Spectrochim. Acta*, 1990, **45B**, 1313.

93. Branch, S., Ebdon, L., Ford, M., Foulkes, M., and O'Neill, P., *J. Anal. At. Spectrom.*, 1991 **6**, 151.

94. Wang, J., Evans, E.H., and Caruso, J.A., *J. Anal. At. Spectrom.*, 1992, 7, 929.

95. Hill, S.J., Ford, M.J., and Ebdon, L., *J. Anal. At. Spectrom.*, 1992, 7, 719.

96. Craig, J.M., and Beauchemin, D, *J. Anal. At. Spectrom.*, 1992, 7, 937.

97. Lam, J.W., and Horlick, G., *Spectrochim. Acta*, 1990, **45B**, 1327.

98. Laborda, F., Baxter, M.J., Crews, H.M., and Dennis, J., *J. Anal. At. Spectrom.*, 1994 9, 727.

99. Sheppard, B.S., Shen, W.-L., Davidson, T.M., and Caruso, J.A., *J. Anal. At. Spectrom.*, 1990, 5, 697.

100. Smith, F.G., Wiederin, D.R., and Houk, R.S., *Anal. Chem.*, 1991, **63**, 1458.

101. Shibata, N., Fudagawa, N., and Kubota, M., *Spectrochim. Acta*, 1992, **47B**, 505.

102. Ford, M.J., Ebdon, L., Hutton, R.C., and Hill, S.J., *Anal. Chim. Acta*, 1994, **285**, 23.

103. Hill, S.J., Ford, M.J., and Ebdon, L., *J. Anal. At. Spectrom.*, 1992, 7, 1157.

104. Ebdon, L., Ford, M.J., Hutton, R.C., and Hill, S.J., *Appl. Spectrosc.*, 1994, **48**, 507.

105. Ruzicka, J., and Hansen, E.H., *Anal. Chim. Acta*, 1975, **78**, 145.

106. Ruzicka, J., and Christian, G.D., *Analyst*, 1990, **115**, 475.

107. Ruzicka, J., and Hansen, E.H., "Flow Injection Analysis", 2nd Ed., Wiley and Sons, New York, 1988.

108. Hirata, S., Honda, K., and Kumamaru, T., *Anal. Chim. Acta*, 1989, **221**, 65.

109. Hartenstein, S.D., Ruzicka, J., and Christian, G.D., *Anal. Chem.*, 1985, **57**, 21.

110. Karlberg, B., and Pacey, G.E., "Flow Injection Analysis. A Practical Guide", Elsevier, Amsterdam, 1989.

111. Valcarcel, M., and Luque de Castro, M.D., "Flow Injection Analysis. Principles and Applications", Ellis Horwood, Chichester, 1987.

112. Karlberg, B., and Thelander, S., *Anal. Chim. Acta*, 1978, **98**, 1.

113. Nord, L., and Karlberg, B., *Anal. Chim. Acta*, 1981, **125**, 199.

114. Svensson, G., and Anfalt, T., *Clin. Chim. Acta*, 1982, **119**, 7.

115. Baadenhuijsen, H., and Seuren-Jacobs, H.E.H., *Clin. Chem*, 1979, **25**, 443.

116. Hansen, E.H., and Ruzicka, J., *Anal. Chim. Acta*, 1976, **87**, 353.

117. van Staden, J.F., and Basson, W.D., *Lab. Pract.*, 1980, **29**, 1279.

118. Gorton, L., and Ogren, L., *Anal. Chim. Acta*, 1981, **130**, 45.

119. Schothorst, R.C., and den Boef, G., *Anal. Chim. Acta*, 1983, **153**, 133.

120. Petit de Pena, Y., Gallego, M., and Valcarcel, M., *J. Anal. At. Spectrom.*, 1994 **9**, 691.

121. Hall, G.E.M., and Pelchat, J.C., *J. Anal. At. Spectrom.*, 1993, **8**, 1059.

122. Kelly, T.A., and Christian, G.D., *Talanta* 1982, **29**, 1109.

123. Olsen, S., Pessenda, L.C.R., Ruzicka, J., and Hansen, E.H., *Analyst*, 1983, **108**, 905.

124. Mohammad, B., Ure, A.M., and Littlejohn, D., *J. Anal. At. Spectrom.*, 1992, **7**, 695.

125. Fang, Z., and Welz, B., *J. Anal. At. Spectrom.*, 1989, **4**, 543.

126. Shah, A., and Devi, S., *Anal. Chim. Acta*, 1990, **236**, 469.

127. Hirata, S., Honda, K., and Kumamaru, T., *Anal. Chim. Acta*, 1989, **221**, 65.

128. Liu, Y., and Ingle, J.D., *Anal. Chem.*, 1989, **61**, 525.

129. Peng, X., Jiang, Z., and Zen, Y., *Anal. Chim. Acta*, 1993, **283**, 887.

130. Hirata, S., Umezaki, Y., and Ikeda, M., *Anal. Chem.*, 1986, **58**, 2602.

131. Kumamaru, T., Matsuo, H., Okamoto, Y., and Ikeda, M., *Anal. Chim. Acta*, 1986, **181**, 271.

132. Mukai, H., Ambe, Y., and Morita, M., *J. Anal. At. Spectrom.*, 1990, **5**, 75.

133. Ebdon, L., Fisher, A., Handley, H., and Jones, P., *J. Anal. At. Spectrom.*, 1993, **8**, 979.

134. Esser, B.K., Volpe, A., Kenneally, J.M., and Smith, D.K., *Anal. Chem.*, 1994, **66**, 1736.

135. Plantz, M.R., Fritz, J.S., Smith, F.G., and Houk, R.S., *Anal. Chem.*, 1989, **61**, 149.

136. Orians, K.J., and Boyle, E.A., *Anal. Chim. Acta*, 1993, **282**, 63.

137. Ida, I., Yoshikawa, H., Ishibashi, Y., and Gunji, N., *ICP Newsletter*, 1990, **16**, 388.

138. James, D.L., The Specialist, Thermo Electron Ltd (13 Sept. 1990).

139. Cox, A.G., Cook, I.G., and McLeod, C.W., *Analyst*, 1985, **110**, 331.

140. Ebdon, L., Fisher, A.S., and Worsfold, P.J., *J. Anal. At. Spectrom.*, 1994, **9**, 661.

141. Trojanowicz, M., and Pyrzynska, K., *Anal. Chim. Acta*, 1994, **287**, 247.

142. Glennon, J.D., and Srijaranai, S., *Analyst*, 1990, **115**, 627.

143. Ma, R., van Mol, W., and Adams, F., *Anal. Chim. Acta*, 1994, **285**, 33.

144. Elmahadi, H.A.M., and Greenway, G.M., *J. Anal. At. Spectrom.*, 1994, **9**, 547.

145. Robards, K., Starr, P., and Patsalides, E., *Analyst*, 1991, **116**, 1247.

146. Chau, Y.K., *Analyst*, 1992, **117**, 571.

147. Hamilton, R.J., and Sewell, P.A., "Introduction to High-Performance Liquid Chromatography", Chapman and Hall, London, 1977.

148. Meyer, V.R., "Practical High-Performance Liquid Chromatography", John Wiley and Sons, Chichester, 1988.

149. Ebdon, L., Hill, S. and Ward, R.W., *Analyst*, 1986, **111**, 1113.

150. Ebdon, L., Hill, S. and Ward, R.W., *Analyst*, 1987, **112**, 1.

151. Gast, C.H., Kraak, J.C., Poppe, H. and Maessen, F.J.M.J., *J. Chromatogr.*, 1979, **185**, 549.

152. Fraley, D.M., Yates, D. and Manahan, S.E., *Anal. Chem.*, 1979, **51**, 2225.

153. Whaley, B.S., Snable, K.R. and Browner, R.F., *Anal. Chem.*, 1982, **54**, 162.

154. Meinhard, J.E., *ICP Newsletter*, 1976, **2**, 163.

155. Novak, J.W., Lillie, D.E., Boorn, A.W. and Browner, R.F., *Anal. Chem.*, 1980, **52**, 579.

156. Maessen, F.J.M.J., Seeverens, P.J.H. and Krevning, G., *Spectrochim. Acta*, 1984, **39B**, 1171.

157. Maessen, F.J.M.J., Krevning, G. and Balke, J., *Spectrochim. Acta*, 1986, **41B**, 3.

158. Wiederin, D.R., Houk, R.S., Winge, R.K. and D'Silva, A.P., *Anal. Chem.*, 1990, **62**, 1155.

159. Ebdon, L., Evans, E.H. and Barnett, N.W.J., *J. Anal. At. Spectrom.*, 1989, **4**, 505.

160. Hausler, D.W. and Taylor, L.T., *Anal. Chem.*, 1981, **53**, 1223.

161. Boorn, A.W. and Browner, R.F., *Anal. Chem.*, 1982, **54**, 1402.

162. Hill, S., Hartley, J. and Ebdon, L., *J. Anal. At.Spectrom.*, 1992, **7**, 23.

163. Jinno, K., Nakanishi, S. and Fujimoto, C., *Anal. Chem.*, 1985, **57**, 2229.

164. Jinno, K., Tsuchida, H., Nakanishi, S., Hirata, Y. and Fujimoto, C., *Appl. Spectrosc.*, 1983, **37**, 258.

165. Lawrence, K.E., Rice, G.W. and Fassel, V.A., *Anal. Chem.*, 1984, **56**, 292.

166. McCarthy, J.P., Caruso, J.A. and Fricke, F.L., *J.Chromatogr. Sci.*, 1983, **21**, 389.

167. Suyani, H., Creed, J., Davidson, T. and Caruso, J., *J. Chromatogr. Sci.*, 1989, **27**, 139.

168. McLaren, J.W., Mykytivk, A.P., Willie, S.N. and Berman, S.S., *Anal. Chem.*, 1985, **57**, 2907.

169. Doherty, W. and Vander Voet, A., *Can. J. Spectrosc.*, 1986, **30**, 135.

170. Thompson, J.J. and Houk, R.S., *Anal. Chem.*, 1986, **58**, 2541.

171. Jiang, S., Palmieri, J.S., Fritz, J.S. and Houk, R.S., *Anal. Chim. Acta*, 1987, **200**, 559.

172. Shen, W.-L., Vela, N.P., Sheppard, B.S. and Caruso, J.A., *Anal. Chem.*, 1991, **63**, 1491.

173. Kumar, U.T., Vela, N.P., Dorsey, J.G., and Caruso, J.A., *J. Chromatogr.* 1993, **655**, 340.

174. Bushee, D.S., *Analyst*, 1988, **113**, 1167.

175. Huang, C.-J., Jiang, S.-J., *Anal. Chim. Acta.*, 1994, **289**, 205.

176. Beauchemin, D., Bednas, M.E., Berman, S.S., McLaren, J.W., Sui, K.W.M. and Sturgeon, R.E., *Anal. Chem.*, 1988, **60**, 2209.

177. Beauchemin, D., Siu, K.W.M., McLaren, J.W. and Berman, S.S., *J. Anal. At. Spectrom.*, 1989, **4**, 285.

178. Shibata, Y. and Morita, M., *Anal. Sci.*, 1989, **5**, 107.

179. Larsen, E.H., Pritzl, G., and Hansen, S.H., *J. Anal. At.Spectrom.*, 1992, **7**, 23.

180. Branch, S., Ebdon, L., and O'Neill, P., *J. Anal. At.Spectrom.*, 1994, **9**, 33.

181. Suyani, H., Heitkemper, D., Creed, J. and Caruso, J., *Appl. Spectrosc.*, 1989, **43**, 962.

182. Shen, W.-L., Vela, N.P., Sheppard, B.S. and Caruso, J.A., *Anal. Chem.*, 1991, **63**, 1491.

183. McLaren, J.W., Siu, K.W.M., Lam, J.W., Willie, S.N., Maxwell, P.S., Palepu, A., Koether, M. and Berman, S.S., *Fresenius J. Anal. Chem.*, 1990, **337**, 721.

184. Beauchemin, D., Micklethwaite, R.K., Van Loon, G.W. and Hay, G.W., *Chem. Geol.*, 1992, **95**, 187.

185. Klinkenberg, H., Van der Waal, S., Frusch, J., Terwint, L. and Beeren, T., *At. Spectrosc.*, 1990, **11**, 199.

186. Mason, A.Z., Storms, S.D. and Jenkins, K.D., *Anal. Biochem.*, 1990, **186**, 187.

187. Gerken, B. and Barnes, R.M., *Anal. Chem.*, 1991, **63**, 283.

188. Crews, H.M., Dean, J.R., Ebdon, L. and Massey, R.C., *Analyst*, 1989, **114**, 895.

189. Matz, S.G., Elder, R.C. and Tepperman, K., *J. Anal. At. Spectrom.*, 1989, **4**, 767.

190. Owen, L.M.W., Crews, H.M., Hutton, R.C., and Walsh, A., *Analyst*, 1992, **117**, 649.

191. Dean, J.R., Ebdon, L., Foulkes, M.E., Crews, H.M., and Massey, R.C., *J. Anal. At. Spectrom.*, 1994, **9**, 615.

192. Bushee, D.S., Moody, J.R. and May, J.C., *J. Anal. At. Spectr.*, 1989, **4**, 773.

193. Kawabata, K., Kishi, Y., Kawaguchi, O., Watanabe, Y. and Inoue, Y., *Anal. Chem.*, 1991, **63**, 2137.

194. Jiang, S. and Houk, R.S., *Spectrochim. Acta.*, 1988, **43B**, 405.

195. Brown, M.A., Kim, I.S., Roehl, R., Sasinos, F.I. and Stephens, R.D., *Chemosphere*, 1989, **19**, 1921.

196. Braverman, D.S., *J. Anal. At. Spectrom.*, 1992, **7**, 43.

197. Shum, S.C.K., Neddersen, R. and Houk, R.S., *Analyst*, 1992, **117**, 577.

198. Roehl, R., and Alforque, M.M., *At. Spectrosc.*, 1990, **11**, 210.

199. Al Rashdan, A., Vela, N.P., Caruso, J.A., and Heitkemper, D.T., *J. Anal. At. Spectrom.*, 1992, **7**, 551.

200. Sheppard, B.S., Caruso, J.A., Heitkemper, D.T. and Wolnik, K.A., *Analyst*, 1992, **117**, 971.

201. Takatera, K., and Watanabe, T., *Anal. Sci.*, 1991, **7**, 695.

202. Shum, S.C.K., Pang, H., and Houk, R.S., *Anal. Chem.*, 1992, **64**, 2444.

203. O'Neill, P., "Environmental Chemistry", George Allen and Unwin Ltd, London, 1985.

204. Unesco Tech. Pap. Mar. Sci.., no. 38. Paris: Unesco 1981.

205. Chester, R., "Marine Geochemistry", Unwin Hyman, London, 1990.

206. Riley, J.P., and Skirrow, G., Editors, "Chemical Oceanography", Academic Press Ltd, London, 1975.

207. Hoover, T.B., EPA Literature Review, 600/3-78-064, 1978.

208. Bruland, K.W., In Riley, J.P., and Chester, R. (Ed.), "Chemical Oceanography", vol.8, Academic Press, London, 1983.

209. Fagerstrom, T. and Jernelov, A., *Water Research*, 1972, **6**, 1193.

210. Ahmed,R., May, K. and Stoeppler, M., *Fresenius Z. Anal. Chem.*, 1987, **326**, 510.

211. Goto, M., Shibakawa, T., Arita, T. and Ishii, D., *Anal. Chim. Acta*, 1982, **140**, 179.

212. Chiba, K., Yoshida, K., Tanabe, K., Haraguchi, H. and Fuwa, K., *Anal. Chem.*, 1983, **55**, 450.

213. Brezinska, A., van Loon, J., Williams, D., Oguma, K., Fuwa, K. and Haraguchi, H., *Spectrochim. Acta*, 1983, **38B**, 1339.

214. Wang, Y.-C. and Whang, C.-W., *J. Chromatogr.*, 1993, **628**, 133.

215. Sarzanini, C., Sacchero, G., Aceto, M., Abollino, O. and Mentasti, E., *J. Chromatogr.* 1992, **626**, 151.

216. Ebdon, L., and Carpenter, R.C., *Anal. Chim. Acta*, 1987, **200**, 551.

217. Ebdon, L., and Carpenter, R.C., *Anal. Chim. Acta*, 1988, **209**, 135.

218. Miller, J.C., and Miller, J.N., "Statistics for Analytical Chemistry" 2nd. ed., Ellis Horwood, Chichester, 1988.

219. Adams, M.J., in Haswell, S.J., Editor, "A Practical Guide to Chemometrics", Marcel Dekker, New York, 1992.

220. Irons, G.P., B.Sc. Final Year Project, University of Hull, 1990.

221. Isshiki, K., Sohrin, Y., Karatani, H., and Nakayama, E., *Anal. Chim. Acta,* 1989, **224**, 55.

222. Kingston, H.M., Barnes, I.L., Brady, T.J., Rains, T.C. and Champ, M.A., *Anal. Chem.*, 1978, **50**, 2064.

223. Pai, S.-C., Fang, T.-H., Chen, C.-T.A., and Jeng, K.L., *Marine. Chem.*, 1990, **29**, 295.

224. Laboratory of the Goverment Chemist, Certified Reference Materials, Issue no.2, 1991.

225. Crouch, T.H., and Klee, C.B., *Biochem.*, 1980, **19**, 3692.

226. Fassett, J.D., and Kingston, H.M., *Anal. Chem.*, 1985, **57**, 2474.

227. Dionex Technical Note 25, Dionex Corporation, 1992.

228. Heithmar, E.M., Hinners, T.A., Rowan, J.T., and Riviello, J.M., *Anal. Chem.*, 1990, **62**, 857.

229. Siriraks, A., Kingston, H.M., and Riviello, J.M., *Anal. Chem.*, 1990, **62**, 1185.

230. Long, S.E., and Martin, T.D., Method 200.10, Environmental Monitoring Systems Laboratory, U.S. Environmental Protection Agency, 1992.

231. Weber, J.H., *Chemosphere*, 1993, **26**, 2063.

232. Clark, R.B., "Marine Pollution", Clarendon Press, Oxford, 1986.

233. Bernhard, M., UNEP Regional Seas Reports and Studies No.98, UNEP, 1988.

234. Matsunaga, K., and Takahashi, S., *Anal. Chim. Acta,* 1976, **87**, 487.

235. Vermeir, G., Vandecasteele, C., Temmerman, E., Dams, R., and Versieck, J., *Mikrochim. Acta,* 1988, **111**, 305.

236. Vargas, M.C., and Romero, R.A., *At. Spectrosc.*, 1989, **10**, 160.

237. Thompson, K.C., and Godden, R.G., *Analyst,* 1975, **100**, 544.

238. Hutton, R.C., and Preston, B., *Analyst,* 1980, **105**, 981.

239. Godden, R.G., and Stockwell, P.B., *J. Anal. At. Spectrom.*, 1989 **4**, 301.

240. Haswell, S.J., Ed., "Atomic Absorption Spectrometry", Elsevier, Amsterdam, 1991.

241. Lindstedt, G., *Analyst,* 1970, **95**, 264.

242. Farey, B.J., Nelson, R.H., and Rolph, M.G., *Analyst,* 1978, **103**, 656.

243. Emteborg, H., Baxter, D.C., and Frech, W., *Analyst,* 1993, **118**, 1007.

244. Hanna, C.P., Tyson, J.F., and McIntosh S., *Anal. Chem.*, 1993, **65**, 653.

245. Guo, T., and Baasner, J., *Anal. Chim. Acta,* 1993, **278**, 189.

246. Canada Rudner, P., Garcia de Torres, A., and Cano Pavon, J.M., *J. Anal. At. Spectrom.*, 1993 **8**, 705.

247. Jian, W., and McLeod, C.W., *Mikrochim. Acta,* 1992, **109**, 117.

248. Schneider, C.A., Schulze, H., Baasner, J., McIntosh, S., and Hanna, C., *Int. Laboratory,* 1994, April, 13.

249. Stroh, A., and Vollkopf, U., *J. Anal. At. Spectrom.*, 1993 **8**, 35.

250. Smith, J., "Personal Communication".

251. Holak, W., *Analyst,* 1982, **107**, 1457.

252. Munaf, E., Haraguchi, H., Ishii, D., Takeuchi, T., and Goto, M., *Anal. Chim. Acta,* 1990, **235**, 399.

253. Sarzanini, C., Sacchero, G., Aceto, M., Abollino, O., and Mentasti, E., *J. Chrom.*, 1992, **626**, 151.

254. Sarzanini, C., Sacchero, G., Aceto, M., Abollino, O., and Mentasti, E., *Anal. Chim. Acta,* 1994, **284**, 661.

255. Bushee, D., Young, D., Krull, I.S., Savage, R.N., and Smith, S.B., *J. Liq. Chrom.*, 1982, **5**, 693.

256. Krull, I.S., Bushee, D., Schleicher, R.G., and Smith, S.B., *Analyst,* 1986, **111**, 345.

PUBLICATIONS

1. Bloxham, M.J., Worsfold, P.J. and Hill, S.J., The Analysis of Trace Metals in Sea Water by ICP-MS and Related Techniques. *Analytical Proceedings,* 1993, **30**, 159.

2. Hill, S.J., Bloxham, M.J. and Worsfold, P.J., Chromatography Coupled With Inductively Coupled Plasma-Atomic Emission Spectrometry and Inductively Coupled Plasma-Mass Spectrometry: A Review, *Journal of Analytical Atomic Spectrometry,* 1993, **8**, 1.

3. Bloxham, M.J., Worsfold, P.J. and Hill, S.J., Matrix Suppression in Sea-water Analysis Using Inductively Coupled Plasma-Mass Spectrometry with Mixed Gas Plasmas, *Analytical Proceedings Including Analytical Communications,* 1994, **31**, 95.

4. Bloxham, M.J., Worsfold, P.J. and Hill, S.J., Determination of Trace Metals in Sea-water and the On-line Removal of Matrix Interferences by Flow Injection With Inductively Coupled Plasma-Mass Spectrometry, *Journal of Analytical Atomic Spectrometry,* 1994, **9**, 935.

5. Speciation of Mercury in Sea water by Liquid Chromatography Coupled with Inductively Coupled Plasma-Mass Spectrometry, To be submitted.

PRESENTATIONS

1. *Speciation of Trace Metals in Sea Water Using Liquid Chromatography Coupled with Inductively Coupled-Plasma Mass Spectrometry,* Poster presented at Research and Development Topics in Analytical Chemistry, University of Birmingham, 7-8 July 1992.

2. *Matrix Suppression in Inductively Coupled Plasma Mass Spectrometry Using Mixed Gas Plasmas*, Poster presented at Research and Development Topics in Analytical Chemistry, University of Bradford, 16-17 July 1993.

3. *On-line Removal of Matrix Interferences in Sea Water by Flow Injection with Inductively Coupled Plasma-Mass-Spectrometric Detection,* Poster presented at 1994 Winter Conference on Plasma Spectrochemistry, San Diego, USA, 10-15 January 1994.

4. *On-line Removal of Matrix Interferences in Sea Water by Flow Injection with Inductively Coupled Plasma-Mass Spectrometric Detection,* Poster presented at Research and Development Topics in Analytical Chemistry, University of Hertfordshire, 18-19 July 1994.

5. *Determination of Trace Metals in Sea-water and the On-line Removal of Matrix Interferences by Flow Injection With Inductively Coupled Plasma-Mass Spectrometric Detection,* Lecture presented at Seventh Biennial National Atomic Spectroscopy Symposium, University of Hull, 20-22 July 1994.